MR08-05

(10 Oct. - 10 Nov. 2008)

Preliminary Cruise Report
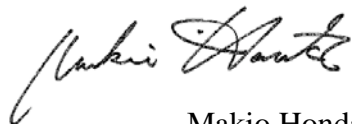
JUST DO IT

2008 Dec.

JAMSTEC

Note

This cruise report is a preliminary documentation published in approximately a month after the end of this cruise.   It may not be corrected even if changes on contents are found after publication.   It may also be changed without notice.   Data on the cruise report may be raw or not processed.   Please ask the principal investigator and parsons in charge of respective observations for the latest information and permission before using.   Users of data are requested to submit their results to JAMSTEC.

12 December 2008

Principal Investigator of MR08-05

Makio Honda
MIO, JAMSTEC

Cruise Report ERRATA of the Photosynthetic Pigments part

page	Error	Correction
99	Ethyl-apo-8'-carotenoate	trans-β-Apo-8'-carotenal

Contents of MR08-05 Preliminary Cruise Report

Cover sheet: the first prize of MR08-05 cruise report cover sheet contest by M. Kitamura (photo) and M. Honda (design)

A. Cruise summary

1. Cruise information

(1) Cruise designation (research vessel)
MR08-05 (R/V MIRAI)

(2) Cruise title
The study of ecosystem and materials' cycle in the North Pacific

(3) Principal Investigator (PI): Makio Honda
JAMSTEC Mutsu Institute for Oceanography (MIO)

(4) Science proposals of cruise

S/N	Affiliation	PI	Proposal titles
MR08-39	JAMSTEC IORGC	Kunio YONEYAMA	Continuous surface meteorological measurements as a basic dataset.
MR08-40	JAMSTEC FRCGC	Sanae CHIBA	Community structure of surface zooplankton and its role on material' vertical transport
MR08-41	NIES	Nobuo SUGIMOTO	Study of distribution and optical characteristics of ice/water clouds and marine aerosols
MR08-43	Nagoya Univ.	Hiromi YAMAZAWA	Underway monitoring of low atmospheric and seawater radon (Rd) with high-sensitive radon detector
MR08-44	Tokyo Univ.	Koji HAMASAKI	Micrometer particles size spectrum and microbial activities in a twilight zone
MR08-45	JAMSTEC IORGC	Naoyuki KURITA	Rain and seawater sampling for stable isotopes
MR08-46	Ryukyu Univ.	Takeshi MATSUMOTO	Standardization of marine geophysical data and its application to the ocean floor geodynamics studies
MR08-47	Kyoto Univ.*	Toshi NAGATA	Full-depth analysis of microbial community structures and their auto- and heterotrophic activities
MR08-48	Chiba Univ.	Masao NAKANISHI	Study of the Pacific plate tectonics
MR08-49	Okayama Univ.	Osamu TSUKAMOTO	Surface atmospheric turbulent flux measurement
MR08-50	Chiba Univ.	Toshiaki TAKANO	Study of the global distribution and structure of oceanic cloud
MR08-51	NIES	Masao UCHIDA	Pilot study on carbon cycle of Marine Crenarchaeota in the North Pacific using geochemical and molecular biological approaches
MR08-82	Nagoya Univ.**	Toshiro SAINO	Stable carbon and nitrogen isotopes of suspended particles

* Present affiliation: Tokyo University

** Present affiliation: JAMSTEC IORGC

(5) Cruise period (port call)
10 October 2008 (Dutch Harbor) – 10 November 2008 (Onahama)

(6) Cruise region (geographical boundary)
The western North Pacific (60°N – 40°N, 140°E – 165°W)

(7) Cruise truck and stations

2 Cruise Participants

	Name	Affiliation	Appointment	Tel
1	Makio HONDA （Principal Investigator）	Mutsu Institute for Oceanography (MIO) Institute of Observational Research for Global Change (IORGC) Japan Agency for Marine-Earth Science and Technology (JAMSTEC)	Sub Leader	0175-45-1071
2	Minoru KITAMURA （Deputy PI）	Extremobiosphere Research Center (XBR) JAMSTEC	Researcher	046-867-9527
3	Kazuhiko MATSUMOTO	MIO, IORGC JAMSTEC	Researcher	0175-45-1071
4	Hajime KAWAKAMI	MIO, IORGC JAMSTEC	Researcher	Same as above
5	Masahide WAKITA	Same as above	Researcher	Same as above
6	Tetsuichi FIJIKI	MIO, JAMSTEC	Researcher	Same as above
7	Sanae CHIBA	Frontier Research Center for Global Change (FRCGC) JAMSTEC	Senior scientist	045-778-5604
8	Katsunori YOSHIDA	Safety and Environment Management Office, JAMSTEC	Engineer	046-867-9104
9	Noriyuki OHYA	Nagoya University	Graduated student	052-789-5134
10	Koji HAMASAKI	Tokyo University	Associate professor	03-5351-6337
11	Hideki FUKUDA	Same as above	Assistant professor	Same as above
12	Ayako OKAMOTO	Same as above	Same as above	Same as above
13	Taichi YOKOKAWA	Netherlands Oceanographic Institution Tokyo University	Post doctor	Same as above
14	Fumihiro YAMAZAKI	Chiba university	Graduate student	043-290-3311
15	Yukiko KUROKI	Tsukuba University	Graduate student	029-850-2042
16	Chie SATO	Same as above	Same as above	Same as above
17	Shiro YOSHIDA	Same as above	Undergraduate student	Same as above
18	Fuyuki SHIBATA （Principal Marine Tech.）	Marine Works Japan Inc. (MWJ)	Marine Technician	045-787-0041
19	Hiroshi MATSUNAGA	Same as above	Same as above	Same as above
20	Masanori ENOKI	Same as above	Same as above	Same as above
21	Masaki TAGUCHI	Same as above	Same as above	Same as above
22	Ai YASUDA	Same as above	Same as above	Same as above
23	Tatsuya TANAKA	Same as above	Same as above	Same as above
24	Katsunori SAGISHIMA	Same as above	Same as above	Same as above
25	Tomoyuki TAKAMORI	Same as above	Same as above	Same as above
26	Misato KUWAHARA	Same as above	Same as above	Same as above
27	Yasuhiro ARII	Same as above	Same as above	Same as above
28	Hiroki USHIROMURA	Same as above	Same as above	Same as above
29	Ayaka HATSUYAMA	Same as above	Same as above	Same as above
30	Miyo IKEDA	Same as above	Same as above	Same as above
31	Yoshiko ISHIKAWA	Same as above	Same as above	Same as above
32	Hayato MATSUSHITA	Same as above	Same as above	Same as above

33	Shoko TATAMISASHI	Same as above	Same as above	Same as above
34	Tomonori WATAI	Same as above	Same as above	Same as above
35	Yuichi SONOYAMA	Same as above	Same as above	Same as above
36	Ken-ichiro SATO	Same as above	Same as above	Same as above
37	Yusuke SATO	Same as above	Same as above	Same as above
38	Kento FUKABORI	Same as above	Same as above	Same as above
39	Hiroyuki HAYASHI	Same as above	Same as above	Same as above
40	Wataru TOKUNAGA (Principal Marine Tech.)	Global Ocean Development Inc. (GODI)	Same as above	045-849-6630
41	Kazuho YOSHIDA	Same as above	Same as above	Same as above

3. Overview of MR08-05

(1) Objective

      To collect oceanographic data in late autumn in the northwestern North Pacific for the sake of understanding cycles of chemical substances focusing on CO_2 and role of ecosystem in materials' cycle

(2) Overview of MR08-05

      Main mission of this cruise was to collect oceanographic data in late autumn in the northwestern North Pacific for the sake of understanding of cycles of chemical substances focusing on CO_2 and role of ecosystem such as zooplankton and bacteria in materials' cycle.

      As same as previous cruises, we suffered from bad weather and sea condition. However we successfully conducted most of all comprehensive observation scheduled at most of all stations unlike we expected.

(Observation in the Bering Sea)

      We could conduct comprehensive biogeochemical observation (measurements of dissolved materials, primary productivity, phyto-plankton pigments, grazing pressure, bacteria production and collection of zooplankton with IONESS) in the open sea of the Bering Sea for the first time.

      Although it was autumn season, biomass of phytoplankton is large (concentration of chlorophyll is > 1.5 mg m^{-3}) and diatom was pre-dominant (Fig. 1), which is indicating that the Bering Sea is indeed "Sea of Silica" (Tsunogai and Noriki, 1979). In addition, we could conduct "transect" observation from the central part of the Bering Sea (57°N) to the former time-series station KNOT (44° N) in the northwestern North Pacific. We measured vertical profiles of dissolved oxygen, nutrients, carbon species and chlorofluorocarbon each one-degree (Fig.2). These results will supply important information about exchange of water and chemical substances between the northwestern North Pacific and the Bering Sea.

Fig.1 Concentration of chlorophyll for respective major phyto-planktons

Fig.2 Vertical section of silicate (upper panel) and oxygen (lower panel) from station AB (57°N) to station KNOT (44°N)

(Observation for study of the role of ecosystem in materials' cycle)

At several major stations including our time-series station K2, measurements of primary productivity, phytoplankton pigments, and sinking particles and suspended particles using the drifting buoy, in situ Large Volume Pump and Laser system (LISST) were conducted. On the other hand, collection of zooplankton using "giant" plankton net (IONESS) and measurements of grazing pressure and bacteria production were also conducted. Based on the preliminary results, primary productivity (PP) at station K2 was approximately 200 mg-C m^{-2} day^{-1} and approximately 60% of PP was grazed by micro-zooplankton. In near future, these results, especially bacteria production measured with radioisotope, will become very informative about the role of ecosystem in the materials' cycle.

(Time-series observation with mooring system)

Mooring system with automatic water sampler, optical sensor package, and sediment traps, which was deployed in September 2007, was successfully recovered. Base on the first inspection of collected materials below 300 m, materials' flux were low in winter and increased from late spring to autumn (Fig. 3). After recovery of samples and data, replacement of new battery, and initialization of each samplers, this mooring system was re-deployed on 28 October. This mooring system will be recovered in January 2010.

Fig.3 Seasonal variability of total mass flux based on measurement of heights of flux in collecting cups at 300m, 540m, 1000m and 4810m.

B. Text

1. Outline of MR08-05

Makio HONDA (JAMSTEC MIO)
Principal Investigator of MR07-05

1.1 Cruise summary

(1) Objective

To collect oceanographic data in late autumn in the northwestern North Pacific for the sake of understanding cycles of chemical substances focusing on CO_2 and role of ecosystem in materials' cycle

(2) Overview of MR08-05

Main mission of this cruise was to collect oceanographic data in late autumn in the northwestern North Pacific for the sake of understanding of cycles of chemical substances focusing on CO_2 and role of ecosystem such as zooplankton and bacteria in materials' cycle.

As same as previous cruises, we suffered from bad weather and sea condition. However we successfully conducted most of all comprehensive observation scheduled at most of all stations unlike we expected.

Fig.1 Concentration of chlorophyll for respective major phyto-planktons

(Observation in the Bering Sea)

We could conduct comprehensive biogeochemical observation (measurements of dissolved materials, primary productivity, phyto-plankton pigments, grazing pressure, bacteria production and collection of zooplankton with IONESS) in the open sea of the Bering Sea for the first time.

Although it was autumn season, biomass of phytoplankton is large (concentration of chlorophyll is > 1.5 mg m^{-3}) and diatom was pre-dominant (Fig. 1), which is indicating that the Bering Sea is indeed "Sea of Silica" (Tsunogai and Noriki, 1979). In addition, we could conduct "transect" observation from the central part of the Bering Sea (57°N) to the former time-series station KNOT (44° N) in the northwestern North Pacific. We measured vertical profiles of dissolved oxygen, nutrients, carbon species and chlorofluorocarbon each one-degree (Fig.2). These results will supply important information about exchange of water and chemical substances between the northwestern North Pacific and the Bering Sea.

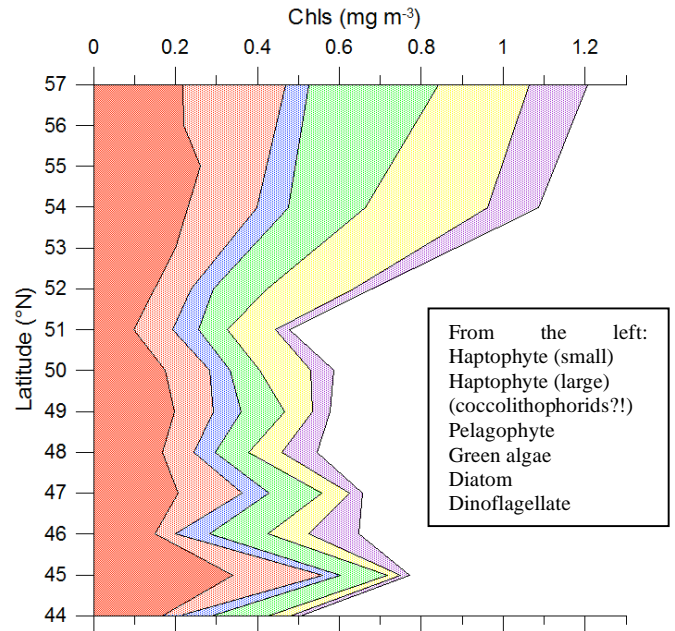(Observation for study of the role of ecosystem in materials' cycle)

At several major stations including our time-series station K2, measurements of primary productivity, phytoplankton pigments, and sinking particles and suspended particles using the drifting buoy, in situ Large Volume Pump and Laser system (LISST) were conducted. On the other hand, collection of zooplankton using "giant" plankton net (IONESS) and measurements of grazing pressure and bacteria production were also conducted. Based on the preliminary results, primary productivity (PP) at station K2 was approximately 200

Fig.2 Vertical section of silicate (upper panel) and oxygen (lower panel) from station AB (57°N) to station KNOT (44°N)

mg-C m^{-2} day^{-1} and approximately 60% of PP was grazed by micro-zooplankton. In near future, these results, especially bacteria production measured with radioisotope, will become very informative about the role of ecosystem in the materials' cycle.

(Time-series observation with mooring system)

Mooring system with automatic water sampler, optical sensor package, and sediment traps, which was deployed in September 2007, was successfully recovered.
Base on the first inspection of collected materials below 300 m, materials' flux were low in winter and increased from late spring to autumn (Fig. 3). After recovery of samples and data, replacement of new battery, and initialization of each samplers, this mooring system was re-deployed on 28 October. This mooring system will be recovered in January 2010.
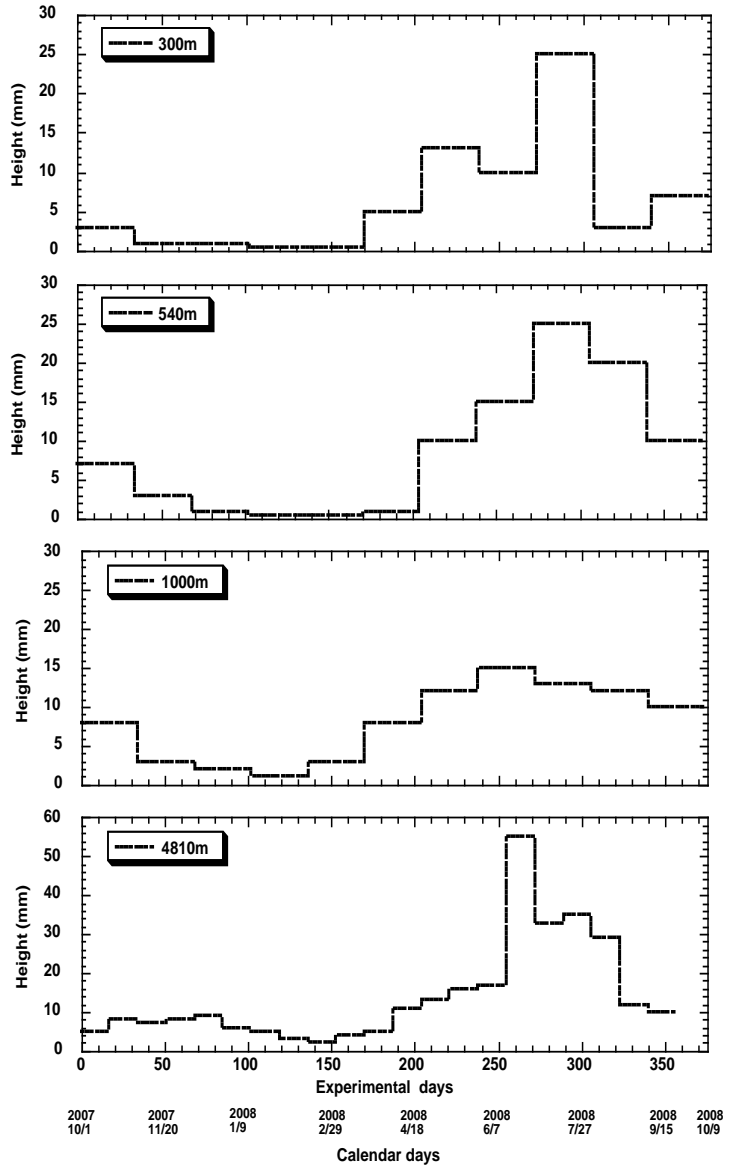
Fig.3 Seasonal variability of total mass flux based on measurement of heights of flux in collecting cups at 300m, 540m, 1000m and 4810m.

(3) Scientific gears

All hydrocasts were conducted using 36-position 12 liter Niskin bottles carousel system with SBE CTD-DO system, fluorescence and transmission sensors. JAMSTEC MIO scientists and MWJ (Marine Work Japan Co. Ltd.) technician group were responsible for analyzing water sample for salinity, dissolved oxygen, nutrients, CFCs, total carbon contents, alkalinity and pH. Cruise participants from JAMSTEC MIO, XBR and FRCGC, Tsukuba University, Tokyo University, Chiba University and Nagoya University helped to divide seawater from Niskin bottles to sample bottles for analysis. Surface water was collected with bucket.

Optical measurement in air and underwater was conducted with PAR sensor (RAMSES-ACC) and SPMR/SMSR called "Free Fall".

For collecting suspended particles at stationK2, Large Volume Pump (LVP) was deployed.

For observing in situ particles, optical sensor called LISST (Laser In Situ Scattering and Transmissometer) was deployed by University of Tokyo.

GODI technicians group undertook responsibility for underway current direction and velocity measurements using an Acoustic Current Profiler (ADCP), geological measurements (topography, geo-magnetic field and gravity), and collecting meteorological data.

For collection of zooplankton, NORPAC plankton net, and IONESS were deployed.

For conducting in situ incubation for measurement of primary productivity and collecting sinking particles at station K2, drifter was deployed at station K2.

For observing vertical profile of primary productivity optically, FRRF was deployed.

In order to conduct time-series observation in physical, chemical and biological activity, JAMSTEC BGC mooring was recovered and re-deployed at station K2. The BGC consisted of a optical sensor package (BLOOMS) at around 35 m, two automatic water samplers (RAS) at around 35 m and 200 m with CT sensor and depth sensor, and 5 sediment traps at 150, 550, 1000 and 5000 m.

Please read text for more detail information and other instruments used for oceanographic and meteorological or atmospheric observation.
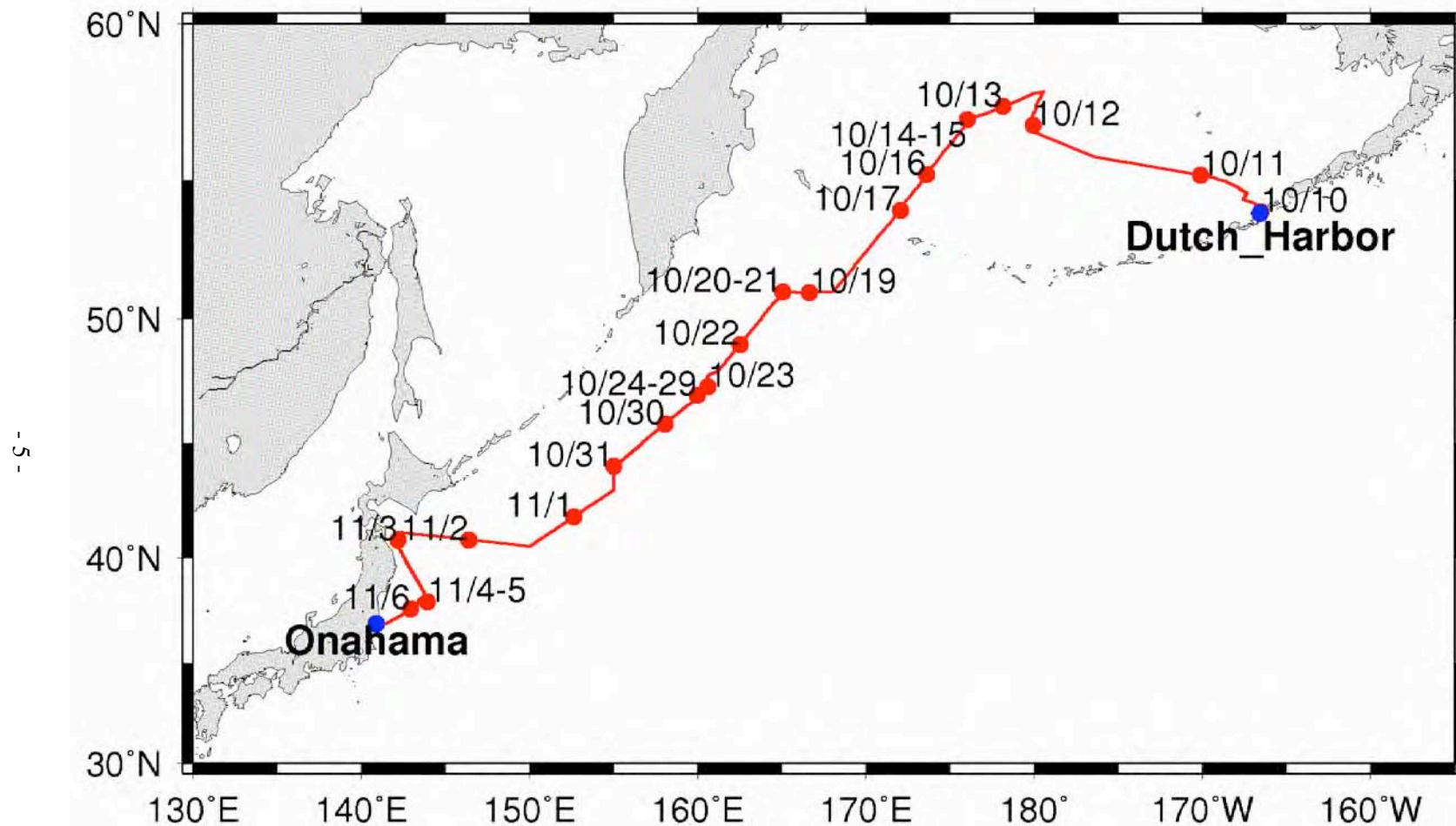
1.2.2   Cruise log

SMT		UTC		Position		Events
Date	Time	Date	Time	Lat.	Lon.	
10/10	14:10	10/10	22:10	55-39N	166-34W	Departure of Dutch Harbor (SMT=UTC-8hr)
	22:00	10/11	6:00	-	-	Time adjustment -1hour (SMT=UTC-9hr)
10/11	8:30		17:30	-	-	Surface sea water sampling pump start
	22:00	10/12	7:00	-	-	Time adjustment -1hour (SMT=UTC-10hr)
10/12	1:34		15:34	55-47.99N	176-29.87W	ARGO float deployment #01
	10:18	10/13	0:18	56-35.92N	179-59.82E	ARGO float deployment #02
	22:00		8:00	-	-	Time adjustment -1hour (SMT=UTC-11hr)
10/13	22:00	10/14	9:00	-	-	Time adjustment -1hour (SMT=UTC-12hr)
10/14	4:18		16:18	57-00N	176-00E	Arrival at Station No.1 (AB)
	4:58		16:58	56-59.47N	176-00.55E	CTD cast #01 (3,863m)
	9:59		21:59	56-59.76N	175-59.83E	Free fall #01
	10:22		22:22	56-59.90N	175-59.63E	FRRF #01
	10:49		22:49	56-59.90N	175-59.63E	CTD cast #02 (200m)
	12:32	10/15	0:32	57-00.04N	175-59.32E	CTD cast #03 (3,792m)
	15:30		3:30	57-01.75N	175-59.23E	FRRF #02
	15:55		3:55	57-02.10N	175-59.37E	LISST #01
	17:10		5:10	57-02.38N	175-59.49E	CTD cast #04 (300m)
	18:57		6:57	56-59.96N	175-59.84E	CTD cast #05 (3,000m)
	21:03		9:03	57-00N	175-59E	Calibration for magnetometer #01
10/15	4:58		16:58	57-00.15N	176-00.08E	FRRF #03
	5:26		17:26	57-00.64N	176-00.20E	CTD cast #06 (200m)
	7:30		19:30	57-00.06N	176-00.09E	Large Volume Pump (LVP) cast #01 (200m, 1 hour)
	9:02		21:02	56-50.32N	176-00.01E	FRRF #04
	9:56		2:56	56-58.80N	176-00.78E	Multiple core sampling #01 (3,813m)

13:30 10/16 1:30	57-00.73N	175-59.01E	IONESS #01 (500m)
16:13	4:13	56-59.98N	175-59.35E	NORPAC net #01 (50 m, 50 m)
16:42	4:42	57-00.34N	175-58.90E	ARGO float deployment #03
18:30	6:30	57-00.03N	175-59.07E	LVP cast #02 (200m, 6 hour)
23:54	11:54	-	-	Departure of Station No.1 (AB)
10/16 3:37	15:37	56-12.08N	175-00.23E	ARGO float deployment #04
4:54	16:54	56-00N	174-40E	Arrival at Station No.2
4:55	16:55	55-59.69N	174-39.51E	CTD cast #07 (3,833m)
7:48	19:48	-	-	Departure of Station No.2
13:00 10/17 1:00	55-00N	173-40E	Arrival at Station No.3
13:05	1:05	54-59.46N	173-20.95E	CTD cast #08 (3,861m)
16:18	4:18	-	-	Departure of Station No.3
21:24	9:24	54-00N	172-00E	Arrival at Station No.4
10/17 09:18	21:18	53-59.18N	172-00.82E	CTD cast #09 (3,881m)
12:18 10/18 00:18	-	-	Departure of Station No.4
17:18	5:18	53-00N	170-40E	Arrival at Station No.5
17:24	5:24	52-59.71N	170-39.89E	CTD cast #10 (1,156m)
18:42	6:42	-	-	Departure of Station No.5
22:00	10:00	-	-	Time adjustment -1hour (SMT=UTC-13hr)
23:06	12:06	52-00N	169-20E	Arrival at Station No.6
23:09	12:09	51-59.57N	169-20.43E	CTD cast #11 (4,664m)
24:00	13:00	-	-	Passing the International date line
				(Skipped 10/18 of SMT and SMT=UTC+11h)

10/19 2:48	15:48	-	-	Departure of Station No.6
11:27	10/19 00:27	50-59.80N	166-39.50E	Free Fall #02
16:12	5:12	51-00N	165-00E	Arrival at Station No.7 (K1)
16:19	5:19	50-59.48N	165-00.90E	CTD cast #12 (4,784m)
21:25	10:25	50-58.31N	165-01.30E	Multiple core sampling #02 (4,836m)
10/20 4:27	17:27	51-00.05N	164-59.34E	CTD cast #12 (200m)
6:29	19:29	51-00.81N	164-59.55E	Surface drifting float buoy deployment
6:34	19:34	51-01.09N	164-59.42E	FRRF #05
8:03	21:03	51-01.91N	165-00.34E	CTD cast #14 (300m)
8:44	21:44	51-01.86N	165-01.01E	FRRF #06
9:08	22:08	51-01.75N	165-01.92E	LISST #02
10:26	23:26	51-01.48N	165-02.68E	NORPAC net #02 (61m, 158m, 58m)
11:10	10/20 0:10	51-01.13N	165-03.83E	Free Fall #03
11:35	0:35	51-01.12N	165-04.81E	FRRF #07
13:05	2:05	50-59.07N	165-03.98E	CTD cast #15 (4,784m)
16:38	5:38	50-58.75N	165-03.33E	FRRF #08
17:56	6:56	50-58.79N	165-03.57E	NORPAC net #03 (150m, 50m, 50m)
18:31	7:31	50-59.17N	165-03.74E	FRRF #09
19:00	8:00	50-59.42N	165-04.37E	CTD cast #16 (3,000m)
10/21 6:58	19:58	51-03.59N	165-17.24E	Surface drifting float buoy recovery
8:00	21:00	51-03.10N	165-17.87E	LVP cast #03 (200m, 1 hour)
9:31	22:31	51-02.91N	165-17.37E	CTD cast #17 (200m)
10:18	23:18	51-03.01N	165-17.87E	IONESS #02 (400m)
12:49	10/21 1:49	50-59.45N	165-13.41E	ARGO float deployment #05
14:30	3:30	51-00.15N	165-01.25E	LVP cast #03 (200m, 5 hour)
19:48	8:48	-	-	Departure of Station No.7 (K1)
10/22 1:30	14:30	50-00N	163-45E	Arrival at Station No.8

1:36	14:36	50-00.51N	163-45.86E	CTD cast #18 (5,850m)
5:48	18:48	-	-	Departure of Station No.8
11:12 10/22 0:12		49-00N	162-30E	Arrival at Station No.9
11:15	0:15	48-59.11N	162-29.39E	CTD cast #19 (5,587m)
15:18	4:18	-	-	Departure of Station No.9
20:54	9:54	48-00N	161-15E	Arrival at Station No.10
20:55	9:55	47-59.12N	161-14.61E	CTD cast #20 (5,356m)
10/23 00:42	13:42	-	-	Departure of Station No.10
22:30	11:30	47-00N	160-00E	Arrival at Station No.11 (K2)
10/24 9:03	22:03	46-59.31N	159-58.81E	CTD cast #21 (5,192m)
13:47 1024 2:47		46-58.10N	159-55.90E	NORPAC net #04 (150m, 52m, 50m)
15:15	4:15	46-59.52N	159-59.66E	CTD cast #22 (5,188m)
19:33	8:33	46-95.85N	160-00.22E	CTD cast #23 (1,000m)
20:32	9:32	46-59.60N	160-00.16E	NORPAC net #05 (160m, 53m, 51m)
10/25 11:24 10/25 0:24		47-03.12N	159-58.39E	BGC mooring recovery (on deck)
11:49	0:49	47-02.06N	159-59.54E	Free Fall #02
13:00	2:00	47-00.81N	159-59.74E	CTD cast #24 (300m)
13:46	2:46	47-01.08N	160-00.84E	LISST #03
19:28	8:28	47-00.53N	159-59.66E	IONESS #03 (400m)
10/26 16:02 10/26 5:02		46-59.94N	160-00.23E	CTD cast #25 (200m)
17:27	6:27	47-00.41N	160-01.65E	CTD cast #26 (5,000m)
20:29	9:29	47-00.76N	160-02.30E	NORPAC net #06 (152m, 53m, 53m)
10/27 4:57	17:57	47-00.09N	160-00.25E	FRRF #10
5:24	18:24	47-00.23N	150-00.75E	CTD cast #27 (1,000m)
6:58	19:58	47-00.27N	160-01.04E	FRRF #11

7:58	20:58	46-59.99N	159-59.97E	CTD cast #28 (200m)
8:57	21:57	47-00.27N	159-59.86E	FRRF #12
10:09	23:09	46-59.89N	159-59.73E	Surface drifting float buoy deployment
10:44	23:44	46-58.94N	160-00.64E	Free Fall #05
11:04 10/27	0:04	46-58.91N	160-00.64E	FRRF #13
11:53	0:53	46-59.09N	160-01.21E	IONESS #04 (400m)
14:20	3:20	46-59.17N	160-06.56E	FRRF #14
15:45	4:45	46-59.98N	160-05.83E	LVP cast #04 (200m, 1 hour)
17:20	6:20	47-00.86N	160-04.68E	FRRF #15
18:02	7:02	47-01.46N	160-05.43E	Releaser response check (200m)
20:45	9:45	47-12.16N	160-08.31E	LVP cast #05 (1,000m, 4.5 hour)
10/28 7:58	20:58	46-59.86N	160-01.00E	CTD cast #29 (900m)
9:59	22:59	47-02.10N	160-01.67E	Surface drifting float buoy recovery (on deck)
11:07 10/28	0:07	47-02.72N	160-02.59E	IONESS #05 (1,000m)
14:25	3:25	46-59.93E	159-56.03E	CTD cast #29 (200m)
16:30	5:30	46-59.61N	160-00.61E	LVP cast #05 (200m, 5 hour)
10/29 6:55	19:55	47-07.42N	160-02.19E	Bucket surface water sampling #01 (60lit.)
8:05	21:05	47-07.00N	159-54.96E	BGC mooring deployment
-	-	47-00.36N	159-58.16E	BGC mooring Fixed position
13:55 10/29	2:55	46-59.64N	159-58.04E	NORPAC net #07 (151m, 50m, 50m)
16:38	5:38	46-59.43N	159-57.36E	Multiple core sampling #03 (5,210m)
20:26	9:26	47-02.27N	160-00.63E	IONESS #06 (1,000m)
10/30 00:06	13:06	-	-	Departure of Station No.11 (K2)
07:06	20:06	46-00N	158-20E	Arrival of Station No.12
7:08	20:08	45-59.79N	158-20.15E	CTD cast #31 (4,869m)
10:45	23:45	45-58.89N	158-20.01E	ARGO float deployment #06
10:48	23:48	-	-	Departure of Station No.12

17:36	10/30 6:36	45-00N	156-40E	Arrival of Station No.13
17:40	6:40	44-59.34N	156-40.09E	CTD cast #32 (4,898m)
21:06	10:06	-	-	Departure of Station No.13
10/31 8:48	21:48	44-00N	155-00E	Arrival of Station No.14 (KNOT)
8:59	21:59	44-00.18N	155-00/47E	Free Fall #06
9:20	22:20	43-59.99N	154-59.96E	Bucket surface water sampling #2 (100lt)
9:23	22:23	44-00.02N	154-59.89E	FRRF #15
9:47	22:47	44-00.12N	154-59.66E	CTD cast #33 (200m)
10:27	23:27	44-00.36N	154-59.30E	NORPAC net #08 (332m, 160m, 52m, 50m)
11:28	10/31 0:28	44-00.84N	154-58.87E	Free Fall #067
11:46	0:46	44-01.30N	154-59.01E	FRRF #16
12:11	1:11	44-01.33N	154-59.01E	CTD cast #34 (300m)
12:55	1:55	44-01.99N	154-59.27E	LISST #04
14:12	3:12	44-02.34N	154-59.77E	FRRF #17
14:38	3:38	44-02.32N	154-59.99E	CTD cast #35 (5,317m)
21:26	10:26	44-00.29N	155-00.23E	FRRF #18
21:52	10:53	44-00.11N	155-00.51E	NORPAC net #09 (332m, 183m, 51m, 55m)
22:54	11:54	-	-	Departure of Station No.14 (KNOT)
11/1 22:00	11/1 11:00	-	-	Time adjustment -1hour (SMT=UTC+10hr)
11/2 22:00	11/2 12:00	-	-	Time adjustment -1hour (SMT=UTC+9hr)
11/3 6:12	21:12	41-07N	142-08E	Arrival of Station No.15 (SK)
6:15	21:15	41-07.20N	142-08.13E	CTD cast #36 (1,000m)
7:56	22:56	41-06.96N	142-08.00E	Multiple core sampling #04 (1,133m)
9:08	11/3 0:08	41-06.96N	142-08.00E	CTD cast #37 (300m)
10:12	1:12	-	-	Departure of Station No.15
11/4 6:03	21:03	37-57.86N	143-57.05E	Dynacon CTD cable free fall (6,000m)

11/5 8:09	11/4 23:09	37-58.74N	143-23.61E	No. 11 Winch cable free fall (1,700m)
10:00	11/5 2:00	37-59N	143-24E	Calibration for magnetometer #02
11/6 15:30	11/6 6:30	-	-	Surface sea water sampling pump stop
11/7 9:00	11/7 0:00	??	??	Arrival of Onahama

1.3 Cruise Participants

	Name	Affiliation	Appointment	Tel
1	Makio HONDA（Principal Investigator）	Mutsu Institute for Oceanography (MIO) Institute of Observational Research for Global Change (IORGC) Japan Agency for Marine-Earth Science and Technology (JAMSTEC)	Sub Leader	0175-45-1071
2	Minoru KITAMURA（Deputy PI）	Extremobiosphere Research Center (XBR) JAMSTEC	Researcher	046-867-9527
3	Kazuhiko MATSUMOTO	MIO, IORGC JAMSTEC	Researcher	0175-45-1071
4	Hajime KAWAKAMI	MIO, IORGC JAMSTEC	Researcher	Same as above
5	Masahide WAKITA	Same as above	Researcher	Same as above
6	Tetsuichi FIJIKI	MIO, JAMSTEC	Researcher	Same as above
7	Sanae CHIBA	Frontier Research Center for Global Change (FRCGC) JAMSTEC	Senior scientist	045-778-5604
8	Katsunori YOSHIDA	Safety and Environment Management Office, JAMSTEC	Engineer	046-867-9104
9	Noriyuki OHYA	Nagoya University	Graduated student	052-789-5134
10	Koji HAMASAKI	Tokyo University	Associate professor	03-5351-6337
11	Hideki FUKUDA	Same as above	Assistant professor	Same as above
12	Ayako OKAMOTO	Same as above	Same as above	Same as above
13	Taichi YOKOKAWA	Netherlands Oceanographic Institution Tokyo University	Post doctor	Same as above
14	Fumihiro YAMAZAKI	Chiba university	Graduate student	043-290-3311
15	Yukiko KUROKI	Tsukuba University	Graduate student	029-850-2042
16	Chie SATO	Same as above	Same as above	Same as above
17	Shiro YOSHIDA	Same as above	Undergraduate student	Same as above
18	Fuyuki SHIBATA（Principal Marine Tech.）	Marine Works Japan Inc. (MWJ)	Marine Technician	045-787-0041
19	Hiroshi MATSUNAGA	Same as above	Same as above	Same as above
20	Masanori ENOKI	Same as above	Same as above	Same as above
21	Masaki TAGUCHI	Same as above	Same as above	Same as above
22	Ai YASUDA	Same as above	Same as above	Same as above
23	Tatsuya TANAKA	Same as above	Same as above	Same as above
24	Katsunori SAGISHIMA	Same as above	Same as above	Same as above
25	Tomoyuki TAKAMORI	Same as above	Same as above	Same as above
26	Misato KUWAHARA	Same as above	Same as above	Same as above
27	Yasuhiro ARII	Same as above	Same as above	Same as above
28	Hiroki USHIROMURA	Same as above	Same as above	Same as above
29	Ayaka HATSUYAMA	Same as above	Same as above	Same as above
30	Miyo IKEDA	Same as above	Same as above	Same as above
31	Yoshiko ISHIKAWA	Same as above	Same as above	Same as above

32	Hayato MATSUSHITA	Same as above	Same as above	Same as above
33	Shoko TATAMISASHI	Same as above	Same as above	Same as above
34	Tomonori WATAI	Same as above	Same as above	Same as above
35	Yuichi SONOYAMA	Same as above	Same as above	Same as above
36	Ken-ichiro SATO	Same as above	Same as above	Same as above
37	Yusuke SATO	Same as above	Same as above	Same as above
38	Kento FUKABORI	Same as above	Same as above	Same as above
39	Hiroyuki HAYASHI	Same as above	Same as above	Same as above
40	Wataru TOKUNAGA (Principal Marine Tech.)	Global Ocean Development Inc. (GODI)	Same as above	045-849-6630
41	Kazuho YOSHIDA	Same as above	Same as above	Same as above

2 General observation

2.1 Meteorological observations

2.1.1 Surface Meteorological Observation

Makio HONDA (JAMSTEC)
Kunio YONEYAMA (JAMSTEC) Principal Investigator / Not on-board
Wataru TOKUNAGA (Global Ocean Development Inc., GODI)
Kazuho YOSHIDA (GODI)

1) Objectives

Surface meteorological parameters are observed as a basic dataset of the meteorology. These parameters bring us the information about the temporal variation of the meteorological condition surrounding the ship.

(2) Methods

Surface meteorological parameters were observed throughout the MR08-05 cruise. During this cruise, we used two systems for the observation.

    i. MIRAI Surface Meteorological observation (SMET) system

    ii. Shipboard Oceanographic and Atmospheric Radiation (SOAR) system

    i. MIRAI Surface Meteorological observation (SMET) system

Instruments of SMET system are listed in Table.2.1.1-1 and measured parameters are listed in Table.2.1.1-2. Data were collected and processed by KOAC-7800 weather data processor made by Koshin-Denki, Japan. The data set consists of 6-second averaged data.

    ii. Shipboard Oceanographic and Atmospheric Radiation (SOAR) system

SOAR system designed by BNL (Brookhaven National Laboratory, USA) consists of major three parts.

a) Portable Radiation Package (PRP) designed by BNL – short and long wave downward radiation.

b) Zeno Meteorological (Zeno/Met) system designed by BNL – wind, air temperature, relative humidity, pressure, and rainfall measurement.

c) Scientific Computer System (SCS) developed by NOAA (National Oceanic and Atmospheric Administration, USA) – centralized data acquisition and logging of all data sets.

SCS recorded PRP data every 6 seconds, while Zeno/Met data every 10 seconds. Instruments and their locations are listed in Table.2.1.1-3 and measured parameters are listed in Table.2.1.1-4.

We checked the following sensors, before and after the cruise for the quality control as post processing.

    i. Young Rain gauge (SMET and SOAR)

Inspect of the linearity of output value from the rain gauge sensor to change input value by adding fixed quantity of test water.

    ii. Barometer (SMET and SOAR)

Comparison with the portable barometer value, PTB220CASE, VAISALA.
iii. Thermometer (air temperature and relative humidity) (SMET and SOAR)
Comparison with the portable thermometer value, HMP41/45, VAISALA.

(3) Preliminary results

Figures 2.1.1 shows the time series of the following parameters;

Wind (SOAR)
Air temperature (SOAR)
Relative humidity (SOAR)
Precipitation (SOAR, Capacitive rain gauge)
Short/long wave radiation (SOAR)
Pressure (SMET)
Sea surface temperature (EPCS)
Significant wave height (SMET)

(4) Data archives

These meteorological data will be submitted to the Marine-Earth Data and Information Department (MEDID) of JAMSTEC just after the cruise. Corrected data sets will be available from K. Yoneyama of JAMSTEC.

(5) Remarks

i. SST (Sea Surface Temperature) data were available in the following periods.
18:54UTC, 11 Oct. - 6:30UTC, 6 Nov.
ii. Smet ORG cleaning
4:42UTC, 17 Oct.
0:36UTC, 31 Oct.

Table.2.1.1-1 Instruments and installations of MIRAI Surface Meteorological observation system

Sensors	Type	Manufacturer	Location (altitude from surface)
Anemometer	KE-500	Koshin Denki, Japan	foremast (24 m)
Tair/RH	HMP45A	Vaisala, Finland	
with 43408 Gill aspirated radiation shield R.M. Young, USA			compass deck (21 m)
			starboard side and port side
Thermometer: SST	RFN1-0	Koshin Denki, Japan	4th deck (-1m, inlet -5m)
Barometer	AP370	Koshin Denki, Japan	captain deck (13 m)
			weather observation room
Rain gauge	50202	R. M. Young, USA	compass deck (19 m)
Optical rain gauge	ORG-815DR	Osi, USA	compass deck (19 m)
Radiometer (short wave)	MS-801	Eiko Seiki, Japan	radar mast (28 m)
Radiometer (long wave)	MS-202	Eiko Seiki, Japan	radar mast (28 m)
Wave height meter	MW-2	Tsurumi-seiki, Japan	bow (10 m)

Table.2.1.1-2 Parameters of MIRAI Surface Meteorological observation system

	Parameter	Units	Remarks
1	Latitude	degree	
2	Longitude	degree	
3	Ship's speed	knot	Mirai log, DS-30 Furuno
4	Ship's heading	degree	Mirai gyro, TG-6000, Tokimec
5	Relative wind speed	m/s	6sec./10min. averaged
6	Relative wind direction	degree	6sec./10min. averaged
7	True wind speed	m/s	6sec./10min. averaged
8	True wind direction	degree	6sec./10min. averaged
9	Barometric pressure	hPa	adjusted to sea surface level
			6sec. averaged
10	Air temperature (starboard side)	degC	6sec. averaged
11	Air temperature (port side)	degC	6sec. averaged
12	Dewpoint temperature (starboard side)	degC	6sec. averaged
13	Dewpoint temperature (port side)	degC	6sec. averaged
14	Relative humidity (starboard side)	%	6sec. averaged
15	Relative humidity (port side)	%	6sec. averaged
16	Sea surface temperature	degC	6sec. averaged
17	Rain rate (optical rain gauge)	mm/hr	hourly accumulation
18	Rain rate (capacitive rain gauge)	mm/hr	hourly accumulation
19	Down welling shortwave radiation	W/m^2	6sec. averaged
20	Down welling infra-red radiation	W/m^2	6sec. averaged
21	Significant wave height (bow)	m	hourly
22	Significant wave height (aft)	m	hourly
23	Significant wave period (bow)	second	hourly
24	Significant wave period (aft)	second	hourly

Table.2.1.1-3 Instrument and installation locations of SOAR system

Sensors(*Zeno/Met*)	Type	Manufacturer	Location (altitude from surface)
Anemometer	05106	R.M. Young, USA	foremast (25 m)
Tair/RH	HMP45A	Vaisala, Finland	
with 43408 Gill aspirated radiation shield		R.M. Young, USA	foremast (23 m)
Barometer	61202V	R.M. Young, USA	
with 61002 Gill pressure port	R.M. Young, USA		foremast (22 m)
Rain gauge	50202	R. M. Young, USA	foremast (24 m)
Optical rain gauge	ORG-815DA	Osi, USA	foremast (24 m)

Sensors (*PRP*)	Type	Manufacturer	Location (altitude from surface)
Radiometer (short wave)	PSP	Epply Labs, USA	foremast (24 m)
Radiometer (long wave)	PIR	Epply Labs, USA	foremast (24m)
Fast rotating shadowband radiometer		Yankee, USA	foremast (24 m)

Table.2.1.1-4 Parameters of SOAR system

	Parameter	Units	Remarks
1	Latitude	degree	
2	Longitude	degree	
3	SOG	knot	
4	COG	degree	
5	Relative wind speed	m/s	
6	Relative wind direction	degree	
7	Barometric pressure	hPa	
8	Air temperature	degC	
9	Relative humidity	%	
10	Rain rate (optical rain gauge)	mm/hr	
11	Precipitation (capacitive rain gauge)	mm	reset at 50 mm
12	Down welling shortwave radiation	W/m^2	
13	Down welling infra-red radiation	W/m^2	
14	Defuse irradiance	W/m^2	
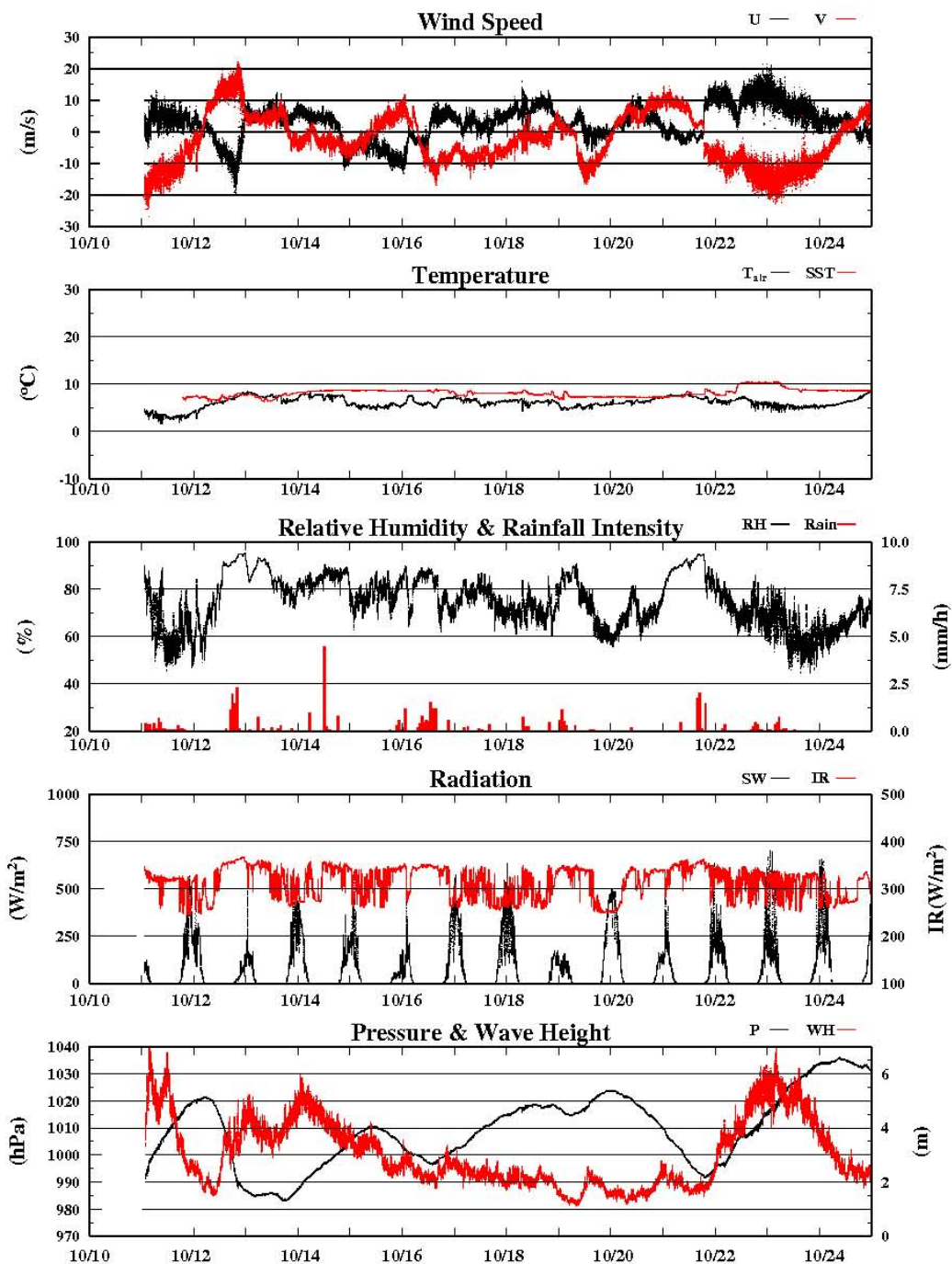
Fig.2.1.1-1 Time series of surface meteorological parameters during the MR08-05 cruise
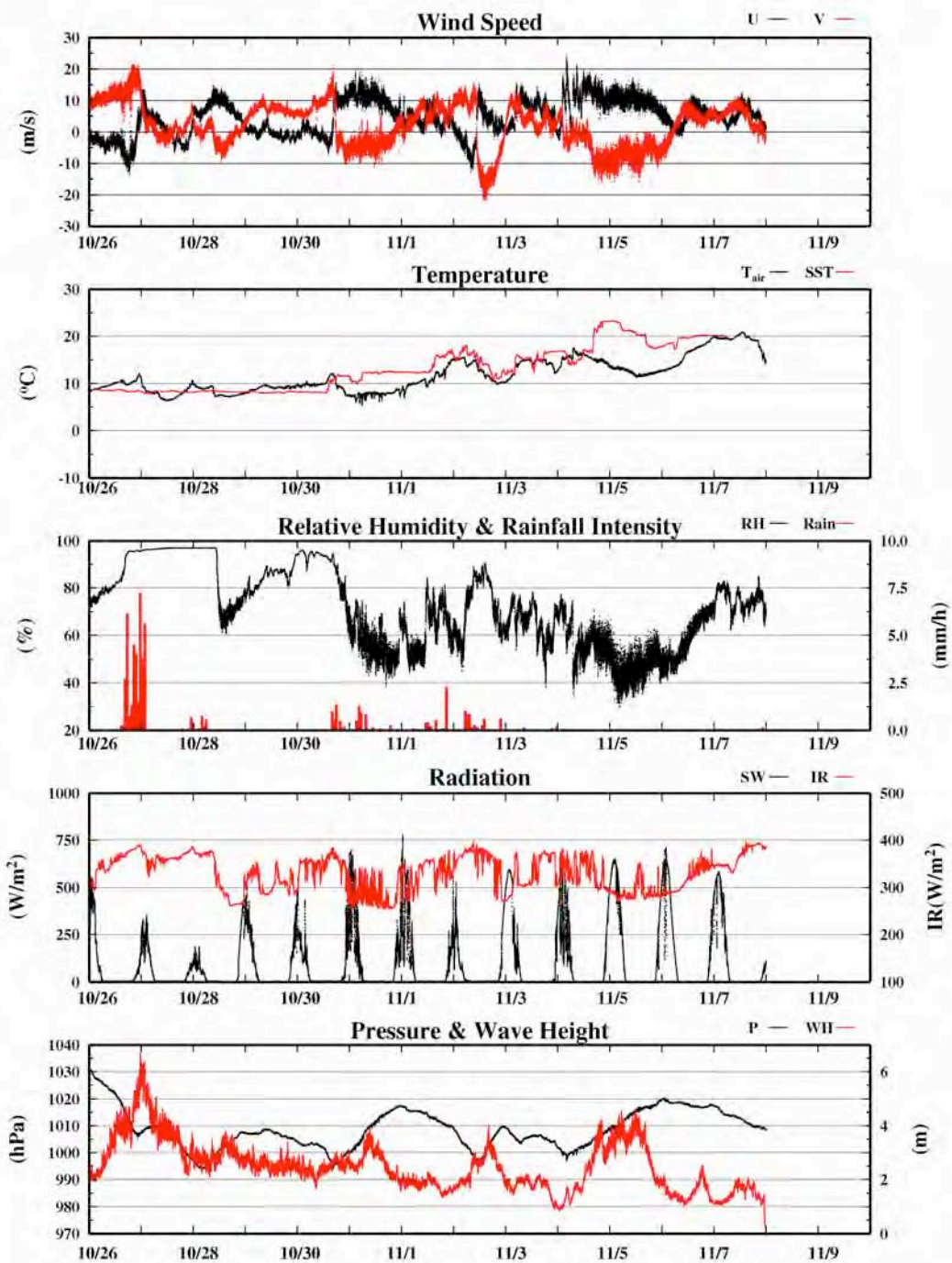
Fig.2.1.1-2 Time series of surface meteorological parameters during the MR08-05 cruise

2.1.2 Ceilometer Observation

Makio HONDA (JAMSTEC)
Kunio YONEYAMA (JAMSTEC) Principal Investigator / Not on-board
Wataru TOKUNAGA (Global Ocean Development Inc., GODI)
Kazuho YOSHIDA (GODI)

(1)   Objectives

The information of cloud base height and the liquid water amount around cloud base is important to understand the process on formation of the cloud. As one of the methods to measure them, the ceilometer observation was carried out.

(2)   Parameters

1.   Cloud base height [m].
2.   Backscatter profile, sensitivity and range normalized at 30 m resolution.
3.   Estimated cloud amount [oktas] and height [m]; Sky Condition Algorithm.

(3)   Methods

We measured cloud base height and backscatter profile using ceilometer (CT-25K, VAISALA, Finland) throughout the MR08-05 cruise from the departure of Dutch Harbor on 10 October 2008 to arrival of Onahama on 7 November 2008.

Major parameters for the measurement configuration are as follows;

Laser source:	Indium Gallium Arsenide (InGaAs) Diode
Transmitting wavelength:	905±5 mm at 25 degC
Transmitting average power:	8.9 mW
Repetition rate:	5.57 kHz
Detector:	Silicon avalanche photodiode (APD)
	Responsibility at 905 nm: 65 A/W
Measurement range:	0 ~ 7.5 km
Resolution:	50 ft in full range
Sampling rate:	60 sec
Sky Condition	0, 1, 3, 5, 7, 8 oktas (9: Vertical Visibility)
	(0: Sky Clear, 1:Few, 3:Scattered, 5-7: Broken, 8: Overcast)

On the archive dataset, cloud base height and backscatter profile are recorded with the resolution of 30 m (100 ft).

(4)   Preliminary results

Figure 2.1.2-1 shows the time series of the lowest, second and third cloud base height.

(5)   Data archives

The raw data obtained during this cruise will be submitted to the Marine-Earth Data and Information Department (MEDID) in JAMSTEC.

(6)   Remarks

1.   We did not collect data in the territorial waters of U.S.A in the following periods.
            14:10UTC 10 Oct. – 2:01UTC11 Oct.

2.   Window cleaning;
       4:42UTC, 17 Oct.
       0:31UTC, 31 Oct.
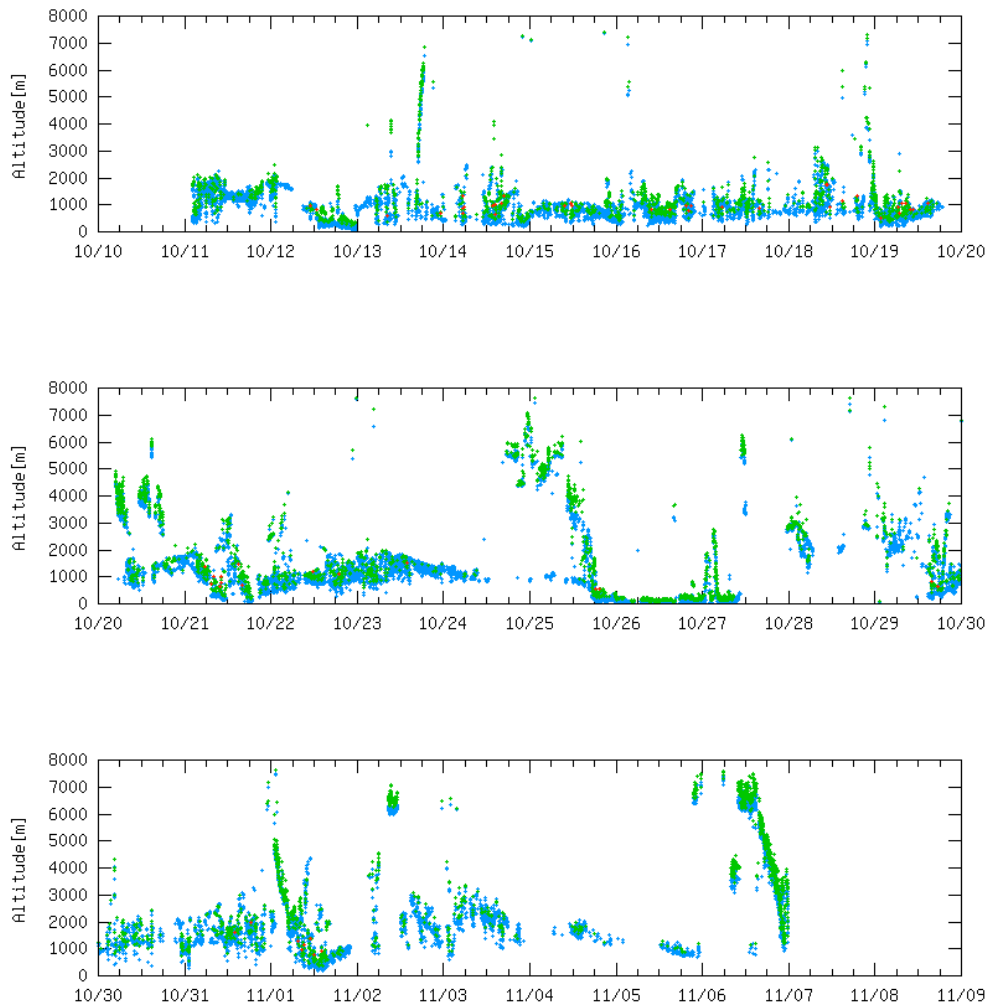
Fig.2.1.2-1   Lowest (blue), 2nd (green) and 3rd(red) cloud base height during the cruise.

2.1.3 Lidar observations of clouds and aerosols

Nobuo SUGIMOTO
(National Institute for Environmental Studies, NIES, not on board),
Ichiro MATSUI (NIES, not on board)
Atsushi SHIMIZU (NIES, not on board)
Tomoaki NISHIZAWA (NIES, not on board)
(lidar operation was supported by Chiba University)

(1) Objectives

Objectives of the observations in this cruise is to study distribution and optical characteristics of ice/water clouds and marine aerosols using a two-wavelength lidar.

(2) Measured parameters
- Vertical profiles of backscattering coefficient at 532 nm
- Vertical profiles of backscattering coefficient at 1064 nm
- Depolarization ratio at 532 nm

(3) Method

Vertical profiles of aerosols and clouds were measured with a two-wavelength lidar. The lidar employs a Nd:YAG laser as a light source which generates the fundamental output at 1064 nm and the second harmonic at 532 nm. Transmitted laser energy is typically 30 mJ per pulse at both of 1064 and 532 nm. The pulse repetition rate is 10 Hz. The receiver telescope has a diameter of 20 cm. The receiver has three detection channels to receive the lidar signals at 1064 nm and the parallel and perpendicular polarization components at 532 nm. An analog-mode avalanche photo diode (APD) is used as a detector for 1064 nm, and photomultiplier tubes (PMTs) are used for 532 nm. The detected signals are recorded with a transient recorder and stored on a hard disk with a computer. The lidar system was installed in a container which has a glass window on the roof, and the lidar was operated continuously regardless of weather. Every 10 minutes vertical profiles of four channels (532 parallel, 532 perpendicular, 1064, 532 near range) are recorded.

(4) Results

Figure 1 shows vertical distribution of clouds and aerosols detected by the lidar. Top panel indicates the intensity of backscatter at visible wavelength. Cloud base is indicated red color in the panel, and blue or green colors correspond to aerosols. Light blue color indicate weak scattering from molecules. Throughout the cruise cloud appeared around 1 – 2 km height, and higher altitude were obscured by these clouds. However we cloud observe some high clouds on Oct 27-28, and it showed greater depolarization ratio (middle panel) which means the particles have irregular (non spherical) shape. And also on Oct 24 and 05 Nov depolarization ratio in the aeorosl layers around 2 – 4 km was higher than usual. It suggests that a long-range transported dust or smoke plumes arrived in the oceanic region.
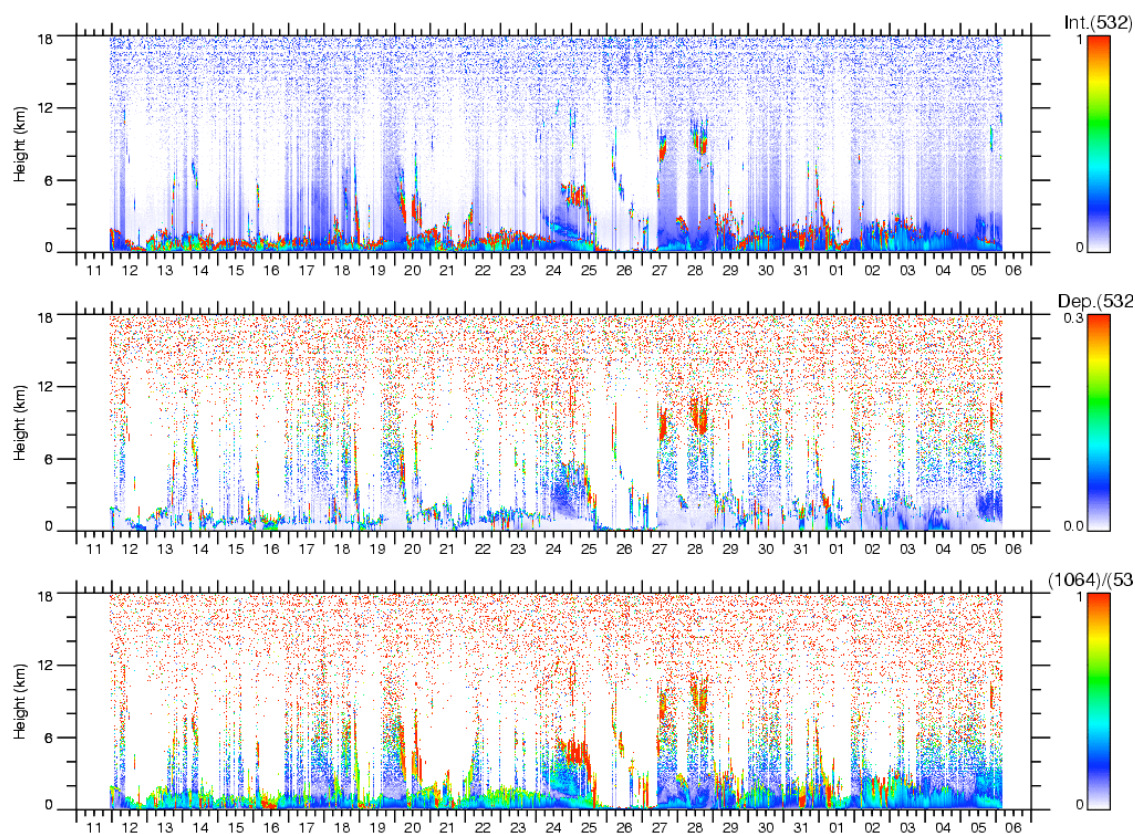
Figure 1: Time-height sections of (top) backscatter intensity at 532 nm, (middle) depolarization ratio at 532 nm, and (bottom) ratio of backscatter intensities at 1064nm and 532 nm, during Oct 11 and Nov 6, 2008.

(5) Data archive
- raw data
    lidar signal at 532 nm
    lidar signal at 1064 nm
    depolarization ratio at 532 nm
    temporal resolution 10min/ vertical resolution 6 m
    data period (UTC):   Oct 11 – Nov 6, 2008
- processed data (plan)
    cloud base height, apparent cloud top height
    phase of clouds (ice/water)
    cloud fraction
    boundary layer height (aerosol layer upper boundary height)
    backscatter coefficient of aerosols
    particle depolarization ratio of aerosols

(6) Data policy and Citation
        Contact NIES lidar team (nsugimot/i-matsui/shimizua/nisizawa@nies.go.jp) to utilize lidar data for productive use.

2.1.4 Rain Sampling for Stable Isotope Measurement

Naoyuki KURITA (JAMSTEC) Principal Investigator
Kimpei ICHIYANGI (JAMSTEC)
Hironori FUDEYASU (Hawaii Univ.)

(1) Objective

Stable isotopes in water (HDO and $H_2^{18}O$) are powerful tool to study for hydrological cycle over the ocean. In order to make a global isotope map over the Ocean region that number of isotope data is limited, sampling of rainwater was performed for stable isotope analyses throughout the MR08-05 cruise from Dutch Harbor on October 11, 2008 to Japan on November 07, 2008.

(2) Method

Rainwater samples gathered in rain collector were collected just after precipitation events have ended. The collected sample was then transferred into glass bottle (6ml) immediately after the measurement of precipitation amount.

(3) Results

Sampling of rain water for isotope analysis is summarized in Table 2.1.4-1 (18 samples). Described rainfall amount is calculated from the collected amount of precipitation.

(4) Data archive

Isotopes (HDO, $H_2^{18}O$) analysis will be done at IORGC/JAMSTEC, and then analyzed isotopes data will be submitted to JAMSTEC Data Management Office.

Table 2.1.4-1 Summary of precipitation sampling for isotope analysis.

	Start				End				Rain (mm)
	Date	Time (UT)	Lon	Lat	Date	Time (UT)	Lon	Lat	
R-1	11-Oct	02:00	167-14W	54-16N	12-Oct	19:07	179-38W	56-31N	3.5
R-2	12-Oct	19:14	179-41W	56-32N	13-Oct	1:18	179-58E	57-13N	1.4
R-3	13-Oct	01:18	179-58E	57-13N	13-Oct	16:11	179-22E	57-42N	1.5
R-4	13-Oct	16:20	179-20E	57-42N	14-Oct	16:30	176-00E	57-00N	4.6
R-5	14-Oct	16:36	176-00E	57-00N	15-Oct	23:23	176-01E	56-59N	0.3
R-6	15-Oct	23:25	176-01E	56-59N	16-Oct	3:05	176-01E	56-59N	0.9
R-7	16-Oct	03:09	176-01E	56-59N	16-Oct	19:53	174-38E	55-59N	7.7
R-8	16-Oct	19:59	174-37E	55-58N	17-Oct	9:50	172-00E	54-00N	0.3

R-9	17-Oct	09:50	172-00E	54-00N	18-Oct	12:57	169-20E	52-00N	0.3
R-10	18-Oct	12:57	169-20E	52-00N	19-Oct	5:17	165-00E	51-00N	2.0
R-11	19-Oct	05:20	165-00E	51-00N	19-Oct	21:18	165-00E	51-02N	0.2
R-12	19-Oct	21:23	165-00E	51-02N	21-Oct	20:16	163-27E	49-46N	4.6
R-13	21-Oct	21:20	163-26E	49-45N	26-Oct	0:30	160-00E	46-59N	4.3
R-14	26-Oct	00:32	160-00E	46-59N	27-Oct	6:40	160-05E	47-01N	1.9
R-15	27-Oct	06:40	160-05E	47-01N	29-Oct	22:20	158-20E	46-00N	0.2
R-16	29-Oct	22:14	158-20E	46-00N	31-Oct	22:24	153-16E	42-09N	2.0
R-17	31-Oct	22:28	153-15E	42-08N	1-Nov	11:00	150-16E	40-38N	0.2
R-18	1-Nov	11:00	150-16E	40-38N	1-Nov	23:20	146-58E	40-45N	0.1

2.1.5 Global Distribution of Clouds above Oceans

Toshiaki TAKANO (Chiba University): Principal Investigator
Hideji ABE (Chiba University) : Student, Doctor Course 2
Jun YAMAGUCHI (Chiba University) : Student, Doctor Course 2
Fumihiro YAMAZAKI (Chiba University) : Student, Master Course 2
Hajime OKAMOTO (Tohoku University)
Nobuo SUGIMOTO (National Institute for Environmental Studies)

(1) Objective

Main objective for this plan is to detect vertical structure of cloud and precipitation in the observed regions and obtain global distribution and characteristics of cloud above oceans. Combinational use of the millimeter wave radar and lidar is recognized to be a powerful tool to study vertical distribution of cloud microphysics, i.e., particle size and liquid/ice water content (LWC/IWC).

The infrared radiometer (hereafter IR) is used to derive the temperature of the cloud base and emissivity of the thin ice clouds. Main objectives are to use study clouds and climate system in tropics by the combination of IR with active sensors such as lidar and 95GHz cloud radar. From these integrated approach, it is expected to extend our knowledge of clouds and climate system. Special emphasis is made to retrieve cloud microphysics in upper part of clouds, including sub-visual clouds that are recognized to be a key component for the exchange of water amount between troposphere and stratosphere. Since June 2006, spaceborn radar and lidar systems, CloudSat and CALIPSO are providing vertical and global distribution of clouds and aerosols. One important aim is to observe the same clouds and aerosols by the observational systems on R/V Mirai. Combination of space-based and ship based observations should provide the unique opportunity to study the complete system of theses clouds and aerosols in relation to its environments. We also added the new function for the protection of precipitation.

(2) Method

Basic output from millimeter wave radar is cloud occurrence, radar reflectivity factor and cloud microphysics. In order to derive reliable cloud amount and cloud occurrence, we need to have radar and lidar for the same record. Radar / lidar retrieval algorithm has been developed in Tohoku University. The algorithm is applied to water cloud in low level and also cirrus cloud in high altitude. In order to analyze the radar data, it is first necessary to calibrate the signal to convert the received power to radar reflectivity factor, which is proportional to backscattering coefficient in the frequency of interest. Then we can interpolate radar and lidar data to match the same time and vertical resolution. Finally we can apply radar/lidar algorithm to infer cloud microphysics.

IR instrument directly provides broadband infrared temperature (9.6-10.5μm).

General specifications of IR system (KT 19II, HEITRONICS)

Temperature range	-100 to 100°C
Accuracy	0.5^{o}C
Mode	24hours
Time resolution	1 min.
Field of view	Less than 1° (will be estimated later)
Spectral region	9.6-10.5μm

This is converted to broadband radiance around the wavelength region. This is further combined with the lidar or radar for the retrieval of cloud microphysics such as optical thickness at visible wavelength, effective particle size. The applicability of the retrieval technique of the synergetic use of radar/IR or lidar/IR is so far limited to ice clouds. The microphysics of clouds from these techniques will be compared with other retrieval technique such as radar/lidar one or radar with multi-parameter.

When the rain is observed by the rain sensor installed in the IR observing system, the radiometer is automatically rotated and stops at the downward position in order to prevent from the rain drops attached on the lens surface.

(3) Results
a)   95GHz Cloud Profiling Radar
(operated by T.Takano et al., Chiba Univ.)

The time height cross-section of radar reflectivity factor obtained in Oct 26. 2008, during MR-08-05 cruise. Vertical extent is 20km. It is seen that there is a cloud layer around 8km in height which is getting lower and gives rain layers below it.
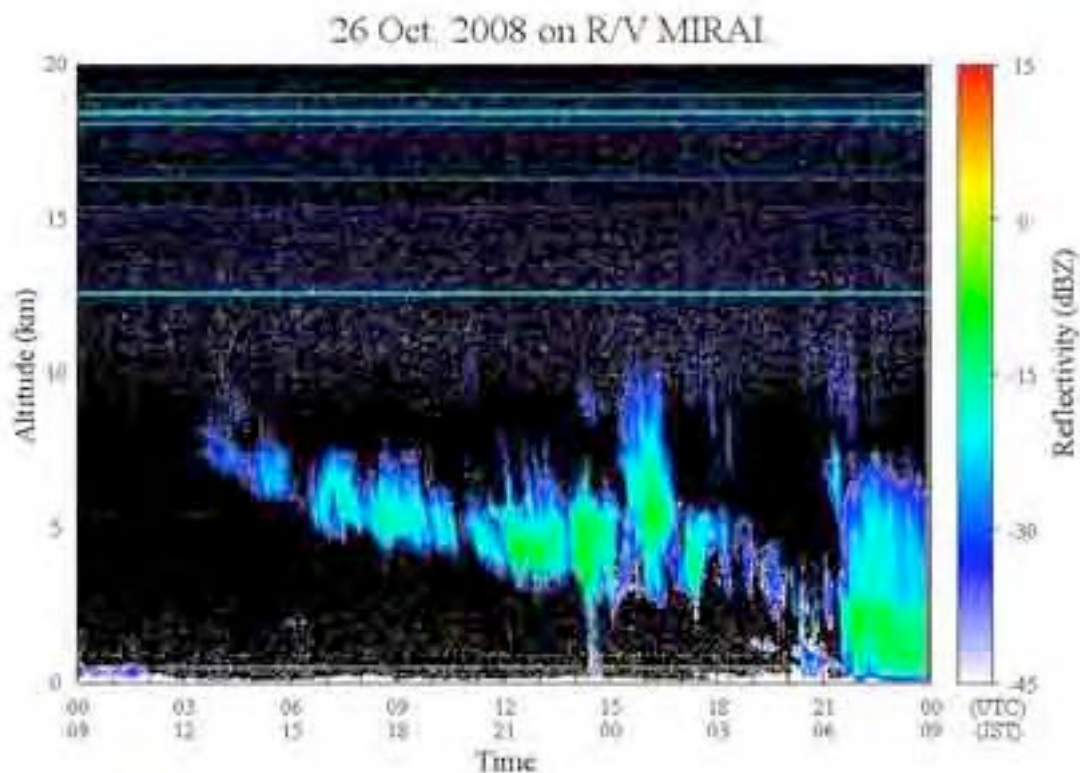
Fig 2.1.5.-1.   Time height cross section of radar reflectivity factor in dBZe
in Oct. 26, 2008 during MR08-05 cruise.

The data archive server is set inside Chiba University and the original data and the results of the analyses will be available from us.

The cloud radar was successfully operated for 24 hours during the cruise.

b) Infrared radiometer

(operated by H.Okamoto et al., Tohoku Univ.)

Fig. 2.1.5.-2. displays the temperature measured by IRT on October 26 , 2008.　The horizontal line denotes the hours (UTC) and vertical axis is the temperature. The location is 46.59^{o}N and 160.06^{o}E. The very low temperature of below -40°C corresponds to clear sky. One of the key feature of infrared temperature in the mid-latitude region is that there is relatively weak contribution of water vapor and the infrared temperature is determined by the emission due to clouds and also water vapor under cloudy conditions, though the effect of water vapor is much weaker than in the tropics regions.

The temperature between -40°C and -10°C actually in good correspondence to the occurrence of ice clouds detected by the radar and lidar such as close to just 3-5 UTC and after 6 UTC. Precipitation occurred after 21 UTC and IRT measurements were not conducted in such cases.
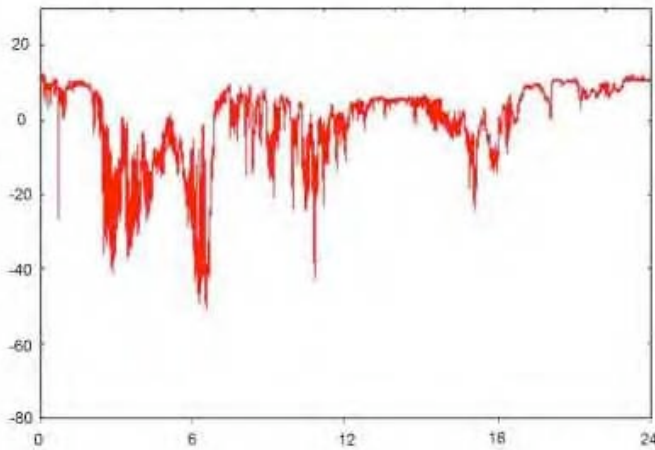
Fig 2.1.5.-2. Temperature measured by the IRT in Oct.26, 2008, during MR08-05 cruise.

The data archive server is set inside Tohoku University and the original data and the results of the analyses will be available from us.

Basically the IRT is operated for 24 hours. The automatic rain protection system works very fine.

c) Lidar　　　　　(operated by N.Sugimoto et al., NIES)

Fig. 2.1.5.-3. shows the data obtain with Lidar of NIES on October 26 , 2008, during MR08-05.　The horizontal line denotes the hours (UTC) and vertical axis is the height from the sea level

.
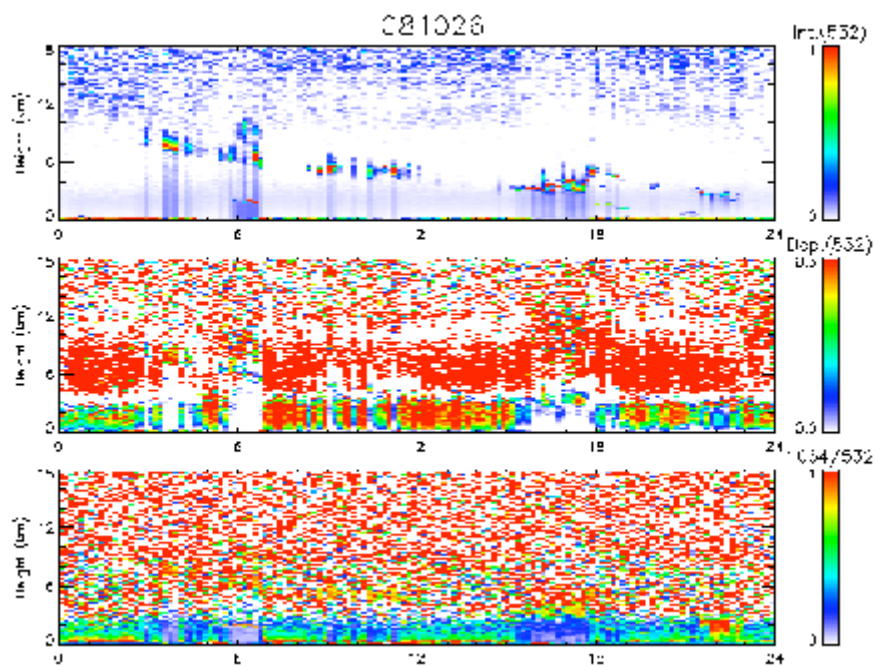
Fig 2.1.5.-3. Lidar data measured in Oct.26, 2008. during MR08-05 cruise.

The data archive server is set inside NIES and the original data and the results of the analyses will be available from us.

Lidar was successfully operated for 24 hours during the cruise.

2.1.6 Air-sea surface eddy flux measurement

Osamu TSUKAMOTO (Okayama University) Principal Investigator   * not on board
Fumiyoshi KONDO (Okayama University)   * not on board
Hiroshi ISHIDA (Kobe University)   * not on board
Wataru TOKUNAGA (Global Ocean Development Inc. (GODI))
Kazuho YOSHIDA (GODI)

(1) Objective

To better understand the air-sea interaction, accurate measurements of surface heat and fresh water budgets are necessary as well as momentum exchange through the sea surface. In addition, the evaluation of surface flux of carbon dioxide is also indispensable for the study of global warming. Sea surface turbulent fluxes of momentum, sensible heat, latent heat, and carbon dioxide were measured by using the eddy correlation method that is thought to be most accurate and free from assumptions. These surface heat flux data are combined with radiation fluxes and water temperature profiles to derive the surface energy budget.

(2) Instruments and Methods

The surface turbulent flux measurement system (Fig. 2.1.6-1) consists of turbulence instruments (Kaijo Co., Ltd.) and ship motion sensors (Kanto Aircraft Instrument Co., Ltd.). The turbulence sensors include a three-dimensional sonic anemometer-thermometer (Kaijo, DA-600) and an infrared hygrometer (LICOR, LI-7500). The sonic anemometer measures three-dimensional wind components relative to the ship. The ship motion sensors include a two-axis inclinometer (Applied Geomechanics, MD-900-T), a three-axis accelerometer (Applied Signal Inc., QA-700-020), and a three-axis rate gyro (Systron Donner, QRS-0050-100). LI7500 is a CO_2/H_2O turbulence sensor that measures turbulent signals of carbon dioxide and water vapor simultaneously. These signals are sampled at 10 Hz by a PC-based data logging system (Labview, National Instruments Co., Ltd.). By obtaining the ship speed and heading information through the Mirai network system it yields the absolute wind components relative to the ground. Combining wind data with the turbulence data, turbulent fluxes and statistics are calculated in a real-time basis. These data are also saved in digital files every 0.1 second for raw data and every 1 minute for statistic data.

(3) Observation log

The observation was carried out throughout this cruise.

(4) Data Policy and citation

All data are archived at Okayama University, and will be open to public after quality checks and corrections. Corrected data will be submitted to JAMSTEC Marine-Earth Data and Information Department.
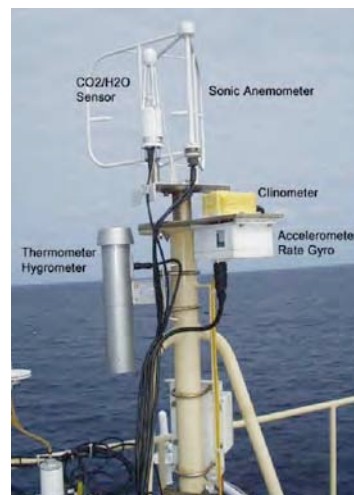
Fig. 2.1.6-1 Turbulent flux measurement system on the top deck of the foremast

2.1.7 Ocean Radon Flux across Air-Sea Interface

Noriyuki OYA (Nagoya Univ.)
Hiromi YAMAZAWA (Nagoya Univ.) not on board

(1) Objectives

The concentrations of ^{222}Rn in near-surface seawater and atmosphere were continuously observed in order to evaluate the ocean radon flux across the air-sea interface. Thirteen near-surface seawater samplings were carried out for the ^{226}Ra concentration measurements after the cruise. The radon flux was estimated from the measurements of radon concentrations, wind speed and sea surface temperature by using the model of Wanninkhof (1992) for gas transfer velocity.

(2) Instrument and Method

i. Instrument

Radon observation system consisted of two high sensitivity radon detectors, degasification units for radon gas dissolved in seawater, a radon-free air producing module and a radon data collection system. The method of radon detection is electrostatic collection of daughter nuclei of ^{222}Rn, and α-spectrometry using PIN photodiode. The volume of radon detector vessel is 70 liter. In order to keep the background at a very low level, the inside of the vessel is electro-polished. The background level of two radon detectors was measured during a period of a month before this cruise. The result of background run is 12.9(^{214}Po count/day) giving detection limit of 0.01(Bq/m^3). This radon detector was developed for continuous monitoring of low level radon concentration in the Super-Kamiokande experiment (Takeuchi et al 1999).

ii. Method

The sample atmospheric air was taken from the fore mast with air sampling platform at the height of 12.5m from sea level into the sea surface water monitoring laboratory, R/V MIRAI for radon concentration analysis. Sample of atmospheric air was directly introduced into other radon detector after an electronic-dehumidifier with the flow rate of 6 liter/min.

A radon free air producing module was used to produce radon-free air for degasification of radon from sea water. It consisted of charcoal(active carbon granular), copper fiber, a cooling device and a drying machine. Seawater was pumped up from sea surface at depth for 4.5m, which was successively flowed into the top of the degasification units with average flow rate of 2.0 liter/min and radon free air was supplied to the bottom of one with average flow rate 2.0 liter/min. Radon free air was supplied continuously into the degasification units and its exhaled air was then introduced into one of the radon detectors after electronic-dehumidifier with dew-point temperature 0.1(deg C).

Measured α-rays energy spectra from two radon detectors were processed to evaluate radon concentrations of atmospheric air and seawater by an analysis system installed in a note-PC. The analysis was conducted for every 10 minute interval.. Radon concentrations, flow rate, temperature, and dew-point of sample air, and flow rate and temperature of seawater were monitored continuously..

(3) Preliminary Results

The data presented in the following are preliminary ones. Therefore, their values may be revised due to reviews and refinement of the analysis.

i. Radon Concentration in Atmospheric Air

Hourly average of atmospheric radon concentration was measured from October-10 to November-7, 2008. Fig.1 shows atmospheric radon concentration in Cruise MR08-05. The concentration varied within the range from 1 to 10 Bq m^{-3} for the most of the observation period. The high concentration above a few Bq m^{-3} would be caused by advection of continental air. It is interesting to notice that these high concentration episodes were observed several times. These data will be utilized to analyze atmospheric transport of continental contaminants in the northeastern Pacific Ocean. .
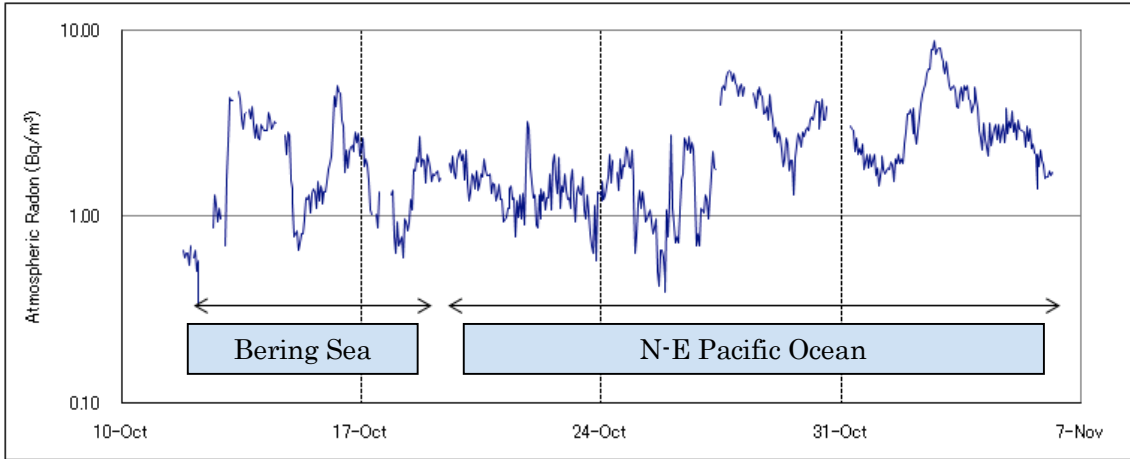
Fig.1 Atmospheric Radon Concentration in Cruise MR08-05 from October-10 to November-7, 2008.

ii. Radon Concentration in Seawater

Seawater radon measurements of RUN#1～RUN#10 were carried out from October-10 to November-7, 2008. During this period, data were obtained for 606 hours. The period was divided in to ten runs to maintain the radon trap rate of the radon-free air producing module   at a planned level and to keep a copper filter working properly. The seawater radon concentration Cw can be estimated by

$$Cw=C(1+\alpha)Fa/Fw \quad (1)$$

where C is the radon concentration in exhaled air from the degasification unit and measured by the high sensitivity radon detector, Fa and Fw are the flow rates of radon-free air and sample seawater, respectively. Coefficient α is the radon solubility depend on sample seawater temperature. Fig.2 shows the hourly average of seawater radon concentration in the cruise MR08-05. Table 1 shows RUN#, RUN time, navigation sea area,   in RUN#1～RUN#10, respectively.

The concentration varied from 0.5 to 2.0 Bq m^{-3}, with a rapid fluctuations superimposed on gentle variations. One of the possible cause of these variations is temporally changing wind speed. However, factors contributing to cause these variations should be analyzed carefully in the later analysis.
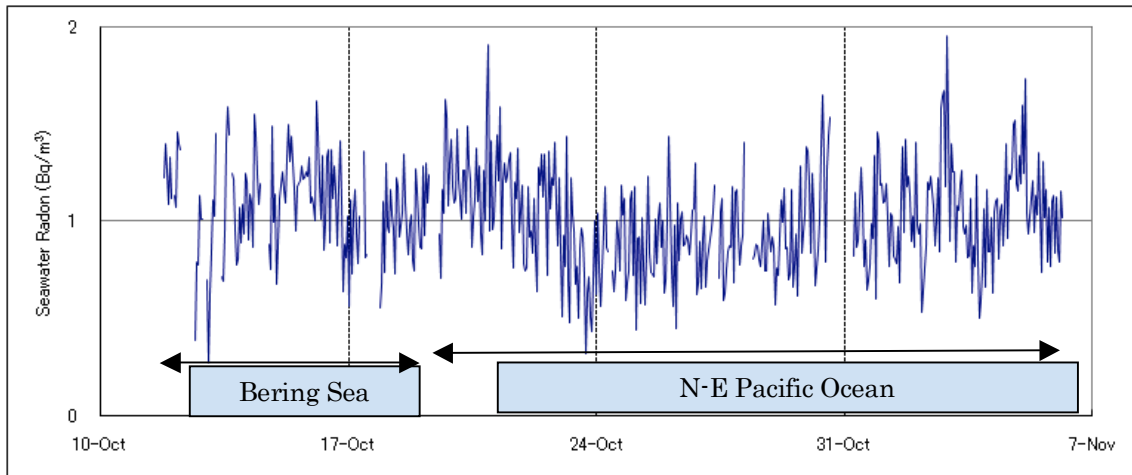
Fig.2 Seawater Radon Concentration in Cruise MR08-05 from October-10 to November-7, 2008.

Table 1 , RUN#0 to RUN#10 in Cruise MR08-05 from October-10 to November-7, 2008.

海水	run time		observation area			
			start		end	
No.	start	end	Lat	Lon	Lat	Lon
#1	2008/10/11 17:55	2008/10/12 1:05	54-59.91N	168-54.89W	55-20.81N	171-52.30W
#2	2008/10/12 1:36	2008/10/15 2:21	55-22.12N	172-05.78W	57-00.98N	175-58.91E
#3	2008/10/15 2:50	2008/10/18 3:02	57-01.18N	175-58.80E	53-26.12N	171-17.73E
#4	2008/10/18 3:23	2008/10/21 4:05	53-22.17N	171-11.82E	51-00.44N	165-02.41E
#5	2008/10/21 4:30	2008/10/24 4:08	51-00.55N	165-02.97E	46-59.47N	159-59.95E
#6	2008/10/24 4:29	2008/10/27 4:53	46-59.67N	160-00.07E	47-00.06N	160-05.62E
#7	2008/10/27 5:15	2008/10/30 5:14	47-00.32N	160-05.26E	45-11.66N	156-59.73E
#8	2008/10/30 6:00	2008/11/2 6:54	45-04.96N	156-48.28E	40-53.14N	145-18.99E
#9	2008/11/2 7:44	2008/11/5 6:50	40-54.06N	145-08.82E	37-48.49N	143-15.22E
#10	2008/11/5 7:47	2008/11/6 5:25	37-47.89N	143-14.23E	37-35.15N	142-50.79E

iii. Ocean Radon Flux Across Air-Sea Interface

One of the short-hand way of estimating ocean radon flux is the used of the model of Wanninkhoh(1992) for gas transfer velocity containing a quadratic dependence on wind speed. The flux of soluble radon gas across the air-sea interface can be expressed as

$$F = k(C_w - \alpha C_a) \qquad (2)$$

where k is the gas transfer velocity, Cw is seawater radon concentration and Ca is atmosphere radon concentration near the air-sea interface, and α is the Ostwald solubility coefficient. The k is a function of the interfacial turbulence, the kinematic viscosity of the seawater μ, and the diffusion coefficient of gas, D. The dependence of k on the last two terms is expressed as the Schmidt number Sc$= \mu$/D. k is proportional Sc$^{-0.5}$ for an interface with waves. For steady winds, relationship between gas transfer and wind speed is taken to be following form by Wanninkhoh,

$$k = 0.31 u^2 (Sc/660)^{-0.5} \qquad (3)$$

where 660 is the Schmidt number of CO_2 in seawater at $20°C$ and u is wind speed. In the Wanninkhoh paper, radon Schmidt number

$$Sc = A - Bt + Ct^2 - Dt^3 \qquad (4)$$

where A=3412.8, B=224.3, C=6.7954, D=0.083, and t is sea surface temperature (deg C). And radon solubility coefficient

$$\alpha = 9.12(273+t)/273(17+t) \qquad (5)$$

Ocean radon flux across the air-sea interface was calculated by using equations (2) to (5) with observation results of Ca, Cw, u, t .

Fig.3 shows the hourly ocean radon flux in RUN#1～RUN#10. Although the values should be checked for the quality of raw data especially ones around November 6, it is interesting to notice that the radon flux was not unidirectional. The values were within the range from -0.15 to 0.15 mBq m^{-2} s^{-1} for most of the period. The negative flux (downward) would be caused by relatively high atmospheric concentration of radon transported from near-by continents. Long-range radon transport simulations will be carried out to analyze the features in these data.
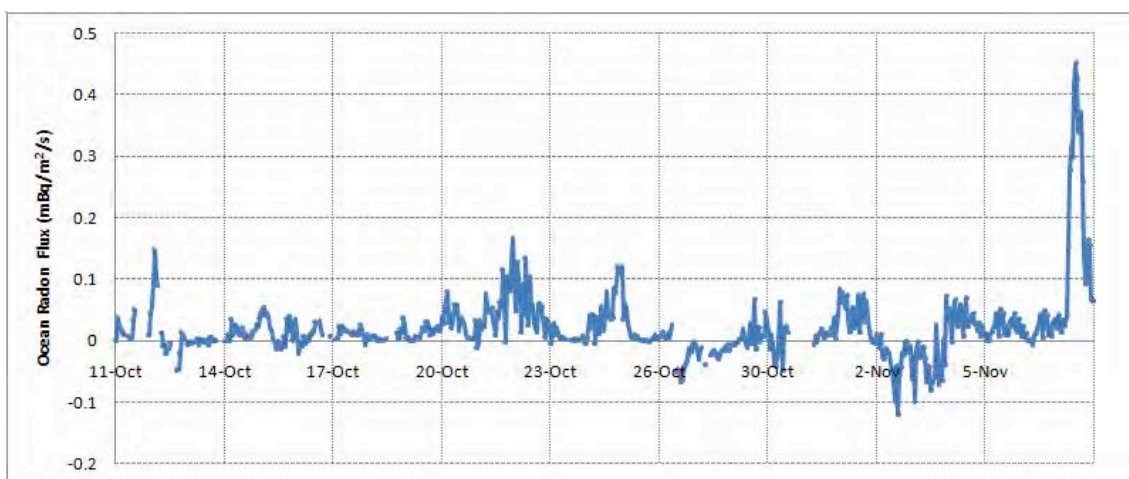
Fig.3 Ocean Radon Flux in Cruise MR08-05 from October-10 to November-7, 2008.

(4) Further data quality check

These preliminary results will be checked for the uncertainty of the calibration factor of radon concentration and the difference of detection efficiency between two high sensitivity radon detectors. ^{226}Ra concentration of seawater samples will be measured with a low background γ -spectrometry. The ^{226}Ra data will enable us to calculate radon concentration deficits from the equilibrium and to evaluate the ocean surface flux independently.

References

Y. Takeuchi, K.Okumura, T.Kajita, S.Tasaka, H.Hori, M.Nemoto, H.Okazawa : Development of high sensitivity radon detectors, Nuclear Instruments and Methods in Physics Research, A421, 334-341, 1999.

Rik Wanninkhof : Relationship Between Wind Speed and Gas Exchange Over the Ocean, Journal of Geophysical Research, Vol. 97, 7373-7382, 1992.

2.2 Physical oceanographic observation

2.2.1 CTD casts and water sampling

Masahide WAKITA (JAMSTEC)：Principal Investigator
Tomoyuki TAKAMORI (MWJ)：Operation Leader
Hiroshi MATSUNOGA (MWJ)
Masaki TAGUCHI (MWJ)
Hiroyuki HAYASHI (MWJ)

(1) Objective
        Investigation of oceanic structure.

(2) Parameters
        Temperature (Primary and Secondary)
        Conductivity (Primary and Secondary)
        Pressure
        Dissolved Oxygen
        Fluorescence
        Transmissometer
        Photosynthetically Active Radiation

(3) Instruments and Methods

CTD/Carousel Water Sampling System, which is a 36-position Carousel water sampler (CWS) with Sea-Bird Electronics, Inc. CTD (SBE9plus), was used during this cruise. 12-litter Niskin Bottles were used for sampling seawater. The sensors attached on the CTD were temperature (Primary and Secondary), conductivity (Primary and Secondary), pressure, dissolved oxygen, oxygen optode, oxygen Rinko, deep ocean standards thermometer, altimeter, Fluorescence, Transmittancy and PAR. Salinity was calculated by measured values of pressure, conductivity and temperature. The CTD/CWS was deployed from starboard on working deck.

The CTD raw data were acquired on real time using the Seasave-Win32 (ver.7.17a) provided by Sea-Bird Electronics, Inc. and stored on the hard disk of the personal computer. Seawater was sampled during the up cast by sending fire commands from the personal computer. We sampled seawater for analysis of salinity, dissolved oxygen, nutrients, and total alkalinity (routine cast).

The package was lowered into the water from the starboard side and held 10 m beneath the surface for about 1 minute in order to activate the pump. After the pump was activated the package was lifted to the surface, and the package was lowered again at a rate of about 1.0 m/s to 1.2m/s. For the up cast, the package was lifted at a rate of 1.2 m/s except for bottle firing stops. At each bottle firing stops, the bottle was fired.

Data processing procedures and used utilities of SBE Data Processing-Win32 (ver.7.17a) and SEASOFT were as follows:

  (The process in order)
 DATCNV : Convert the binary raw data to engineering unit data. DATCNV also extracts bottle
          information where scans were marked with the bottle confirm bit during
          acquisition.

TCORP (original module) : Corrected the pressure sensitivity of the temperature (SBE3) sensor. S/N 1464 : 8.94556e-008 (degC/dbar)

BOTTLESUM : Create a summary of the bottle data. The data were averaged over 4.4 seconds.

ALIGNCTD : Convert the time-sequence of sensor outputs into the pressure sequence to ensure that all calculations were made using measurements from the same parcel of water. Oxygen data are systematically delayed with respect to depth mainly because of the long time constant of the oxygen sensor and of an additional delay from the transit time of water in the pumped pluming line. This delay was compensated by 5 seconds advancing oxygen sensor output (oxygen voltage) relative to the temperature data. Prototype of the oxygen Rinko data is also delayed by slightly slow response time to the sensor. The delay was compensated by 2 seconds advancing

WILDEDIT : Mark extreme outliers in the data files. The first pass of WILDEDIT obtained an accurate estimate of the true standard deviation of the data. The data were read in blocks of 1000 scans. Data greater than 10 standard deviations were flagged. The second pass computed a standard deviation over the same 1000 scans excluding the flagged values. Values greater than 20 standard deviations were marked bad. This process was applied to all variables.

CELLTM : Remove conductivity cell thermal mass effects from the measured conductivity. Typical values used were thermal anomaly amplitude alpha = 0.03 and the time constant 1/beta = 7.0.

FILTER : Perform a low pass filter on pressure with a time constant of 0.15 second. In order to produce zero phase lag (no time shift) the filter runs forward first then backwards.

WFILTER : Perform a median filter to remove spikes in the fluorescence and Transmittancy data. A median value was determined by 49 scans of the window.

SECTIONU (original module of SECTION) : Select a time span of data based on scan number in order to reduce a file size. The minimum number was set to be the starting time when the CTD package was beneath the sea-surface after activation of the pump. The maximum number of was set to be the end time when the package came up from the surface. Data for estimation of the CTD pressure drift were prepared before SECTION.

LOOPEDIT : Mark scans where the CTD was moving less than the minimum velocity of 0.0 m/s (traveling backwards due to ship roll).

DESPIKE (original module) : Remove spikes of the data. A median and mean absolute deviation was calculated in 1-dbar pressure bins for both down and up cast, excluding the flagged values. Values greater than 4 mean absolute deviations from the median were marked bad for each bin. This process was performed 2 times for temperature, conductivity, oxygen voltage (SBE43), oxygen optode and oxygen Rinko data.

DERIVE : Compute oxygen (SBE43)

BINAVG : Average the data into 1-dbar pressure bins.

DERIVE : Compute salinity, potential temperature, and sigma-theta.

SPLIT : Separate the data from an input .cnv file into down cast and up cast files.

Configuration file
     MR0805a.con (File name; S01M01～S04M02)
     MR0805b.con (File name; S04M03～S07M02)
     MR0805c.con (File name; S07M03～S07M04)
     MR0805d.con (File name; S07M05)
     MR0805e.con (File name; S07M06)
     MR0805f.con (File name; S08M01～S15M02)

Specifications of the sensors are listed below.
     CTD：SBE911plus CTD system
       Under water unit：
         SBE9plus (S/N 09P79492-0575, Sea-Bird Electronics, Inc.)
         Pressure sensor：Digiquartz pressure sensor (S/N 79492)
              Calibrated Date：04 Aug. 2008
         SBE9plus (S/N 09P27443-0677, Sea-Bird Electronics, Inc.)
         Pressure sensor：Digiquartz pressure sensor (S/N 79511)
              Calibrated Date：27 Mar. 2008
       Temperature sensors：
         Primary：SBE03-04/F (S/N 031464, Sea-Bird Electronics, Inc.)
              Calibrated Date：16 Jul. 2008
         Secondary：SBE03plus (S/N 03P4815, Sea-Bird Electronics, Inc.)
              Calibrated Date：19 Nov. 2007
       Conductivity sensors：
         Primary：SBE04C (S/N 042435, Sea-Bird Electronics, Inc.)
              Calibrated Date：08 Jul. 2008
           SBE04C (S/N 042854, Sea-Bird Electronics, Inc.)
              Calibrated Date：18 Apr. 2008
         Secondary：SBE04C (S/N 042036, Sea-Bird Electronics, Inc.)
              Calibrated Date：23 Jan. 2008
      Dissolved Oxygen sensors：
         Primary：SBE43 (S/N 430330, Sea-Bird Electronics, Inc.)
              Calibrated Date：28 Jun. 2008
     Oxygen Optode：Oxygen Optode 3830 (S/N 001, Aanderaa Instruments, Inc.)
     Prototype Oxygen Rinko：Rinko (S/N 006, Alec Electronics Co. Ltd.)
     Deep Ocean Standards Thermometer：
             SBE35 (S/N 0045, Sea-Bird Electronics, Inc.)
             Calibrated Date：08 Feb. 2008
     Altimeter：Benthos PSA-916T (S/N 1100, Teledyne Benthos, Inc.)
     Fluorometer：Chlorophyll Fluorometer (S/N 2936, Seapoint Sensors, Inc.)
     Transmissometer：Transmittancy (S/N CST-207RD, WET Labs, Inc.)
     PAR：Photosynthetically Active Radiation (S/N 0049 Satlantic Inc)
     Carousel water sampler：
            SBE32 (S/N 3227443-0391, Sea-Bird Electronics, Inc.)

     Deck unit：SBE11plus (S/N 11P7030-0272, Sea-Bird Electronics, Inc.)

(5) Preliminary results

Total 39 casts of CTD measurements have been carried out (see table1 below).

Table.1 MR08-05 CTD Cast table

Stnnbr	Castno	Date(UTC) (mmddyy)	Time(UTC) Start	Time(UTC) End	BottomPosition Latitude	BottomPosition Longitude	Depth	Wire Out	Max Depth	Max Pressure	CTD Filename	Remark
S01	1	10/14/08	17:03	19:49	56-59.83N	176-00.27E	3813.0	3848.6	3792.4	3861.8	S01M01	
S01	2	10/14/08	22:53	23:24	57-00.00N	175-59.26E	3812.0	201.9	201.3	202.2	S01M02	
S01	3	10/15/08	00:36	03:18	57-00.11N	175-59.76E	3811.0	3861.8	3792.3	3862.6	S01M03	
S01	4	10/15/08	05:15	05:49	57-02.34N	175-59.44E	3810.0	296.0	297.8	301.1	S01M04	
S01	5	10/15/08	07:02	08:50	57-00.01N	176-00.37E	3810.0	3031.8	3001.4	3049.7	S01M05	
S01	6	10/15/08	17:31	17:58	57-00.55N	176-00.17E	3811.0	199.8	200.1	202.6	S01M06	
S02	1	10/16/08	17:00	19:46	55-59.99N	174-39.93E	3852.0	3885.3	3832.9	3904.7	S02M01	
S03	1	10/17/08	01:10	04:12	55-00.06N	173-19.99E	3879.0	3889.1	3861.4	3933.0	S03M01	No.10 bottle miss fire
S04	1	10/17/08	09:31	-	54-00.05N	172-00.04E	-	-	3694.0	3760.0	S04M01	CTD trouble. Stopped observation.
S04	2	10/17/08	16:02	-	53-59.60N	171-59.38E	-	-	-	-	S04M02	CTD trouble. Stopped observation.
S04	3	10/17/08	21:23	00:15	53-59.76N	171-59.94E	3899.0	3979.4	3880.6	3951.9	S04M03	CTD trouble
S05	1	10/18/08	05:28	06:39	52-59.96N	170-39.94E	1063.0	1176.3	1157.2	1171.2	S05M01	CTD trouble
S06	1	10/18/08	12:13	15:41	52-00.00N	169-20.09E	4670.0	4716.2	4664.2	4757.0	S06M01	CTD trouble and No.10 bottle miss fire
S07	1	10/19/08	05:23	08:35	50-59.99N	165-00.20E	4838.0	4877.2	4785.4	4882.2	S07M01	
S07	2	10/19/08	17:31	17:58	51-00.02N	164-59.96E	4803.0	197.6	200.5	202.1	S07M02	
S07	3	10/19/08	21:07	21:35	51-01.09N	165-00.29E	4748.0	297.0	298.1	300.8	S07M03	
S07	4	10/20/08	02:10	05:30	50-59.73N	165-03.10E	4823.0	4879.1	4784.0	4881.7	S07M04	CTD trouble
S07	5	10/20/08	08:04	09:48	50-59.28N	165-03.91E	4810.0	3041.9	-	3049.2	S07M05	
S07	6	10/20/08	22:36	22:58	51-02.90N	165-17.47E	5149.0	198.4	200.1	201.9	S07M06	
S08	1	10/21/08	14:40	18:45	50-00.07N	163-45.03E	5869.0	5942.6	5849.9	5982.1	S08M01	
S09	1	10/22/08	00:20	04:12	48-59.85N	162-29.92E	5602.0	5663.9	5586.8	5709.6	S09M01	
S10	1	10/22/08	09:59	13:36	48-00.03N	161-14.92E	5360.0	5461.8	5360.5	5475.7	S10M01	
S11	1	10/23/08	22:07	02:38	46-59.78N	160-00.01E	5219.0	5336.5	5192.2	5300.3	S11M01	
S11	2	10/24/08	04:19	07:37	46-59.65N	160-00.21E	5210.0	5232.2	5189.7	5190.2	S11M02	
S11	3	10/24/08	08:37	09:22	46-59.95N	160-00.20E	5192.0	1011.9	1006.3	1017.6	S11M03	
S11	4	10/25/08	02:04	02:37	47-00.78N	159-59.65E	5205.0	301.7	302.5	305.1	S11M04	
S11	5	10/26/08	05:06	05:28	46-59.94N	160-00.15E	5189.0	196.7	200.3	203.9	S11M05	
S11	6	10/26/08	06:31	09:19	47-00.18N	160-01.06E	5209.0	5059.0	5001.2	5103.2	S11M06	
S11	7	10/26/08	18:29	19:29	47-00.14N	160-00.56E	5194.0	1010.9	1001.0	1011.3	S11M07	
S11	8	10/26/08	21:03	21:34	46-59.95N	159-59.98E	5186.0	198.2	200.1	200.5	S11M08	
S11	9	10/27/08	21:02	21:48	46-59.80N	160-00.96E	5230.0	899.4	895.4	906.4	S11M09	
S11	10	10/28/08	03:30	03:50	46-59.92N	159-55.95E	5205.0	199.1	201.5	203.5	S11M10	
S12	1	10/29/08	20:12	23:38	45-59.99N	158-20.06E	4881.0	4913.7	4869.2	4966.7	S12M01	
S13	1	10/30/08	06:44	10:04	44-59.84N	156-40.10E	4920.0	4949.8	4898.4	4995.6	S13M01	
S14	1	10/30/08	22:51	23:18	44-00.09N	154-59.71E	5306.0	198.2	200.2	201.8	S14M01	
S14	2	10/30/08	01:16	01:48	44-01.23N	154-59.01E	5317.0	299.1	301.5	304.5	S14M02	
S14	3	10/31/08	03:42	07:20	44-02.46N	154-59.98E	5330.0	5355.9	5317.5	5428.5	S14M03	
S15	1	11/02/08	21:20	22:08	41-07.06N	142-07.96E	1133.0	1007.8	1003.1	1013.4	S15M01	
S15	2	11/03/08	00:12	01:06	41-06.90N	142-07.99E	1134.0	300.4	300.4	302.8	S15M02	

(6) Troubles

PAR sensor was flooded from Stn.S01(File name ; S01M03). Therefore I removed a PAR sensor from Stn.S08.

A noise occurred for data in Stn.04 (File name; S04M01, S04M02, S04M03), Stn.05 (File name; S05M01), Stn.06 (File name; S06M01) and Stn.07 (File name; S07M04). Therefore I removed a noise and carried out data handling.

At the Stn.S07 (File name; S07M05), the primary sensors showed unusual profile due to flowing of a copepod into the pumped pluming line.

At the Stn.S03 (File name; S03M01) and Stn.S07 (File name; S06M01), Niskin bottle #10 Miss fire.

(7) Data Policy

All raw and processed CTD data files were copied onto DVD-ROM. The data will be submitted to the Data Integration and Analyses Group (DIAG), JAMSTEC, and will be opened to public via "R/V MIRAI Data Web Page" in JAMSTEC home page.

2.2.2 Salinity measurement

Masahide WAKITA   (JAMSTEC)：**Principal Investigator**
Tatsuya TANAKA   (MWJ)：**Operation Leader**
Hiroki USHIROMURA   (MWJ)

(1) Objectives

　　　　To measure bottle salinity obtained by CTD casts, bucket sampling, and EPCS.

(2) Method

　a. Salinity Sample Collection

　　　Seawater samples were collected with 12 liter Niskin-X bottles, bucket, and EPCS. The salinity sample bottle of the 250ml brown grass bottle with screw cap was used for collecting the sample water. Each bottle was rinsed three times with the sample water, and was filled with sample water to the bottle shoulder. The bottle was stored for more than 24 hours in the laboratory before the salinity measurement.

　　　　The kind and number of samples taken are shown as follows；

Table 1 Kind and number of samples

Kind of Samples	Number of Samples
Samples for CTD and Bucket	577
Samples for EPCS	29
Total	606

　b. Instruments and Method

　　　　The salinity analysis was carried out on R/V MIRAI during the cruise of MR08-05 using the salinometer (Model 8400B "AUTOSAL"； Guildline Instruments Ltd.: S/N 62556) with an additional peristaltic-type intake pump (Ocean Scientific International, Ltd.). A pair of precision digital thermometers (Model 9540； Guildline Instruments Ltd.) were used. The thermometer monitored the ambient temperature and the other monitored a bath temperature.

　　　　The specifications of AUTOSAL salinometer and thermometer are shown as follows；

Salinometer (Model 8400B "AUTOSAL"； Guildline Instruments Ltd.)
　　Measurement Range　　　：　0.005 to 42 (PSU)
　　Accuracy　　　　　　　：　Better than ±0.002 (PSU) over 24 hours
　　　　　　　　　　　　　　　　　　　　without re-standardization
　　Maximum Resolution　　：　Better than ±0.0002 (PSU) at 35 (PSU)

Thermometer (Model 9540； Guildline Instruments Ltd.)
　　Measurement Range　　　：　-40 to +180 deg C
　　Resolution　　　　　　　：　0.001
　　Limits of error ±deg C　　：　0.01 (24 hours @ 23 deg C ±1 deg C)
　　Repeatability　　　　　　：　±2 least significant digits

　　　　The measurement system was almost the same as Aoyama *et al.* (2002). The salinometer was operated in the air-conditioned ship's laboratory at a bath temperature of 24 deg C. The ambient temperature varied from approximately 21 deg C to 25 deg C, while the

bath temperature was very stable and varied within +/- 0.004 deg C on rare occasion. The measurement for each sample was done with the double conductivity ratio and defined as the median of 31 readings of the salinometer. Data collection was started 10 seconds after filling the cell with sample and it took about 10 seconds to collect 31 readings by a personal computer. Data were taken for the sixth and seventh filling of the cell. In the case of the difference between the double conductivity ratio of these two fillings being smaller than 0.00002, the average value of the double conductivity ratio was used to calculate the bottle salinity with the algorithm for practical salinity scale, 1978 (UNESCO, 1981). If the difference was greater than or equal to 0.00003, an eighth filling of the cell was done. In the case of the difference between the double conductivity ratio of these two fillings being smaller than 0.00002, the average value of the double conductivity ratio was used to calculate the bottle salinity. In the case of the double conductivity ratio of eighth filling did not satisfy the criteria above, we measured a ninth filling or a tenth filling of the cell and calculated the bottle salinity above. The measurement was conducted in about 7 - 14 hours per day and the cell was cleaned with soap after the measurement of the day.

(3) Preliminary Result
　a. Standard Seawater
　　　　Standardization control of the salinometer was set to 670 and all measurements were done at this setting. The value of STANDBY was 5504 +/- 0001 and that of ZERO was 0.0-0001 +/- 0001. The conductivity ratio of IAPSO Standard Seawater batch P148 was 0.99982 (the double conductivity ratio was 1.99964) and was used as the standard for salinity. We measured 36 bottles of P148.

　　　　Fig.2.2.2-1 shows the history of the double conductivity ratio of the Standard Seawater batch P148 before correction. The average of the double conductivity ratio was 1.99962 and the standard deviation was 0.00001, which is equivalent to 0.0003 in salinity.

　　　　Fig.2.2.2-2 shows the history of the double conductivity ratio of the Standard Seawater batch P148 after correction. The average of the double conductivity ratio after correction was 1.99964 and the standard deviation was 0.00001, which is equivalent to 0.0002 in salinity.

　　　　The specifications of SSW used in this cruise are shown as follows ;

batch	:	P148
conductivity ratio	:	0.99982
salinity	:	34.993
preparation date	:	10-October-2006
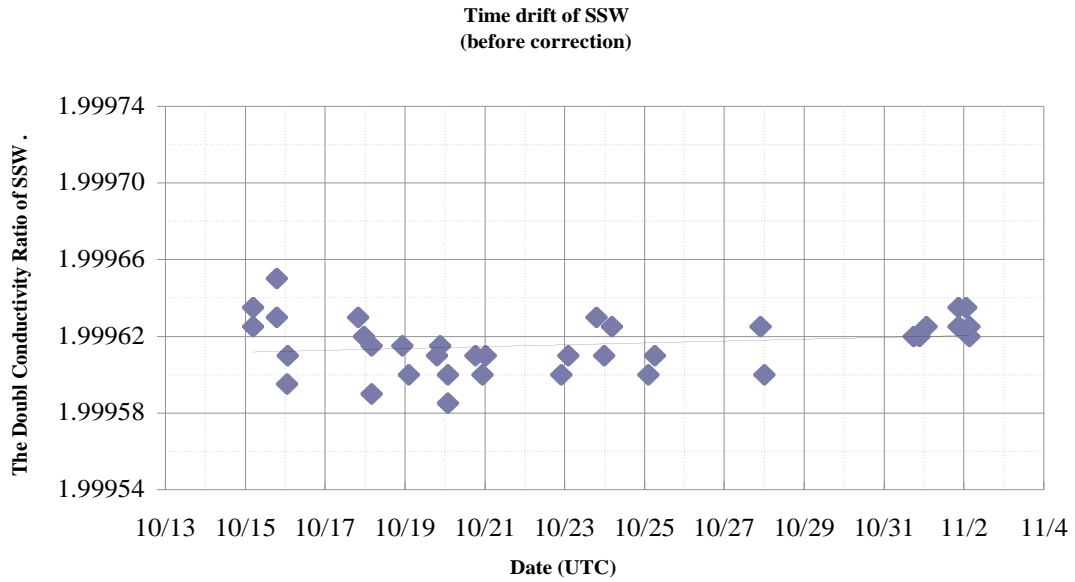
Fig.1 The history of the double conductivity ratio for the Standard Seawater batch P148
(before correction)
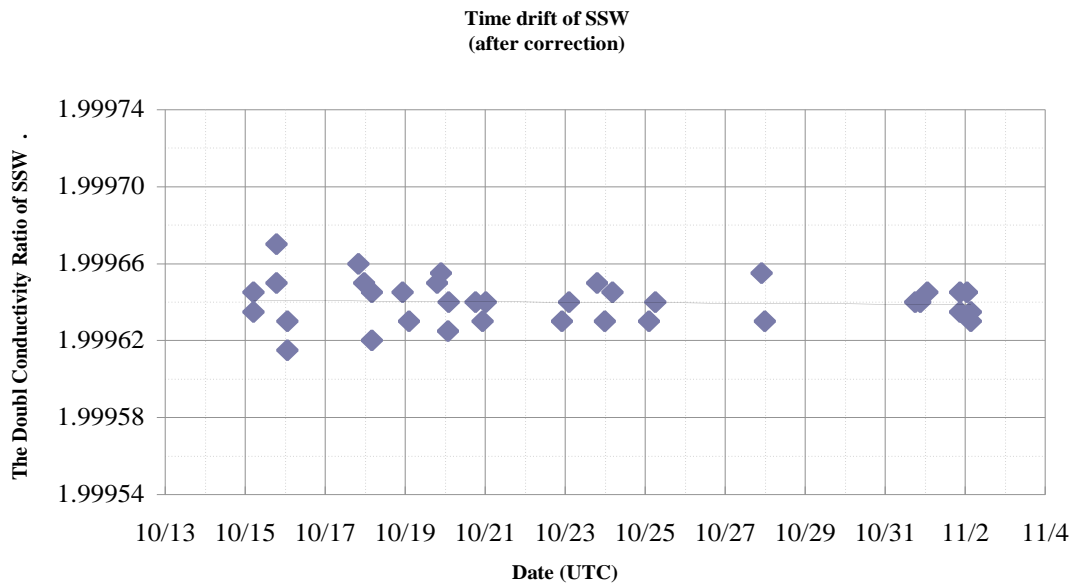
Fig.2 The history of the double conductivity ratio for the Standard Seawater batch P148
(after correction)

b. Sub-Standard Seawater

Sub-standard seawater was made from deep-sea water filtered by a pore size of 0.45 micrometer and stored in a 20-liter container made of polyethylene and stirred for at least 24 hours before measuring. It was measured about every 6 samples in order to check for the possible sudden drifts of the salinometer.

c. Replicate Samples

We estimated the precision of this method using 76 pairs of replicate samples taken from the same Niskin bottle. The average and the standard deviation of absolute deference among 76 pairs of replicate samples were 0.0003 and 0.0002 in salinity, respectively.

(4) Data archive

These raw datasets will be submitted to JAMSTEC Data Integration and Analyses Group (DIAG).

(5) Reference

・Aoyama, M., T. Joyce, T. Kawano and Y. Takatsuki : Standard seawater comparison up to P129. Deep-Sea Research, I, Vol. 49, 1103～1114, 2002

・UNESCO : Tenth report of the Joint Panel on Oceanographic Tables and Standards. UNESCO Tech. Papers in Mar. Sci., 36, 25 pp., 1981

2.3 Sea surface monitoring: EPCS

Masahide WAKITA (JAMSTEC MIO): Principal Investigator
Yoshiko ISHIKAWA (MWJ)
Yasuhiro ARII (MWJ)

(1) Objectives

   To measure temperature, salinity, dissolved oxygen, and fluorescence of the sea surface water in the western North Pacific Ocean.

(2) Instruments and Methods

   The *Continuous Sea Surface Water Monitoring System* (Nippon Kaiyo Co. Ltd.) that equips five sensors of 1) salinity, 2) temperatures (two sensors), 3) dissolved oxygen and 4) fluorescence can continuously measure their values for the sea surface water. Salinity is calculated by conductivity on the basis of PSS78. Specifications of these sensors are listed below.

   This system is settled in the "*sea surface monitoring laboratory*" on R/V MIRAI, and sea surface water was continuously pumped up to the system through a vinyl-chloride pipe. The flow rate for the system is manually controlled by several valves with its value of 12 L min^{-1} except for the fluorometer (about 0.5 L min^{-1}). Each flow rate is monitored with respective flow meter.   The system is connected to shipboard LAN-system, and measured data is stored in a hard disk of PC every 1-minute together with time (UTC) and position of the ship.

   a) Temperature and Conductivity sensor
      Model: SBE-21, SEA-BIRD ELECTRONICS, INC.
      Serial number: 2126391-3126
      Measurement range: Temperature -5 to +35℃, Conductivity 0 to 7 S m^{-1}
      Resolution: Temperatures 0.001℃, Conductivity 0.0001 S m^{-1}
      Stability: Temperature 0.01℃ 6 months^{-1}, Conductivity 0.001 S m^{-1} month^{-1}

   b) Bottom of ship thermometer
      Model: SBE 3S, SEA-BIRD ELECTRONICS, INC.
      Serial number: 032607
      Measurement range: -5 to +35℃
      Resolution: ±0.001℃
      Stability: 0.002℃ year^{-1}

   c) Dissolved oxygen sensor
      Model: 2127A, Hach Ultara Analytics Japan, INC.
      Serial number: 61230
      Measurement range: 0 to 14 ppm
      Accuracy: ±1% in ±5℃ of correction temperature
      Stability: 5% month^{-1}

   d) Fluorometer
      Model: 10-AU-005, TURNER DESIGNS
      Serial number: 5562 FRXX

Detection limit: 5 ppt or less for chlorophyll a
Stability: 0.5% month^{-1} of full scale

e) Flow meter
   Model: EMARG2W, Aichi Watch Electronics LTD.
   Serial number: 8672
   Measurement range: 0 to 30 L min^{-1}
   Accuracy: <= ±1%
   Stability: <= ±1% day^{-1}

The monitoring period (UTC) during this cruise are listed below.
            Start: 2008/10/11 19:24   Stop: 2008/11/05 05:20

(3) Preliminary Result
        Preliminary data of temperature, salinity, dissolved oxygen, fluorescence at sea surface are shown in Fig.1. We took the surface water samples once a day to compare sensor data with bottle data of salinity, dissolved oxygen. For the compensation sample of the fluorescence, we took a total of 4 times (after the beginning of the continuous monitoring, before and after the exchanging the flowcell, before the end of the continuous monitoring). The results are shown in Fig.2, 3, Table1. All the salinity samples were analyzed by the Guildline 8400B "AUTOSAL", and dissolve oxygen samples were analyzed by Winkler method. Fluorescence samples were analyzed by Non-acidification method, using 10-AU-005,TURNER DESIGNS.

(4) Date archive
        The data were stored on a CD-R, which will be submitted to JAMSTEC, and will be opened to public via "R/V MIRAI Data Web Page" in JAMSTEC homepage.
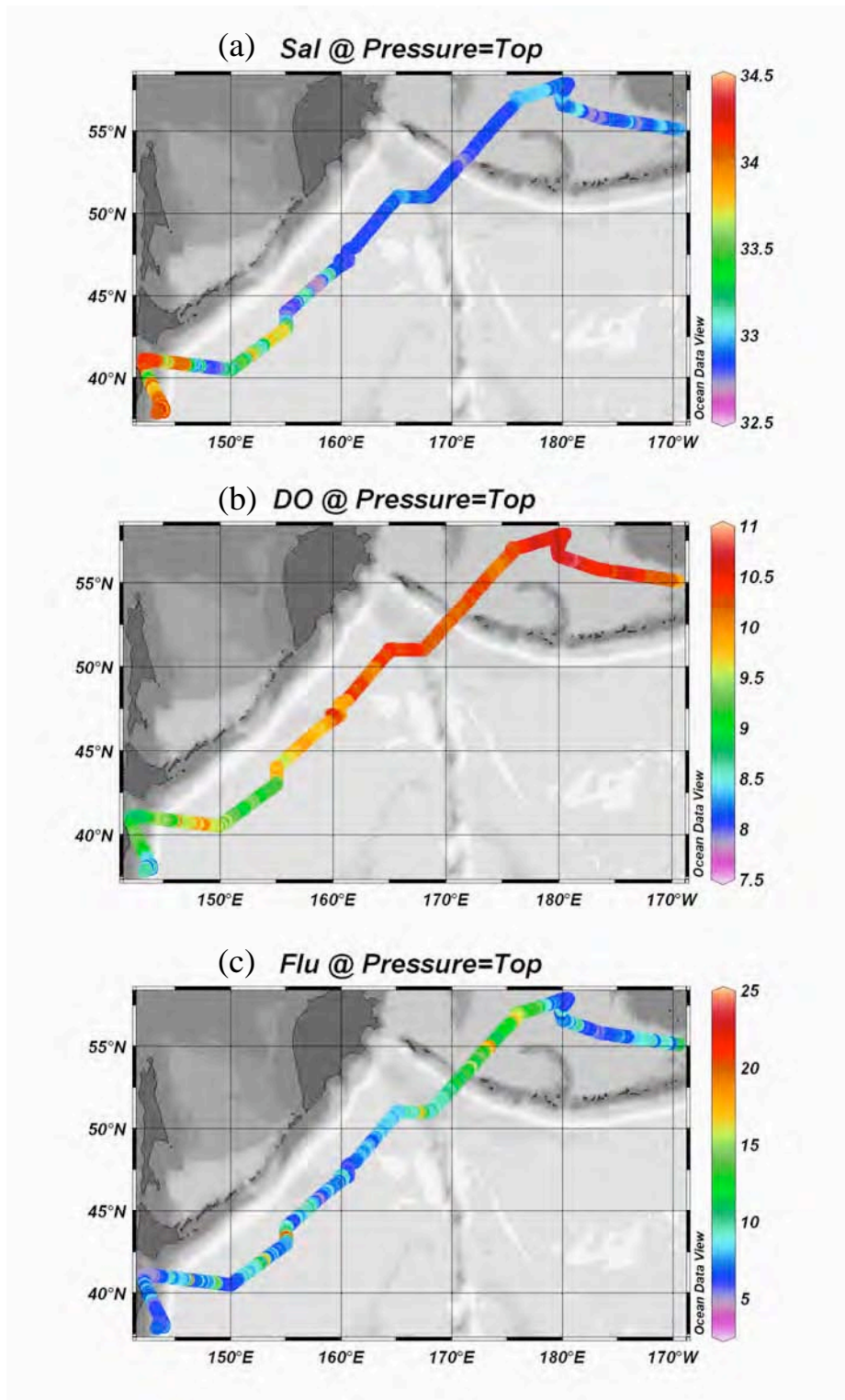
Fig.1 Contour line of salinity(a), dissolved oxygen(b), fluorescence(c) of the sea surface water during this cruise.
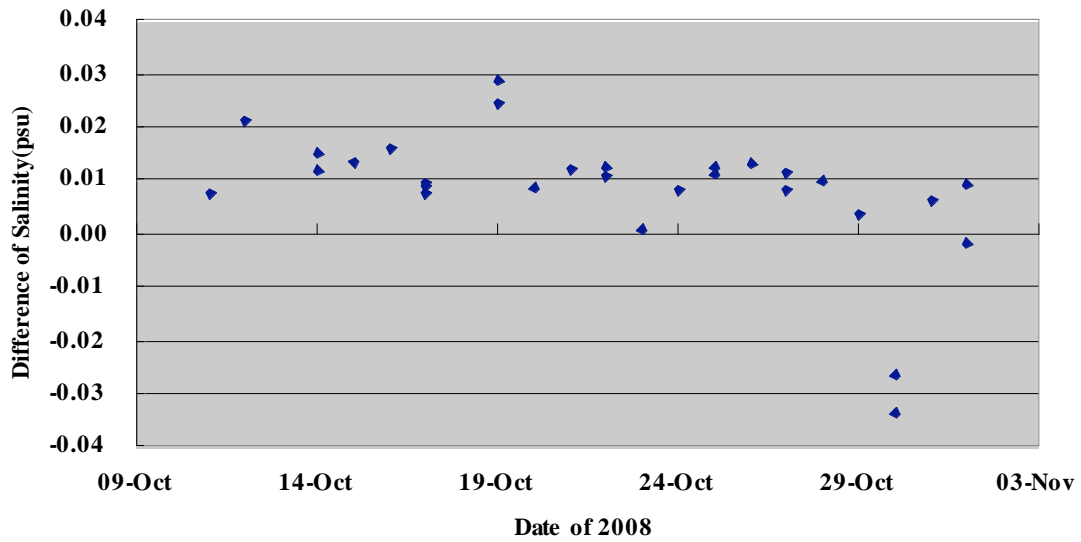
Fig.2　Difference of salinity between sensor data and bottle data.　The mean difference is 0.0085psu.
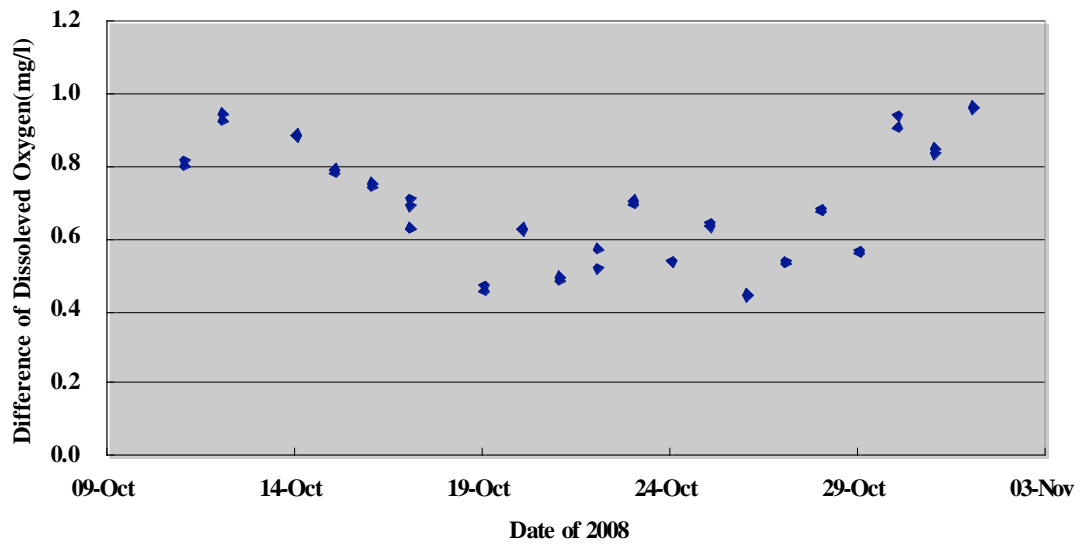
Fig.3　Difference of dissolved oxygen between sensor data and bottle data.　The mean difference is 0.6926mg/l.

Table 1 Comparison of the fluorescence with the bottle chlorophyll a during MR08-05

Date [UTC]	Time [UTC]	fluorescence	Bottle Chlorophyll a (µg/L)	
			Non-Acidification Method	Acidification Method
2008/10/11[*1]	23:02	9.123	1.73	1.60
2008/10/21[*2]	04:30	10.660	0.83	0.75
2008/10/21[*3]	06:30	8.230	0.81	0.72
2008/11/01[*4]	00:31	18.640	1.94	1.90

*1: Water was sampled immediately after the beginning of the continuous monitoring.
*2: Water was sampled before exchanging the flowcell.
*3: Water was sampled after exchanging the flowcell.
*4: Water was sampled finishing of before the continuous monitoring.

2.4 Dissolved oxygen measurement

Masahide WAKITA (JAMSTEC): Principal Investigator
Masanori ENOKI (MWJ)
Miyo IKEDA (MWJ)
Misato KUWAHARA (MWJ)

(1)Objectives
Determination of dissolved oxygen in seawater by Winkler titration.

(2) Measured parameters
Dissolved oxygen of sampled seawater

(3) Instruments and Methods
a. Reagents
Pickling Reagent I: Manganous chloride solution (3M)
Pickling Reagent II: Sodium hydroxide (8M) / sodium iodide solution (4M)
Sulfuric acid solution (5M)
Sodium thiosulfate (0.025M)
Potassium iodate (0.001667M)

b. Instruments:
Burette for sodium thiosulfate;
APB-510 manufactured by Kyoto Electronic Co. Ltd. / 10 cm^3 of titration vessel
Burette for potassium iodate;
APB-510 manufactured by Kyoto Electronic Co. Ltd. / 10 cm^3 of titration vessel
Detector and Software; Automatic photometric titrator manufactured by Kimoto Electronic
Co. Ltd.

c. Sampling
Following procedure is based on the WHP Operations and Methods (Dickson, 1996).
Seawater samples were collected with Niskin bottle attached to the CTD-system.
Seawater for oxygen measurement was transferred from Niskin sampler bottle to a volume
calibrated flask (ca. 100 cm^3).   Three times volume of the flask of seawater was overflowed.
Temperature was measured by digital thermometer during the overflowing.   Then two reagent
solutions (Reagent I and II) of 0.5 cm^3 each were added immediately into the sample flask and
the stopper was inserted carefully into the flask. The sample flask was then shaken vigorously to
mix the contents and to disperse the precipitate finely throughout.   After the precipitate has
settled at least halfway down the flask, the flask was shaken again vigorously to disperse the
precipitate.   The sample flasks containing pickled samples were stored in a laboratory until
they were titrated.

d. Sample measurement
At least two hours after the re-shaking, the pickled samples were measured on board.
A magnetic stirrer bar and 1 cm^3 sulfuric acid solution were added into the sample flask and
stirring began.   Samples were titrated by sodium thiosulfate solution whose morality was
determined by potassium iodate solution.   Temperature of sodium thiosulfate during titration

was recorded by a digital thermometer.   During this cruise we measured dissolved oxygen concentration using two sets of the titration apparatus (DOT-01 and DOT-03).   Dissolved oxygen concentration (μmol kg^{-1}) was calculated by sample temperature during seawater sampling, salinity of the sample, and titrated volume of sodium thiosulfate solution without the blank.

e. Standardization and determination of the blank

Concentration of sodium thiosulfate titrant (ca. 0.025M) was determined by potassium iodate solution. Pure potassium iodate was dried in an oven at 130°C. 1.7835g potassium iodate weighed out accurately was dissolved in deionized water and diluted to final volume of 5 dm^3 in a calibrated volumetric flask (0.001667M). 10 cm^3 of the standard potassium iodate solution was added to a flask using a calibrated dispenser. Then 90 cm^3 of deionized water, 1 cm^3 of sulfuric acid solution, and 0.5 cm^3 of pickling reagent solution II and I were added into the flask in order. Amount of sodium thiosulfate titrated gave the morality of sodium thiosulfate titrant.

The blank from the presence of redox species apart from oxygen in the reagents was determined as follows. Firstry, 1 cm^3 of the standard potassium iodate solution was added to a flask using a calibrated dispenser.   Then 100 cm^3 of deionized water, 1 cm^3 of sulfuric acid solution, and 0.5 cm^3 of pickling reagent solution II and I were added into the flask in order. Secondary, 2 cm^3 of the standard potassium iodate solution was added to a flask using a calibrated dispenser.   Then 100 cm^3 of deionized water, 1 cm^3 of sulfuric acid solution, and 0.5 cm^3 of pickling reagent solution II and I were added into the flask in order. The blank was determined by difference between the first and second titrated volumes of the sodium thiosulfate.

Table 2. shows results of the standardization and the blank determination during this cruise.

Table 1 Results of the standardization and the blank determinations during this cruise.

Date	KIO₃		Na₂S₂O₃	DOT-01		DOT-02		Samples
(UTC)	#	bottle		E.P.(mL)	Blank	E.P.(mL)	Blank	(Stations)
2008/10/11	3	20080722-03-07	20070613-25-1	3.960	-0.003	3.961	-0.003	S01 cast1, S01 cast2
2008/10/11	-	CSK	20070613-25-1	3.958	-	3.959	-	-
2008/10/16	3	20080722-03-08	20070613-25-1	3.961	-0.002	3.963	-0.002	S02 cast1, S03 cast1, S04 cast3, S05 cast1, S06 cast1, S07 cast1, S07 cast2
2008/10/19		20080722-03-09	20070613-25-1	3.962	-	3.962	-	
2008/10/21		20080722-03-10	20070613-25-1	3.960	-0.002	3.962	0.000	
2008/10/21		20080722-03-10	20070613-25-2	3.966	-0.002	3.967	0.000	S08 cast1 S09 cast1 S10 cast1 S11 cast1 S11 cast8
2008/10/22	4	20080722-04-01	20070613-25-2	3.963	-0.001	-	-	
2008/10/29		20080722-04-02	20070613-25-2	3.962	-0.001	3.963	0.000	S12 cast8, S13 cast8
2008/10/31		20080722-04-03	20070613-25-2	3.960	-0.001	3.962	0.000	
2008/10/31		20080722-04-03	20070613-27-1	3.963	-0.002	3.963	0.000	S14 cast1, S14 cast3
2008/11/01		20080722-04-04	20070613-27-1	3.964	-0.001	3.965	0.000	
2008/11/01	-	CSK	20070613-27-1	3.960	-	3.961	-	

\# Batch number of the KIO₃ standard solution.

f. Reproducibility of sample measurements

Replicate samples were taken at every CTD cast; usually these were 5 - 10 % of seawater samples of each cast during this cruise. Results of the replicate samples were shown in Table 2. and this histogram shown in Fig.2. The standard deviation was calculated by a procedure (SOP23) in DOE (1994).

Table 2 Results of the replicate samples measurements

Number of replicate sample pairs	Oxygen concentration (μmol/kg)
	Standard Deviation.
47	0.09

*Computation of a replicates sample measurements removed samples which is a difference not less than UCL at the Fig .2 .
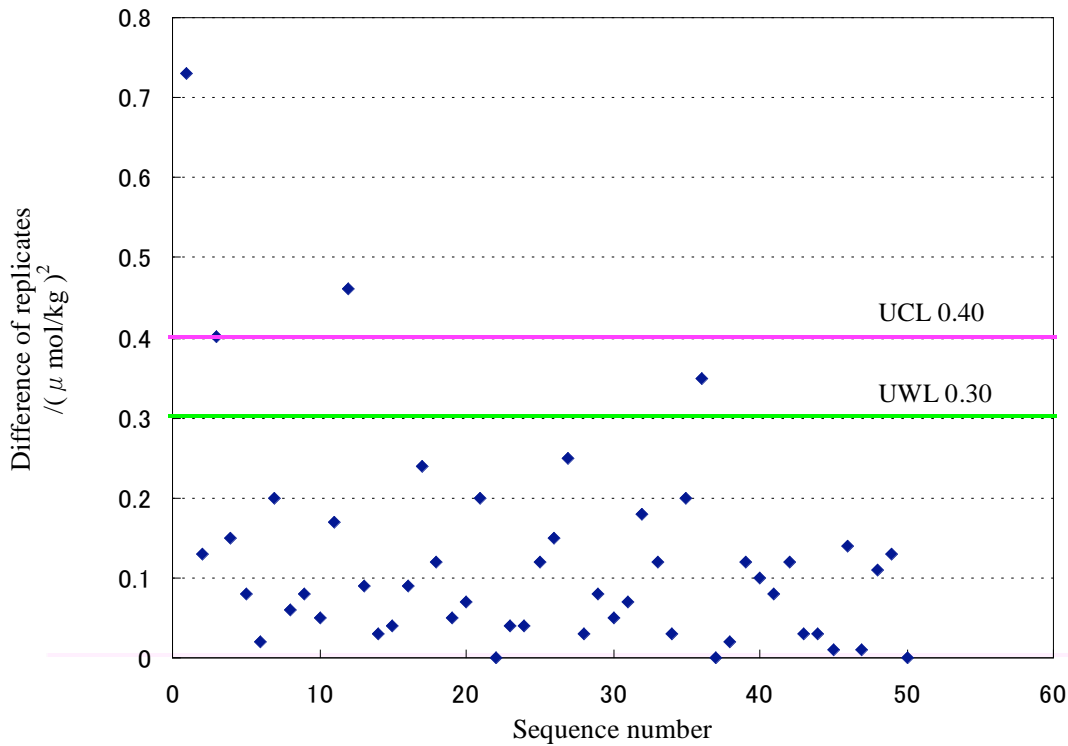
Fig. 2   Results of the replicate samples measurements

*This chart was on the based of the SOP22 in Guide to best practices for ocean CO_2 measurements.

(4) Preliminary Result
　　　During this cruise, we measured oxygen concentration in 551 seawater samples at 18 stations.

(5) Data policy and citation
　　　All data will be submitted to Chief Scientist.

(6) Reference

 Dickson, Determination of dissolved oxygen in sea water by Winkler titration. (1996)
Dickson et al., Guide to best practices for ocean CO_2 measurements. (2007)
Culberson, WHP Operations and Methods July-1991 "Dissolved Oxygen", (1991)
Japan Meteorological Agency, Oceanographic research guidelines（Part 1）. (1999)
KIMOTO electric CO. LTD., Automatic photometric titrator DOT-01 Instruction manual.

2.5 Nutrients

Masahide WAKITA   (JAMSTEC): Principal Investigator
Junji MATSUSHITA   (MWJ)
Kenichiro SATO   (MWJ)
Yusuke SATO   (MWJ)

(1) Objectives

The vertical and horizontal distributions of the nutrients are one of the most important factors on the primary production. On the other hand, nutrients data are used to study of climate changes as chemical tracers of seawater mass movement. During this cruise nutrient measurements will give us the important information on the mechanism of the primary production and/or seawater circulation.

(2) Measured Parameters

Nitrate, Nitrite, Silicate (Although silicic acid is correct, we use silicate because a term of silicate is widely used in oceanographic community), Phosphate and Ammonia. See below for further details.

(3) Instruments and Methods

Nutrient analysis was performed on the BRAN+LUEBBE TRAACS 800 system. The laboratory temperature was maintained between 23-25 deg C.

a. Measured Parameters

Nitrate + nitrite and nitrite are analyzed according to the modification method of Grasshoff (1970). The sample nitrate is reduced to nitrite in a cadmium tube inside of which is coated with metallic copper. The sample stream with its equivalent nitrite is treated with an acidic, sulfanilamide reagent and the nitrite forms nitrous acid, which reacts with the sulfanilamide to produce a diazonium ion. N1-Naphthylethylene- diamine added to the sample stream then couples with the diazonium ion to produce a red, azo dye. With reduction of the nitrate to nitrite, both nitrate and nitrite react and are measured; without reduction, only nitrite reacts. Thus, for the nitrite analysis, no reduction is performed and the alkaline buffer is not necessary. Nitrate is computed by difference. Absorbance of 550 nm by azo dye in analysis is measured using a 3 cm length cell for Nitrate and 5 cm length cell for nitrite.

The silicate method is analogous to that described for phosphate. The method used is essentially that of Grasshoff et al. (1983), wherein silicomolybdic acid is first formed from the silicic acid in the sample and added molybdic acid; then the silicomolybdic acid is reduced to silicomolybdous acid, or "molybdenum blue," using L-ascorbic acid as the reductant. Absorbance of 630 nm by silicomolybdous acid in analysis is measured using a 3 cm length cell.

The phosphate analysis is a modification of the procedure of Murphy and Riley (1962). Molybdic acid is added to the seawater sample to form phosphomolybdic acid, which is in turn reduced to phosphomolybdous acid using L-ascorbic acid as the reductant. Absorbance of 880 nm by phosphomolybdous acid in analysis is measured using a 5 cm length cell.

Ammonia in seawater is mixed with an alkaline solution containing EDTA, ammonia as gas state is formed from seawater. The ammonia (gas) is absorbed in sulfuric acid solution by way of 0.1 µm pore size membrane filter (ADVANTEC PTFE) at the dialyzer attached to analytical system. The ammonia absorbed in acid solution is determined by coupling with phenol and hypochlorite solution to from an indophenol blue compound. Absorbance of 630 nm by

indophenol blue compound in analysis is measured using a 3 cm length cell.

b. Standard

Silicate standard solution, the silicate primary standard, was obtained from Merck, Ltd.. This standard solution, traceable to SRM from NIST was 1000 mg per litter. Since this solution is alkaline solution of 0.5 M NaOH, an aliquot of 40 ml solution were diluted to 500 ml together with an aliquot of 20 ml of 1 M HCl. Primary standard for nitrate (KNO_3) and phosphate (KH_2PO_4) were obtained from Merck, Ltd., nitrite ($NaNO_2$) and ammonia ((NH_4)$_2SO_4$) were obtained from Wako Pure Chemical Industries, Ltd..

c. Sampling Procedures

Samples were drawn into virgin 10 ml polyacrylate vials that were rinsed 3 times before sampling without sample drawing tubes. Sets of 4 to 6 different concentrations for nitrate, nitrite, silicate, phosphate and ammonia of the shipboard standards were analyzed at beginning and end of each group of analysis. The standard solutions of highest concentration were measured every 8to 16 samples and were used to evaluate precision of nutrients analysis during the cruise. We also used reference material for nutrients in seawater, RMNS (KANSO Co., Ltd., lots AS, AT and AU), for every runs to secure comparability on nutrient analysis throughout this cruise.

d. Low Nutrients Sea Water (LNSW)

Surface water having low nutrient concentration was taken and filtered using 0.45 μm pore size membrane filter. This water is stored in 20-liter cubitainer with paper box. The concentrations of nutrient of this water were measured carefully in April 2007.

(4) Results

Analytical precisions were 0.07% (55.0 μM) for nitrate, 0.09% (1.17 μM) for nitrite, 0.07% (170 μM) for silicate, 0.13% (3.63 μM) for phosphate, 0.36% (4.0 μM) for ammonia in terms of median of precision, respectively.

Results of RMNS analysis are shown in Table 3.1-1.

(5) Remarks

The phosphate data at S01, S02 and S03 was corrected by RMNS.

(6) Archive

All data will be submitted to JAMSTEC Data Integration and Analyses Group (DIAG) and is currently under its control.

(7) Reference

Grasshoff, K. (1970), Technicon paper, 691-57.

Grasshoff, K., Ehrhardt, M., Kremling K. et al. (1983), Methods of seawater analysis. 2nd rev. Weinheim: Verlag Chemie, Germany, West.

Murphy, J., and Riley, J.P. (1962), Analytica chim. Acta 27, 31-36.

Table 3.1-1   Summary of RMNS concentrations in this cruise.

μmol/kg

		NO$_3$	NO$_2$	SiO$_2$	PO$_4$	NH$_4$
RM-AS	avg	0.11	0.02	1.66	0.071	0.83
	stdev	0.02	0.00	0.08	0.008	0.03
	n=	18	18	18	18	5
RM-AT	avg	7.50	0.02	17.91	0.579	0.74
	stdev	0.02	0.00	0.07	0.008	0.01
	n=	18	18	18	18	5
RM-AU	avg	29.90	0.02	66.38	2.175	0.55
	stdev	0.04	0.00	0.10	0.010	0.01
	n=	34	34	34	34	9

2.6 pH measurement

Masahide WAKITA (JAMSTEC MIO)
Ayaka HATSUYAMA (MWJ)
Tomonori WATAI (MWJ)

(1) Introduction

Since the global warming is becoming an issue world-widely, studies on the greenhouse gases such as CO_2 are drawing high attention. Because the ocean plays an important role in buffering the increase of atmospheric CO_2, studies on the exchange of CO_2 between the atmosphere and the sea becomes highly important. When CO_2 dissolves in water, chemical reaction takes place and CO_2 alters its appearance into several species. The concentrations of the individual species of CO_2 system in solution cannot be measured directly, however, two of the four measurable parameters (alkalinity, total dissolved inorganic carbon, pH and pCO_2) can estimate each concentration of CO_2 system (Dickson et al., 2007). Seawater acidification associated with CO_2 uptake into the ocean possibly changes oceanic ecosystem and garners attention recently. We here report on board measurements of pH during MR08-05cruise.

(2) Apparatus and performance
(2)-1 Seawater sampling

Seawater samples were collected with CTD system mounted 12 L Niskin bottles at 14 stations. Seawater was sampled in a 300 ml borosilicate glass bottle that was previously soaked in 5 % non-phosphoric acid detergent (pH13) solution at least 3 hours and was cleaned by fresh water for 5 times and Milli-Q deionized water for 3 times. A sampling silicone rubber tube with PFA tip was connected to the Niskin bottle when the sampling was carried out. The glass bottles were filled from the bottom smoothly, without rinsing, and were overflowed for 2 times bottle volume (20 seconds) with care not to leave any bubbles in the bottle. The water in the bottle was sealed by a glass made cap gravimetrically fitted to the bottle mouth without additional force. After collecting the samples on the deck, the bottles were carried into the lab and put in the water bath kept about 25 ℃ before the measurement.

(2)-2 Seawater analyses

The pH ($-\log[H^+]$) of the seawater was measured spectrophotometry by a pH measuring system (Nippon ANS) using a scheme of Clayton and Byrne (1993). The sampled seawater in the glass bottle is transferred to a sample cell in the spectrophotometer (Carry 50 Scan, Varian) via dispensing unit. The length and volume of the cell are 8 cm and 13 ml, respectively, and its temperature is kept at 25.00 ± 0.05 °C in a thermostated compartment. The pH is calculated by measuring two sets of absorbance at three wavelengths (730, 578 and 434 nm). One is the absorbance of seawater sample before injecting an indicator solution and another is the one after the injection. For mixing the indicator solution and the seawater sufficiently, they are circulated through the line by a peristaltic pump about 3.5 minutes before the measurement.

The pH is calculated based on the following equation:

$$pH = pK_2 + \log((A1 / A2 - 0.00691)/(2.2220 - 0.1331(A1 / A2)))$$

where A1 and A2 represents the difference of absorbance at 578 and 434 nm between before and after the injection, respectively, and pK_2 is a function of water temperature and salinity. The absorbance of wavelength at 730 nm is used to subtract the variation of absorbance caused by

the system.

To keep the highly analysis precision, some treatments were carried out during the cruise. The indicator solution, *m*-cresol purple (2 mmol), was produced on board a ship, and retained in a 1000 ml DURAN laboratory bottle. We conditioned an indicator solution 5 times to keep its absorbance ratio in a range of 1.52 - 1.61. The check was made by a spare spectrophotometer using a cell with its path length of 0.5 mm. For mixing the seawater and the indicator solution sufficiently, TYGON tube used on the peristaltic pump was periodically renewed. Absorbance measurements were done 15 times during each analysis, and the stable last five values are averaged and used for above listed calculation.

 (3) Preliminary results

A replicate analysis of seawater sample was made at 10, 50, 200, 1200 and 4000 m depth of every observation point and the difference between each pair of analyses was plotted on a range control chart (see Figure 1). The average of the difference was 0.0012 pH units (n=46 pairs) and its standard deviation 0.0010 pH units. These values were lower than the value recommended by Dickson et al. (2007).

(4) Data Archive

All data will be submitted to JAMSTEC and is currently under its control.

(5) Reference

Clayton, T.D. and R.H. Byrne (1993): Spectrophotometric seawater pH measurements: total hydrogen ion concentration scale calibration of *m*-cresol purple and at-sea results, Deep-Sea Research 40, 2115-2129.

Dickson, A. G., C. L. Sabine and J. R. Christian, Eds. (2007): Guide to best practices for ocean CO_2 measurements, PICES Special Publication 3, 199pp.

Fig. 1 Range control chart of the absolute differences of duplicate measurements of pH carried out during the cruise. AVE represents the average value, UCL upper control limit (UCL = AVE * 3.267), and UWL upper warning limit (UWL = AVE * 2.512) (Dickson et al., 2007).

2.7 Dissolved inorganic carbon-DIC

Masahide WAKITA   **(JAMSTEC MIO)**
Yoshiko ISHIKAWA   **(MWJ)**
Yasuhiro ARII   **(MWJ)**

(1) Objective

Concentrations of CO_2 in the atmosphere are now increasing at a rate of 1.5 ppmv y^{-1} owing to human activities such as burning of fossil fuels, deforestation, and cement production. It is an urgent task to estimate as accurately as possible the absorption capacity of the oceans against the increased atmospheric CO_2, and to clarify the mechanism of the CO_2 absorption, because the magnitude of the anticipated global warming depends on the levels of CO_2 in the atmosphere, and because the ocean currently absorbs 1/3 of the 6 Gt of carbon emitted into the atmosphere each year by human activities.

Since the global warming is becoming an issue world-widely, studies on green house gases such as CO_2 are drawing high attention. Because the ocean plays an important role in buffering the increase of atmospheric CO_2, surveys on the exchange of CO_2 between the atmosphere and the sea becomes highly important. When CO_2 dissolves in water, chemical reaction takes place and CO_2 alters its appearance into several species. Unfortunately, concentrations of the individual species of CO_2 system in solution cannot be measured directly. There are, however, four parameters that could be measured; total alkalinity, total dissolved inorganic carbon, pH and pCO_2. When more than two of the four parameters are measured, the concentration of CO_2 system in the water can be estimated (Dickson et al., 2007). We here report on-board measurements of DIC performed during the MR08-05 cruise.

(2) Methods, Apparatus and Performance
(2)-1 Seawater sampling

Seawater samples were collected by 12L Niskin bottles at 14 stations. Among these stations, deep and shallow casts were carried out for 4 stations. When shallow casts were performed, surface seawater samples were also collected by a bucket. Seawater was sampled in a 300ml glass bottle (SCHOTT DURAN) that was previously soaked in 5% non-phosphoric acid detergent (pH13) solution at least 3 hours and was cleaned by fresh water for 5 times and Milli-Q deionized water for 3 times. A sampling tube was connected to the Niskin bottle when the sampling was carried out. The glass bottles were filled from the bottom, without rinsing, and were overflowed for 20 seconds. They were sealed using the 29mm polyethylene inner lids with care not to leave any bubbles in the bottle. After collecting the samples on the deck, the glass bottles were removed to the lab to be measured. Prior to the analysis, 3ml of the sample (1% of the bottle volume) was removed from the glass bottle in order to make a headspace. The samples were then poisoned with 100μl of over saturated solution of mercury chloride within one hour from the sampling point. After poisoning, the samples were sealed using the 31.9mm polyethylene inner lids. The samples were stored in a refrigerator at approximately 5degC until analyzed.

(2)-2 Seawater analysis

Measurements of DIC were made with total CO_2 measuring system (systems A; Nippon ANS, Inc.). The system comprise of seawater dispensing system, a CO_2 extraction system and a coulometer (Model 5012, UIC Inc.)

The seawater dispensing system has an auto-sampler (6 ports), which takes seawater

into a glass bottle and dispenses the seawater to a pipette of nominal 21ml volume by PC control. The pipette was kept at 20 ± 0.05 degC by a water jacket, in which water from a thermostatic water bath (LP-3110, ADVANTEC) set at 20 degC is circulated.

CO$_2$ dissolved in a seawater sample is extracted in a stripping chamber of the CO$_2$ extraction system by adding phosphoric acid (10% v/v). The stripping chamber is made approx. 25 cm long and has a fine frit at the bottom. The acid is added to the stripping chamber from the bottom of the chamber by pressurizing an acid bottle for a given time to push out the right amount of acid. The pressurizing is made with nitrogen gas (99.9999%). After the acid is transferred to the stripping chamber, a seawater sample kept in a pipette is introduced to the stripping chamber by the same method as that for adding an acid. The seawater reacted with phosphoric acid is stripped of CO$_2$ by bubbling the nitrogen gas through a fine frit at the bottom of the stripping chamber. The CO$_2$ stripped in the chamber is carried by the nitrogen gas (flow rates of 140ml min^{-1}) to the coulometer through a dehydrating module. The module consists of two electric dehumidifiers (kept at 0.5 degC) and a chemical desiccant (Mg(ClO$_4$)$_2$).

The measurement sequence such as 2% CO$_2$ gas in a nitrogen base, system blank (phosphoric acid blank), and seawater samples (6 samples) was programmed to repeat. The measurement of 2% CO$_2$ gas was made to monitor response of coulometer solutions (from UIC, Inc.).

(3) Preliminary results

During the cruise, 547 samples were analyzed for DIC. A replicate analysis was performed at the interval decided beforehand and the difference between each pair of analyses was plotted on a range control chart (see Figure 1). The average of the differences was 1.0μmol/kg (n=52). The standard deviation was 0.9μmol/kg, which indicates that the analysis was accurate enough according to the guide (Dickson et al., 2007).

(4) Data Archive

All data will be submitted to JAMSTEC Data Integration and Analyses Group (DIAG) and is currently under its control.

(5) Reference
Dickson, A. G., Sabine, C. L. & Christian, J. R. (2007), Guide to best practices for ocean CO$_2$ measurements; PICES Special Publication 3, 199pp.
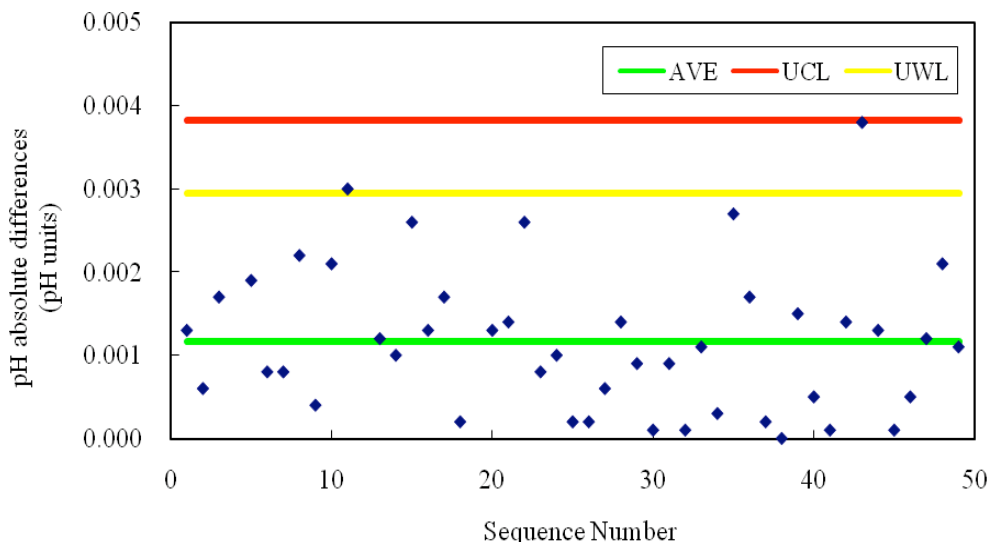
Fig. 1 Range control chart of the absolute differences of replicate measurements carried out in the analysis of DIC during the MR08-05 cruise. UCL and UWL represents the upper control limit (UCL=AVE*3.267) and upper warning limit (UWL=AVE*2.512), respectively.

2.8 Total Alkalinity

Masahide WAKITA (JAMSTEC)
Ayaka HATSUYAMA (MWJ)
Tomonori WATAI (MWJ)

(1) Objective

Since the global warming is becoming an issue world-widely, studies on green house gases such as CO_2 are drawing high attention. Because the ocean plays an important role in buffering the increase of atmospheric CO_2, surveys on the exchange of CO_2 between the atmosphere and the sea becomes highly important. When CO_2 dissolves in water, chemical reaction takes place and CO_2 alters its appearance into several species. Unfortunately, concentrations of the individual species of CO_2 system in solution cannot be measured directly. There are, however, four parameters that could be measured; total alkalinity, total dissolved inorganic carbon, pH and pCO_2. When two of the four parameters are measured, the concentration of CO_2 system in the water could be estimated (Dickson et al., 2007). We here report on-board measurements of total alkalinity performed during the MR08-05 cruise.

(2) Measured Parameters

Total Alkalinity, TA

(3) Apparatus and performance
(3)-1 Seawater sampling

Seawater samples were collected at 14 stations in 12L Niskin bottles mounted on the CTD system. Samples for TA analysis were transferred into 125 ml glass bottles (SCHOTT DURAN) using a sampling tube, filled from the bottom without rinsing, and overflowed for 10 seconds. These bottles were pre-washed by soaking in 5% non-phosphoric acid detergent (pH=13) for more than 3 hours and then rinsed 5 times with tap water and 3 times with Milli-Q deionized water. After the sampling, bottles filled with seawater sample were put in a water bath kept at 25 ℃ for one hour before the analysis.

(3)-2 Seawater analysis

Measurement of alkalinity was made using a spectrophotometric systems (Nippon ANS, Inc.).

The system comprises of water dispensing unit and a spectrophotometer (Cary 50 Scan, Varian). For an indicator, bromocresol green sodium (BCG) was used. Calculation of TA was made based on a single step acid addition procedure (Yao and Byrne, 1998).

Sample seawater of approx. 40 ml is transferred from a sample bottle into water-jacketed (25.00 ± 0.05 ℃) titration cell. Then, sample seawater circulated through the line between the titration and pH cells by a peristaltic pump. The length and volume of the pH cell are 8 cm and 13 ml, respectively. First, absorbencies of seawater itself were measured at three wavelengths (750, 616 and 444 nm). Then, 0.05 M HCl + 4×10^{-5} M BCG in 0.65 M NaCl solution was added using a titrator (Metrohm, Dosimat 765). The concentration of BCG in the final solution was approx. 2-3 μM. Then the solution was stirred and circulated through titration and pH cells with purging N_2 gas for 6 minutes to allow CO_2 degassing and to mix the acid-indicator solution and seawater sufficiently. After the pump was stopped, the absorbencies of solution were measured at the same wavelengths. The excess hydrogen ion concentration was

calculated based on the following equation (Yao and Byrne, 1998):

$$pH_T = 4.2699 + 0.002578(35 - S) + \log\left(\frac{A_{616}/A_{444} - 0.00131}{2.3148 - 0.1299(A_{616}/A_{444})}\right) - \log(1 - 0.01005S),$$

where A_{616}/A_{444} indicate absorbance ratio at 25°C and S is salinity of the sample. The alkalinity of a seawater sample that has been acidified and purged of CO_2 can written as follows:

$$A_T = \left[\left(N_A V_A - (H^+)_{ASW} \, dsw \, V_{ASW}\right)/V_{SW} \times 10^6\right]/dsw$$

where A_T is the alkalinity of a seawater sample (μmol/kg), N_A is the concentration of the added acid (mol/l), V_A is the volume of the added acid (ml), V_{SW} is the volume of the seawater sample (ml), $(H^+)_{ASW}$ is the excess hydrogen ion concentration in the acidified seawater (mol/kg), V_{ASW} is the volume of the acidified seawater calculated as $V_{SW} + V_A$ (ml), dsw is sample seawater density at 25°C and S.

The acid titrant was made from 0.6M HCl solution, calibrated by Na_2CO_3 using Gran's plot technique. The concentrations of two batches of acid titrant used during the cruise were 0.049974mol/l (batch:070621-3), calculated from concentration, volume and density of 0.6M HCl and the volume of flask.

(4) Preliminary results

A few replicate samples were taken at most of stations and the difference between each pair of analyses was plotted on a range control chart (see Figure 1). The average of the difference was 0.5μmol/kg (n=49). The standard deviation was 0.4μmol/kg, which indicates that the analysis was accurate enough according to the guide (Dickson et al., 2007).

(5) Data Archive

All data will be submitted to JAMSTEC and is currently under its control.

(6) References
Yao, W. and Byrne, R. H. (1998), Simplified seawater alkalinity analysis: Use of linear array spectrometers. Deep-Sea Research Part I, Vol. 45, 1383-1392.
Dickson, A. G., Sabine, C. L. & Christian, J. R. (2007), Guide to best practices for ocean CO2 measurements; PICES Special Publication 3, 199pp.

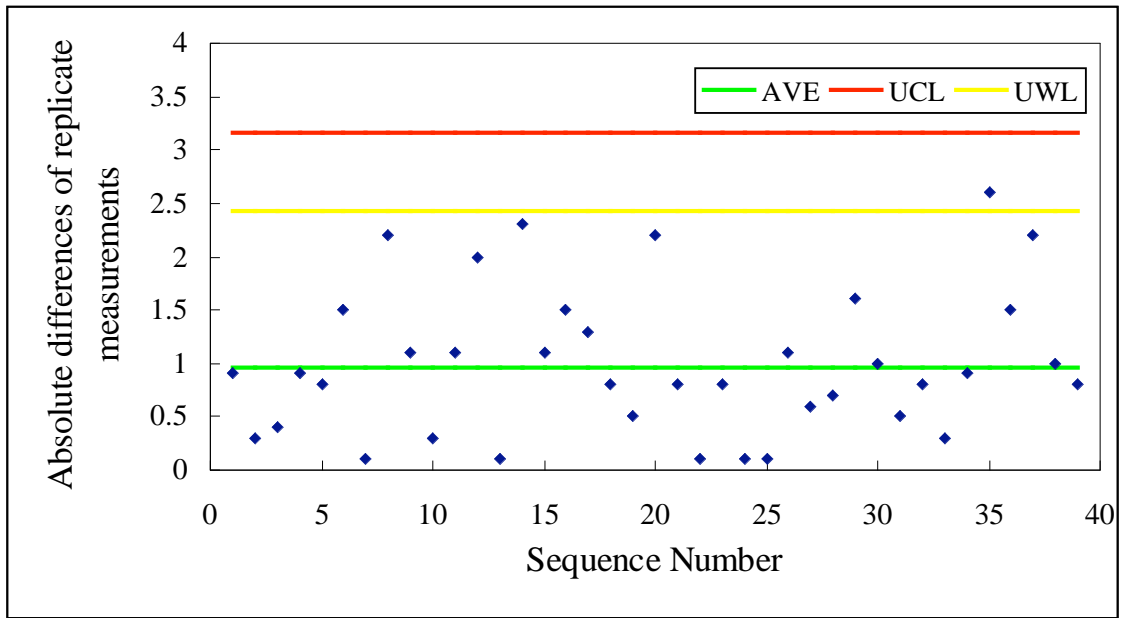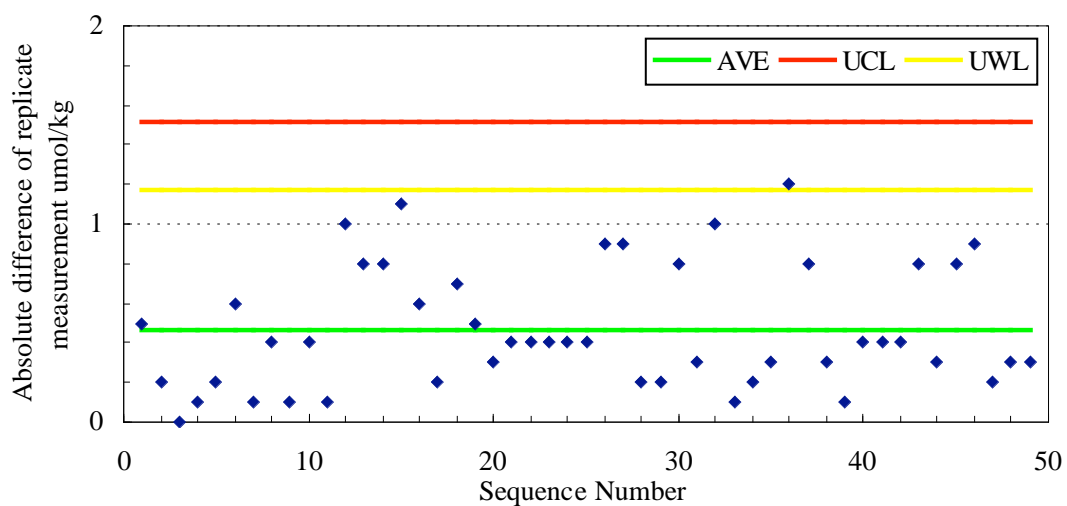Fig. 1 Range control chart of the absolute differences of replicate measurements of TA carried out during this cruise. UCL and UWL represents the upper control limit (UCL=AVE*3.267) and upper warning limit (UWL=AVE*2.512), respectively.

2.9 Underway pCO$_2$

Masahide WAKITA   **(JAMSTEC MIO)**
Yoshiko ISHIKAWA   **(MWJ)**
Yasuhiro ARII   **(MWJ)**

(1) Objectives

Concentrations of CO$_2$ in the atmosphere are now increasing at a rate of 1.5 ppmv y^{-1} owing to human activities such as burning of fossil fuels, deforestation, and cement production. It is an urgent task to estimate as accurately as possible the absorption capacity of the oceans against the increased atmospheric CO$_2$, and to clarify the mechanism of the CO$_2$ absorption, because the magnitude of the anticipated global warming depends on the levels of CO$_2$ in the atmosphere, and because the ocean currently absorbs 1/3 of the 6 Gt of carbon emitted into the atmosphere each year by human activities.

Since the global warming is becoming an issue world-widely, studies on green house gases such as CO$_2$ are drawing high attention. Because the ocean plays an important role in buffering the increase of atmospheric CO$_2$, surveys on the exchange of CO$_2$ between the atmosphere and the sea becomes highly important. When CO$_2$ dissolves in water, chemical reaction takes place and CO$_2$ alters its appearance into several species. Unfortunately, concentrations of the individual species of CO$_2$ system in solution cannot be measured directly. There are, however, four parameters that could be measured; total alkalinity, total dissolved inorganic carbon, pH and pCO$_2$. When more than two of the four parameters are measured, the concentration of CO$_2$ system in the water can be estimated (Dickson et al., 2007). We here report on board measurements of pCO$_2$ performed during MR08-05 cruise.

(2) Methods, Apparatus and Performance

Concentrations of CO$_2$ in the atmosphere and the sea surface were measured continuously during the cruise using an automated system with a non-dispersive infrared gas analyzer (NDIR; BINOS^{TM}).

The automated system was operated by on one and a half hour cycle. In one cycle, standard gasses, marine air and equilibrated air with surface seawater within the equilibrator were analyzed subsequently. The concentrations of the standard gas were 299.90, 349.99, 399.94 and 449.99 ppm.

To measure marine air concentrations (mol fraction) of CO$_2$ in dry air (xCO$_2$-air), marine air sampled from the bow of the ship (approx.30m above the sea level) was introduced into the NDIR by passing through a mass flow controller which controls the air flow rate at about 0.5 L/min, a cooling unit, a perma-pure dryer (GL Sciences Inc.) and a desiccant holder containing Mg(ClO$_4$)$_2$.

To measure surface seawater concentrations of CO$_2$ in dry air (xCO$_2$-sea), marine air equilibrated with a stream of seawater within the equilibrator was circulated with a pump at 0.7-0.8L/min in a closed loop passing through two cooling units, a perma-pure dryer and a desiccant holder containing Mg(ClO$_4$)$_2$. The seawater taken by a pump from the intake placed at the approx. 4.5m below the sea surface flowed at a rate of 5-6L/min in the equilibrator. After that, the equilibrated air was introduced into the NDIR.

(3) Preliminary results

Concentrations of CO_2 (xCO_2) of marine air and surface seawater are shown in Fig.1.
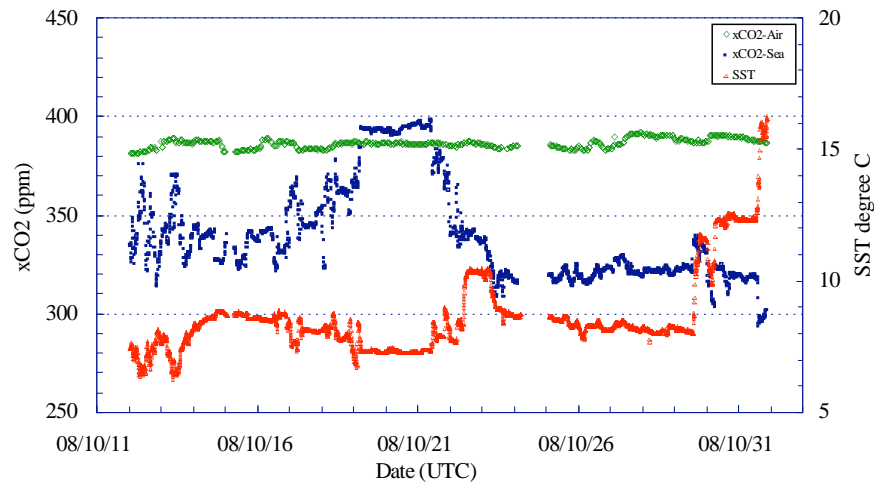
Fig. 1 Temporal changes of concentrations of CO_2 (xCO_2) in atmosphere (green) and surface seawater (blue), and SST (red).

(4) Data Archive

All data will be submitted to JAMSTEC and is currently under its control.

(5) Reference

Dickson, A. G., Sabine, C. L. & Christian, J. R. (2007), Guide to best practices for ocean CO_2 measurements; PICES Special Publication 3, 199pp.

3. Special Observation

3.1.1 Recovery and Deployment

Makio HONDA (JAMSTEC MIO)
Masaki TAGUCHI (MWJ)
Hiroshi MATSUNAGA (MWJ)
Tomoyuki TAKAMORI (MWJ)
Tatsuya TANAKA (MWJ)
Toru IDAI (MWJ) not on board

The one BGC mooring system was designed for biogeochemistry at Station K-2 in the Western Subarctic Gyre. We recovered BGC mooring, which was deployed at MR07-05, at Station K-2. It is 47N / 160E, where is close to station KNOT and, however, structure of water mass is more stable than station KNOT. Sea floor topography was surveyed with Sea Beam during MR01-K04 Leg.2. In order to place the top of mooring systems in the surface euphotic layer, precise water depths for mooring positions was measured by an altimeter (Datasonics PSA900D) mounted on CTD / CWS.

This BGC mooring system was re-deployed at Station K-2. Mooring works took approximately 5 hours for each mooring system. After sinker was dropped, we positioned the mooring systems by measuring the slant ranges between research vessel and the acoustic releaser. The position of the mooring is finally determined as follow:

Table 3.1.1-1 Mooring positions for respective mooring systems

	Recovery	Deployment
Station & type	K-2 BGC	K-2 BGC
Mooring Number	K2B070911	K2B081028
Date of deployment	Sep. 11th 2007	Oct. 28th 2008
Latitude	47$^°$ 00.27 N	47$^°$ 00.36 N
Longitude	159$^°$ 58.39 E	159$^°$ 58.16 E
Depth	5,206.2 m	5,206.2 m

The BGC mooring consists of a 64" syntactic top float with 3,000 lbs (1,360 kg) buoyancy, instruments, wire and nylon ropes, glass floats (Benthos 17" glass ball), dual releasers (Edgetech) and 4,660 lbs (2,116 kg). sinker with mace plate. Two ARGOS compact mooring locators and one submersible recovery strobe are mounted on the top float. This mooring system was planned 5,216.2 m depth to keep the following time-series observational instruments are mounted approximately 40 ~ 50 m below sea surface. It is 10 m longer than 5,206.2 m real depth because recovered depth sensor which was installed on the RAS shows 10 m deeper than our expected by mooring tilt.

On the recovered BGC mooring, two RAS (Remote Access Sampler) were installed on the 40 m and 200 m with Depth sensors (RIGO) and CT sensors (Arec). BLOOMS (Ocean Optical Sensor) was only installed on the RAS at 200 m. 5 Sediment Traps were installed on the 150 m, 300 m, 540 m, 1,000 m and 5,000 m.

On the deployment BGC mooring, two RAS (Remote Access Sampler) are installed on the 40 m and 200 m CTD (SBE-37) and DO sensors (Arec).   Extra CTD (SBE-37) and Do Sensor (Arec) are mounted on the dual acoustic releasers.   BLOOMS (Ocean Optical Sensor) is only installed on the RAS at 200 m.   4 Sediment Traps are installed on the 150 m, 540 m, 1,000 m and 5,000 m.

Details for each instrument are described later (section 3.1.2).   Serial numbers for instruments are as follows:

Table 3.1.1-2   Serial numbers of instruments

Recovery		Deployment	
Station and type	K-2 BGC	Station and type	K-2 BGC
Mooring Number	K2B070911	Mooring Number	K2B081028
ARGOS	18842 / 52112	ARGOS	18841 / 52111
ARGOS ID	18577 / 5374	ARGOS ID	18570 / 5373
Strobe	N02-044	Strobe	N02-043
RAS (40m)	ML11241-09	RAS (40m)	ML11241-07
BLOOMS	OCR-504-TCSW-57	BLOOMS	OCR-504-TCSW-57
RIGO Depth Sensor	DP1142	SBE-37	2755
AREC CT Sensor	1136	AREC DO sensor	002
RAS (200m)	ML11241-11	RAS (200m)	ML11241-08
RIGO Depth Sensor	DP1158	SBE-37	2756
AREC CT Sensor		AREC DO sensor	003
Sediment Trap×5		Sediment Trap×4	
Mark7-21 (150m)	878	Mark7-13 (150m)	ML11241-22
Mark7-13 (300m)	ML11241-22	Mark7-13 (540m)	ML11241-25
Mark7-13 (540m)	ML11241-25	Mark7-13(1000m)	ML11241-24
Mark7-13(1000m)	ML11241-24	Mark7-21(5000m)	989
Mark7-21(5000m)	989		
Releaser	027815	Releaser	027864
	027825	Releaser	027867
		SBE-37	2757
		AREC DO sensor	005

Table 3.1.1-3 Recovery BGC Mooring Record BGC Mooring

Mooring Number   K2B070911

Project	Time-Series	Depth	5,206.2	m
Area	North Pacific	Planned Depth	5,216.2	m
Station	K-2 BGC	Length	5,186.0	m
Target Position	**47°00.350** N	Depth of Buoy	30	m
	159°58.326 E	Period	1	year
ACOUCTIC RELEASERS				
Type	Edgetech	Edgetech		
Serial Number	27815	27825		
Receive F.	11.0 kHz	11.0 kHz		
Transmit F.	12.0 kHz	12.0 kHz		
RELEASE C.	**344657**	**344176**		
Enable C.	361035	356736		
Disable C.	361073	356770		
Battery	2 year	2 year		
Release Test	FINE	FINE		
RECOVERY				
Recorder	Tatsuya Tanaka	Work Distance	1.4	Nmile
Ship	R/V MIRAI	Send Enable C.	19:11	
Cruise No.	MR08-05	Slant Renge	-	msec
Date	2008/10/25	Send Release C.	19:43	
Weather	C	Discovery Buoy	19:43	
Wave Hight	2.3 m	Pos. of Top Buoy	47°00.36	N
Depth	5214 m		159°58.20	E
Ship Heading	<008>	Pos. of Start	47°00.75	N
Ship Ave.Speed	0.5 knot		159°58.39	E
Wind	<185> 7.1 m/s	Pos. of Finish	47°02.12	N
Current	<015> 0.5 knot		159°59.05	E

Note: 10/24 19:11 Although sent enable command from ship's SSBL, no response. Then send a signal from after deck using a transduser and confirm wake up and release successfully.

Table 3.1.1-4 Recovery BGC Mooring Working Time Record

MOORING NO.　K2B070911　　　　DATE 2008/10/24　　　Name : T.Tanaka

I T E M	S/N	Switch		On deck		Note
Top Buoy 015162-02	A:18842/52112	☑		☑	21:34	
ARGOS and Flasher		☑		☑		I
5m 3/4" PC Chain						G
RAS	ML11241-09	☑		☑	21:34	
Depth & Arec CT Sensor	DP1142/1136	☑		☑		ZE
3-TON Swivel						E
106 m 5/16" Wire	B	☑				MX
3m 5/16' Wire Coated	TRAP01	☑				L
Sediment Trap_150m	878	☑		☑	21:48	D
1.5m 16mm T-Chain						E
40m 5/16" Wire	C-2	☑				E
3m 5/16' Wire Coated	RAS01	☑				EZ
RAS	ML11241-11	☑		☑	21:56	
Depth Sensor	DP1158	☑		☑		E
3-TON Swivel						E
94m 5/16" Wire	G-01	☑				M
3m 5/16" Wire Coated	TRAP02	☑				L
Sediment Trap_300m	ML11241-22	☑		☑	22:03	XD
5m 16mm T-Chain						E
183m 5/16" Wire	S-05	☑				E
50m 5/16" Wire Coated	I-4	☑				L
Sediment Trap_540m	ML11241-25	☑		☑	22:18	XD
5m 16mm T-Chain						E
403m 5/16" Wire	F	☑				E
43m 5/16" Wire	DK	☑				M
3m 5/16" Wire Coated	TRAP04	☑				M
Sediment Trap_1000m	ML11241-24	☑		☑	22:36	YD
2m 16mm T-Chain						E
3-TON Swivel						B
500m 1/4" Wire	B-6	☑				A
500m 1/4" Wire	B-7	☑			22:48	B
(8) 17" Glass Balls					23:00	FC
500m 1/4" Wire	B-8	☑				A
500m 1/4" Wire	D	☑			23:12	B
(8) 17" Glass Balls					23:22	FC
368m 1/4" Wire	T	☑				A
200m 1/4" Wire	P-05	☑				A
100m 1/4" Wire	NN	☑			23:36	A
100m 1/4" Wire	LL	☑			23:40	A
100m 1/4" Wire	KK	☑			23:43	A
(14) 17" Glass Balls					23:50	B
472m 1/4" Wire	C	☑				FFFC
368m 1/4" Wire	U	☑			23:59	A
50m 1/4" Wire	E-2	☑			0:06	A
3m 5/16" Wire Coated	TRAP05	☑				K
Sediment Trap_4810m	989	☑		☑	0:10	K
2m 16mm T-Chain						YD
300m 1/4" Wire	BB-05	☑				B
5m 16mm T-Chain						C
(48) 17" Glass Balls					0:21	F
5m 16mm T-Chain						FFFF
3-TON Swivel						G
Dual Releases	27815	☑		☑	0:24	J
	27825	☑		☑		

Notes:
- B-7 & B-8 were tangled. cut & connected B-7 & B-8 directly
- D & T were tangled. Cut & connected D & T directly
- KK & C were tangled. cut & connected D & T directly
- BB-5 & Glass Balls were tangled

Table 3.1.1-5 detail of Recovery BGC Mooring system.

#	Mooring ID / Description	S/N	Joint	Depth Item Length (m)	Item Weight (kg)	Mooring Length (m)	Mooring Weight (kg)	Above Bottom (m)	Mooring Depth (m)	
1	64" Syntatic Sphere			2.27	-1360.78		-1360.78	5185.73	30.47	30
2	Hardware		I	0.28	3.63	2.55	-1357.15	5183.46	32.74	
3	**5** Meters 3/4" Proof Coil Chain			5.00	40.01	7.55	-1317.14	5183.18	33.02	
4	Hardware		G	0.25	2.40	7.80	-1314.74	5178.18	38.02	
5	Instrument - "RAS"	ML11241-09	Z	2.25	51.00	10.05	-1263.74	5177.93	38.27	
6	Hardware		E	0.24	2.00	10.29	-1261.74	5175.68	40.52	
7	3-TON Miller Swivel			0.16	3.17	10.45	-1258.57	5175.45	40.75	
8	Hardware		E	0.24	2.00	10.68	-1256.57	5175.29	40.91	
9	**106** Meters 5/16" Wire	B		106.19	22.64	116.87	-1233.93	5175.05	41.15	
10	Hardware		M	0.24	1.93	117.11	-1232.00	5068.86	147.34	
11	**3** Meters 5/16" Wire Coated	TRAP01		3.00	0.64	120.11	-1231.36	5068.63	147.57	
12	Hardware		L	0.24	2.19	120.35	-1229.17	5065.63	150.57	
13	Sediment Trap	878	X	3.57	55.68	123.92	-1173.49	5065.39	150.81	150
14	Hardware		D	0.06	2.00	123.98	-1171.49	5061.82	154.38	
15	**1.5** Meters 16mm T-Chain			1.50	8.34	125.48	-1163.15	5061.76	154.44	
16	Hardware		E	0.24	2.00	125.71	-1161.15	5060.26	155.94	
17	**40** Meters 5/16" Wire	C-2		40.07	8.54	165.78	-1152.61	5060.02	156.18	
18	Hardware		E	0.24	1.93	166.02	-1150.68	5019.95	196.25	
19	**3** Meters 5/16" Wire Coated	RAS01		3.00	0.64	169.02	-1150.04	5019.72	196.48	
20	Hardware		E	0.24	2.00	169.25	-1148.04	5016.72	199.48	
21	Instrument - "RAS"	ML11241-11	Z	2.43	51.00	171.68	-1097.04	5016.48	199.72	200
22	Hardware		E	0.24	2.00	171.92	-1095.04	5014.05	202.15	
23	3-TON Miller Swivel			0.16	3.17	172.08	-1091.87	5013.82	202.38	
24	Hardware		E	0.24	2.00	172.31	-1089.87	5013.66	202.55	
25	**94** Meters 5/16" Wire	G-1		94.15	20.07	266.46	-1069.80	5013.42	202.78	
26	Hardware		M	0.24	1.93	266.70	-1067.87	4919.27	296.93	
27	**3** Meters 5/16" Wire Coated	TRAP02		3.00	0.64	269.70	-1067.23	4919.04	297.16	
28	Hardware		L	0.24	2.19	269.94	-1065.04	4916.04	300.16	
29	Sediment Trap	ML11241-22	X	3.70	55.70	273.64	-1009.34	4915.80	300.40	300
30	Hardware		D	0.06	2.00	273.70	-1007.34	4912.10	304.10	
31	**1.5** Meters 16mm T-Chain			1.50	8.34	275.20	-999.00	4912.04	304.16	
32	Hardware		E	0.24	2.00	275.43	-997.00	4910.54	305.66	
33	**183** Meters 5/16" Wire	S-05		183.60	39.14	459.03	-957.86	4910.30	305.90	
34	Hardware		E	0.24	2.00	459.27	-955.86	4726.70	489.50	
35	**50** Meters 5/16" Wire with eal	I-4		50.07	10.68	509.34	-945.18	4726.47	489.73	
36	Hardware		L	0.24	2.19	509.58	-942.99	4676.40	539.81	
37	Sediment Trap	ML11241-25	X	3.69	55.70	513.27	-887.29	4676.16	540.05	540
38	Hardware		D	0.06	2.00	513.33	-885.29	4672.47	543.74	
39	**5** Meters 16mm T-Chain			5.00	27.80	518.33	-857.49	4672.41	543.80	
40	Hardware		E	0.24	2.00	518.56	-855.49	4667.41	548.80	
41	**403** Meters 5/16" Wire	F		403.72	86.07	922.28	-769.42	4667.17	549.03	
42	Hardware		E	0.24	2.00	922.52	-767.42	4263.45	952.75	
43	**43** Meters 5/16" Wire	DK		43.55	9.28	966.07	-758.14	4263.22	952.98	
44	Hardware		M	0.24	1.93	966.30	-756.21	4219.67	996.53	
45	**3** Meters 5/16" Wire Coated	TRAP04		3.00	0.64	969.30	-755.57	4219.43	996.77	
46	Hardware		M	0.24	2.19	969.54	-753.38	4216.43	999.77	
47	Sediment Trap	ML11241-24	Y	3.95	55.70	973.49	-697.68	4216.19	1000.01	1000
48	Hardware		D	0.06	2.00	973.55	-695.68	4212.24	1003.96	
49	**2** Meters 16mm T-Chain			2.00	11.12	975.55	-684.56	4212.18	1004.02	
50	Hardware		E	0.24	2.00	975.79	-682.56	4210.18	1006.02	
51	3-TON Miller Swivel			0.16	3.17	975.95	-679.39	4209.95	1006.25	

#	Description	Code		Value	Value	Value	Value	Value	Value	
52	Hardware		B	0.23	1.65	976.18	-677.74	4209.79	1006.41	
53	**500** Meters 1/4" Wire	B-6		501.36	70.50	1477.53	-607.24	4209.56	1006.64	
54	Hardware		A	0.21	1.33	1477.74	-605.91	3708.20	1508.00	
55	**500** Meters 1/4" Wire	B-7		501.34	70.50	1979.09	-535.42	3707.99	1508.21	
56	Hardware		B	0.23	1.65	1979.32	-533.77	3206.65	2009.55	
57	4-17" Glassballs on 16mm T-Chain			4.00	-79.36	1983.32	-613.13	3206.42	2009.78	
58	Hardware		F	0.24	2.00	1983.55	-611.13	3202.42	2013.78	
59	4-17" Glassballs on 16mm T-Chain			4.00	-79.36	1987.55	-690.49	3202.18	2014.02	
60	Hardware		C	0.24	1.65	1987.79	-688.84	3198.18	2018.02	
61	**500** Meters 1/4" Wire	B-8		501.33	70.49	2489.12	-618.34	3197.94	2018.26	
62	Hardware		A	0.21	1.33	2489.33	-617.01	2696.62	2519.58	
63	**500** Meters 1/4" Wire	D		501.31	70.49	2990.63	-546.52	2696.41	2519.79	
64	Hardware		B	0.23	1.65	2990.86	-544.87	2195.10	3021.10	
65	4-17" Glassballs on 16mm T-Chain			4.00	-79.36	2994.86	-624.23	2194.87	3021.33	
66	Hardware		F	0.24	2.00	2995.10	-622.23	2190.87	3025.33	
67	4-17" Glassballs on 16mm T-Chain			4.00	-79.36	2999.10	-701.59	2190.64	3025.56	
68	Hardware		C	0.24	1.65	2999.34	-699.94	2186.64	3029.56	
69	**368** Meters 1/4" Wire	T		368.90	51.87	3368.24	-648.07	2186.40	3029.80	
70	Hardware		A	0.21	1.33	3368.45	-646.74	1817.50	3398.70	
71	**200** Meters 1/4" Wire	P-05		200.84	28.24	3569.29	-618.50	1817.29	3398.91	
72	Hardware		A	0.21	1.33	3569.50	-617.17	1616.45	3599.76	
73	**100** Meters 1/4" Wire	NN		99.95	14.05	3669.45	-603.11	1616.24	3599.97	
74	Hardware		A	0.21	1.33	3669.66	-601.78	1516.29	3699.91	
75	**100** Meters 1/4" Wire	LL		100.03	14.07	3769.69	-587.72	1516.08	3700.12	
76	Hardware		A	0.21	1.33	3769.90	-586.39	1416.05	3800.15	
77	**100** Meters 1/4" Wire	KK		100.02	14.06	3869.92	-572.32	1415.84	3800.36	
78	Hardware		B	0.23	1.65	3870.15	-570.67	1315.81	3900.39	
79	2-17" Glassballs on 16mm T-Chain			2.00	-39.68	3872.15	-610.35	1315.58	3900.62	
80	Hardware		F	0.24	2.00	3872.39	-608.35	1313.58	3902.62	
81	4-17" Glassballs on 16mm T-Chain			4.00	-79.36	3876.39	-687.71	1313.35	3902.85	
82	Hardware		F	0.24	2.00	3876.62	-685.71	1309.35	3906.85	
83	4-17" Glassballs on 16mm T-Chain			4.00	-79.36	3880.62	-765.07	1309.11	3907.09	
84	Hardware		F	0.24	2.00	3880.86	-763.07	1305.11	3911.09	
85	4-17" Glassballs on 16mm T-Chain			4.00	-79.36	3884.86	-842.43	1304.88	3911.32	
86	Hardware		C	0.24	1.65	3885.10	-840.78	1300.88	3915.32	
87	**472** Meters 1/4" Wire	C		472.25	66.40	4357.35	-774.38	1300.64	3915.56	
88	Hardware		A	0.21	1.33	4357.56	-773.05	828.39	4387.81	
89	**368** Meters 1/4" Wire	U		368.98	51.88	4726.54	-721.17	828.18	4388.02	
90	Hardware		A	0.21	1.33	4726.75	-719.84	459.20	4757.00	
91	**50** Meters 1/4" Wire	E-2		50.13	7.05	4776.87	-712.79	458.99	4757.21	
92	Hardware		K	0.20	1.33	4777.07	-711.46	408.86	4807.34	
93	**3** Meters 1/4" Wire Coated	TRAP05		3.00	0.42	4780.07	-711.04	408.66	4807.54	
94	Hardware		K	0.20	1.33	4780.27	-709.71	405.66	4810.54	
95	Sediment Trap	989	Y	3.82	55.70	4784.09	-654.00	405.46	4810.74	**4810.8**
96	Hardware		D	0.06	2.00	4784.15	-652.00	401.64	4814.56	
97	**2** Meters 16mm T-Chain			2.00	11.12	4786.15	-640.88	401.58	4814.62	
98	Hardware		B	0.23	1.65	4786.38	-639.23	399.58	4816.62	
99	**300** Meters 1/4" Wire	BB-05		301.55	42.40	5087.94	-596.83	399.35	4816.85	
100	Hardware		C	0.24	1.65	5088.18	-595.18	97.80	5118.40	
101	5 Meters 16mm T-Chain			5.00	27.80	5093.18	-567.38	97.56	5118.64	
102	Hardware		F	0.24	2.00	5093.41	-565.38	92.56	5123.64	
103	4-17" Glassballs on 16mm T-Chain			4.00	-79.36	5097.41	-644.74	92.32	5123.88	
104	Hardware		F	0.24	2.00	5097.65	-642.74	88.32	5127.88	
105	4-17" Glassballs on 16mm T-Chain			4.00	-79.36	5101.65	-722.10	88.09	5128.11	
106	Hardware		F	0.24	2.00	5101.88	-720.10	84.09	5132.11	
107	4-17" Glassballs on 16mm T-Chain			4.00	-79.36	5105.88	-799.46	83.85	5132.35	
108	Hardware		F	0.24	2.00	5106.12	-797.46	79.85	5136.35	
109	4-17" Glassballs on 16mm T-Chain			4.00	-79.36	5110.12	-876.82	79.62	5136.58	

110	Hardware	F	0.24	2.00	5110.35	-874.82	75.62	5140.58		
111	4-17" Glassballs on 16mm T-Chain		4.00	-79.36	5114.35	-954.18	75.38	5140.82		
112	Hardware	F	0.24	2.00	5114.59	-952.18	71.38	5144.82		
113	4-17" Glassballs on 16mm T-Chain		4.00	-79.36	5118.59	-1031.54	71.15	5145.05		
114	Hardware	F	0.24	2.00	5118.82	-1029.54	67.15	5149.05		
115	4-17" Glassballs on 16mm T-Chain		4.00	-79.36	5122.82	-1108.90	66.91	5149.29		
116	Hardware	F	0.24	2.00	5123.06	-1106.90	62.91	5153.29		
117	4-17" Glassballs on 16mm T-Chain		4.00	-79.36	5127.06	-1186.26	62.68	5153.52		
118	Hardware	F	0.24	2.00	5127.29	-1184.26	58.68	5157.52		
119	4-17" Glassballs on 16mm T-Chain		4.00	-79.36	5131.29	-1263.62	58.44	5157.76		
120	Hardware	F	0.24	2.00	5131.53	-1261.62	54.44	5161.76		
121	4-17" Glassballs on 16mm T-Chain		4.00	-79.36	5135.53	-1340.98	54.21	5161.99		
122	Hardware	F	0.24	2.00	5135.76	-1338.98	50.21	5165.99		
123	4-17" Glassballs on 16mm T-Chain		4.00	-79.36	5139.76	-1418.34	49.97	5166.23		
124	Hardware	F	0.24	2.00	5140.00	-1416.34	45.97	5170.23		
125	4-17" Glassballs on 16mm T-Chain		4.00	-79.36	5144.00	-1495.70	45.74	5170.46		
126	Hardware	F	0.24	2.00	5144.23	-1493.70	41.74	5174.46		
127	5 Meters 16mm T-Chain		5.00	27.80	5149.23	-1465.90	41.50	5174.70		
128	Hardware	F	0.24	2.00	5149.46	-1463.90	36.50	5179.70		
129	3-TON Miller Swivel		0.16	3.20	5149.63	-1460.70	36.27	5179.93		
130	Hardware	G	0.25	2.40	5149.88	-1458.30	36.11	5180.09		
131	Dual EGG Acoustic Releases	J	1.95	66.04	5151.82	-1392.26	35.86	5180.34		
132	Hardware	G	0.25	2.40	5152.07	-1389.86	33.91	5182.29		
133	5 Meters 16mm T-Chain		5.00	27.80	5157.07	-1362.06	33.66	5182.54		
134	Hardware	H	0.26	2.85	5157.33	-1359.21	28.66	5187.54		
135	**20** Meters 1" Nylon		21.92	6.54	5179.25	-1352.67	28.40	5187.80		
136	Hardware	H	0.26	2.85	5179.51	-1349.82	6.48	5209.72		
137	5 Meters 16mm T-Chain		5.00	27.80	5184.51	-1322.02	6.22	5209.98		
138	Hardware	H	0.26	2.40	5184.77	-1319.62	1.22	5214.98	**Design**	
139	4666 Lb Ww Anchor		0.96	2116.46	5185.73	796.84	0.96	5215.24	**Depth**	
	OVERALL MOORING LENGTH		**5185.73**					5216.20	**5216.2**	

Fig. 3.1.1-1 Recovery BGC Mooring Figure

Column 1

30 m -
Light [N02-042]
Double ARGOS [18842 / 52112]
64" Syntactic Sphere [015162]
3/4" SH
7/8" END Link
3/4" SH
5 m 3/4" PC Chain
3/4" SH
3/4" SL
5/8" SH
RAS [ML11241-09]
Bloom [OCR-504-TCSW-57]
Depth Sensor [DP1142]   540 m -
(4) 1m Chain Bridal
5/8" SH
5/8" SL
5/8" SH
3 ton Swivel
5/8" SH
5/8" SL
5/8" SH
106 m 5/16" Wirerope [B]
5/8" SS SH
3/4" SS SL
5/8" SS SH
3 m 5/16" Wirerope [TRAP01]
5/8" SS SH
3/4" SS SL
150m -
(3) 1m Titanium Bridal
Sediment Trap [878]
(3) 1 m 3/8" Chain Bridal
5/8" SH
1.5 m 16mm T-Chain
5/8" SH
5/8" SL
5/8" SH
40 m 5/16" Wirerope [C-2]
5/8" SH
5/8" SL
5/8" SH
3 m 5/16" Wirerope [RAS01]
5/8" SH
5/8" SL
5/8" SH
200m -
RAS [ML11241-11]
Depth Sensor [DP1158]
(4) 1m Chain Bridal
5/8" SH
5/8" SL
5/8" SH
3 ton Swivel
5/8" SH
5/8" SL
5/8" SH
94 m 5/16" Wirerope [G-01]
5/8" SS SH
3/4" SS SL
5/8" SS SH
3 m 5/16" Wirerope [TRAP02]
5/8" SS SH
3/4" SS SL
300 m -
(3) 1m Titanium Bridal
Sediment Trap [ML11241-22]
(3) 1 m 3/8" Chain Bridal
5/8" SH

Column 2

1.5 m 16mm T-Chain
5/8" SH
5/8" SL
5/8" SH
183 m 5/16" Wirerope [S-05]
5/8" SH
5/8" SL
50 m 5/16" Wirerope
(Coated) with eal Grip [I-4]
5/8" SS SH
3/4" SS SL
(3) 1m TitaniumBridal
Sediment Trap [ML11241-25]
(3) 1 m 3/8" Chain Bridal
5/8" SH
5 m 16mm T-Chain
5/8" SH
5/8" SL
5/8" SH
403 m 5/16" Wirerope [F]
5/8" SH
5/8" SL
5/8" SH
43 m 5/16" Wirerope [DK]
5/8" SS SH
3/4" SS SL
5/8" SS SH
3 m 5/16" Wirerope [TRAP04]
5/8" SS SH
3/4" SS SL
5/8" SS SH
(3) 1m Wire Bridal
Sediment Trap [ML11241-24]
1,000m -
(3) 1 m 3/8" Chain Bridal
5/8" SH
2 m 16mm T- Chain
5/8" SH
5/8" SL
5/8" SH
3 ton Swivel
5/8" SH
5/8" SL
1/2" SH
500 m 1/4" Wirerope [B-6]
1/2" SH
5/8" SL
1/2" SH
500 m 1/4" Wirerope [B-7]
1/2" SH
5/8" SL
1/2" SH
(4) 17" Glass Balls
on 16mm T-Chain
5/8" SH
3/4" SL
5/8" SH
(4) 17" Glass Balls
on 16mm T-Chain
5/8" SH
3/4" SL
1/2" SH
500 m 1/4" Wirerope [B-8]

Column 3

1/2" SH
5/8" SL
1/2" SH
500 m 1/4" Wirerope [D]
1/2" SH
5/8" SL
5/8" SH
(4) 17" Glass Balls
on 16mm T-Chain
5/8" SH
3/4" SL
5/8" SH
(4) 17" Glass Balls
on 16mm T-Chain
5/8" SH
3/4" SL
1/2" SH
368 m 1/4" Wirerope [T]
1/2" SH
5/8" SL
1/2" SH
200 m 1/4" Wirerope [P-05]
1/2" SH
5/8" SL
1/2" SH
100 m 1/4" Wirerope [NN]
1/2" SH
5/8" SL
1/2" SH
100 m 1/4" Wirerope [LL]
1/2" SH
5/8" SL
1/2" SH
100 m 1/4" Wirerope [KK]
1/2" SH
5/8" SL
5/8" SH
(2) 17" Glass Balls
on 16mm T-Chain
5/8" SH
3/4" SH
5/8" SH
(4) 17" Glass Balls
on 16mm T-Chain
5/8" SH
3/4" SH
5/8" SH
(4) 17" Glass Balls
on 16mm T-Chain
5/8" SH
3/4" SL
5/8" SH
(4) 17" Glass Balls
on 16mm T-Chain
5/8" SH
3/4" SL
1/2" SH
472 m 1/4" Wirerope [C]
1/2" SH
5/8" SL
1/2" SH
368 m 1/4" Wirerope [U]
1/2" SH
5/8" SL
1/2" SH

Column 4

50 m 1/4" Wirerope [E-2]
1/2" SS SH
3/4" SS SL
1/2" SS SH
3 m 5/16" Wirerope [TRAP05]
1/2" SS SH
3/4" SS SL
1/2" SS SH
(3) 1m Wire Bridal
Sediment Trap [989]
(3) 1 m 3/8" Bridal
5/8" SH
2 m 16mm T-Chain
5/8" SH
5/8" SL
1/2" SH
300 m 1/4" Wirerope [BB-05]
1/2" SH
3/4" SL
5/8" SH
5 m 16mm T- Chain
5/8" SH
3/4" SL
5/8" SH
(4) 17" Glass Balls
on 16mm T-Chain   ×12
5/8" SH
3/4" SL
5/8" SH
5 m 16mm T- Chain
5/8" SH
3/4" SL
5/8" SH
3 ton Swivel
5/8" SH
3/4" SL
3/4" SH
Dual Edgetech Releases
[27815 / 27825]
1/2" Trawler Chain
Master Link
3/4" SH
3/4" SL
5 m 16mm T-Chain
5/8" SH
3/4" SL
7/8" SH
20 m 1" Nylon
7/8" SH
3/4" SL
5/8" SH
5 m 16mm T-Chain
5/8" SH
3/4" SL
7/8" SH
2.28 ton Anchor
Water Depth = 5206.2 m

JPAC NW-PACIFIC **BGC MEX** MOORING

Station **K-2**, 5206.2m
MR07-05 設置

Table 3.1.1-6 Deployment BGC Mooring Record

Mooring Number	K2B081028			
Project	Time-Series	Depth	5,206.2	m
Area	North Pacific	Planned Depth	5,216.2	m
Station	K-2 BGC	Length	5,186.0	m
Target Position	**47°00.350** N	Depth of Buoy	30	m
	159°58.326 E	Period	1	year
ACOUCTIC RELEASERS				
Type	Edgetech	Edgetech		
Serial Number	27864	27867		
Receive F.	11.0 kHz	11.0 kHz		
Transmit F.	14.0 kHz	14.0 kHz		
RELEASE C.	**344421**	**344573**		
Enable C.	357724	360536		
Disable C.	357762	360570		
Battery	2 years	2 years		
Release Test	OK	OK		
DEPLOYMENT				
Recorder	Tatsuya Tanaka	Start	7.3	Nmile
Ship	R/V MIRAI	Overshoot	531	m
Cruise No.	MR08-05	Let go Top Buoy	21:08	
Date	2008/10/28	Let go Anchor	1:13	
Weather	C to bc	Sink Top Buoy	2:02	
Wave Hight	2.5 m	Pos. of Start	47°07.00	N
Depth	5220 m		159°54.96	E
Ship Heading	<161>	Pos. of Drop. Anc.	47°00.03	N
Ship Ave.Speed	1.8 knot		159°58.46	E
Wind	<150> 5.9 m/s	Pos. of Mooring	47°00.36	N
Current	<170> 0.5 cm/sec		159°58.16	E

Table 3.1.1-7 Deployment BGC Mooring Working Time Record

MOORING NO. K2B081028   DATE 2008/10/28   Name : T.Tanaka

I T E M	S/N		Switch		TIME			DAMAGE	PIN	Note
Top Buoy 015162-02	A:18841/52111	✓	20:05	✓	21:08					
ARGOS and *Flasher*	F:N02-043	✓	20:55	✓		I	✓	✓	✓	
5m 16mm T-Chain		✓				G	✓	✓	✓	
RAS	ML11241-07	✓	10/28	☐	21:08					
SBE37	2755	✓	01:00	✓						
DO	002	✓	01:00	✓		ZE	✓	✓	✓	
3-TON Swivel		✓				E	✓	✓	✓	
106 m 5/16" Wire	T08-C	✓				E	✓	✓	✓	
3m 5/16" Wire Coated	TRAP03	✓				LX	✓	✓	✓	
Sediment Trap_150m	ML11241-22	✓		☐	21:17	D	✓	✓	✓	
2.2 m 13mm Strong-Chain		✓				E	✓	✓	✓	
40m 5/16" Wire	T08-E1	✓				E	✓	✓	✓	
3m 5/16" Wire Coated	RAS01	✓								
RAS	ML11241-08	✓	10/28	☐		EZ	✓	✓	✓	
SBE37	2756	✓	01:00	✓	21:21					
DO	003	✓	01:00	✓		E	✓	✓	✓	
3-TON Swivel		✓				E	✓	✓	✓	
94m 5/16" Wire	G-2	✓				E	✓	✓	✓	
3m 5/16" Wire Coated	TRAP05	✓				L	✓	✓	✓	
5 m 16mm T-Chain		✓				E	✓	✓	✓	
230m 5/16" Wire	T08-B	✓				E	✓	✓	✓	
3m 5/16" Wire Coated	TRAP04	✓				L	✓	✓	✓	
Sediment Trap_540m	ML11241-25	✓		✓	21:35	XD	✓	✓	✓	
1.6 m 13mm Strong-Chain		✓				E	✓	✓	✓	
450m 5/16" Wire	T08-A	✓				E	✓	✓	✓	
3m 5/16" Wire Coated	TRAP02	✓				L	✓	✓	✓	
Sediment Trap_1000m	ML11241-24	✓		✓	21:48	YD	✓	✓	✓	
4 m 16mm T-Chain		✓				E	✓	✓	✓	
3-TON Swivel		✓				B	✓	✓	✓	
500m 1/4" Wire	T08-F1	✓			21:57	A	✓	✓	✓	
500m 1/4" Wire	T08-F2	✓				B	✓	✓	✓	
(8) 17" Glass Balls		✓			22:09	FC	✓	✓	✓	
500m 1/4" Wire	T08-F3	✓			22:17	A	✓	✓	✓	
500m 1/4" Wire	T08-F4	✓				B	✓	✓	✓	
(8) 17" Glass Balls		✓			22:27	FC	✓	✓	✓	
500m 1/4" Wire	T08-F5	✓			22:35	A	✓	✓	✓	
500m 1/4" Wire	T08-F6	✓				B	✓	✓	✓	
(12) 17" Glass Balls		✓			22:46	FFC	✓	✓	✓	
500m 1/4" Wire	T08-F7	✓			22:55	A	✓	✓	✓	
200m 1/4" Wire	T08-H1	✓			23:02	A	✓	✓	✓	
50m 1/4" Wire	T08-I	✓				A	✓	✓	✓	
5m 1/4" Wire	adj.	✓				A	✓	✓	✓	
3m 5/16" Wire Coated	TRAP01	✓				L	✓	✓	✓	
Sediment Trap_4810m	989	✓		✓	23:08	YD	✓	✓	✓	
7 m 16mm T-Chain		✓				B	✓	✓	✓	
300m 1/4" Wire	T08-G	✓				C	✓	✓	✓	
5m 16mm T-Chain		✓				FFFF	✓	✓	✓	
(44) 17" Glass Balls		✓			23:25	F	✓	✓	✓	
5m 16mm T-Chain		✓				F	✓	✓	✓	
3-TON Swivel		✓								
Release 01	27864	✓	20:48	✓		G	✓	✓	✓	
Release 02	27867	✓		☐	23:06					
CTD	2757	✓	01:00	✓						
DO	005	✓	01:00	✓		JG	✓	✓	✓	
5m 16mm T-Chain		✓				H	✓	✓	✓	
20m 1" Nylon		✓				H	✓	✓	✓	
5m 16mm T-Chain		✓				H	✓	✓	✓	
2.28 ton Mace Anchor		✓			1:13					

Table 3.1.1-8 detail of deployment BGC Mooring system.

	Description	S/N	Joint	Item Length (m)	Item Weight (kg)	Mooring Length (m)	Mooring Weight (kg)	Above Bottom (m)	Mooring Depth (m)	
1	64" Syntatic Sphere			2.27	-1360.78		-1360.78	5185.72	30.48	**30**
2	Hardware		I	0.28	3.63	2.55	-1357.15	5183.45	32.75	
3	**5** Meters 16mm T-Chain			5.00	27.80	7.55	-1329.35	5183.17	33.03	
4	Hardware		G	0.25	2.40	7.80	-1326.95	5178.17	38.03	
5	Instrument - "RAS"	ML11241-07	Z	2.30	51.00	10.10	-1275.95	5177.92	38.28	
6	Hardware		E	0.24	2.00	10.34	-1273.95	5175.62	40.58	
7	3-TON Miller Swivel			0.16	3.17	10.50	-1270.78	5175.38	40.82	
8	Hardware		E	0.24	2.00	10.73	-1268.78	5175.22	40.98	
9	**106** Meters 5/16" Wire	T08-C		106.20	22.64	116.93	-1246.14	5174.99	41.21	
10	Hardware		E	0.24	1.93	117.17	-1244.21	5068.79	147.41	
11	**3** Meters 5/16" Wire Coated	TRAP03		3.00	0.64	120.17	-1243.57	5068.55	147.65	
12	Hardware		L	0.24	2.19	120.41	-1241.38	5065.55	150.65	
13	Sediment Trap	ML11241-22	X	3.57	55.68	123.98	-1185.69	5065.31	150.89	**150**
14	Hardware		D	0.06	2.00	124.04	-1183.69	5061.74	154.46	
15	**2.2** Meters 13mm Strong-Chain			2.20	5.65	126.24	-1178.04	5061.68	154.52	
16	Hardware		E	0.24	2.00	126.47	-1176.04	5059.48	156.72	
17	**40** Meters 5/16" Wire	T08-E1		40.08	8.54	166.55	-1167.49	5059.25	156.95	
18	Hardware		E	0.24	1.93	166.78	-1165.56	5019.17	197.03	
19	**3** Meters 5/16" Wire Coated	RAS01		3.00	0.64	169.78	-1164.93	5018.94	197.26	
20	Hardware		E	0.24	2.00	170.02	-1162.93	5015.94	200.26	
21	Instrument - "RAS"	ML11241-08	Z	2.30	51.00	172.32	-1111.93	5015.70	200.50	**200**
22	Hardware		E	0.24	2.00	172.55	-1109.93	5013.40	202.80	
23	3-TON Miller Swivel			0.16	3.17	172.72	-1106.76	5013.17	203.03	
24	Hardware		E	0.24	2.00	172.95	-1104.76	5013.01	203.20	
25	**94** Meters 5/16" Wire	G-2		94.15	20.07	267.10	-1084.69	5012.77	203.43	
26	Hardware		E	0.24	1.93	267.33	-1082.76	4918.62	297.58	
27	**3** Meters 5/16" Wire Coated	TRAP05		3.00	0.64	270.33	-1082.12	4918.39	297.81	
28	Hardware		E	0.24	2.19	270.57	-1079.93	4915.39	300.81	
29	**5** Meters 13mm Strong-Chain			5.00	12.85	275.57	-1067.08	4915.15	301.05	
30	Hardware		E	0.24	2.00	275.80	-1065.08	4910.15	306.05	
31	**230** Meters 5/16" Wire	T08-B		230.27	49.09	506.07	-1015.99	4909.92	306.28	
32	Hardware		E	0.24	2.00	506.30	-1013.99	4679.65	536.55	
33	**3** Meters 5/16" Wire Coated	TRAP04		3.00	0.64	509.30	-1013.35	4679.42	536.78	
34	Hardware		L	0.24	2.19	509.54	-1011.16	4676.42	539.78	
35	Sediment Trap	ML11241-25	X	3.69	55.70	513.23	-955.45	4676.18	540.02	**540**
36	Hardware		D	0.06	2.00	513.29	-953.45	4672.49	543.71	
37	**1.6** Meters 13mm Strong-Chain			1.60	4.11	514.89	-949.34	4672.43	543.77	
38	Hardware		E	0.24	2.00	515.13	-947.34	4670.83	545.37	
39	**450** Meters 5/16" Wire	T08-A		450.95	96.14	966.08	-851.21	4670.59	545.61	
40	Hardware		E	0.24	1.93	966.31	-849.28	4219.64	996.56	
41	**3** Meters 5/16" Wire Coated	TRAP02		3.00	0.64	969.31	-848.64	4219.41	996.79	
42	Hardware		L	0.24	2.19	969.55	-846.45	4216.41	999.79	
43	Sediment Trap	ML11241-24	Y	3.95	55.70	973.50	-790.75	4216.17	1000.03	**1000**
44	Hardware		D	0.06	2.00	973.56	-788.75	4212.22	1003.98	
45	**4** Meters 13mm Strong-Chain			4.00	10.28	977.56	-778.47	4212.16	1004.04	
46	Hardware		E	0.24	2.00	977.80	-776.47	4208.16	1008.04	
47	3-TON Miller Swivel			0.16	3.17	977.96	-773.30	4207.92	1008.28	
48	Hardware		B	0.23	1.65	978.19	-771.65	4207.76	1008.44	
49	**500** Meters 1/4" Wire	T08-F1		501.72	70.55	1479.90	-701.10	4207.53	1008.67	
50	Hardware		A	0.21	1.33	1480.11	-699.77	3705.82	1510.38	
51	**500** Meters 1/4" Wire	T08-F2		501.75	70.55	1981.87	-629.22	3705.61	1510.59	
52	Hardware		B	0.23	1.65	1982.10	-627.57	3203.86	2012.35	
53	4-17" Glassballs on 13mm S-Chain			4.00	-91.32	1986.10	-718.89	3203.63	2012.58	
54	Hardware		F	0.24	2.00	1986.33	-716.89	3199.63	2016.58	
55	4-17" Glassballs on 13mm S-Chain			4.00	-91.32	1990.33	-808.21	3199.39	2016.81	
56	Hardware		C	0.24	1.65	1990.57	-806.56	3195.39	2020.81	
57	**500** Meters 1/4" Wire	T08-F3		501.76	70.55	2492.33	-736.00	3195.15	2021.05	
58	Hardware		A	0.21	1.33	2492.54	-734.67	2693.39	2522.81	
59	**500** Meters 1/4" Wire	T08-F4		501.74	70.55	2994.28	-664.12	2693.18	2523.02	

#	Description	Code							
60	Hardware		B	0.23	1.65	2994.51	-662.47	2191.44	3024.76
61	4-17" Glassballs on 13mm S-Chain			4.00	-91.32	2998.51	-753.79	2191.21	3024.99
62	Hardware		F	0.24	2.00	2998.74	-751.79	2187.21	3028.99
63	4-17" Glassballs on 13mm S-Chain			4.00	-91.32	3002.74	-843.11	2186.98	3029.22
64	Hardware		C	0.24	1.65	3002.98	-841.46	2182.98	3033.22
65	**500** Meters 1/4" Wire	T08-F5		501.51	70.52	3504.49	-770.94	2182.74	3033.46
66	Hardware		A	0.21	1.33	3504.70	-769.61	1681.23	3534.97
67	**500** Meters 1/4" Wire	T08-F6		501.67	70.54	4006.37	-699.07	1681.02	3535.18
68	Hardware		B	0.23	1.65	4006.60	-697.42	1179.35	4036.85
69	4-17" Glassballs on 13mm S-Chain			4.00	-91.32	4010.60	-788.74	1179.12	4037.08
70	Hardware		F	0.24	2.00	4010.84	-786.74	1175.12	4041.08
71	4-17" Glassballs on 13mm S-Chain			4.00	-91.32	4014.84	-878.06	1174.88	4041.32
72	Hardware		F	0.24	2.00	4015.07	-876.06	1170.88	4045.32
73	4-17" Glassballs on 13mm S-Chain			4.00	-91.32	4019.07	-967.38	1170.65	4045.55
74	Hardware		C	0.24	1.65	4019.31	-965.73	1166.65	4049.55
75	**500** Meters 1/4" Wire	T08-F7		501.75	70.55	4521.06	-895.18	1166.41	4049.79
76	Hardware		A	0.21	1.33	4521.27	-893.85	664.66	4551.54
77	**200** Meters 1/4" Wire	T08-H1		200.32	28.17	4721.59	-865.68	664.45	4551.75
78	Hardware		A	0.21	1.33	4721.80	-864.35	464.13	4752.07
79	**50** Meters 1/4" Wire			50.00	7.03	4771.80	-857.32	463.92	4752.28
80	Hardware		A	0.21	1.33	4772.01	-855.99	413.92	4802.28
81	**5** Meters 1/4" Wire			5.00	0.70	4777.01	-855.29	413.71	4802.49
82	Hardware		B	0.20	1.33	4777.21	-853.96	408.71	4807.49
83	**3** Meters 5/16" Wire Coated	TRAP01		3.00	0.64	4780.21	-853.32	408.51	4807.69
84	Hardware		L	0.20	1.33	4780.41	-851.99	405.51	4810.69
85	Sediment Trap	989	Y	3.82	55.70	4784.23	-796.29	405.31	4810.89	**4810.8**
86	Hardware		D	0.06	2.00	4784.29	-794.29	401.49	4814.71
87	**7** Meters 13mm Strong-Chain			7.00	17.99	4791.29	-776.30	401.43	4814.77
88	Hardware		B	0.23	1.65	4791.52	-774.65	394.43	4821.77
89	**300** Meters 1/4" Wire	T08-G		300.63	42.27	5092.16	-732.37	394.20	4822.00
90	Hardware		C	0.24	1.65	5092.40	-730.72	93.56	5122.64
91	5 Meters 16mm T-Chain			5.00	27.80	5097.40	-702.92	93.32	5122.88
92	Hardware		F	0.24	2.00	5097.63	-700.92	88.32	5127.88
93	4-17" Glassballs on 16mm T-Chain			4.00	-79.36	5101.63	-780.28	88.09	5128.11
94	Hardware		F	0.24	2.00	5101.87	-778.28	84.09	5132.11
95	4-17" Glassballs on 16mm T-Chain			4.00	-79.36	5105.87	-857.64	83.85	5132.35
96	Hardware		F	0.24	2.00	5106.10	-855.64	79.85	5136.35
97	4-17" Glassballs on 16mm T-Chain			4.00	-79.36	5110.10	-935.00	79.62	5136.58
98	Hardware		F	0.24	2.00	5110.34	-933.00	75.62	5140.58
99	4-17" Glassballs on 16mm T-Chain			4.00	-79.36	5114.34	-1012.36	75.38	5140.82
100	Hardware		F	0.24	2.00	5114.57	-1010.36	71.38	5144.82
101	4-17" Glassballs on 16mm T-Chain			4.00	-79.36	5118.57	-1089.72	71.15	5145.05
102	Hardware		F	0.24	2.00	5118.81	-1087.72	67.15	5149.05
103	4-17" Glassballs on 16mm T-Chain			4.00	-79.36	5122.81	-1167.08	66.91	5149.29
104	Hardware		F	0.24	2.00	5123.04	-1165.08	62.91	5153.29
105	4-17" Glassballs on 16mm T-Chain			4.00	-79.36	5127.04	-1244.44	62.68	5153.52
106	Hardware		F	0.24	2.00	5127.28	-1242.44	58.68	5157.52
107	4-17" Glassballs on 16mm T-Chain			4.00	-79.36	5131.28	-1321.80	58.44	5157.76
108	Hardware		F	0.24	2.00	5131.51	-1319.80	54.44	5161.76
109	4-17" Glassballs on 16mm T-Chain			4.00	-79.36	5135.51	-1399.16	54.21	5161.99
110	Hardware		F	0.24	2.00	5135.75	-1397.16	50.21	5165.99
111	4-17" Glassballs on 16mm T-Chain			4.00	-79.36	5139.75	-1476.52	49.97	5166.23

112	Hardware	F	0.24	2.00	5139.98	-1474.52	45.97	5170.23	
113	4-17" Glassballs on 16mm T-Chain		4.00	-79.36	5143.98	-1553.88	45.74	5170.46	
114	Hardware	F	0.24	2.00	5144.22	-1551.88	41.74	5174.46	
115	5 Meters 16mm T-Chain		5.00	27.80	5149.22	-1524.08	41.50	5174.70	
116	Hardware	F	0.24	2.00	5149.45	-1522.08	36.50	5179.70	
117	3-TON Miller Swivel		0.16	3.20	5149.61	-1518.88	36.27	5179.93	
118	Hardware	G	0.25	2.40	5149.86	-1516.48	36.11	5180.09	
119	Dual EGG Acoustic Releases	J	1.95	66.04	5151.81	-1450.44	35.86	5180.34	
120	Hardware	G	0.25	2.40	5152.06	-1448.04	33.91	5182.29	
121	5 Meters 16mm T-Chain		5.00	27.80	5157.06	-1420.24	33.66	5182.54	
122	Hardware	H	0.26	2.85	5157.32	-1417.39	28.66	5187.54	
123	20 Meters 1" Nylon		21.92	6.54	5179.24	-1410.85	28.40	5187.80	
124	Hardware	H	0.26	2.85	5179.50	-1408.00	6.48	5209.72	
125	5 Meters 16mm T-Chain		5.00	27.80	5184.50	-1380.20	6.22	5209.98	
126	Hardware	H	0.26	2.40	5184.76	-1377.80	1.22	5214.98	**Design Depth**
127	4666 Lb Ww Anchor		0.96	2116.46	5185.72	738.66	0.96	5215.24	
	OVERALL MOORING LENGTH		**5185.72**					5216.20	**5216.2**

64" Syntactic Sphere
Light [N02-043]
Double ARGOS CML
[18841 / 52111]

3/4" Shackle
7/8" END Link
3/4" Shackle

5 m 16mm T-Chain

3/4" Shackle
3/4" Link
5/8" Shackle

RAS [ML11241-07]
Bloom [OCR-504-TCSW-57]
CTD [2755]、DO [002]
1m Chain Bridle × 4
5/8" Shackle
5/8" Link
5/8" Shackle
3 ton Swivel
5/8" Shackle
5/8" Link
5/8" Shackle

106 m 5/16" Wire Rope
[T08-C]
5/8" Shackle
5/8" Link
5/8" Shackle
3 m 5/16" Wire Rope
[TRAP03]
5/8" SUS Shackle
3/4" SUS Link
1m Titanium Bridle

Sediment Trap
150m [ML11241-22]
1 m 3/8" Chain Bridle
5/8" Shackle

2.2 m 13mm Strong Chain
5/8" Shackle
5/8" Link
5/8" Shackle
40 m 5/16" ワイヤー
[T08-E1]
5/8" Shackle
5/8" Link
5/8" Shackle
3 m 5/16" ワイヤー
[RAS01]
5/8" Shackle
3/4" Link
5/8" Shackle

RAS [ML11241-08]
CTD [2756]、DO[003]
1 m 3/8" Chain Bridle
5/8" Shackle
5/8" Link
5/8" Shackle
3 ton Swivel
5/8" Shackle
5/8" Link
5/8" Shackle

94 m 5/16" Wire Rope
[G-2]
5/8" Shackle
5/8" Link
5/8" Shackle
3 m 5/16" Wire Rope
[TRAP05]
5/8" Shackle
5/8" Link
5/8" Shackle

5 m 16mm T-Chain
5/8" Shackle
5/8" Link
5/8" Shackle

---

230 m 5/16" Wire Rope
[T08-B]
5/8" Shackle
5/8" Link
5/8" Shackle
3 m 5/16" Wire Rope
[TRAP04]
5/8" SUS Shackle
5/8" SUS Link
1m Titanium Bridle

Sediment Trap
540m [ML11241-25]
1 m 3/8" Chain Bridle
5/8" Shackle

1.6 m 13mm Strong Chain
5/8" Shackle
5/8" Link
5/8" Shackle

450 m 5/16" Wire Rope
[T08-A]
5/8" Shackle
5/8" Link
5/8" Shackle
3 m 5/16" Wire Rope
[TRAP02]
5/8" SUS Shackle
3/4" SUS Link
1m Wire Bridle

Sediment Trap
1000m [ML11241-24]
1 m 3/8" Chain Bridle
5/8" Shackle

4 m 13mm Strong Chain
5/8" Shackle
5/8" Link
5/8" Shackle
3 ton Swivel
5/8" Shackle
5/8" Link
1/2" Shackle

500 m 1/4" Wire Rope
[T08-F1]
1/2" Shackle
5/8" Link
1/2" Shackle

500 m 1/4" Wire Rope
[T08-F2]
1/2" Shackle
3/4" Link
5/8" Shackle

17" Glass Ball × 4 on the
4m 13mm Strong Chain
5/8" Shackle
3/4" Link
5/8" Shackle

17" Glass Ball × 4 on the
4m 13mm Strong Chain
5/8" Shackle
3/4" Link
1/2" Shackle

500 m 1/4" Wire Rope
[T08-F3]

1/2" Shackle
5/8" Link
1/2" Shackle

500 m 1/4" Wire Rope
[T08-F4]
1/2" Shackle
3/4" Link
5/8" Shackle

17" Glass Ball × 4 on the
4m 13mm Strong Chain

5/8" Shackle
3/4" Link
5/8" Shackle

17" Glass Ball × 4 on the
4m 13mm Strong Chain

5/8" Shackle
3/4" Link
1/2" Shackle

500 m 1/4" Wire Rope
[T08-F5]
1/2" Shackle
5/8" Link
1/2" Shackle
500 m 1/4" Wire Rope
[T08-F6]
1/2" Shackle
3/4" Link
5/8" Shackle

17" Glass Ball × 4 on the
4m 13mm Strong Chain

5/8" Shackle
3/4" Link
5/8" Shackle

17" Glass Ball × 4 on the
4m 13mm Strong Chain

5/8" Shackle
3/4" Link
5/8" Shackle

17" Glass Ball × 4 on the
4m 13mm Strong Chain

5/8" Shackle
3/4" Link
1/2" Shackle

500 m 1/4" Wire Rope
[T08-F7]
1/2" Shackle
5/8" Link
1/2" Shackle

200 m 1/4" Wire Rope
[T08-H1]
1/2" Shackle
5/8" Link
1/2" Shackle

50 m 1/4" Wire Rope
[T08-I]
1/2" Shackle
5/8" Link
1/2" Shackle
5 m 1/4" Wire Rope
[adj.]
1/2" Shackle
5/8" Link
5/8" Shackle

---

3 m 5/16" Wire Rope
[TRAP01]
5/8" SUS Shackle
3/4" SUS Link
1m Wire Bridle

Sediment Trap
4810m [989]
1 m 3/8" Chain Bridle
5/8" Shackle

7 m 13mm Strong Chain
5/8" Shackle
5/8" Link
1/2" Shackle

300 m 1/4" Wire Rope
[T08-G]
1/2" Shackle
3/4" Link
5/8" Shackle

5 m 16mm T-Chain
5/8" Shackle
3/4" Link
5/8" Shackle

17" Glass Ball × 4 on the
4m 13mm Strong Chain (×11)

5/8" Shackle
3/4" Link
5/8" Shackle

5 m 16mm T-Chain
5/8" Shackle
5/8" Link
5/8" Shackle
3 ton Swivel
5/8" Shackle
5/8" Link
3/4" Shackle

Acoustic Releaser × 2
[27864 / 27867]
CTD[2757]、DO[005]

2 m 13mm Dual Strong Chain

1" Master Link
3/4" Shackle
3/4" Link
5/8" Shackle

5 m 16mm T-Chain
5/8" Shackle
3/4" Link
7/8" Shackle

20 m 1" Nylon Rope

7/8" Shackle
3/4" Link
5/8" Shackle

5 m 16mm T-Chain
5/8" Shackle
3/4" Link
7/8" Shackle

2.28 ton Anchor

JPAC NW-PACIFIC **BGC** Mooring

MR08-05 Station **K-2**, 5206.2m
2008/10/28 **Deployment**

Table 3.1.1-2 Deployment BGC Mooring Figure.

3.1.2 Instruments

On mooring systems, the following instruments are installed.

(1) ARGOS CML (Compact Mooring Locator)

The Compact Mooring Locator is a subsurface mooring locator based on SEIMAC's Smart Cat ARGOS PTT (Platform Terminal Transmitter) technology.   Using CML, we can know when our mooring has come to the surface and its position.   The CML employs a pressure sensor at the bottom.   When the CML is turned ON, the transmission is started immediately every 90 seconds and then when the pressure sensor works ON by approximately 10 dbar, the transmission is stopped.   When the top buoy with the CML comes to the surface, the pressure sensor will work OFF and the transmission will be started.   Smart Cat transmissions will be initiated at this time, allowing us to locate our mooring.   Depending on how long the CML has been moored, it will transmit for up to 120 days on a 90 second repetition period.   Battery life, however, is affected by how long the CML has been moored prior to activation.   A longer pre-activation mooring will mean less activation life.

Principle specification is as follows:
(Specification)

Transmitter:	Smart Cat PTT
Operating Temp.:	+35 [deg] to –5 [deg]
Standby Current:	80 microamps
Smart Cat Freq.:	401.650 MHz
Battery Supply:	7-Cell alkaline D-Cells
Ratings:	+10.5VDC nom., 10 Amp Hr
Hull:	6061-T6 Aluminum
Max Depth:	1,000 m
Length:	22 inches
Diameter:	3.4 inches
Upper flange:	5.60 inches
Dome:	Acrylic
Buoyancy:	-2.5 (negative) approx.
Weight	12 pounds approx.

(2) Submersible Recovery Strobe

The NOVATECH Xenon Flasher is intended to aid in the marking or recovery of oceanographic instruments, manned vehicles, remotely operated vehicles, buoys or structures. Due to the occulting (firing closely spaced bursts of light) nature of this design, it is much more visible than conventional marker strobes, particularly in poor sea conditions.
(Specification)

Repetition Rate:	Adjustable from 2 bursts per second to 1 burst every 3 seconds.
Burst Length:	Adjustable from 1 to 5 flashes per burst. 100 ms between flashes nominal.
Battery Type:	C-cell alkaline batteries.
Life:	Dependent on repetition rate and burst length. 150 hours with a one flash burst every 2 seconds.

Construction:	Awl-grip painted, Hard coat anodized 6061 T-6 aluminum housing.
Max. Depth:	7,300m
Daylight-off:	User selected, standard
Pressure Switch:	On at surface, auto off when submerged below 10m.
Weight in Air:	4 pounds
Weight in Water:	2 poundsOutside
Diameter:	1.7 inches nominal
Length:	21-1/2 inches nominal

(3) Depth Sensor

RMD Depth sensor is digital memory type and designed for mounting on the plankton net and instrument for mooring and so on. It is small and right weight for easy handling. Sampling interval is chosen between 2 and 127 seconds or 1 and 127 minutes and sampled Time and Depth data. The data is converted to personal computer using exclusive cable (printer interface).

(Specification)

Model:	RMD-500
Operating Depth:	0 ~ 500m
Precision:	0.5% (F.S.)
Accuracy:	1/1300
Memory:	65,534 data (128kbyte)
Battery:	lithium battery (CR2032) DC6V
Battery Life:	65,000 data or less than 1 year
Sample interval:	2 ~ 127 seconds or 1 ~ 127 minutes
Broken Pressure:	20MPa
Diameter:	50mm
Length:	150mm
Main Material:	vinyl chloride resin
Cap material:	polyacetal resin
Weight:	280g

(4) AREC CT Sensor (Not re-deploy)

AREC CT sensor is digital memory type and designed for mounting on the plankton net and instrument for mooring and so on.   It is small and right weight for easy handling.   Sampling interval is chosen 1 second or 1, 2 and 10 minutes.   The data is converted to personal computer using exclusive cable (serial port).

(Specification)

Model:	COMPACT-CT
Operating Depth:	0 ~ 500m
T-Sensor Range:	-5~40°C
T-Sensor Precision:	0.001°C
T-Sensor Accuracy:	±0.02°C
C-Sensor Range:	0~60 mS/cm

C-Sensor Precision:	0.001 mS/cm
C-Sensor Accuracy:	±0.02 mS/cm
Memory:	2Mbyte flash memory
Battery:	lithium battery (CR2) DC3V
Battery Life:	178439 data
Sample interval:	1 seconds or 1, 2 and 10 minutes
Diameter:	40mm
Length:	202mm
Main Material:	titanium
Weight in water:	265g

(5) CTD SBE-37

The SBE 37-SM MicroCAT is a high-accuracy conductivity and temperature (pressure optional) recorder with internal battery and memory. Designed for moorings or other long duration, fixed-site deployments, the MicroCAT includes a standard serial interface and nonvolatile FLASH memory. Constructed of titanium and other non-corroding materials to ensure long life with minimum maintenance, the MicroCAT's depth capability is 7000 meters; it is also available with an optional 250-meter plastic *ShallowCAT* housing.

(Specification)

Measurement Range

Conductivity: 0 - 7 S/m (0 - 70 mS/cm)

Temperature: -5 to 35 °C

Optional Pressure: 7000 (meters of deployment depth capability)

Initial Accuracy

Conductivity: 0.0003 S/m (0.003 mS/cm)

Temperature: 0.002 °C

Optional Pressure: 0.1% of full scale range

Typical Stability (per month)

Conductivity: 0.0003 S/m (0.003 mS/cm)

Temperature: 0.0002 °C

Optional Pressure: 0.004% of full scale range

Resolution

Conductivity: 0.00001 S/m (0.0001 mS/cm)

Temperature: 0.0001 °C

Optional Pressure: 0.002% of full scale range

Time Resolution 1 second

Clock Accuracy 13 seconds/month

Quiescent Current * 10 microamps

Optional External Input Power 0.5 Amps at 9-24 VDC

Housing, Depth Rating, and Weight (without pressure sensor)

Standard Titanium, 7000 m (23,000 ft)

Weight in air: 3.8 kg (8.3 lbs)

Weight in water: 2.3 kg (5.1 lbs)

(sampling parameter)

Sampling start time: Oct. 28th 2008 01:00:00
Sampling interval: 1800 seconds

(6) AREC DO Sensor
       AREC DO (Compact Optode) sensor is digital memory type and designed for mounting on the plankton net and instrument for mooring and so on.   It is small and right weight for easy handling.   Sampling interval is chosen 1 second or 1, 2 and 10 minutes.   The data is converted to personal computer using exclusive cable (serial port).
 (Specification)

Model:	COMPACT-Optode
Sensor Type:	Fluorescence quenching
Operating Range:	0 ~ 120%
Precision:	0.4%
Accuracy:	within 5%
Memory:	2Mbyte flash memory
Battery:	lithium battery 7Ah
Battery Life:	172800 data
Sample interval:	1,2,5,10,15,20 and 30 seconds
Diameter:	54mm
Length:	272mm
Main Material:	titanium
Weight in water:	0.6kg
Broken Pressure:	60MPa

(sampling parameter)
    Sampling start time: Oct. 28th 2008 01:00:00
    Sampling interval: 1800 seconds

(7) RAS (Remotely Access Sampler)
       There are four major components mounted within the RAS: (1) the controller housing, (2) the pump assembly, (3) the multi-port valve, and (4) the sample containers.   The principle of water sampling is that the pump draws out water in the sample container in which the collapsed sample bag is mounted. This creates a pressure gradient that pushes ambient seawater through the intake and into the inflating sample bag.
       Length, width and Height are 73 cm, 73 cm, and 114 cm, respectively, and weight with empty sample containers is 110 kg in air and 57 kg in water. The RAS instruments were loaded with acid-cleaned, 500 ml–capacity bags made of the following 3 laminated layers; a thin exterior Mylar® film for protection, a vacuum coated aluminum foil layer for blocking solar radiation and minimizing gas diffusion and an interior, Teflon® film for reinforcement and insulation of sample water from the Al layer.   Each bag was pre-loaded with a preservative solution (1 ml $HgCl_2$ solution: 3.6 g $HgCl_2$ in 100 ml distilled water) [*], connected to a distribution valve and placed within a sturdy 600 ml sample container (acrylic sheathe) within the instrument. The remaining spaces within sheathes were filled with seawater before deployment. There are 49 identical bag assemblages on a RAS. Of these, 48 were used to sample seawater on a scheduled sequence. The remaining bag was filled with 6M HCl that was used to flush the intake path before each water

sampling procedure in order to avoid biofouling.

Normally, the RAS multi-port valve resides in a home position that block all intake paths. Five minutes before sampling, the multi-port valve aligns with the intake path and the cleansing acid bag and a <u>5 ml jet of 6M HCl flushes the intake manifolds</u>[*].   After a one-minute pause, the same path was rinsed with 100 ml of *in situ* seawater. Then the multi-port valve aligns the intake valve to a designated sampling bag assemblage. As the seawater is removed from the acrylic sheathe by operating the pump in reverse to the previous flush stage, the resultant low pressure induces the *in situ* water to move into the sampling bag. To minimize cross contamination of water samples, the graphite-gear pump is not exposed to the sample water but only to the evacuated distilled water in the sheathes. Execution records documenting sample timing, estimated sample volume, flushing periods, and electricity consumption were logged by the RAS instruments and retrieved from the memory on recovery.

This time, RAS was installed at approximately 50 m and 200m.

Note 1: $HgCl_2$ of 1 ml (not 2 ml as the previous deployment) was add to respective sampling bag.

Note 2: This time, flushing inlet with HCl was not scheduled in order to avoid the effect of acid on carbonate chemistry.

(8) BLOOMS

The Bio-optical Long-term Optical Ocean Measuring System package (BLOOMS) consisted of a WETLabs fluorometer and a Satlantic Inc. spectral radiometer (OCR-504-ICWS; Halifax, Canada) along with data acquisition / storage systems and a pressure housing.   The BLOOMS was mounted on the frame of the RAS for measurements of chlorophyll *a* (chl-*a*) concentrations as a proxy for phytoplankton biomass (fluorometer) and downwelling spectral irradiance at four wavelengths (412, 443, 490, and 555 nm).   The optical system was kept free of biofouling by use of copper shutters.

Measurement started on 10:00 26 October 2008 (LST).   The values of Ed at 4 wavelengths were measured every hour during the local daytime period (19:00 - 7:00 UTC).

(7) Sediment trap

A time-series sediment trap with 21 cups were installed at approximately 5000 m. Three traps with 13 cups were installed at 150 m, 550 m and 1000 m.   Before deployment, collecting cups were filled up with deep seawater (~ 2000 m) based <u>10 %</u> buffered formalin. <u>NaCl of 50 g was add</u> to this solution of 10L to increase salinity by 5 per-mil.

3.1.3 Sampling schedule

Sediment trap and RAS will collect samples under the following schedule.

Sediment Trap

	Opening day		Opening day
	21 cup		13 cup
	(5000)		(150, 550, 1000)
int	17	int	34
1	2008.11.1	1	2008.11.1
2	2008.11.18		
3	2008.12.5	2	2008.12.5
4	2008.12.22		
5	2009.1.8	3	2009.1.8
6	2009.1.25		
7	2009.2.11	4	2009.2.11
8	2009.2.28		
9	2009.3.17	5	2009.3.17
10	2009.4.3		
11	2009.4.20	6	2009.4.20
12	2009.5.7		
13	2009.5.24	7	2009.5.24
14	2009.6.10		
15	2009.6.27	8	2009.6.27
16	2009.7.14		
17	2009.7.31	9	2009.7.31
18	2009.8.17		
19	2009.9.3	10	2009.9.3
20	2009.9.20		
21	2009.10.7	11	2009.10.7
	2009.10.24	12	2009.11.10
		13	2009.12.14

close

2010.1.17

MR10-01 cruise	2010 1/21-2/24

RAS (40m and 200m)

	preservative:		1 ml HgCl2
	No flushing inlet with HCl		
	Interver (days):	9.00	
	Sampling date and time		
1	2008.11.1 12:00	25	2009.6.5 12:00
2	2008.11.10 12:00	26	2009.6.14 12:00
3	2008.11.19 12:00	27	2009.6.23 12:00
4	2008.11.28 12:00	28	2009.7.2 12:00
5	2008.12.7 12:00	29	2009.7.11 12:00
6	2008.12.16 12:00	30	2009.7.20 12:00
7	2008.12.25 12:00	31	2009.7.29 12:00
8	2009.1.3 12:00	32	2009.8.7 12:00
9	2009.1.12 12:00	33	2009.8.16 12:00
10	2009.1.21 12:00	34	2009.8.25 12:00
11	2009.1.30 12:00	35	2009.9.3 12:00
12	2009.2.8 12:00	36	2009.9.12 12:00
13	2009.2.17 12:00	37	2009.9.21 12:00
14	2009.2.26 12:00	38	2009.9.30 12:00
15	2009.3.7 12:00	39	2009.10.9 12:00
16	2009.3.16 12:00	40	2009.10.18 12:00
17	2009.3.25 12:00	41	2009.10.27 12:00
18	2009.4.3 12:00	42	2009.11.5 12:00
19	2009.4.12 12:00	43	2009.11.14 12:00
20	2009.4.21 12:00	44	2009.11.23 12:00
21	2009.4.30 12:00	45	2009.12.2 12:00
22	2009.5.9 12:00	46	2009.12.11 12:00
23	2009.5.18 12:00	47	2009.12.20 12:00
24	2009.5.27 12:00	48	2009.12.29 12:00

3.1.4 Preliminary results

(1) RAS depth

        Two automatic water samplers (RAS) was designed to be located at approximately 35 m and 200 m. These RAS depths during deployment were observed each two hours by depth sensors (RIGO RMD-500) attached on RAS frame.

        Although RAS at 35 m and 200 m were sometimes deepened by approximately 30 m, both RAS depth were generally stable and RAS was kept at designed depth before August 2008. However it was noteworthy that both RAS were deepened by 120 m at maximum in August 2008. It is suspected that strong current took place and mooring system at least upper 350 m might be largely forced to be tilted. It might be supported by the fact of low flux collected by sediment trap at 300 m.
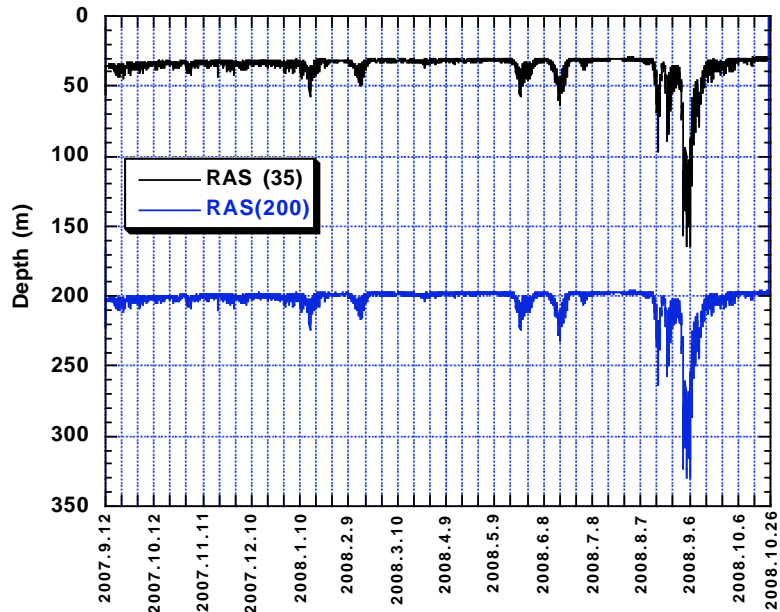
Fig.1 RAS depth

(2) Temperature and salinity at RAS depth

        Conductivity and Temperature sensor (AREC COMPACT-CT) were installed on both RAS frame, and temperature and salinity were observed each twenty minutes during deployment.

        Temperature at deeper RAS depth (~ 200m, $Temp_{(200)}$ hereinafter) was approximately 3.5°C in October 2007. $Temp_{(200)}$ was generally constant all year around although temperature was sometimes lower than 3°C. On the other hand, temperature at shallower RAS depth (~ 35 m, $Temp_{(35)}$ hereinafter) showed seasonal variability. $Temp_{(35)}$ in October 2007 was approximately 9°C and decreased toward winter. Between middle December 2007 and middle June 2008, $Temp_{(35)}$ was lower than $Temp_{(200)}$ with minimum temperature of approximately 1°C in March 2008. After March 2008, $Temp_{(35)}$ increased toward autumn 2008. However its increase was not smooth but had large deviation. In August and September 2008, $Temp_{(35)}$ became lower largely. It is attributed to that $RAS_{(35)}$ was deepened largely during this period.

        Salinity at deeper RAS depth ($Sal_{(200)}$ hereinafter) was generally stable. Average $Sal_{(200)}$ was 34.1 and standard deviation (1σ) was 0.02 during deployment. Salinity at shallower RAS depth ($Sal_{(35)}$ hereinafter) was approximately 32.6 in October 2007 and increased toward February 2008. It was attributed to winter mixing and supply of subsurface water with higher salinity to surface water. After February 2008, $Sal_{(35)}$ decreased toward July 2008. Increase of $Sal_{(35)}$ observed in August and September 2008 was likely caused by increase of RAS depth by 150 m.
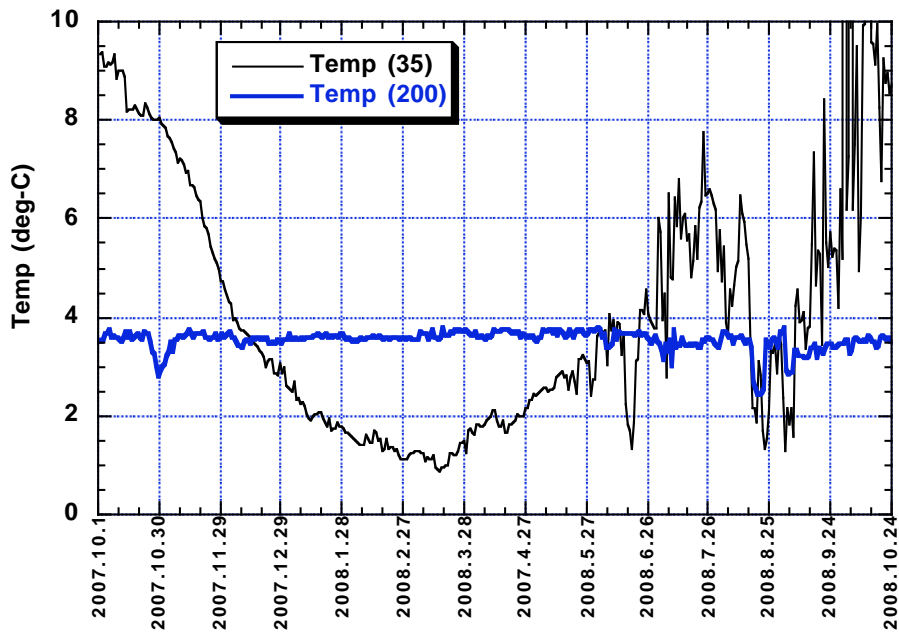
Fig.2 Temperature at RAS depth (~35 m and 200 m)
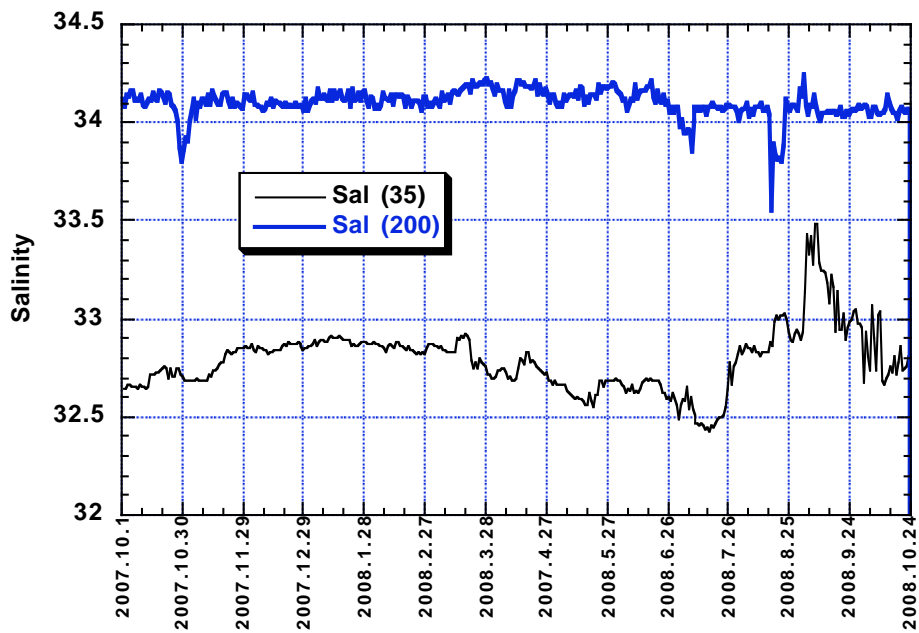
Fig.3 Salinity at RAS depth (~35 m and 200 m)

(4) Chemical analysis of RAS sample
1) Status of RAS sampling (Table 1)

Because of malfunction of Water Flush Path (WFP) valve, RAS at 200 m collected only first four samples.

RAS at 35 m worked following schedule. However sample volume after sample #27 (after late April 2008) was quite small. Judging from the onboard test after recovery, it is suspected that power of suction pump became too weak to collect approximately 500 ml seawater after sample #27. Thus we could not measure dissolved inorganic carbon (DIC) and total alkalinity (TALK) after late April 2008. On several sample bags, there were holes made by corrosion. Salinity of RAS seawater sample was measured by salinometer (AutoLab YEO-KAL). Salinity of RAS sample should be lower than ambient seawater because RAS sample was diluted with preservative (1 ml $HgCl_2$). The smaller sample is, the more dilution effect is. However salinity of half of RAS samples was higher than that of ambient water observed by CT sensor (AREC COMPACT-CT) when sample volume was lower. For RAS sample with hole on sample bag, high salinity should be attributed to contamination of high saline seawater in the sample bag container. We cannot explain high salinity for other RAS sample at this moment. One of possibility is low precision and / or accuracy of salinometer and / or CT sensor. Preliminary results of chemical analysis of shallower RAS sample (~ 35 m) are shown in Fig. 4.

2) Preliminary results of chemical analysis of RAS sample
(a) NO_3

Concentration of normalized NO_3 (N-NO_3) for the first sample (collected on 1 October 2007) was approximately 12 µmol kg^{-1}. This value was comparable to previous value observed at comparable season (Honda and Watanabe, JO 63, 349 - 362, 2007). N-NO_3, except these of contaminated sample, increased toward March 2008. N-NO_3 was approximately 23 µmol kg^{-1}. This value was slightly lower than previous observed data (~ 25 µmol kg^{-1}; Honda and Watanabe, 2007). N-NO_3 started to decrease at April 2008 toward autumn 2008. N-NO_3 for the last sample collected on 1 October 2008 was approximately 11 µmol kg^{-1} and slightly lower than previous data. This sample was quite small volume and this might affect N-NO_3.

(b) $Si(OH)_4$

Generally, seasonal variability of normalized $Si(OH)_4$ (N-$Si(OH)_4$) was similar to that of N-NO_3. N-$Si(OH)_4$ was low in October, high in early spring and decreased from spring toward autumn. As reported previously (Honda and Watanabe, 2007), decrease from spring to autumn and increase from autumn to next spring is likely attributed to biological activity and winter mixing, respectively. N-$Si(OH)_4$ ranged from 15 to 37 µmol kg^{-1}. Highest value observed in spring in this study was slightly lower than previous values (~ 40 - 45 µmol kg^{-1}, Honda and Watanabe, 2007).

(c) NO_2

Seasonal variability of concentration of normalized NO_2 (N-NO_2) was mirror image of that of N-NO_3 and $Si(OH)_4$ although data was scattered. In general, N-NO_2 started to decrease at autumn October 2007 and became minimum in late February 2008. N-NO_2 started to increase after that toward summer 2008. Thus it is suspected that N-NO_2 was accumulated in the surface mixed layer between spring to autumn when biological activity is active.

(d) PO$_4$

　　　　Seasonal variability of normalized PO$_4$ (N-PO$_4$) between October 2007 and March 2008 was similar to that of N-NO$_3$ and N-Si(OH)$_4$. However N-PO$_4$ were scattered largely after late March. N-PO$_4$ larger than 2 μmol kg^{-1} have been never observed around 35 m by hydrocasting previously (Honda and Watanabe, 2007). Volume of most of these samples was quite small and, thus, sample might be contaminated largely. This time we did not use HCl, which is used for anti-biofouling because we thought that HCl affected PO$_4$ analysis (Honda and Watanabe, 2007). However we cannot judge whether usage of HCl is good or bad for sample analysis based on preliminary result.

(e) Dissolved inorganic carbon (DIC)

　　　　Although normalized DIC concentration (N-DIC) data was scattered, DIC showed same increase as nutrients. N-DIC ranged from approximately 2000 μmol kg^{-1} to 2120 μmol kg^{-1}. Although high value (2120 μmol kg^{-1}) observed in March 2008 was comparable with previous value, low value was smaller than previous value by 50 μmol kg^{-1} (2050 μmol kg^{-1}). As described above, we did not use HCl, which is used for anti-biofouling because we thought HCl affected DIC analysis (Honda and Watanabe, 2007). However DIC became lower than DIC observed by hydrocasting even if seawater was collected without HCl. CO$_2$ degassing might take place during deployment regardless of usage of HCl. Unfortunately RAS sample might not be available for measurement of DIC.

(e) Total alkalinity (TALK)

　　　　Concentration of total alkalinity (TALK) tended to increase from October 2008 toward April 2008. It is likely attributed to supply of subsurface water with higher TALK to surface water. In contrast, normalized TALK (N-TALK) tended to decrease toward April 2008. This trend will be more discussed taking into account for mineralization/remineralization of CaCO$_3$.

Table 1 RAS sample list. Sample with asterisks is one with higher salinity than ambient seawater. Sample volume was suspected from sum of sample volume for respective chemical analysis and weight of remains measured on land laboratory after cruise

Sample Name	Chemical analysis				sample volume	MEMO	sampling day	ExD	salinity	AREC salinity		AREC temp	Depth (m)
	TCO2	ALK	NUTS	SAL									
50m– 1	○	○	○	○	517		2007.10.1	0	32.571	32.667		9.35	37.4
50m– 2	○	○	○	○	511		2007.10.8	7	32.598	32.676		9.31	34.0
50m– 3	○	○	○	○	534		2007.10.16	15	32.618	32.746		8.28	33.1
50m– 4	○	○	○	○	537		2007.10.24	23	32.642	32.772		8.19	33.4
50m– 7	○	○	○	○	439	Hole on sample bag	2007.11.16	46	36.854	32.781	*	6.47	32.7
50m– 8	○	○	○	○	525		2007.11.24	54	32.829	32.834		5.37	32.0
50m– 9	○	○	○	○	568		2007.12.2	62	32.760	32.842		4.35	32.7
50m– 10	○	○	○	○	535		2007.12.10	70	32.764	32.842		3.75	34.0
50m– 11	○	○	○	○	537		2007.12.17	77	32.766	32.860		3.33	33.0
50m– 12	○	○	○	○	535		2007.12.25	85	32.772	32.869		2.85	34.2
50m– 13	○	○	○	○	551		2008.1.2	93	32.785	32.869		2.55	34.2
50m– 14	○	○	○	○	534		2008.1.10	101	32.825	32.877		2.22	35.3
50m– 15	○	○	○	○	535		2008.1.18	109	32.818	32.886		2.03	41.0
50m– 16	○	○	○	○	467	Hole on sample bag	2008.1.25	116	35.511	32.869	*	1.82	34.4
50m– 17	○	○	○	○	493		2008.2.2	124	32.933	32.877	*	1.53	31.6
50m– 18	○	○	○	○	532		2008.2.10	132	32.856	32.869		1.58	35.9
50m– 19	○	○	○	○	537		2008.2.18	140	32.824	32.842		1.30	36.2
50m– 20	○	○	○	○	507		2008.2.25	147	32.905	32.834	*	1.14	32.0
50m– 22	○	○	○	○	460	exit of zooplankton	2008.3.12	163	32.909	32.816	*	1.13	32.3
50m– 23	○	○	○	○	509		2008.3.20	171	33.013	32.886	*	0.99	31.2
50m– 24	○	○	○	○	541		2008.3.28	179	32.942	32.755	*	1.47	31.2
50m– 25	○	○	○	○	522		2008.4.4	186	32.882	32.755	*	1.80	31.2
50m– 26	○	○	○	○	459	Hole on sample bag	2008.4.12	194	32.849	32.711	*	2.09	31.5
50m– 27	○	○	○	○	429	slightly small sample	2008.4.20	202	32.910	32.790	*	1.87	32.2
50m– 28	○	○	○	○	498	slightly small sample	2008.4.28	210	32.891	32.702	*	2.31	30.9
50m– 29	×	×	○	○	169	small sample	2008.5.6	218	32.822	32.685	*	2.59	31.0
50m– 31	×	×	○	○	165	small sample	2008.5.21	233	32.822	32.606	*	2.42	34.8
50m– 35	×	×	○	○	134	small sample	2008.6.21	264	32.832	32.711	*	2.77	39.1
50m– 36	×	×	×	○	169	small sample	2008.6.29	272	32.808	32.606	*	4.35	30.9
50m– 37	×	×	×	○	155	small sample	2008.7.7	280	32.831	32.606	*	3.54	32.1
50m– 44	×	×	○	○	178	small sample	2008.8.30	334	32.822	32.869		4.06	47.5
50m– 46	×	×	○	○	136	small sample	2008.9.15	350	33.005	33.166		6.41	42.9
50m– 47	×	×	○	○	134	small sample	2008.9.23	358	32.772	32.947		6.91	32.1
50m– 48	×	×	○	○	87	quite small sample	2008.10.1	366	30.592	32.702		11.00	31.6

Sample Name	TCO2	ALK	NUTS	SAL	sample volume	MEMO	sampling day	ExD	salinity	AREC salinity		AREC temp	Depth (m)
200m– 1	○	○	○	○	511		2007.10.1	0	33.774	34.120			
200m– 2	○	○	○	○	523	Hole on sample bag	2007.10.8	7	33.815	34.120			
200m– 3	○	○	○	○	514		2007.10.16	15	33.789	34.150			
200m– 4	○	○	○	○	520		2007.10.24	23	33.807	34.140			
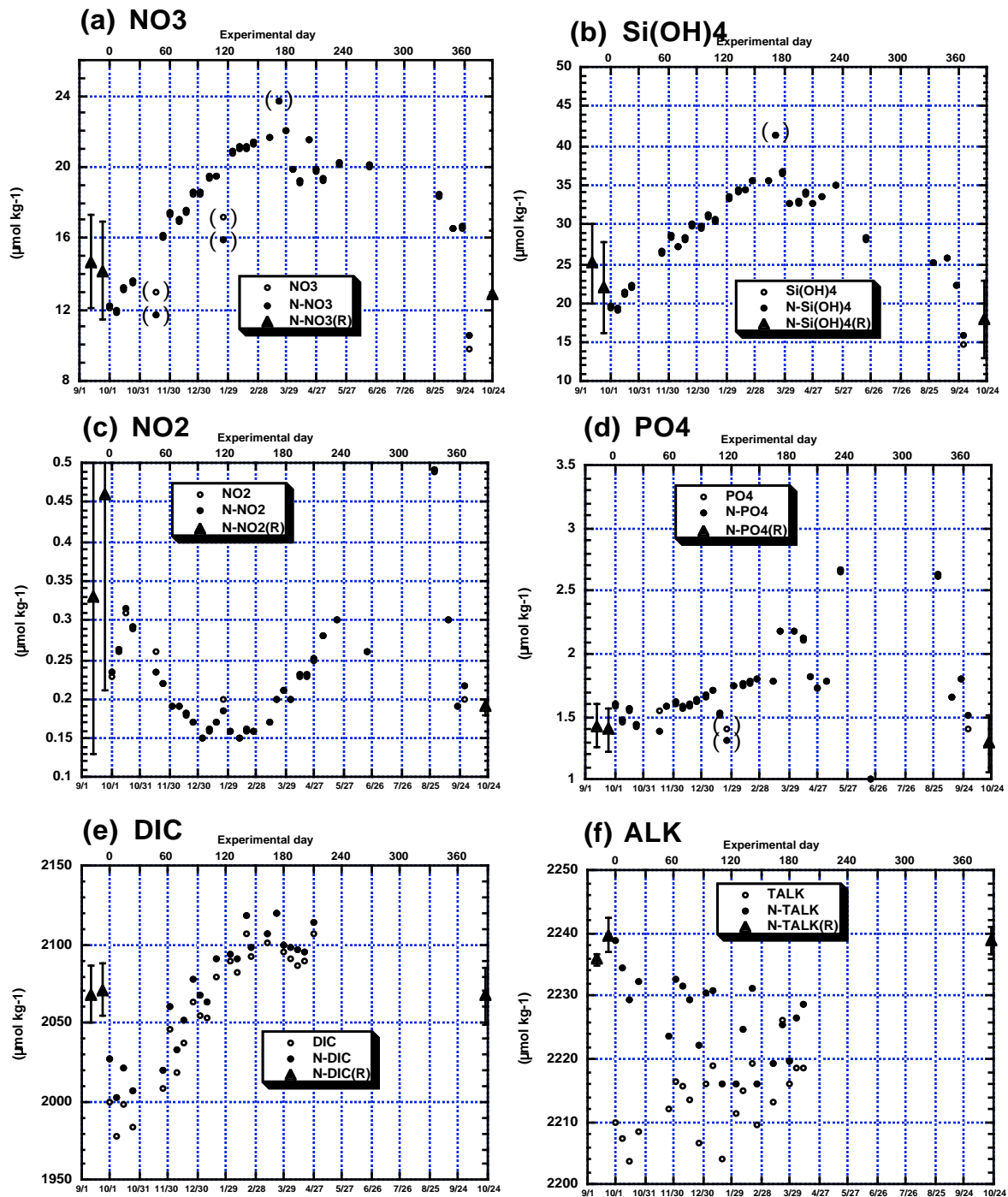
Fig. 4 Preliminary results of chemical analysis of RAS samples at 35 m. (a) NO_3, (b) $Si(OH)_4$, (c) NO_2, (d) PO_4, (e) DIC and (f) ALK. Open circles and closed circles are respected measured data and salinity-normalized data (salinity = 33), respectively. Closed triangles are normalized respective data observed by hydrocasting before and after mooring deployment/recovery. Data in parenthesis probably contaminated with ambient high saline seawater.

(5) Sediment trap

Time-series sediment traps were deployed at 150, 300, 540, 1000 and 4810 m. However a turntable with 21 collecting cups at 150 m disappeared when sediment traps were recovered. Thus no data from 150 m was available.

After recovery, collected samples were observed. In order to estimate amount of sample qualitatively, heights of collected sample was measured with a scale (Fig. 5). It was observed that material fluxes at respective depths decreased toward winter and increased toward summer 2008. With time lag, seasonal variability at respective depths synchronized well. As same as previous results, material fluxes at deepest depth (4810 m) seemed higher than fluxes at shallower depths. Low flux observed in August and early September 2008 at 300 m (sample with asterisk in upper panel of Fig. 5) might be associated with tilt of BGC mooring system judging from increase of RAS depths.
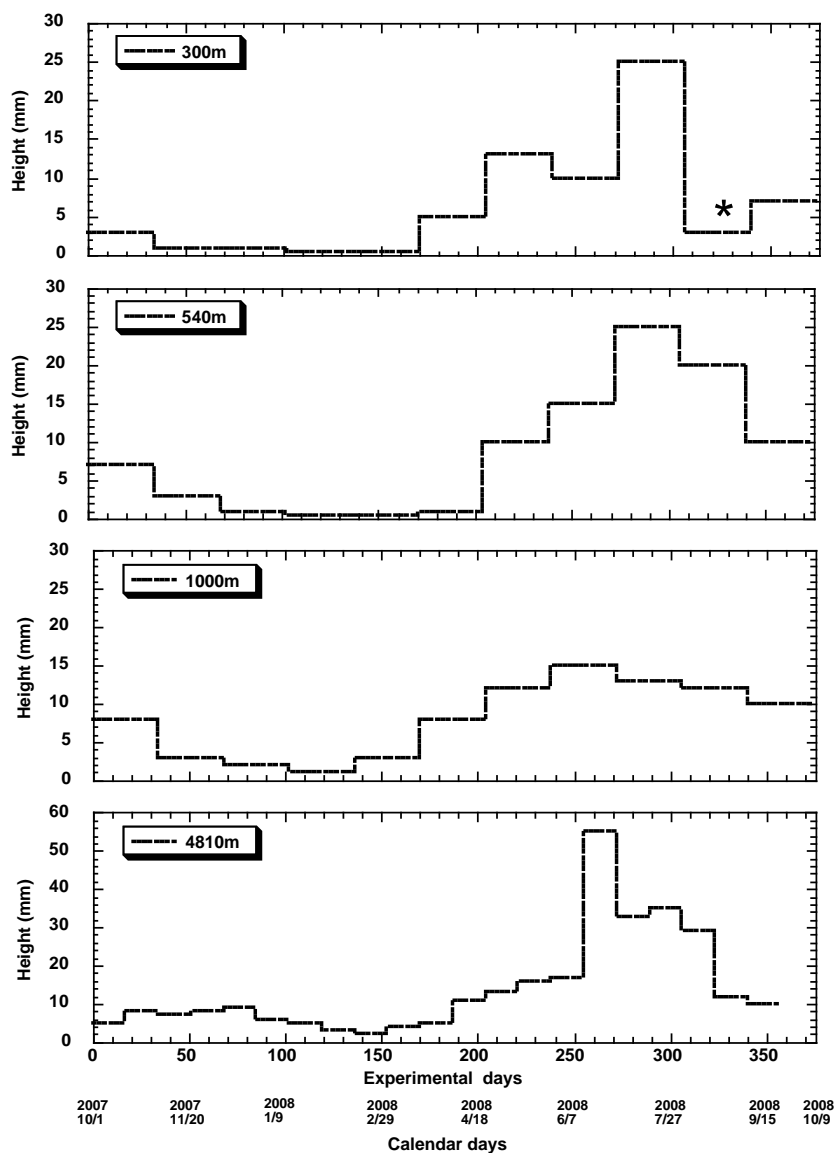
Fig. 5 Seasonal variability in material fluxes at 300, 500, 1000 and 4810 m

3.2 Phytoplankton

3.2.1 Chlorophyll *a* measurements by fluorometric determination

Kazuhiko MATSUMOTO (JAMSTEC); Principal Investigator
Masanori ENOKI (MWJ); Operation Leader
Miyo IKEDA (MWJ); Operator

(1) Objective

Phytoplankton exist various species in the ocean, but the species are roughly characterized by their cell sizes. The objective of this study is to investigate the vertical distribution of phytoplankton as chlorophyll *a* (chl-*a*) by using the fluorometric determination with the size fractionations.

(2) Sampling

We collected samples for total chl-*a* from 9 depths between the surface and 200 m during the deep-cast. We collected samples for total chl-*a* and size-fractionated chl-*a* from 8 depths respectively within the euphotic layer during the shallow-cast. The euphotic layer was determined by the downward irradiance sensor for the experiments of primary productivity at the shallow-casts, and the sampling depths were determined with the light intensity (%) of surface incident irradiance as 100, 50, 25, 10, 5, 2.5, 1 and 0.5%.

(3) Instruments and Methods

Water samples for total chl-*a* were vacuum-filtrated (<0.02MPa) through 25mm-diameter Whatman GF/F filter. Water samples for size-fractionated chl-*a* were sequentially vacuum-filtrated (<0.02MPa) through the three types of 47mm-diameter nuclepore filters (pore size of 10.0μm, 3.0μm and 1.0μm) and the 25mm-diameter Whatman GF/F filter. Phytoplankton pigments retained on the filters were immediately extracted in a polypropylene tube with 7 ml of N,N-dimethylformamide. The tubes were stored at –20°C under the dark condition to extract chl-*a* for 24 hours or more.

Fluorescences of each sample were measured by Turner Design fluorometer (10-AU-005), which was calibrated against a pure chl-*a* (Sigma chemical Co.). We applied two kind of fluorometric determination for the samples of total chl-*a*: "Non-acidification method" (Welschmeyer, 1994) and "Acidification method" (Holm-Hansen *et al*., 1965). Analytical conditions of each method were listed in table 1. Size-fractionated samples were applied only "Non-acidification method".

(4) Preliminary Results

The result of total chl-*a* was shown as the spatial distribution (Figure 1). The result of size-fractionated chl-*a* was shown as the vertical distribution (Figure 2).

(5) Data archives

The processed data file of pigments will be submitted to the JAMSTEC Data Integration and Analyses Group (DIAG) within a restricted period. Please ask PI for the latest information.

(6) Reference

Holm-Hansen, O., Lorenzen, C. J., Holmes, R.W., J. D. H. Strickland 1965.Fluorometric

determination of chlorophyll. *J. Cons. Cons. Int. Explor. Mer.* 30, 3-15.

Welschmeyer, N. A. 1994. Fluorometric analysis of chlorophyll *a* in the presence of chlorophyll *b* and pheopigments. *Limnol. Oceanogr.* 39, 985-1992.

Table 1. Analytical conditions of "Non-acidification method" and "Acidification method" for chlorophyll *a* with Turner Designs fluorometer (10-AU-005).

	Non-acidification method	Acidification method
Excitation filter (nm)	436	340-500
Emission filter (nm)	680	>665
Lamp	Blue Mercury Vapor	Daylight White
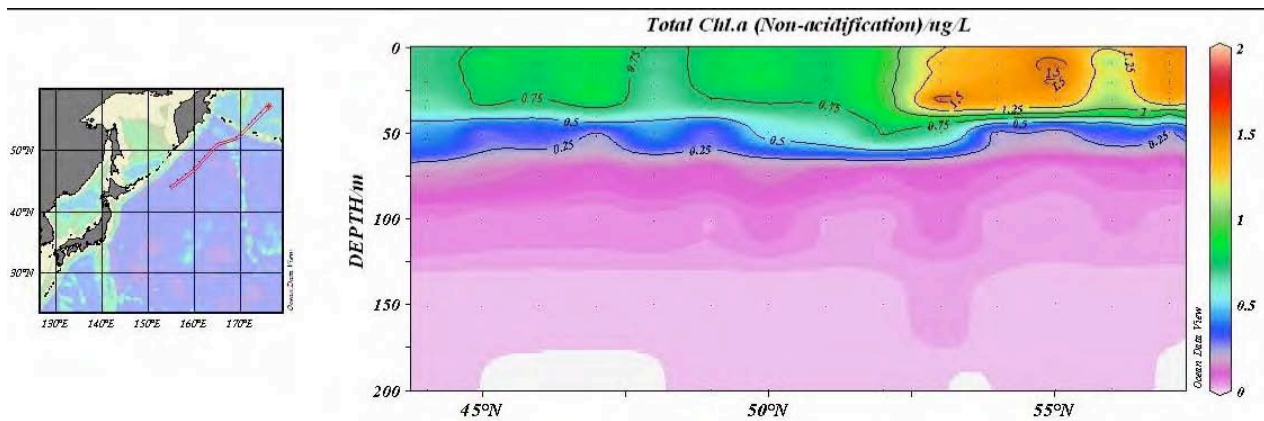
Fig. 1 Spatial distribution of chlorophyll *a* concentration (μg/L) during this cruise.
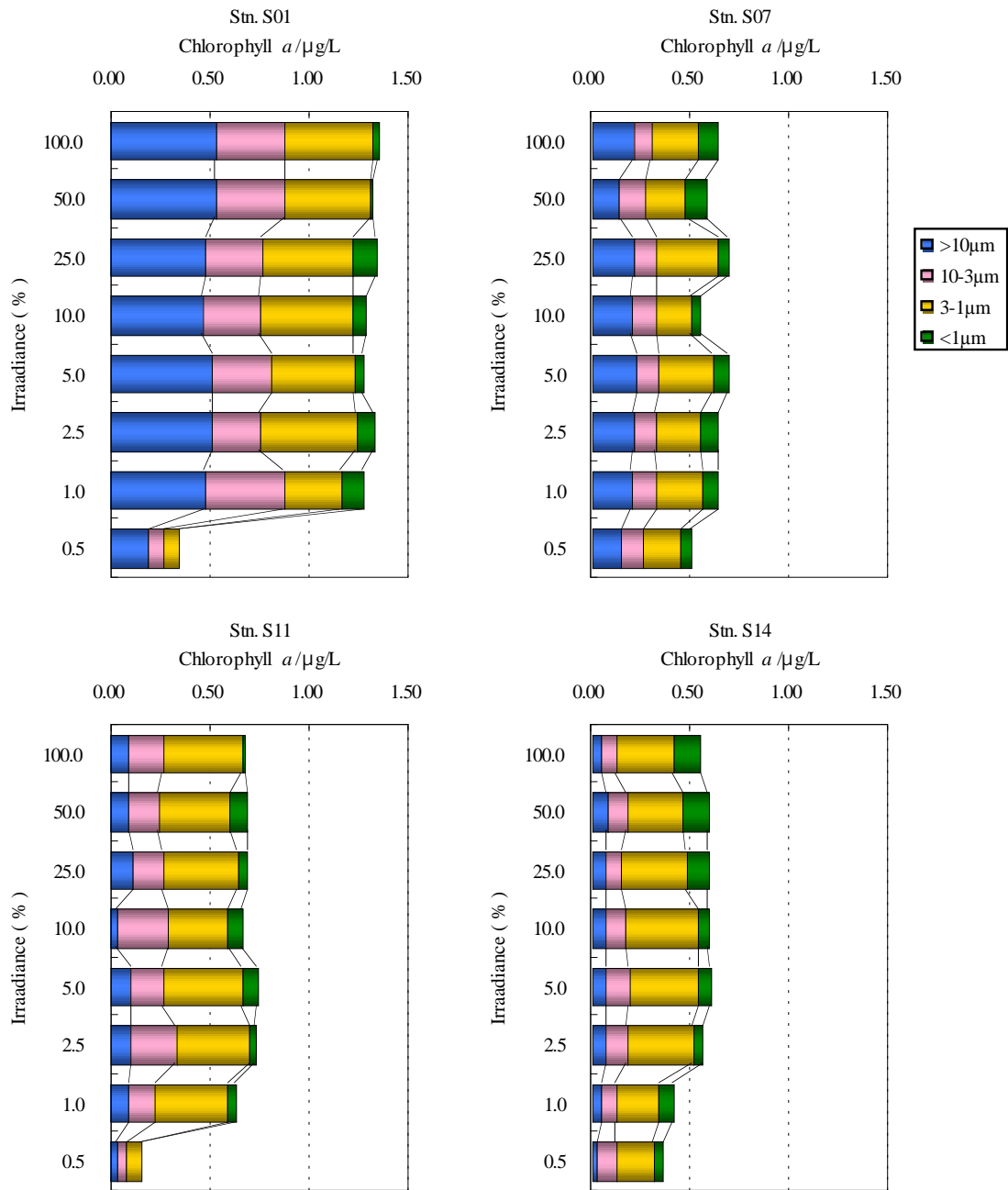
Fig.2 Vertical distribution of size-fractionated chlorophyll *a* during shallow-cast.

3.2.2. HPLC measurements of marine phytoplankton pigments

Kazuhiko MATSUMOTO (JAMSTEC MIO)
Tetsuichi FUJIKI (JAMSTEC MIO)
Yuichi SONOYAMA (MWJ)

(1) Objective

The chemotaxonomic assessment of phytoplankton populations present in natural seawater requires taxon-specific algal pigments as good biochemical markers. A high-performance liquid chromatography (HPLC) measurement is an optimum method for separating and quantifying phytoplankton pigments in natural seawater.

In this cruise, we measured the marine phytoplankton pigments by HPLC to investigate the marine phytoplankton community structure in the northwestern Pacific Ocean.

(2) Methods, Apparatus and Performance

Seawater samples were collected at 8 depths, which were determined by the light intensity as 100, 50, 25, 10, 5, 2.5, 1 and 0.5 % of surface incident irradiance during shallow-cast using Niskin bottles, except for the surface water (100%), which was taken by a bucket. The water samples (5L) were filtrated at a vacuum-pressure below 0.02MPa through the 47 mm-diameter Whatman GF/F filter. To remove retaining seawater in the sample filters, GF/F filters were vacuum-dried in a freezer (-20 °C) within 5 hours. Subsequently, phytoplankton pigments retained on a filter were extracted in a glass tube with 4 ml of N,N-dimethylformamide (HPLC-grade) for at least 24 hours in a freezer (-20 °C), and analyzed by HPLC within a few days.

Residua cells and filter debris were removed through polypropylene syringe filter (pore size: 0.2 μm) before the analysis. The samples (500μl) were injected from the auto-sampler immediately after the addition of pure water (180μl) and internal standard (10μl) with the extracted pigments (420μl). Phytoplankton pigments were quantified based on C8 column method containing pyridine in the mobile phase (Zapata *et al*., 2000). The eluant linear gradients of this method were modified slightly to be fit for our system.

（ⅰ）HPLC System

HPLC System was composed by a Waters modular system (high dwell volume) including 600S controller, 616 pump (low-pressure mixing system), 717 Plus auto-sampler and 996 photodiode array detector (2.4 nm optical resolution).

（ⅱ）Stationary phase

Analytical separations were performed using a YMC C_8 column (150×4.6 mm). The column was thermostatted at 25 °C in the column heater box.

（ⅲ）Mobile phases

The eluant A was a mixture of methanol : acetonitrile : aqueous pyridine solution (0.25M pyridine) (50 : 25 : 25　v : v : v). The eluant B was a mixture of acetonitrile : acetone (80 : 20　v : v). Organic solvents for mobile phases were used reagents of HPLC-grade.

（ⅳ）Calibrations

HPLC was calibrated using the standard pigments (Table 1). We selected Chlorophyll

a, Chlorophyll *b* (Sigma co.) and other 23 pigments (DHI co.). The solvents of pigment standards were displaced to N,N-dimethylformamide and the concentrations were determined with spectrophotometer by using its extinction coefficient.

(ⅴ) Internal standard
　　　Ethyl-apo-8'-carotenoate was added into the samples prior to the injection as the internal standard. When we analyzed samples, the area values of internal standard were slightly higher compared with the earlier measurements of the standard solutions (Chlorophyll *a* and Chlorophyll *b*) because the equipment had not been stabilized yet (Figure 1). So we made corrections for the concentration of samples using internal standard. After the sequence number of 20 (Figure 1), the average of area values was 204630±1827 (n=28), the coefficient of variation was 0.9%.

(ⅵ) Pigment detection and identification
　　　Chlorophylls and carotenoids were detected by photodiode array spectroscopy (350~720nm). Pigment concentrations were calculated from the chromatogram area at different five channels (Table 1).
　　　First channel was allocated at 661.4 nm of wavelength, which is the absorption maximum in red band for Divinyl Chlorophyll *a* and Chlorophyll *a*.
　　　Second channel was allocated at 663.9 nm, which is the absorption maximum in red band for Chlorophyllide *a*, Pheophorbide *a* and Pheophytin *a*.
　　　Third channel was allocated at 457.2nm, which is the absorption maximum in red band for Chlorophyll *b*.
　　　Fourth channel was allocated at 440.0 nm, whichi is the absorption maximum in red band for [3,8-Divinyl]-Protochlorophyllide.
　　　Fifth channel was allocated at 460.0 nm for other pigments. However, we could not acquire satisfactory separation between Zeaxanthin and Lutein, and Neoxanthin and Violaxanthin also could not be separated from other pigments.

(3) Preliminary results
　　　Vertical profiles of major pigments were shown in Figure 2.

(4) Data archives
　　　The processed data file of pigments will be submitted to the JAMSTEC Data Integration and Analyses Group (DIAG) within a restricted period. Please ask PI for the latest information.

(5) Reference
Zapata M, Rodriguez F, Garrido JL (2000)　Separation of chlorophylls and carotenoids from marine phytoplankton : a new HPLC method using a reversed phase C8 column and pyridine-containing mobile phases. Mar. Ecol. Prog. Ser. 195 : 29-45

Table 1. Retention time and wavelength of identification for pigment standards.

No.	Pigment	Retention Time (minute)	Wavelength of identification (nm)
1	Chlorophyll *c3*	10.685	460
2	Chlorophyllide *a*	13.042	663.9
3	[3,8-Divinyl]-Protochlorophyllide	13.917	440
4	Chlorophyll *c2*	14.565	460
5	Peridinin	18.027	460
6	Pheophorbide *a*	20.280	663.9
7	19'-butanoyloxyfucoxanthin	20.955	460
8	Fucoxanthin	21.968	460
9	Neoxanthin	22.248	460
10	Prasinoxanthin	23.572	460
11	19'-hexanoyloxyfucoxanthin	24.200	460
12	Violaxanthin	24.343	460
13	Diadinoxanthin	26.063	460
14	Antheraxanthin	26.682	460
15	Alloxanthin	27.052	460
16	Diatoxanthin	27.488	460
17	Zeaxanthin	27.850	460
18	Lutein	27.927	460
19	Ethyl-apo-8'-carotenoate	29.203	460
20	Crocoxanthin	30.705	460
21	Chlorophyll *b*	31.200	457.2
22	Divinyl Chlorophyll *a*	32.325	661.4
23	Chlorophyll *a*	32.500	661.4
24	Pheophytin a	35.605	663.9
25	Alpha-carotene	35.747	460
26	Beta-carotene	35.948	460
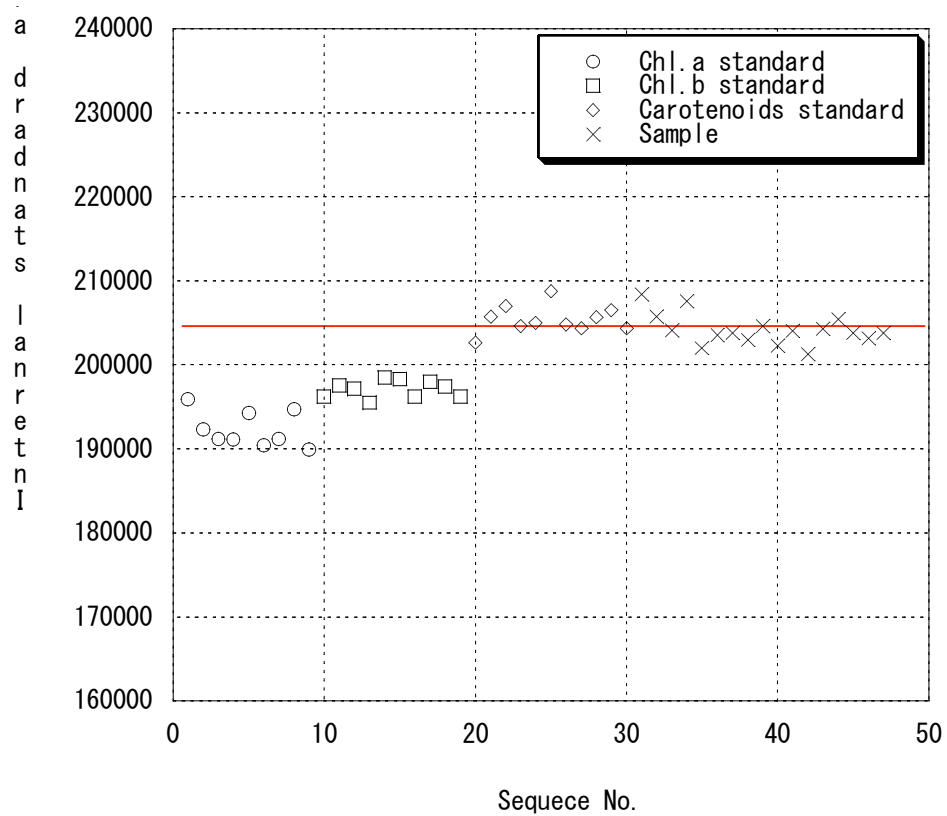
Fig. 1   Variabilities of the chromatogram areas for the internal standard. The average of area values after the sequence number of 20 was indicated with red line.
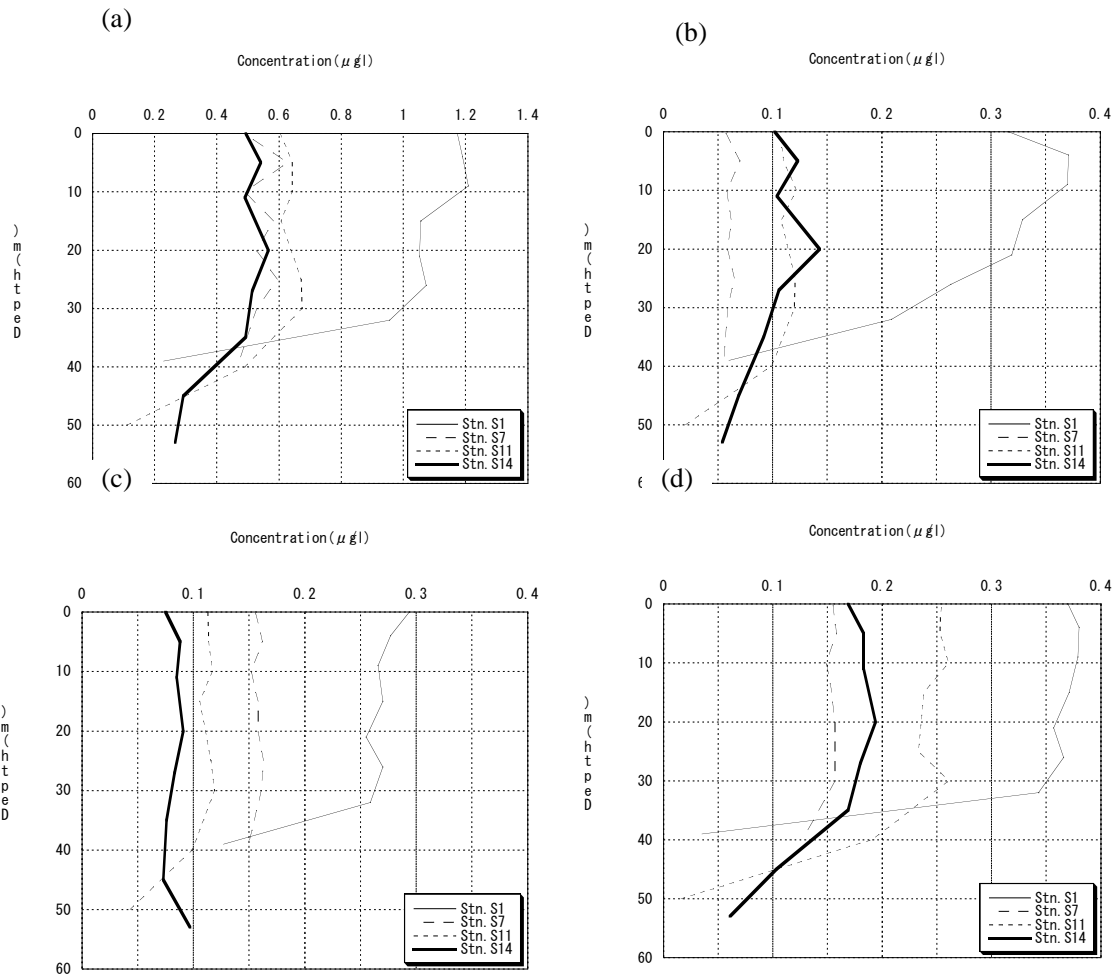
Fig. 2 Vertical distributions of phytoplankton pigments (μg/l) at the station of Stn.S1, S7, S11 and S14. Chlorophyll *a* (a), Chlorophyll *b* (b), Fucoxanthin (c), 19'-Hexanoyloxyfucoxanthin (d) are roughly represented as the abundance of total phytoplankton, green algae, diatoms, and haptophytes, respectively.

3.2.3 Phytoplankton abundances

Kazuhiko MATSUMOTO (JAMSTEC MIO)

(1) Objectives

The main objective of this study is to estimate phytoplankton abundances and their taxonomy in the western North Pacific subarctic gyre and the Bering Sea. Phytoplankton abundances were measured with two kinds of methods: microscopy for large size phytoplankton and flowcytometry for picophytoplankton.

(2) Sampling

Samplings were conducted within the euphotic zone using Niskin bottles, except for the surface water, which was taken by a bucket. Sampling depths were determined to correspond to eight light levels (100%, 50%, 25%, 10%, 5%, 2.5%, 1% and 0.5% of surface incident irradiance). Samplings were carried out at the four observational stations of S01, S07, S11 and S14.

(3) Methods
 1) Microscopy

Water samples were placed in 500 ml plastic bottle and fixed with neutral buffered formalin solution (1% final concentration). The microscopic measurements are scheduled after the cruise.

 2) Flowcytometry
  2)-1 Equipment

The flowcytometry system used in this research was BRYTE HS system (Bio-Rad Laboratories Inc). System specifications are follows:

Light source: 75W Xenon arc lamp
Excitation wavelength: 350-650 nm
Detector: high-performance PMT
Analyzed volume: 75 µl
Flow rate: 10 µl min^{-1}
Sheath fluid: Milli-Q water
Filter block: B2 as excitation filter block, OR1 as fluorescence separator block
B2 and OR1 have ability as follows:

B2:	Excitation filter	390-490 nm
	Beam-splitter	510 nm
	Emission filter	515-720 nm
OR1:	Emission filter 1	565-605 nm
	Beam-splitter	600 nm
	Emission filter 2	>615 nm

  2)-2 Measurements

The water samples were pre-filtered by Nuclepore filter of 3µm pore size. The pre-filtered samples were fixed immediately with glutaraldehyde (1% final concentration) and stored in the dark at 4°C. The analysis by the flow cytometer was acquired on board within 24 hours after the sample fixation. Calibration was achieved with standard beads (Polysciences) of 2.764µm. Standard beads were added into each sample prior to the

injection of flow cytometer as internal standard. Phytoplankton cell populations were estimated from the forward light scatter signal. Acquired data were stored in list mode file and analyzed with WinBryte software. Phytoplankton are classified with prokaryotic cyanobacteria (*Prochlorococcus* and *Synechococcus*) and other eukaryotes on the basis of scatter and fluorescence signals. *Synechococcus* is discriminated by phycoerythrin as the orange fluorescence, while other phytoplankton are recognized by chlorophylls as the red fluorescence without the orange fluorescence. *Prochlorococcus* and picoeukaryotes were distinguished with their cell size.

(4) Preliminary result

Prochlorococcus was not observed in this cruise, whereas *Synechococcus* was numerically dominant through the observation. The abundance of *Synechococcus* increased outside the Bering Sea and showed the highest abundance at the south station of S14.

(5) Data Archive

All data will be submitted to Data Integration and Analysis Group (DIAG), JAMSTEC. Please ask PI for the latest information.
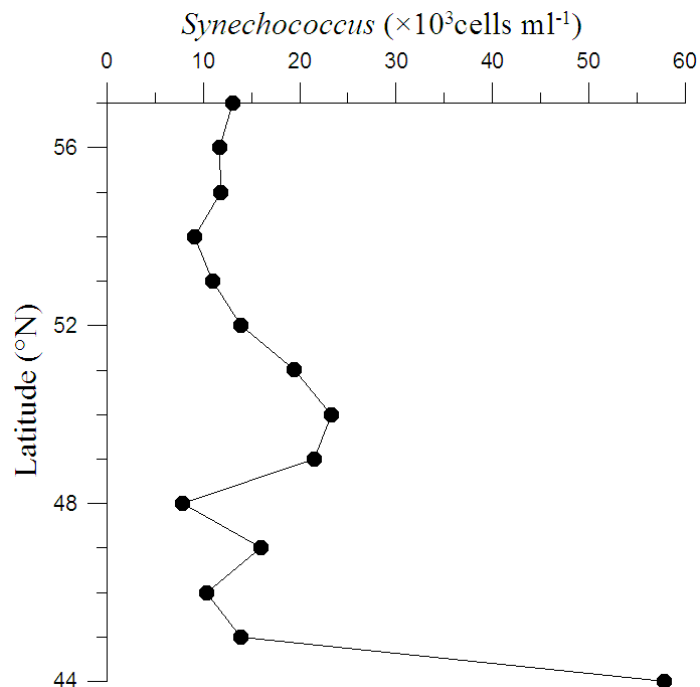
Fig. 1. Latitudinal shift of *Synechococcus* abundances of the surface.

3.3 Th-234 and export flux

Hajime KAWAKAMI (JAMSTEC MIO)
Makio HONDA (JAMSTEC MIO)

(1) Purpose of the study

The fluxes of POC were estimated from Particle-reactive radionuclides (^{234}Th, ^{210}Po) and their relationship with POC in the northwestern North Pacific Ocean.

(2) Sampling

Seawater and suspended particulate sampling for ^{234}Th and POC: 3 stations [stations S1 (AB), S7 (K1), and S11 (K2)] and 8 depths (10m, 20m, 30m, 50m, 75m, 100m, 150m, and 200m) at each station.   Seawater and suspended particulate sampling for ^{210}Po, ^{210}Pb, and POC: 1 station [station S11 (K2)] and 16 depths (10m, 20m, 30m, 50m, 75m, 100m, 150m, 200m, 300m, 400m, 500m, 600m, 700m, 800m, 900m, and 1000m) at each station.   Settling particulate sampling for ^{234}Th: 2 stations [stations S7 (K1) and S11 (K2)] and 4 depths (60 m, 100 m, 150 m, 200 m).

Seawater samples (30 L for ^{234}Th, 10 L for ^{210}Po and ^{210}Pb) were taken from Hydrocast at each depth.   The seawater samples for ^{234}Th and ^{210}Po were filtered through polypropylene cartridge filters with a pore size of 0.8 μm on board immediately after water sampling.

In situ filtering (suspended particulate) samples were taken from large volume pump sampler (Large Volume Pump WTS-6-1-142V, McLane Inc.). Approximately 200L seawater was filtered through GF/F filter at each station at 10–200m depths (for ^{234}Th, ^{210}Po, and POC). Approximately 1 m^3 seawater was filtered through Nitex mesh filter with a pore size of 53μm at each station (for ^{234}Th and POC).   Drifting sediment trap's (settling particulate) samples were filtered with GF/F filter (for ^{234}Th).   Approximately 500L seawater was filtered through GF/F filter at each station at 300–1000m depths (for ^{210}Po, and POC).   The filter samples were divided for radionuclides and POC.

(3) Chemical analyses

Dissolved, particulate and drifting sediment trap's ^{234}Th was purified using anion exchange method.   Purified ^{234}Th was absorbed on 25mm stainless steel disks electrically, and were measured by b-ray counter (LBC-470, Aloka Co. Ltd.).

Dissolved and particulate ^{210}Po was absorbed on 25mm silver disks electrically, and were measured by a-ray counter (Octéte, Seiko EG&G Co. Ltd.).   For total (dissolved + particulate) ^{210}Pb measurement, the same procedure was applied to the seawater samples 18 months later, when ^{210}Po come to radioactive equilibrium with ^{210}Pb.

POC was measured with an elemental analyzer (Perkin-Elmer model 2400) in land-based laboratory.

(4) Preliminary result

The distributions of ^{234}Th, ^{210}Po, and POC will be determined as soon as possible after this cruise.   This work will help further understanding of particle dynamics at the euphotic layer and twilight zone.

3.4 Optical measurement

Makio HONDA (JAMSTEC MIO)
Kazuhiko MATSUMOTO (JAMSTEC MIO)

(1) Objective

The objective of this measurement is to investigate the air and underwater light conditions at respective stations and to determine depths for *in situ* or simulated *in situ* measurement of primary production by using carbon stable isotope (C-13) during late autumn. In addition, optical data can be used for the validation of satellite data.

Moreover, our group (JAMSTEC-MIO) have been conducting time-series observation with using a mooring system in the northwestern North Pacific (NWNP). On this mooring system, optical sensor package called BLOOMS are installed. The BLOOM measures spectral downwelling irradiance and upwelling radiance for four wavelengths (412 nm, 443 nm, 490 nm and 555 nm) and chlorophyll. Another objective of optical observation during this cruise was to know the optical characteristics and to contribute to the evaluation of observed values by BLOOM.

(2) Description of instruments deployed

The instrument consisted of the SeaWiFS Profiling Multichannel Radiometer (SPMR) and SeaWiFS Multichannel Surface Reference (SMSR). The SPMR was deployed in a free fall mode through the water column. The SPMR profiler called "Free Fall" has a 13 channel irradiance sensors (Ed), a 13 channel radiance sensors (Lu), tilt sensor, and fluorometer. The SMSR has a 13 channel irradiance sensors (Es) and tilt meter (Table 1). These instruments observed the vertical profiles of visible and ultra violet light and chlorophyll concentration.

Table 1. Center wavelength (nm) of the SPMR/SMSR

Es	379.5	399.6	412.2	442.8	456.1	490.9	519.0	554.3	564.5	619.5	665.6	683.0	705.9
Ed	380.0	399.7	412.4	442.9	455.2	489.4	519.8	554.9	565.1	619.3	665.5	682.8	705.2
Lu	380.3	399.8	412.4	442.8	455.8	489.6	519.3	554.5	564.6	619.2	665.6	682.6	704.5

Optical measurements by Free Fall were conducted at major stations including our time-series station K2. Measurements should be ideally conducted at median time. However observations were conducted irregularly because of limited ship-time and other observation's convenience (Table 2). The profiler was deployed twice at respective stations to a depth of 100 m. The SMSR was mounted on the anti-rolling system's deck and was never shadowed by any ship structure. The profiler descended at an average rate of 1.0 m/s with tilts of less than 3 degrees except near surface.

Observed data was analyzed by using software "Satlantic PPROSOFT 6" and extinction rate and photosynthetically available radiation (PAR) were computed.

Table 2 Locations of optical observation and principle characteristics
(Date and Time in LST: UTC+11hr.)

Date and Time	Station	Lat./Long.	Surface PAR (quanta cm^{-2} sec^{-1})	Euphotic layer (m)
2008.10.14 10:11	AB	57N/176E	$1.38*10^{16}$	~ 32
2008.10.19 11:00	K1B	50-59.8N/166-39.5E	$1.22*10^{16}$	~ 32
2008.10.20 11:00	K1	51N/165E	$5.33*10^{16}$	~ 40
2008.10.25 11:45	K2	47N/160E	$4.82*10^{16}$	~ 40
2008.10.27 10:45	K2-2	47N/160E	$1.39*10^{16}$	~ 43
2008.10.31 09:00	KNOT	44N/155E	$2.10*10^{16}$	~ 45
2008.10.31 11:30	KNOT-2	44N/155E	$7.55*10^{16}$	~ 45

(3) Preliminary result

We deployed "Free Fall sensor" 7 times (Table 2). Surface PAR ranged from approximately 1.2 x 10^{16} to 7.6 x 10^{16} quanta cm^{-2} sec^{-1}.   The euphotic layer that is defined as water depth with 1 % of surface PAR ranged from 32 to 45 m.   There was tendency that euphotic layer depth increases southward.   It is likely that particulate materials, *i.e.* phytoplankton, in the water column were smaller at the southern station than those at the northern station. The euphotic layer at time-series station K2 was approximately 40 m.

(4) Data archive

Optical data were filed on two types of file.
(BIN file) digital data of upwelling radiance and downwelling irradiance each 1 m from near surface to approximately 100 m for respective wave-lengths with surface PAR data during "Free Fall" deployment
(PAR file) in situ PAR each 1 m from near surface to approximately 100 m with extinction coefficient with surface PAR data during "Free Fall" deployment

These data files will be submitted to JAMSTEC Data Integration and Analyses Group (DIAG).

3.5 Primary productivity and drifting sediment trap

Makio HONDA (JAMSTEC MIO)
Hajime KAWAKAMI (JAMSTEC MIO)
Fuyuki SHIBATA (MWJ)
Ai YASUDA (MWJ)
Kento FUKABORI (MWJ)

3.5.1 Drifting mooring system

In order to conduct *in situ* incubation for measurement of primary productivity and drifting sediment trap experiment at station K2, drifting mooring system (drifter) was deployed. This drifter consists of radar reflector, GPS radio buoy (Taiyo TGB-100), flush light, surface buoy, ropes and sinker.　On this system, incubation bottles at 8 layers and "Knauer" type sediment trap at 4 layers were installed together.　Thanks to the effort by MWJ technicians, drifting mooring system was upgraded on board.　The configuration is shown in Fig. 3.5.1.1.

The drifter was deployed at 19:30 on 19 October (UTC) at station K1 and at 23:00 on 27 October at station K2 (UTC) and recovered after 24 hours.　The drifter's position was monitored by using GPS radio buoy (Taiyo TGB-100).　Fig. 3.5.1.2 shows tracks of the drifter. In general, the drifter tended to drift southeastward at station K2 with rotation.
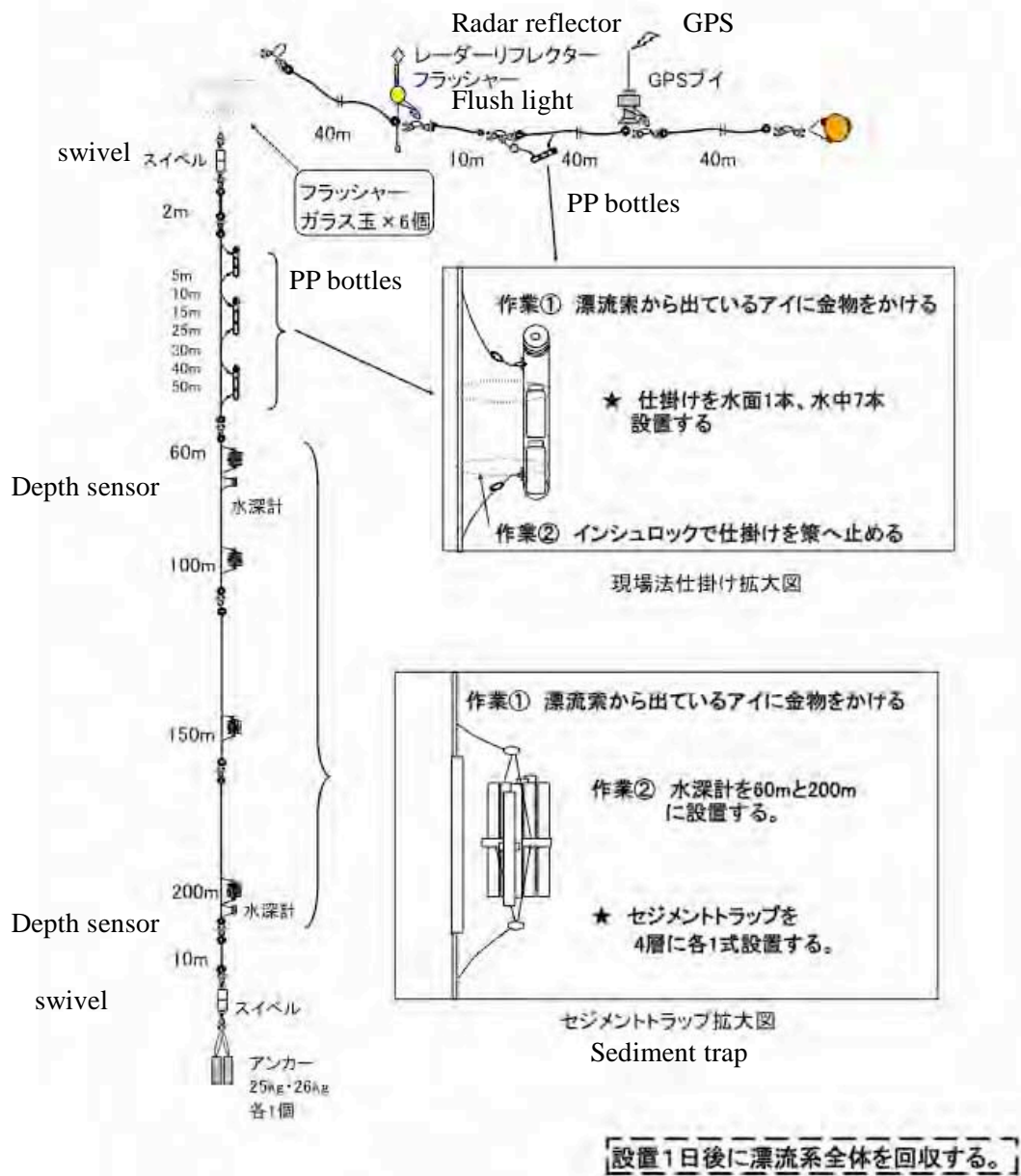
Fig. 3.5.1.1 Drifting mooring system at station K2
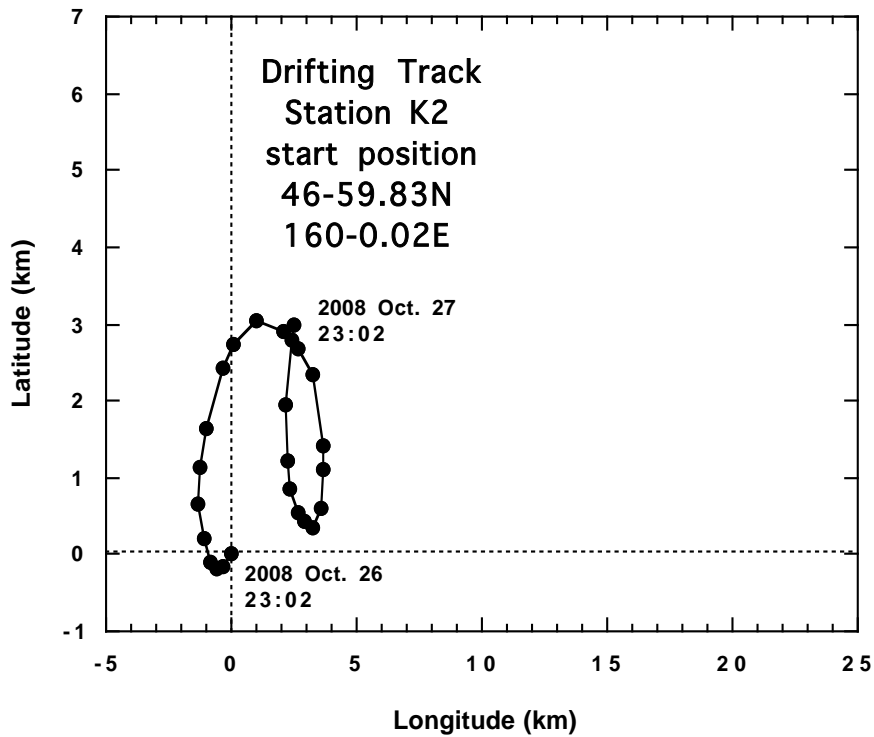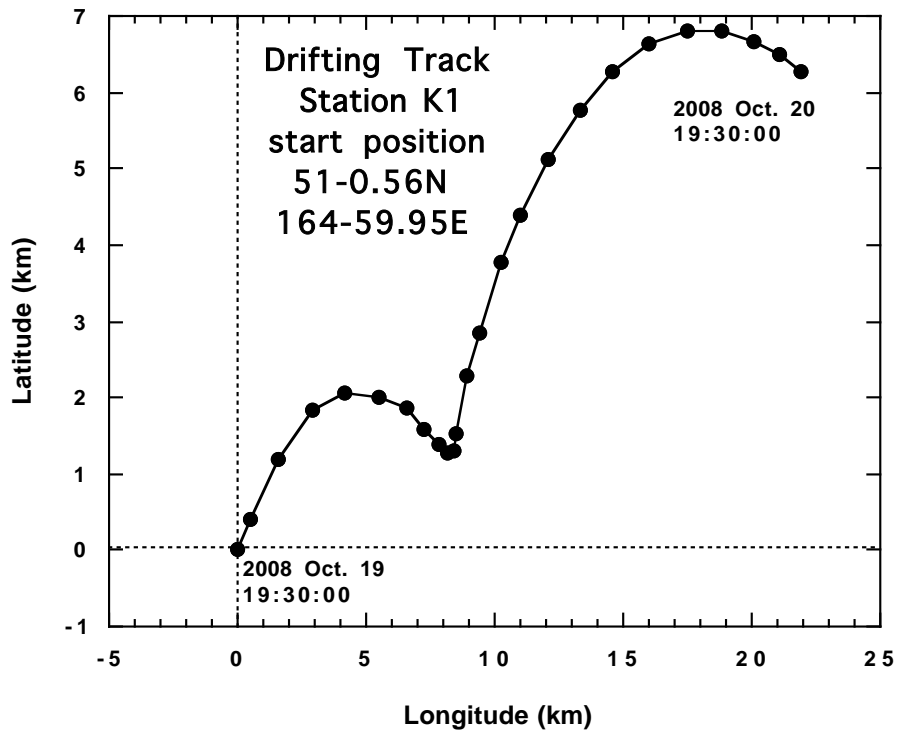
Fig. 3.5.1.2 Track of drifter (GPS buoy) at stations K 1 and K2

3.5.2 Primary productivity

Primary productivity was measured at major stations (AB, K1, K2, KNOT). Incubation for PP measurement at station K1 and K2 were conducted by *in situ* incubation method using the above drifting system and incubation at stations AB and KNOT was conducted by simulated *in situ* incubation method using the light-controlled water bath on deck.

(1) *in-situ* or simulated *in situ* incubation
1) Bottles for incubation and filters

Bottles for incubation are *ca.* 1 liter Nalgen polycarbonate bottles with screw caps. Grass fiber filters (Wattman GF/F 25mm) pre-combusted with temperature of 450° C for at least 2 hours were used for a filtration of phytoplankton after incubation.

2) Incubation

Water samples were collected at 8 layers between the surface and seven pre-determined depths by a bucket or Niskin bottle. These depths corresponded to nominal specific optical depths *i.e.* approximately 50%, 25%, 10%, 5%, 2.5%, 1% and 0.5% light intensity relative to the surface irradiance as determined from the optical profiles obtained by "Free Fall sensor". All samples were spiked with 0.2 μmoles/mL of NaH^{13}CO$_3$ solution. After spike, bottles were installed at respective depths on the drifter and *in situ* incubated (Fig.3.5.1.1) or bottles were incubated in the water baths on deck. Natural light was adjusted to the light level for each depth with blue film. After 24 hours incubation, samples were filtrated through grass fiber filters (Wattman GF/F 25mm). GF/F filters were kept in a freezer on board until analysis.

(2) Soler Irradiance and water temperature during incubation

Fig.3.5.2.1 and 3.5.2.2 show diurnal change of photosynthetically available radiation (PAR) observed by PAR sensor (Trios Optical sensors RAMSES-ACC), and vertical profile of water temperature measured by CTD, respectively. Daily PARs during incubation ranged from 6 to 16 E m^{-2} day^{-1}. However daily PAR during the second incubation at station K2 was quite low. Surface water temperature were 8±1°C except KNOT (~ 12°C). Water temperature was almost constant upper 35-40 m. Water bath on deck for simulated *in situ* incubation was filled up with surface seawater. Thus phytoplankton collected below 35 m at station KNOT and below 40 m at station AB was incubated under higher temperature than actual *in situ* temperature, resulting overestimate of PP.
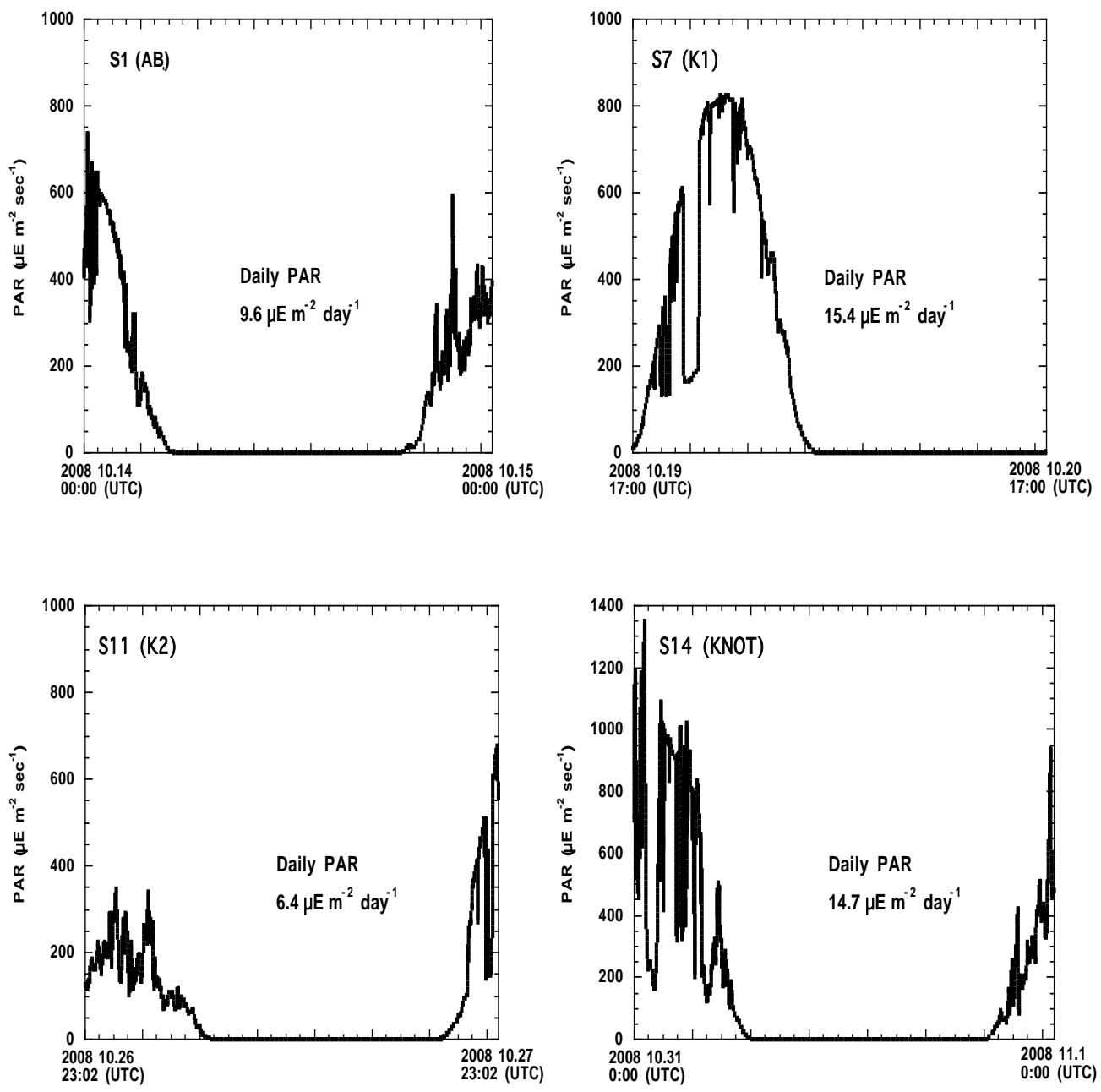
Fig. 3.5.2.1 Photosynthesis Available Radiation (PAR) during *in situ* incubation
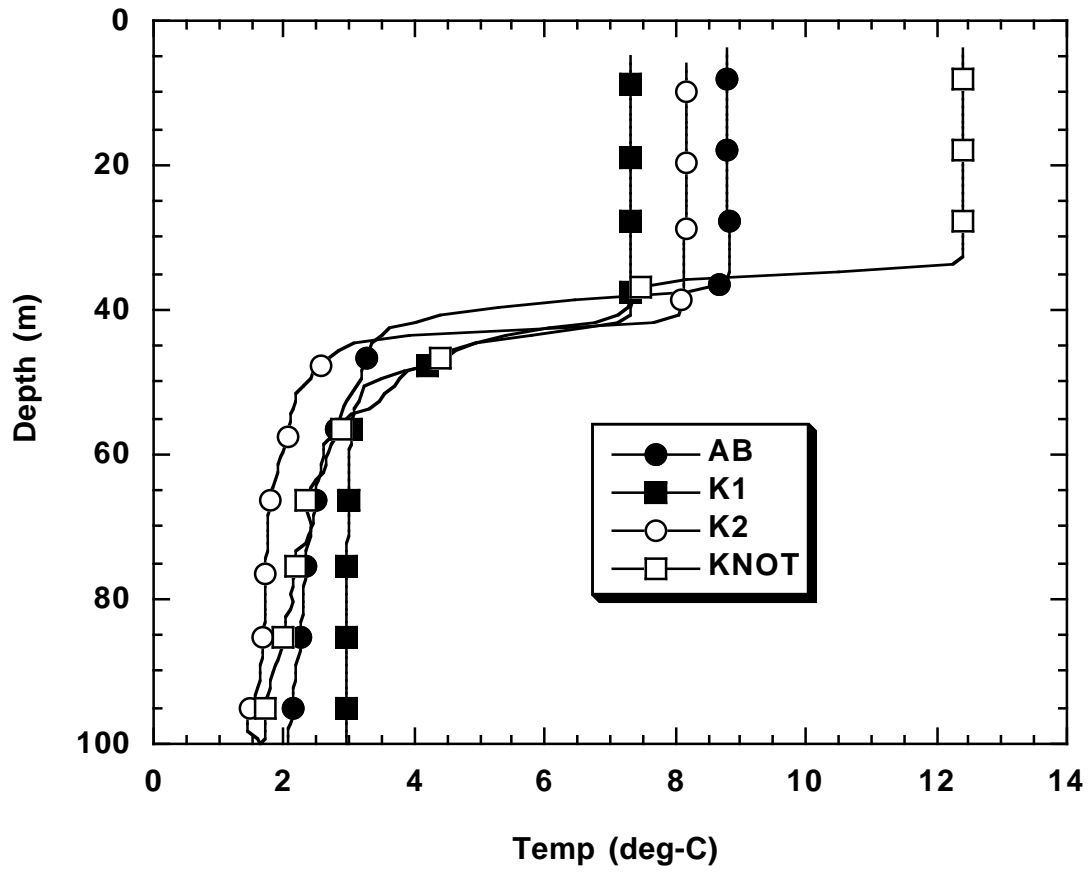
Fig. 3.5.2.2 Vertical profile of water temperature for respective stations observed with CTD .

(3) Measurement

^{13}C of samples were measured by using a mass spectrometer ANCA-SL system on board.

Before analysis, inorganic carbon of samples was removed by an acid treatment in a HCl vapor bath for 4 - 5 h.

Based on the balance of ^{13}C, assimilated organic carbon (ΔPOC) is expressed as follows (Hama *et al*., 1983):

$$^{13}C_{(POC)} \times POC = {}^{13}C_{(sw)} \times \Delta POC + (POC - \Delta POC) \times {}^{13}C_{(0)}$$

This equation is converted to the following equation;

$$\Delta POC = POC \times ({}^{13}C_{(POC)} - {}^{13}C_{(0)}) / ({}^{13}C_{(sw)} - {}^{13}C_{(0)})$$

where $^{13}C_{(POC)}$ is concentration of ^{13}C of particulate organic carbon after incubation, *i.e.*, measured value (%). $^{13}C_{(0)}$ is that of particulate organic carbon before incubation, *i.e.*, that for sample as a blank (1.084 in this cruise).
$^{13}C_{(sw)}$ is concentration of ^{13}C of ambient seawater with a tracer. This value for this study was determined based on the following calculation;

$$^{13}C_{(sw)} (\%) = [(TDIC * 0.011) + 0.0002] / (TDIC + 0.0002) \times 100$$

where TDIC is concentration of total dissolved inorganic carbon at respective bottle depths (mol l^{-1}) and 0.011 is concentration of ^{13}C of natural seawater (1.1 %). 0.0002 is added ^{13}C (mol) as a tracer. Taking into account for the discrimination factor between ^{13}C and ^{12}C (1.025), primary productivity (PP) was, finally, estimated by

$$PP = 1.025 \times \Delta POC$$

The precision (repeatability: standard deviation / average, n = 32) ranged from 0.6% to 28% with average of 4.9%.

(4) Preliminary results

Primary productivity (PP) decreased with depth (Fig. 3.5.2.3). Maximum PP of 30 mg m^{-3} day^{-1} was observed at surface at station AB. Integrated PP at station AB was approximately 450 mg-C m^{-2} day^{-1} and larger than other PP although daily PAR was low. It was attributed to large biomass of phyto-plankton. Integrated PP at station K2 was approximately 210 mg m^{-2} day^{-1}. It is attributed to quite low daily PAR during incubation. Fig. 3.5.2.4 shows seasonal variability in PP observed at station K2 since 2003. Observed PP was one of the lowest PP. It was suspected that PP would decrease more in winter.

(5) Data archived

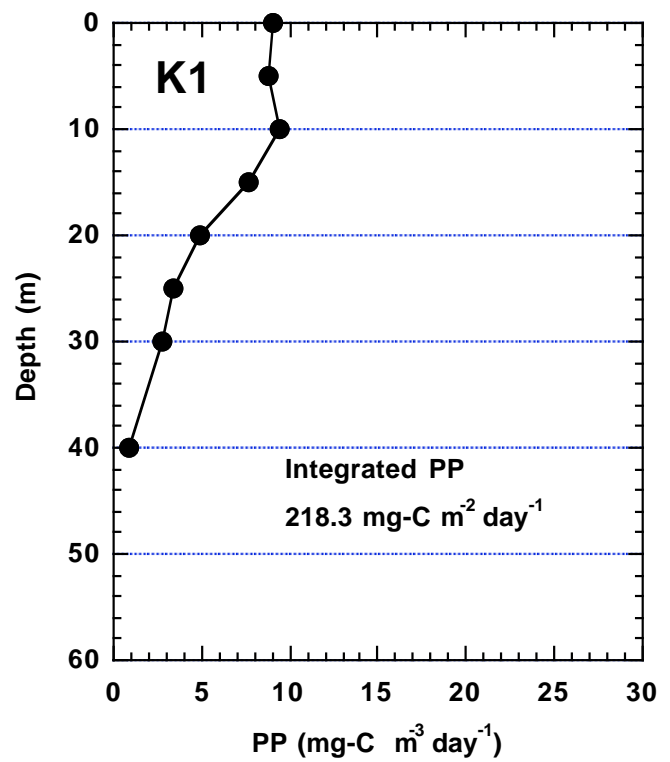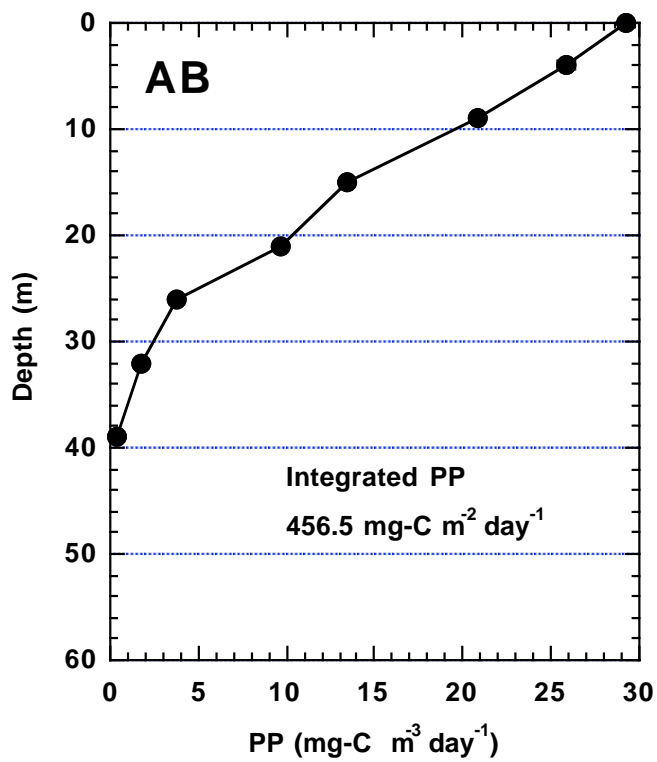All data will be submitted to JAMSTEC Data Integration and Analyses Group (DIAG).
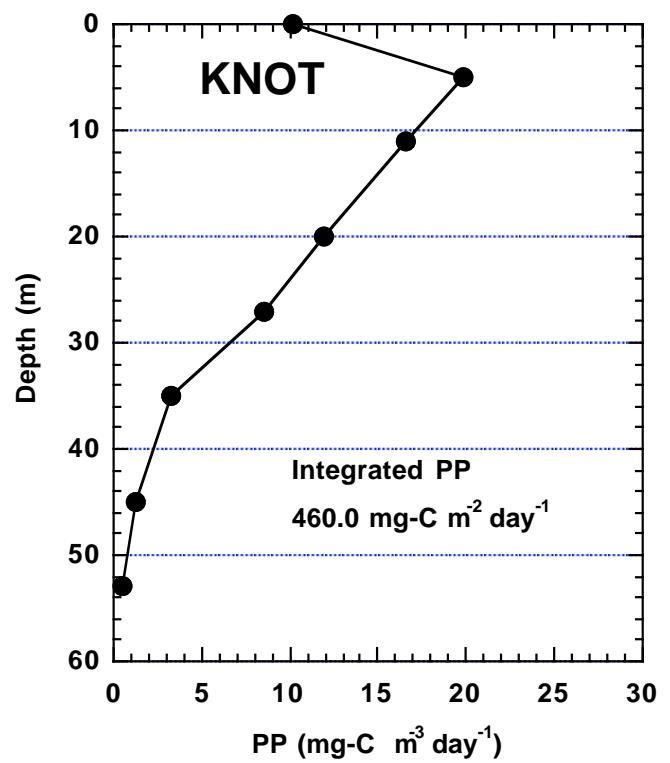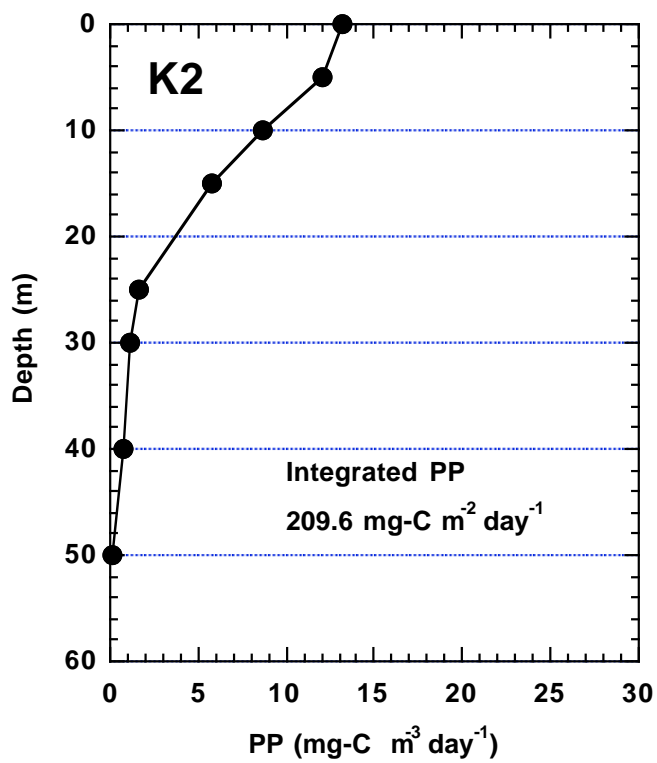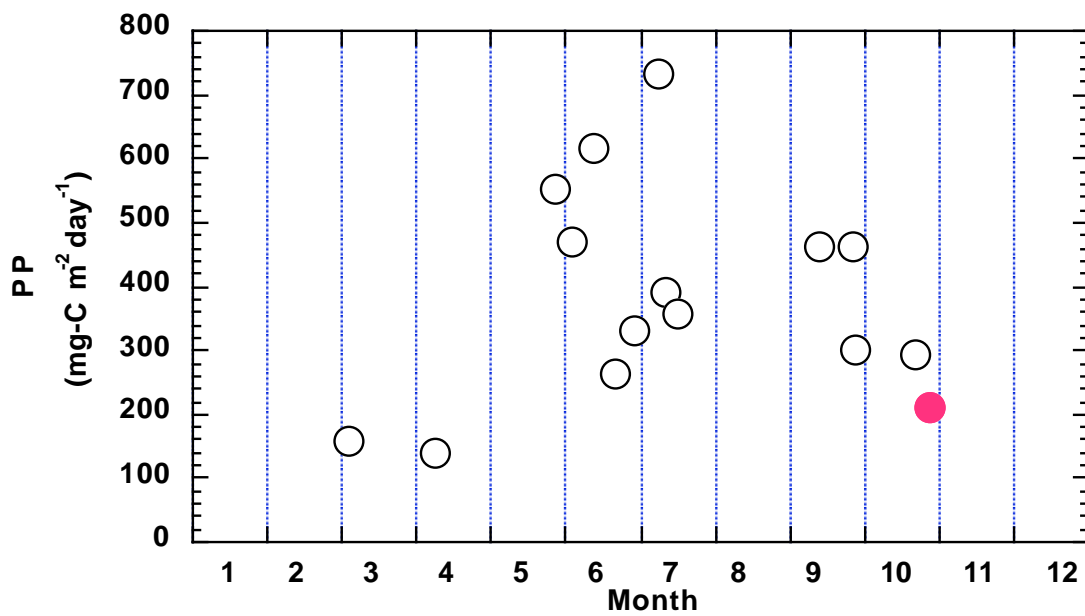
Fig. 3.5.2.3 Primary productivity

Fig. 3.5.2.4 Seasonal variability in PP at station K2 that have been observed since 2003. Red circles are PP observed during this cruise (210 mg-C m^{-2} day^{-1}).

3.5.3 Drifting sediment trap

In order to collect sinking particles and measure carbon flux, radionuclide, and zooplankton, "Knauer type" cylindrical sediment trap (Photo 3.5.3.1) was deployed at stations K1 and K2 where measurement of primary productivity and in situ pumping (LVP) were conducted. This trap consists of 8 individual transparent policarbonate cylinders with baffle (collection area: ca. 0.0038 m^2, aspect ratio: 620 mm length / 75 mm width = 8.27), which were modified from Knauer (1979). Before deployment, each trap was filled with filtrated surface seawater, which salinity is adjusted to ~ 39 PSU by addition of NaCl (addition of 100 mg NaCl to 20 L seawater) were placed in tubes. These were located at approximately 60 m, 100 m, 150 m and 200 m. After recovery, sediment traps were left for half hour to make collected particles settle down to the bottle. After seawater in acrylic tube was dumped using siphonic tube, collecting cups were took off. In laboratory on board, seawater with sinking particles were filtrated on various filters for respective purpose. These were kept in freezer by the day when these were analyzed.
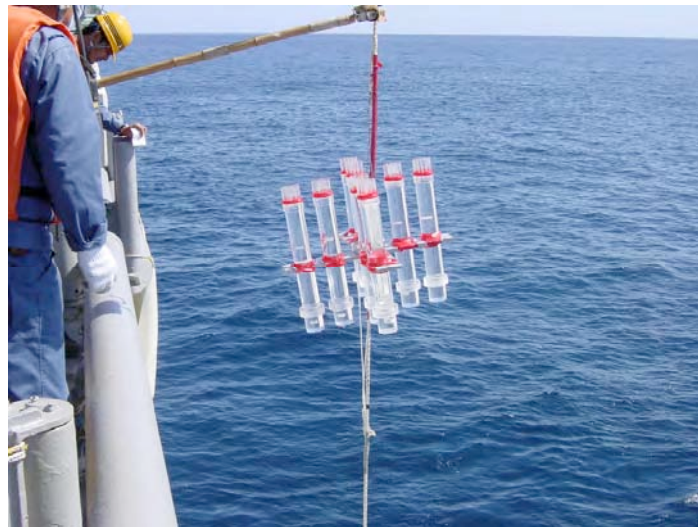
Photo 3.5.3.1 Drifting Sediment Trap

3.5.4 P vs. E curve

Kazuhiko MATSUMOTO   **(JAMSTEC)**
Fuyuki SHIBATA   **(MWJ)**
Ai YASUDA   **(MWJ)**
Kento FUKAHORI   **(MWJ)**

(1) Objectives

The objective of this study is to estimate the relationship between phytoplankton photosynthetic rate (P) and scalar irradiance (E) in the western North Pacific and the Bering Sea.

(2) Sampling

Samplings were carried out at four observational stations of S01, S07, S11 and S14. Water samples were collected at the surface by a bucket, and the depths of 2.5% and 25% of the surface incident irradiance at S01 and 5% depth at S11 by Niskin bottles. We examined the P vs. E curve experiments for size-fractionated samples at S07, S11 and S14.

(3) Methods
1) Incubation

Three incubators filled in water were used, illuminated at one end by a 500W halogen lamp. Water temperature was controlled by circulating water-cooler. Water samples were poured in nine polycarbonate bottles (approx. 1 liter) and arranged in the incubator linearly against the lamp after adding the isotope solutions. The isotope solutions of 13C and 15N were added as same as the primary productivity experiment. All bottles were controlled light intensity by shielding with a neutral density film on lamp side. The light intensities inside the bottles were shown in table 1. The incubations were conducted for three hours round about noon in local time.

2) Measurement

After the incubation, samples were treated as same as the primary productivity experiment.

The analytical function and parameter values used to describe the relationship between the photosynthetic rate (P) and scalar irradiance (E) are best determined using a least-squares procedure from the following equations.

$$P=P_{max}\tanh(\alpha E/P_{max}) : \text{(Jassby and Platt 1976)}$$
$$P=P_{max}(1-e^{-\alpha E/Pmax})e^{-b\alpha E/Pmax} : \text{(Platt et al., 1980)}$$

where, P_{max} is the light-saturated photosynthetic rate, α is the initial slope of the P vs. E curve, b is a dimensionless photoinhibition parameter.

3) Size fractionation experiment

At the station of S07, S11 and S14, the P vs. E curve experiments were conducted for the size-fractionated samples. The collected sample water was filtrated through 3µm and 10µm Nuclepore filter individually before the incubation. The P vs. E curve of three size fractions for <3µm, <10µm and total were acquired from the incubations of filtrated water and non-filtrated

water.

(4) Preliminary result

The experiments of the P vs. E curve of three size fractions are represented in Figure 1. At the lower irradiances, photosynthetic rates were almost directly proportional to the irradiance. As irradiance increases, the slope of the P vs. E curve decreased and the photosynthetic rate eventually reached to a saturation level. With further increase in irradiance, the photosynthetic rates were decreased relative to the saturation level by the photoinhibition.

(5) Data Archive

All data will be submitted to Data Integration and Analysis Group (DIAG), JAMSTEC. Please ask PI for the latest information.

References

Jassby, A.D., Platt, T. 1976. Mathematical formulation of relationship between photosynthesis and light for phytoplankton. Limnology and Oceanography, 21, 540-547.

Platt, T., Gallegos, C.L., Harrison, W.G. 1980. Photoinhibition of photosynthesis in natural assemblages of marine phytoplankton. Journal of Marine Research, 38, 687-701.

Table. 1 Light Intensity of P-E measurements

	Bath A	Bath B	Bath C	Bath C'
Bottle No.	Light Intensity (µE/m2/sec)			
1	2050	2050	1025	2000
2	1100	1150	500	1150
3	500	560	200	550
4	220	220	85	210
5	90	85	60	90
6	40	45	20	45
7	24	25	15	25
8	4.6	5	5	6.5
9	0.29	0.34	0.22	0.22

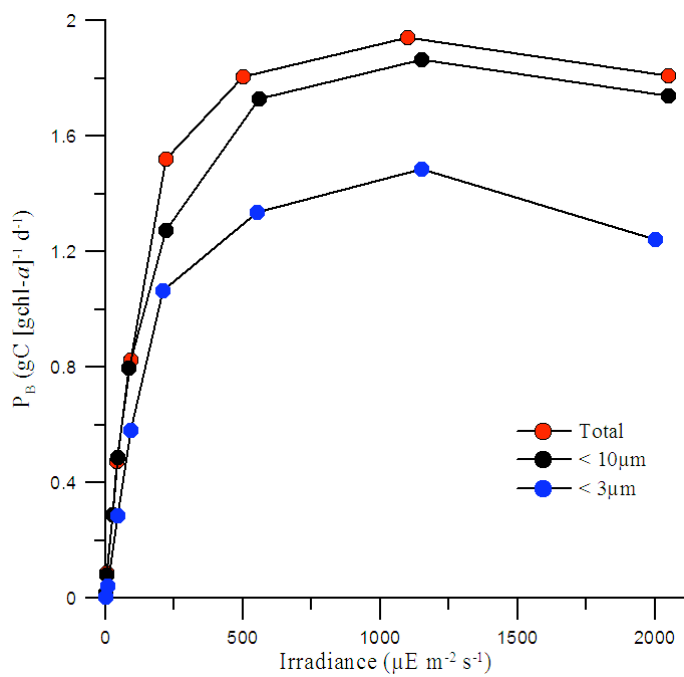*Bath C' was using in size fractionation experiment.

Fig. 1 The experiments of the P vs. E curve of three size fractions at the surface at S07.

3.5.5 New Production

Makio HONDA   (JAMSTEC MIO)
Kazuhiko MATSUMOTO   (JAMSTEC MIO)
Fuyuki SHIBATA   (MWJ)
Ai YASUDA   (MWJ)

(1) Objective

New production is generally defined as "primary production associated with not old or regenerated nitrogen such as NH_3-N, but newly available nitrogen such as NO_3-N". Under steady state condition, new production should be comparable to production that exported from surface layer or transported to the ocean interior. This export production has been observed by sediment trap, and measurement of nutrients and natural radionuclide. In order to observe the new production, measurement of NO_3 uptake rate was conducted with ^{15}N stable isotope tracer when primary productivity was measured.

(2) Method

When *in situ* or simulated *in situ* incubation for measurement of primary production was conducted, ^{15}N-enriched NO_3, $Na^{15}NO_3$, was injected to the incubation bottle, resulting that the final concentration of additional ^{15}N is 0.5 μmol L^{-1}. After incubation, samples are filtered onto Whatman GF/F glass fiber filter. Particulates are converted to N_2 gas and isotope ratios are determined by mass spectrometry on board.

NO_3 uptake rate or new production (NP) was estimated with following equation:

$$NP\ (\mu g\ L^{-1}\ day^{-1}) = (15N_{excess} \times PON) / (^{15}N_{enrich}) / day$$

where $^{15}N_{excess}$, PON and $^{15}N_{enrich}$ are excess ^{15}N (measured ^{15}N minus ^{15}N natural abundance, 0.366 atom%) in the post-incubation particulate sample (%), particulate nitrogen content of the sample after incubation (mg L^{-1}) and ^{15}N enrichment in the dissolved fraction (%), respectively. $^{15}N_{enrich}$ is expressed as follows:

$$^{15}N_{enrich}\ (\%) = {}^{15}N / ({}^{15}N + {}^{14}N) \times 100 - {}^{15}N_n$$

where ^{15}N, ^{14}N and $^{15}N_n$ are concentration of labeled N (0.5 μmol L^{-1}), concentration of unlabeled N (dissolved NO_3 measured as "routine", μmol L^{-1}) and natural abundance of ^{15}N (0.366 atom%), respectively.

Precision of measurement (reproducibility) was 15% on average (n=32).

(3) Preliminary result

Maximum of NO_3 uptake rate was approximately 3.7 mgN m^{-3} day^{-1} and generally decreased with depth (Table 3.5.5.1). NO_3 uptake rate was converted to carbon uptake rate (new production: mgC m^{-3} day^{-1}) with Redfield ratio (C/N = 6.6) and integrated in the euphotic layer. Integrated new production at stations AB, K1, K2 and KNOT were estimated to be approximately366, 333, 210 and 460 mgC m^{-2} day^{-1}, respectively. These corresponded to approximately 80, 152, 24 and 39% of primary productivity at stations AB, K1, K2 and KNOT, respectively.

Table 3.5.5.1 New production measured by ^{15}N

Station	Depth (m)	NO3 uptake rate (mgN m^{-3} day^{-1})	average (mgN m^{-3} day^{-1})	deviation (%)	New production: NP (mgC m^{-3} day^{-1})	Inventory (mgC m^{-2} day^{-1})	Primary Productivity: PP (mgC m^{-2} day^{-1})	NP / PP (%)
AB	0	3.648	3.648	0.000	24.077			
	0	3.648						
	4	3.192	3.372	5.338	22.255	92.664		
	4	3.552						
	9	3.000	2.964	1.215	19.562	197.208		
	9	2.928						
	15	1.560	1.572	0.763	10.375	287.021		
	15	1.584						
	21	1.032	0.996	3.614	6.574	337.867		
	21	0.960						
	26	0.216	0.216	0.000	1.426	357.865		
	26	0.216						
	32	0.048	0.072	33.333	0.475	363.568		
	32	0.096						
	39	-0.024	0.024	200.000	0.158	365.785	456.5	80.1
	39	0.072						

Station	Depth (m)	NO3 uptake rate (mgN m^{-3} day^{-1})	average (mgN m^{-3} day^{-1})	deviation (%)	New production: NP (mgC m^{-3} day^{-1})	Inventory (mgC m^{-2} day^{-1})	Primary Productivity: PP (mgC m^{-2} day^{-1})	NP / PP (%)
K1	0	2.376	2.280	4.211	15.048			
	0	2.184						
	5	2.280	2.148	6.145	14.177	73.062		
	5	2.016						
	10	2.280	2.100	8.571	13.860	143.154		
	10	1.920						
	15	1.632	1.908	14.465	12.593	209.286		
	15	2.184						
	20	0.840	0.936	10.256	6.178	256.212		
	20	1.032						
	25	0.552	0.660	16.364	4.356	282.546		
	25	0.768						
	30	0.744	0.804	7.463	5.306	306.702		
	30	0.864						
	40	-0.072	0.000	#DIV/0!	0.000	333.234	218.3	152.6
	40	0.072						

Table 3.5.5.1 continued

Station	Depth (m)	NO3 uptake rate (mgN m⁻³ day⁻¹)	average (mgN m⁻³ day⁻¹)	deviation (%)	New production: NP (mgC m⁻³ day⁻¹)	Inventory (mgC m⁻² day⁻¹)	Primary Productivity: PP (mgC m⁻² day⁻¹)	NP / PP (%)
K2	0	0.624	0.600	4.000	3.960			
	0	0.576						
	5	0.528	0.492	7.317	3.247	18.018		
	5	0.456						
	10	0.240	0.240	0.000	1.584	30.096		
	10	0.240						
	15	0.120	0.132	9.091	0.871	36.234		
	15	0.144						
	25	0.048	0.048	0.000	0.317	42.174		
	25	0.048						
	30	0.048	0.036	33.333	0.238	43.560		
	30	0.024						
	40	0.024	0.024	0.000	0.158	45.540		
	40	0.024						
	50	0.120	0.096	25.000	0.634	49.500	209.6	23.6
	50	0.072						

Station	Depth (m)	NO3 uptake rate (mgN m⁻³ day⁻¹)	average (mgN m⁻³ day⁻¹)	deviation (%)	New production: NP (mgC m⁻³ day⁻¹)	Inventory (mgC m⁻² day⁻¹)	Primary Productivity: PP (mgC m⁻² day⁻¹)	NP / PP (%)
KNOT	0	0.528	0.456	15.789	3.010			
	0	0.384						
	5	1.464	1.524	3.937	10.058	32.670		
	5	1.584						
	11	1.152	1.236	6.796	8.158	87.318		
	11	1.320						
	20	0.696	0.696	0.000	4.594	144.698		
	20	0.696						
	27	0.288	0.300	4.000	1.980	167.706		
	27	0.312						
	35	0.072	0.060	20.000	0.396	177.210		
	35	0.048						
	45	0.024	0.024	0.000	0.158	179.982		
	45	0.024						
	53	0.048	0.000	#DIV/0!	0.000	180.616	460.0	39.3
	53	-0.048						

3.6 FRRF observation

Tetsuichi FUJIKI (JAMSTEC MIO)
Toshiro SAINO (JAMSTEC IORGC)

(1) Objective

During the past decade, the utilization of active fluorescence techniques in biological oceanography brought significant progress in our knowledge of primary productivity in the oceans. Above all, the fast repetition rate (FRR) fluorometry reduces the primary electron acceptor (Q_a) in photosystem II (PSII) by a series of subsaturating flashlets and can measure a single turnover (ST) fluorescence induction curve in PSII. The PSII parameters, such as the potential photosynthetic activity (F_v/F_m) and the functional absorption cross-section of PSII (σ_{PSII}), derived from the ST fluorescence induction curve can be used to estimate gross primary productivity. In the present study, to gain a better understanding of variability in phytoplankton productivity in the Bering Sea and the western subarctic North Pacific, we measured the PSII parameters and primary productivity using the FRR fluorometry.

(2) Methods

The vertical and spatial variations in and PSII parameters and primary productivity were examined at Stns AB, K1, K2 and KNOT. The FRR fluorometer was moved up and down between surface and 100 m at the rate of 0.2 m s^{-1} using a ship winch. The profiling rate of the observation buoy was set to minimal in order to detect small scale variations (~0.5 m) in measurements. In addition, the photosynthesis-irradiance response curves of phytoplankton assemblage were measured using the FRR fluorometer with the external light attachment.

(3) Preliminary results

The diel variation in gross primary productivity (P^b_{O2}) at K2 measured using the FRR fluorometer were shown in Figure 1.

(4) Data archives

All data will be submitted to JAMSTEC Data Management Office and is currently under its control.

$$P^{b}_{O2} \ (\text{molO}_2 \ \text{molChl} \ a^{-1} \ \text{h}^{-1})$$
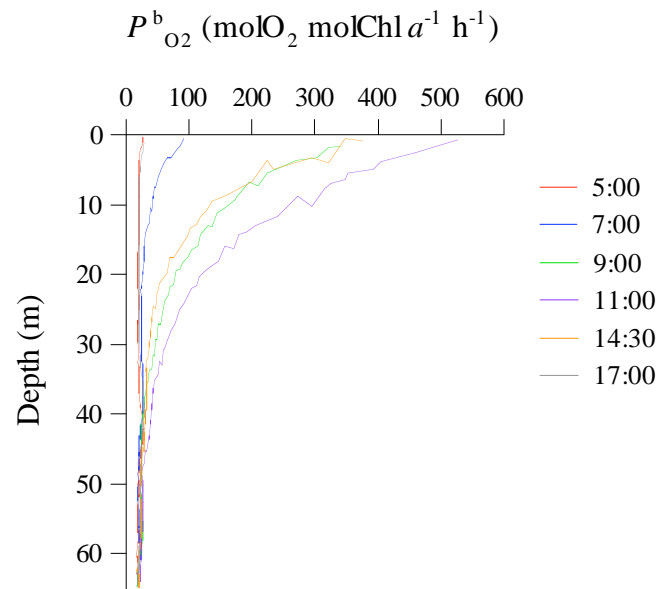
Fig. 1. Diel variation in gross primary productivity (P^{b}_{O2}) at Stn K2 on 27 October 2008 (LST).

3.7 Pilot study on carbon cycle of Marine Crenarchaeota in the North Pacific using geochemical and molecular biological approaches

Masao UCHIDA (NIES; National Institute for Environmental Studies)
Motoo UTSUMI (Univ. of Tsukuba)
Yukiko KUROKI (Univ. of Tsukuba)
Chie SATO (Univ. of Tsukuba)
Shiro YOSHIDA (Univ. of Tsukuba)

(1) Objectives

Marine microbes, especially bacteria, are large and essential components of food webs and elemental cycles in the water column and sediment. Marine bacteria include the two deepest divisions, or domains, Bacteria and Archaea. These domains are identified by genetic distance in the composition of the 16S rRNA gene (Woose et al. 1990). Marine bacteria are small and morphologically simple: rods, spheres and filaments generally less than 1-2 μm in size, but they are highly diverse in terms of both taxonomy and metabolism. There are many different varieties of bacteria existing in the marine ecosystem, but it has been long noted a discrepancy of several orders of magnitude between the number of bacterial cells that can be seen in the oceans by direct count (by epifluorescence microscopy) and the number of colonies that appear on agar plates (e.g. Jannasch and Jones, 1959). In terms of carbon cycling in marine ecosystems, especially for dissolved organic carbon (DOC), one of the most important activities of bacteria is aerobic decomposition. In recent years, it is reported that nonthermophilic Archaea, named crenarchaeota, represent up to 40% of the free-living prokaryotic bacteria community in the water column of the world's oceans (ex. Delong, 1992), and some of their population is chemoautotrophy (ex. Pearson et al. 2001). Therefore, it is important to study the relationship between carbon cycling and archaeal metabolic information in marine ecosystem.

The key aim of this study is to analyze the metabolic characteristics of marine crenarchaeota, and relationship between their biomass, community structures and carbon cycling in the ocean. The objectives of this study are as follow:

1) Collect large volume (50 to 400 L per each sample) of seawater for measuring stable and radioactive isotope ratio of POC, archaeal cell membrane lipids (especially GDGTs), and for analyzing the bacterial gene information,
2) Collect mega volume (c.a. 100,000 L) of surface seawater for measuring radioactive isotope ratio of archaeal cell membrane lipids,
3) Collect surface sediments for investigating archaeal cell membrane lipids (especially GDGTs), and for analyzing the bacterial gene information,

We also collected seawater samples for measuring the radioactive isotope ratio and concentration of DIC and DOC, and for counting bacterial population density (Bacteria and Archaea) in the water column.

(2) Water sample collection during MR08-05

To collect filter samples for studying the stable and radioactive carbon isotope ratio of POC and bacterial cell membrane lipids (especially GDGTs), diversity of

bacterial community and their functional genes, we filtered totally 689 to 1,306 L seawater at 4 stations (Table 1).   These samples were collected from the several depths with X-Niskin water samplers (12 L, General Oceanic), and sea-water in the samplers immediately transferred to 10 L plastic canteens on deck.   The water samples of same depth were filtered with quartz fiber filters (Whatman QM-A, with operational pore size of 0.6 μm, 110 mm in diameter) as soon as possible on board. Then, the filtrates filtered again with 0.2 μm isopore membrane filter (Advantec, 147 mm in diameter). We also collected filter (POC) and filtrate (DOC) samples, and DIC and DI^{14}C samples from routine or exclusive sampling casts at 4 stations (Table 1). Sea-water in the samplers immediately transferred to 5 L plastic canteens for POC and DOC, 250 mL glass bottles for DIC and DI^{14}C on deck.   All water samples for POC and DOC were filtered with QM-A filters (47 mm in diameter) and filtrate was collected in 1 L PE bottles, as soon as possible on board. The filters and filtrates are frozen at -20°C during the cruise.   DIC and DI^{14}C samples were then immediately poisoned with 0.2 mL of a 7.0 % HgCl$_2$ solution and stored at 4 ^{o}C during the cruise.   Surface seawater (sampling depth; 5 m) also collected from surface sea-water supply system during St.K2 survey 25th October 2008 for POM and bacterial cell membrane lipids (120 L), DOM (2 L), DIC and DI^{14}C (each 250 mL).   The filters and DOM samples were frozen at -20°C, DIC and DI^{14}C samples were stored at 4°C during the cruise.

Water samples at several depths of stations were also fixed with formalin (final concentration in the sample was 3.6%, 100 mL x 2 bottles) immediately. About 30 mL of each fixed samples were then filtered with 0.2 μm isopore membrane filter (Whatman, 25 mm in diameter) for counting the population density of Bacteria and Archaea. The filters and the bottles in fixed water sample were frozen at -80°C during the cruise.

To study the radioactive isotope ratio of POC and bacterial cell membrane lipid, and diversity of bacterial community in surface sea-water, we filtered surface sea-water (total 32,320 L, see Table 2) continuously during St.K2 survey (from 24th Oct. to 30th Oct.).   The filtration system was set up in the surface sea-water analysis room in "MIRAI".   The equipment was consist of a) steel-wool part, b) 10 μm size filter part, c) 1.0 μm size filter part, d) 0.5μm size filter part, e) 0.2μm size filter part, and f) flowmeters (inflow and outflow, respectively).   The maximum filtration velocity was about 8 L/min.   Each filter was exchanged new one when the filtration velocity declined under 3 L/min or the filtration period exceeded 4 day.   The collected filters were frozen at -20°C during the cruise.

(3) Core sample collection during MR08-05

Nonthermophilic archaea represent up to 40% of the free-living prokaryotic community in the water column of the world's oceans (1–6), but until recently there has been limited information about the sources of carbon and energy that fuel these organisms. The characteristic membrane lipids of planktonic archaea include glycerol dialkyl glycerol tetraethers (GDGTs). These compounds are ubiquitous in marine sediments and ocean water. The relative abundance of individual GDGTs recovered from sediments is used to reconstruct sea-surface temperatures. This distribution, known as TEX86, has been shown through experimental manipulation of surface-water mesocosm experiments to respond to changes in incubation temperature. The collective metabolic activities of the numerous archaea in the ocean are likely to play a significant role in the cycling of organic carbon (OC) and nutrients, and their membrane lipids show significant

utility for paleoceanography. However, neither the metabolic requirements of the natural population of marine archaea nor the mechanisms by which these populations record sea-surface temperature are known. In this study, chemoautotrophy in the marine archaea first are investigated by using both 13C and radiocarbon (14C) isotopic measurements of GDGT-derived lipids and biomarkers extracted from sediments, as well as large volume filtration samples from sea water. Using this methods, we can investigate carbon source of archaeal biomass.

In addition, here, we quantify the proportion of marine archaeal lipid that is synthesized by chemoautotrophic production in mesopelagic waters. These results have important implications for biogeochemical cycles and for development of paleoceanographic proxies.

1) Multiple corer (MC)

A Multiple core sampler was used for taking the surface sediment. This core sampler consists of a main body of 620kg-weight and 8 sub-core samplers (I.D. 74mm and length of 60cm).

When we started lowering MC, a speed of wire out was set to be 0.2 m/s., and then gradually increased to the maximum of 1.0 m/s. The corers were stopped at a depth about 100 m above the seafloor for 2-3 minutes to reduce some pendulum motion of the system. After the corers were stabilized, the wire was stored out at a speed of 0.3 m/s., and we carefully watched a tension meter. When the corers touched the bottom, wire tension abruptly decreases by the loss of the corer weight. Immediately after confirmation that the corers hit the bottom, wire out was stopped and winding of the wire was started at a speed of 0.3m/s., until the tension gauge indicates that the corers were lifted off the bottom. After leaving the bottom, winch wire was wound in at the maximum speed. Results of the MC are summarized in Table 3.

2) Soft-X ray photographs

Soft-X ray photographs were taken to observe sedimentary structures of cores. Sediment samples were put into the original plastic cases (200x3x7mm) from cores. Each case has a TEPURA sheel showing cruise code, core number, section number, case number, and section depth (cm), and was rimmed by PARAFILM to seal the sediment.

Soft-X ray photographs were taken to using the device SOFTEX PRO-TEST 150 on board. The condition of X-ray was decided from results of test photographs by each core section. The condition was ranged between 40~50KVp, 2mA, and 150~200 seconds.

All photographs were developed into the negative films by the device FIP-1400 on board.

3) Core Photographs

After splitting each section of piston, pilot and multiple cores into working and archive halves, sectional photographs of archive were taken using a digital camera (Camera body: Nikon D1x / Lens: Nikon AF Zoom-Nikkor 24-50mm). When using the digital camera, shutter speed was 1/160 ~ 1/10 sec (partly 1/160~1/15 sec, 1/160~1/8 sec), F-number was 6.3 (partly 8). sensitivity was ISO 400. File format of raw data is Exif-JPEG. Details for settings were included on property of each file.

References

Delong, E.F. (1992) Proc. Natl. Acad. Sci. USA 89: 5685-5689.

Jannasch, H. W., and Jones, G. E. (1959)   Limnol. Oceanogr. 4:128-139.

Pearson, A., McNichol, A.P., Bentitez-Nelson, B.C., Hayes, J.M. and Eglinton, T.I. (2001) Geochim. Cosmochim. Acta 65: 3123-3137.

Woese, C. R., Kandler, O., and Wheelis, M. L. (1990) Proc. Natl. Acad. Sci. USA 87:4576-4579.

Table 1. List of filtrated sea-water samples for stable and radioactive carbon isotope ratio of (a) POM and bacterial cell membrane lipids, (b) DOM, and (c) DIC and DI^{14}C during MR08-05.

(a) Filter samples for POM and bacterial cell membrane lipids.

sampling date	site information and sampling depth (dBar)	Total filtrated volume (L)
2008.10.14~15	St. AB (50, 100, 200, 1,000 and 3,000)	689
2008.10.19~20	St.K1 (50, 100, 200, 500, 1,000 and 3,000)	820
2008.10.24~25	St. K2 (50, 100, 200, 300, 500, 1,000, 3,000, 5,000)	1,306
2008.11.2~3	St. SK (50, 100, 200, 300, 500 1,000)	843

(b) Filtrated seawater samples for DOM.

sampling date	site information	Total filtrated volume (L)
2008.10.14~15	St. AB	16
2008.10.19~20	St.K1	24
2008.10.24~25	St. K2	41
2008.11.2~3	St. SK	24

(c) Seawater samples for DIC and DI^{14}C.

sampling date	site information	Total volume (L)
2008.10.14~15	St. AB	1.25
2008.10.19~20	St.K1	1.75
2008.10.24~25	St. K2	2.0
2008.11.2~3	St. SK	2.0

Table 2. List of filter samples for bacterial cell membrane lipids from surface sea-water during MR08-05.

sampling date	site information	Total filtrated volume (L)
from 2008/10/24 to 2008/10/30	St.K2	32,320

Table 3. List of multiple cores collected during MR08-05.

Core ID	Date (UTC)	HAND No.	Core length (cm)	Core ID	Date (UTC)	HAND No.	Core length (cm)
MC-01	2008/10/15	HAND1	28.1	MC-03	2008/10/29	HAND1	18.0
		HAND2	26.0			HAND2	29.0
		HAND3	29.1			HAND3	30.7
		HAND4	35.8			HAND4	29.5
		HAND5	31.5			HAND5	31.0
		HAND6	35.2			HAND6	31.3
		HAND7	36.9			HAND7	16.0
		HAND8	31.5			HAND8	29.6
MC-02	2008/10/19	HAND1	29.3	MC-04	2008/11/02	HAND1	32.0
		HAND2	29.5			HAND2	32.3
		HAND3	28.4			HAND3	32.1
		HAND4	11.0			HAND4	32.0
		HAND5	29.8			HAND5	31.5
		HAND6	29.5			HAND6	32.0
		HAND7	29.3			HAND7	31.9
		HAND8	29.7			HAND8	32.0

3.8 Biological observation

3.8.1 Community structure and ecological roles of zooplankton

Minoru KITAMURA (JAMSTEC, XBR)
Sanae CHIBA (JAMSTEC, FRCGC)
Kazuhiko MATSUMOTO (JAMSTEC, MIO)

(1) Objective

Subarctic western North Pacific is known to be a region with high biological draw down of atmospheric CO_2 due to extensive diatom bloom in spring. Time-series biogeochemical observations conducted at the Station K2 have revealed high annual material transportation efficiency to the deep compared to the other time-series sites set in the subtropical regions.

Zooplankton dominated in this regions are large copepods, which mainly feed on diatoms, and supposed to help enhancing Biological Carbon Pump (BCP) function, by repackaging diatoms through the fecal pellet production. However, the reported zooplankton fecal pellet flux to the deep were smaller than expected from the production in the surface layer, suggesting consumption and biological breakdown occurred in surface and mesopelagic layers. In particular, biological processes in the mesopelagic layer are largely unknown.

Besides the fecal pellet production, "active transport" of carbon by ontogenetic migrating copepods, e.g. *Neocalanus* spp. recently was reported large, even equivalent to amount of carbon flux estimated based on the sediment trap experiments. Other copepods, *Metridia* spp. perform extensive diel vertical migration, and could transport large amount of surface carbon to the several hundred meters deep through respiration. Detailed information of timing and biomass of vertical migration of these copepods should be investigated.

With these background, goal of these research is to investigate roles of zooplankton in vertical material transport in the western subarctic North Pacific. We deployed two types of plankton nets to investigate species and size composition of zooplankton from the surface to the greater deep. Microzooplankton were also collected in the surface layer. Since zooplankton researches have been conducted at the K2 during the high productive season, in August 2005, and June-July 2006, we hoped to figure out difference in zooplankton roles in BCP function between the high and the post-high-productive seasons

(2) Materials and methods
Mesozooplankton and micronekton samplings

For collection of stratified sample sets, multiple opening/closing plankton net system, IONESS, was used. This is a rectangular frame trawl with seven nets. Area of the net mouth is 1.5 m^2 when the net frame is towed at 45° in angle, and mesh pore size is 0.33-mm. Researcher can open and close nets at discretion depths and can real time monitor net status. Volume of filtering water of each net is estimated using area of net mouth, towing distance, and filtering efficiency. The area of net mouth is calibrated from frame angle during tow, the towing distance is calculated from revolutions of flow-meter, and the filtering efficiency is 96% which was directory measured. The net system is towed obliquely. Ship speed during net tow was about 2 knot, speeds of wire out and reeling were 0.1-0.7 m/s and 0.1-0.3 m/s, respectively.

Total six tows of IONESS were done. The stratified sampling layers at Stn. K2 were as follows; 0-50, 50-100, 100-150, 150-200, 200-300, 300-400, 400-500, 500-600, 600-700, 700-800, 800-900, 900-1000m. To understand diel vertical migration of mesozooplankton and micronekton, the stratified samplings were conducted during both day and night. On the other

hand, samplings at Stns. AB and K1 were conducted only daytime and maximum depth of tows were 500 and 400m, respectively. Towing data such as date, time, position, filtering volume and etc. are summarized in Table 3.8.1-1.

Collected zooplankton samples were divided using a sample splitter. Subsamples (from 1/8 to 1/32) were frozen (-80°C) for CHN analysis and the remainders were fixed and preserved in 5% formalin-seawater buffered with borax.

Role of Small Copepods in BCP Efficiency (NORPAC net sampling)

Smaller non-calanoid copepods, e.g. *Oithona* spp, are highly abundant and numerically dominant in the surface subarctic North Pacific. Those species are known to feed on the fecal pellets of large copepods and other organic materials, and thus, are suggested to contribute in break down of these particles, resulting in reducing BCP efficiency. We collected those smaller copepods to quantify their biomass and role in carbon transport to subsurface using a twin-type NORPAC net with fine mesh (64 μm and 100 μm) and a flow meter for each.

The net was vertically towed 0-50 m and 0-150 m night and day each at the Station AB, K1, K2, and KNOT (Table 3.8.1-2). Zooplankton collected were preserved in the 5% buffered formalin seawater for the later analysis on species and size composition. For the 100 μm mesh samples taken from 0-50 layer, zooplankton were subdivided by a splitter and a half was frozen in the deep freezer (-80°C) for the later measurement on carbon biomass.

Vertical distribution of surface microzooplankton

Four series of seawater samples were collected on 14, 20, 27 and 31 Oct. at Stations AB, K1, K2 and KNOT. Each series comprises eight waters which collected using bucket and Niskin bottles at different depths. These depths corresponded to nominal specific optical depths approximately 100, 50, 25, 10, 5, 2.5, 1 and 0.5% light intensity relative to the surface irradiance as determined from the optical profiles obtained by ''Free-Fall Sensor''.

Seawater samples were immediately treated with the final concentration of 1% glutaraldehyde and were kept at 4°C until filtering. Each seawater sample were filtered through 1μm pore size Nuclepore fitter, pre-stained by irgalan black, at the low vacuum of 15 cmHg, and were double-stained using DAPI (4'6-diamidino-2-phenylindole dihydrochloride) and proflavine (3-6-diamidino-acridine hemisulfate). Just before the finish of filtering, DAPI was added to sample in filtering funnel for the staining DNA. After the DAPI staining, proflavine was also added for the staining of flagella. Both the staining time is five minute. The working solution of DAPI (10 μg/ml) and proflavine (0.033%) were pre-filtered through 0.45 μm pore size of non-pyrogenic Durapore membrane filter (Millipore, Millex-GX). After the filtering, sample filters put on a slide-glass with one drop of immersion oil, and covered with micro cover glass. All preparations were stored in the deep freezer (-80°C) until the observation.

Above mentioned water samples are for analysis of microzooplankton except for tintiniids. Because filtering volume is little (up to 400 ml), these samples are not appropriate for tintiniids analysis whose abundance is low. So, additional seawater samples for this taxon were collected in the same depths, same time. Collected water samples were immediately filtered (5L) using 20 μm hand net and concentrated ones were fixed in 1% acid Lugol's solution.

Sampling data such as depths or filtering volume are summarized in Table 3.8.1-3.

Table 3.8.1-1. Information of IONESS towing.

Stn.	Data file name	Date and Time in / out	Position in / out	Net No. 0	1	2	3	4	5	6	Remarks
AB	I081015a	2008.10.15 13:33 / 15:25	57° 00.7' N 175° 58.9' E / 56° 58.7' N 175° 59.8' E	0~550~500	500~400 / 1537.4 / 1/8	400~300 / 2255.4 / 1/8	300~200 / 1157.6 / 1/16	200~100 / 934.9 / 1/8	100~50 / 585.7 / 1/8	50~0 / 783.3 / 1/16	
K1	I081021a	2008.10.21 10:27 / 12:28	51° 03.0' N 165° 17.9' E / 50° 59.3' N 165° 15.8' E	0~430~400	400~300 / 1650.2 / -	300~200 / 2234.9 / -	200~150 / 1276.4 / -	150~100 / 1294.0 / -	100~50 / 1255.3 / -	50~0 / 1083.5 / -	
K2	I081025a	2008.10.25 19:29 / 21:24	47° 00.5' N 159° 59.6' E / 46° 57.1' N 160° 01.7' E	0~460~400	400~300 / 1446.3 / 1/16	300~200 / 1124.0 / 1/32	200~150 / 884.7 / 1/16	150~100 / 1017.4 / 1/16	100~50 / 990.5 / 1/16	50~0 / 876.3 / 1/32	
K2	I081027a	2008.10.27 11:55 / 14:01	46° 59.1' N 160° 01.2' E / 46° 58.8' N 160° 06.5' E	0~451~400	400~300 / 1284.5 / 1/32	300~200 / 927.4 / 1/32	200~150 / 1092.1 / 1/32	150~100 / 954.6 / 1/32	100~50 / 1012.1 / 1/16	50~0 / 898.9 / 1/32	
K2	I081028a	2008.10.28 11:08 / 14:06	47° 02.7' N 160° 02.5' E / 46° 59.9' N 159° 55.7' E	0~1050~1000	1000~900 / 1310.4 / 1/8	900~800 / 1665.4 / 1/8	800~700 / 1330.5 / 1/8	700~600 / 1022.8 / 1/8	600~500 / 1716.0 / 1/16	500~400 / 1384.5 / 1/16	
K2	I081029a	2008.10.29 20:27 / 30 0:01	47° 02.2' N 160° 00.6' E / 46° 55.5' N 160° 04.0' E	0~1080~1000	1000~900 / 1492.5 / 1/8	900~800 / 1506.7 / 1/16	800~700 / 1802.7 / 1/16	700~600 / 1558.8 / 1/16	600~500 / 1585.1 / 1/16	500~400 / 1094.7 / 1/32	winch trouble after samplings

Table 3.8.1-2. Summary of NORPAC net samplings

MR08-05
NORPAC net hauls for analysis of community structure and copepods production rate
Samples taken by Twin net were fixed in 5% folmarin sea water
flow-meter No.: XX13 2373, XXX25 3115
Rewind speed: twin net: 1.0 m / sec, single net: 0.5 m / sec

Stn.	Date	Local Time	Net	Sampling Layer (m)	Wire out (m)	Wire angle (°)	revolution XX13	revolution XXX25	Filtering vol. (m³) XX13	Filtering vol. (m³) XX25	sample information XX13	sample information XX25	Remarks
AB	2008.10.15	16:13	Twin	50-0	61	35	832	900	11.6	13.5	1/1	1/1	
	2008.10.15	16:27	Single	50-0	52	15	-	-	-	-	gut pigment	-	
K1-a	2008.10.20	10:28	Twin	50-0	61	35	675	668	9.5	10.0	1/1	1/1	
	2008.10.20	10:38	Twin	150-0	166	25	1647	1695	23.1	25.4	1/2 preserved	1/1	weight changed 10km -> 20kg
	2008.10.20	10:50	Single	50-0	58	30	-	-	-	-	gut pigment	-	
K1-b	2008.10.20	17:56	Twin	150-0	166	25	1590	1570	22.3	23.6	1/1	1/1	
	2008.10.20	18:13	Twin	50-0	58	30	635	712	8.9	10.7	1/1	1/1	
	2008.10.20	18:23	Single	50-0	58	30	-	-	-	-	gut pigment	-	
K2-a	2008.10.24	13:49	Twin	150-0	175	25	2095	2550	29.3	38.3	1/2 preserved	1/1	
	2008.10.24	14:10	Twin	50-0	65	15	695	761	9.7	11.4	1/2 & 1/4 preserved, 1/4 carbon analysis	1/1	weight changed 20km -> 30kg
	2008.10.24	14:20	Single	50-0	50	5	-	-	-	-	gut pigment	-	
K2-b	2008.10.24	20:33	Twin	150-0	160	20	1745	1790	24.4	26.9	1/1	1/1	
	2008.10.24	20:48	Twin	50-0	53	20	628	640	8.8	9.6	1/2 preserved, 1/4 carbon analysis	1/1	
	2008.10.24	20:57	Single	50-0	51	10	-	-	-	-	gut pigment	-	
K2-c	2008.10.26	20:30	Twin	150-0	152	10	1700	1734	23.8	26.0	1/1	1/1	
	2008.10.26	20:47	Twin	50-0	53	20	660	703	9.2	10.5	1/2 preserved, 1/4 carbon analysis	1/1	
	2008.10.26	20:56	Single	50-0	53	20	-	-	-	-	gut pigment	-	
K2-d	2008.10.29	13:55	Twin	150-0	151	5	1505	1548	21.1	23.2	1/1	1/1	
	2008.10.29	14:12	Twin	50-0	50	5	524	575	7.3	8.6	1/2 preserved, 1/4 carbon analysis	1/1	
	2008.10.29	14:20	Single	50-0	50	5	-	-	-	-	gut pigment	-	
KNOT-a	2008.10.31	10:29	Twin	300-0	332	25	3238	3401	45.3	51.0	1/1	1/1	several inds of *Limachina* excluded
	2008.10.31	10:52	Twin	150-0	160	20	1660	1780	23.2	26.7	1/1	1/1	
	2008.10.31	11:08	Twin	50-0	52	15	618	702	8.7	10.5	1/1	1/1	
	2008.10.31	11:17	Single	50-0	50	5	-	-	-	-	gut pigment	-	
KNOT-b	2008.10.31	21:52	Twin	300-0	332	25	3482	3845	45.266	57.675	1/1	1/1	several inds of *Limachina* excluded
	2008.10.31	22:16	Twin	150-0	183	35	2180	2447	28.34	36.705	1/1	1/1	
	2008.10.31	22:36	Twin	50-0	51	10	575	598	7.475	8.97	1/1	1/1	
	2008.10.31	22:46	Single	50-0	55	25	-	-	-	-	gut pigment	-	

Table 3.8.1-3. Information of microzooplankton samplings. * Local ship time.

Stn.	Date*	CTD time*	Sample No.	Sampling depth (m)	Irradiance (%)	Filtering vol. for Tintinid (L)	Filtering vol. for other microzoo (ml)	Funnel No.	Remarks
AB	2008.10.14	10:50-11:25	AB, 23	39	0.5	5	300	1	CTD cast; 2
		(JST+3h)	AB, 24	32	1	5	140	2	
			AB, 25	26	2.5	5	155	3	
			AB, 26	21	5	5	240	4	
			AB, 27	15	10	5	230	5	
			AB, 28	9	25	5	250	6	
			AB, 29	4	50	5	185	3	
			AB, S	0	100	5	235	5	
K1	2008.10.20	4:27-4:59	K1, 23	40	0.5	5	190	1	CTD cast; 2
		(JST+2h)	K1, 24	30	1	5	145	2	
			K1, 25	25	2.5	5	140	3	
			K1, 26	20	5	5	290	4	
			K1, 27	15	10	5	205	5	
			K1, 28	10	25	5	290	6	
			K1, 29	5	50	5	160	2	
			K1, S	0	100	5	275	5	
K2	2008.10.27	8:00-8:35	K2, 23	50	0.5	5	350	1	CTD cast; 8
		(JST+2h)	K2, 24	40	1	5	240	2	
			K2, 25	30	2.5	5	250	3	
			K2, 26	25	5	5	310	4	
			K2, 27	15	10	5	170	5	
			K2, 28	10	25	5	325	6	
			K2, 29	5	50	5	260	2	
			K2, S	0	100	5	275	4	
KNOT	2008.10.31	9:49-10:18	KNOT, 23	53	0.5	5	295	1	CTD cast; 1
		(JST+2h)	KNOT, 24	45	1	5	400	2	
			KNOT, 25	35	2.5	5	190	3	
			KNOT, 26	27	5	5	190	4	
			KNOT, 27	20	10	5	215	5	
			KNOT, 28	11	25	5	320	6	
			KNOT, 29	5	50	5	195	1	
			KNOT, S	0	100	5	300	2	

(3) Preliminary results

Vertical Distribution of mesozooplankton biomass in Stns. AB and K2.

Vertical distributions of mesozooplankton biomass (dry weight) in Stns. AB and K2 are shown in Fig. 3.8.1-1. The dry masses between 200 to 500 m are relatively high. Ontogenetic migratory copepod, *Neocalanus cristatus*, is abundant in the layers.
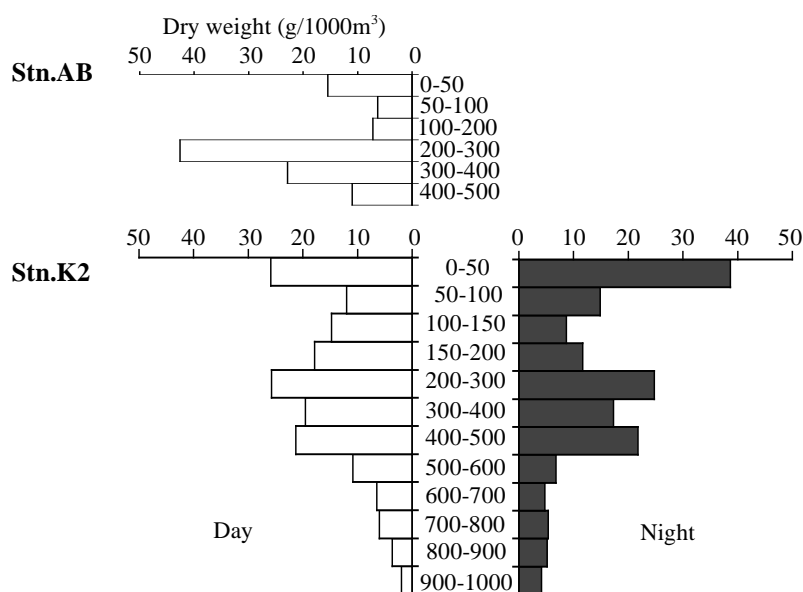
Fig.3.8.1-1. Vertical distribution mesozooplankton dry mass in the stations AB and K2.

(4) Future plans and sample archives
Community structure and ecological role of mesozooplankton
        All IONESS samples preserved in formalin are stored at JAMSTEC, Yokosuka. We will analyze as follows; (1) Vertical distribution of biomass in higher taxa revel (copepods, euphausiids, etc.), and taxa composition based on the carbon weight, (2) Vertical distribution, composition, biomass, minimum carbon requirement and diel vertical migration for each species of dominant three taxa, copepods, euphausiids and chaetognaths, (3) Estimation of carbon transport through respiration of the diel migratory species, (4) Vertical distribution and biomass of ontogenetically migrate copepods, estimation of carbon transport by them, and (5) Vertical distribution and composition of gelatinous animals (Cnidaria, Ctenophore, Polychaeta and Mollusca). Sample observation and sorting will be done under the microscope, carbon weight of each taxon will be calculated using its dry weight and specific conversion factor previously reported. Dr. Okutani, JAMSTEC, who has interesting on planktonic mollusca will join to analysis of the community structure of gelatinous.

        Environmental (T, S) and net status (net number, towing distance, R/V position, etc.) data were recorded during each IONESS tow. All data is under Kitamura and submitted to DMO, JAMSTEC.

Role of Small Copepods in BCP Efficiency
        All samples frozen or preserved in formalin are stored in JAMSTEC, Yokosuka. The formalin preserved samples will be microscopically analyzed to obtain taxonomic composition. Size composition of those samples will be analyzed using an optical zooplankton analyzing system, ZooScan (RECIF Technologies). Once we gain the species and size composition of copepods of each sample, a minimum carbon requirement, ingestion and egestion rates for each species will be estimated based on the total length and ambient water temperature. These data will be compared to information obtained by other biological observations of this cruise, e.g. phytoplankton abundance/composition, microzooplankton grazing, bacterial abundance, and fecal pellets flux obtained from the floating sediment trap samples.

        We have collected NORPAC zooplankton samples in the equivalent way in Jun-July 2006, and September 2007 at the station K2, while this year's observation was conducted in the late October. Using those samples taken in the mid, late and post productive seasons, we aim to investigate seasonal variation of the surface zooplankton community, and estimate how the community change in the surface layer affected the grazing pressure on the primary production and vertical carbon flux.

Vertical distribution of surface microzooplankton
        Frozen filter samples are stored at Mutsu Institute of oceanography, JAMSTEC. And analysis will be consigned to Marine Biological Research institute of Japan Co. LTD., Shinagawa, Tokyo.

        Tintiniids samples are stored in JAMSTEC, Yokosuka. Kitamura will observe and count under microscope. And vertical distribution of tintiniids abundance will be shown.

3.8.2 Grazing pressure of microzooplankton

Minoru KITAMURA (JAMSTEC, XBR)
Sanae CHIBA (JAMSTEC, FRCGC)

(1) Objective

For understand of material export processes from surface to deep ocean, not only estimations of primary productivity or vertical flux but also evaluation of grazing impacts by many types of heterotrophic organisms to the productivity is needed. Grazing by larger organisms might bring about efficient vertical carbon transport through repacking phytoplankton into fecal pellets or active carbon transport by diel and ontogenetic migrator. On the other hand, grazing by smaller organisms might have small impact to vertical export. Identification of influential grazers and quantitative estimation of their grazing rates are essential to discuss the carbon cycle in the ocean. Recently, large grazing pressure of not only the crustacean plankton but also microzooplankton has been recognized in the several area. These micro organisms maybe become important in the northwestern north Pacific in autumn because large calanoid copepods migrate to midwater. Based on this background, we planned to estimate grazing rate of them.

(2) Materials and methods

Five experiments were done through the cruise, 14-15 Oct. (Stn.AB), 20-21 Oct. (Stn.K1), 27-28 and 29-30 Oct. (Stn.K2) and 31 Oct.-1 Nov. (KNOT). For each experiment 40 l of surface water were collected using bucket. Water was pre-screened through 200 μm mesh to exclude larger zooplankton. Dilution series were prepared with 25, 50, 75, and 100% of natural seawater. Filtered water was obtained by direct gravity flow through a compact cartridge filter (ADVANTEC, MCS-020-D10SR). Incubation of the dilute water was done in transparent polycarbonate bottle. Triplicate bottle were prepared. Incubation lasted for 24 h in a tank with continuous flow of surface seawater under natural light conditions. All the water samplings, filtering, and incubate items were soaked in 10% HCl and rinsed Milli-Q water between each use on board. No nutrient was added in the incubation bottles. To measure initial and final chl.*a* concentration, experiment water were filtered onto GF/F filter and extracted 6 ml DMF at $-20°C$ until measurement. Chl.*a* were measured fluorometrically (Welshmeyer method) with a Turner Design fluorometer.

Apparent phytoplankton growth rate (d^{-1}) were calculated using following equation:

$$\text{Apparent growth rate} = (1/t)\ln(P_t/P_0)$$

where t is incubation time (day), P_t and P_0 are final and initial chlorophyll a concentration, respectively. When the apparent phytoplankton growth rate is plotted as a function of dilution factor, the y-intercept and negative slope of the approximate line means true phytoplankton growth (k; d^{-1}) and grazing coefficient of microzooplankton (g: d^{-1}), respectively. According to Verity et al. (1993) and Zhang et al. (2006), microzooplankton grazing pressure on primary production (P_p; %) is calculated as the following equation:

$$P_p = (e^{kt} - e^{(k-g)t}) / (e^{kt}-1)*100$$

Through the three incubation experiments, we tried to estimate true growth rate of phytoplankton, grazing rate of microzooplankton and grazing pressure of microzooplankton on primary production. Incubation states are summarized in Table 3.8.2-1.

References

Verity, P.G., D.K. Stoecker, M.E. Sieracki & J.R. Nelson. 1996. Grazing, growth and mortality of microzooplankton during the 1989 North Atlantic spring bloom at 47°N, 18°W. Deep-Sea Res., 40: 1793-1814.

Zhang, W., H. Li, T. Xiao, J. Zhang, C. Li & S. Sun. 2006. Impact of microzooplankton and copepods on the growth of phytoplankton in the Yellow Sea and East China Sea.

Table 3.8.2-1. Summary of dilution incubation experiments for estimation of microzooplankton grazing pressure during MR08-05, October and November 2008.

Stn.	Date	Time (LST)		Sampling depth	Water temp.	Weather
		Water sampling	Incuvation start end	(m)	(°C)	
AB	2008.10.14	11:00	12:00 12:00	0	8.9	fine rain
K1	2008.10.20	4:30	6:30 6:30	0	7.4	fine
K2-1	2008.10.27	8:00	9:00 9:00	0	8.4	fog
K2-2	2008.10.29	7:00	8:00 8:00	0	8.5	
KNOT	2008.10.31	9:20	10:15 10:15	0	12.4	fine fine

(3) Preliminary results

All measurements of Chl.a and calculations were finished on board. Negative correlation between apparent phytoplankton growth rates and dilution factors is recognized except result of Stn.K1. However, r^2-values are low in the experiments of Stns. AB and K2-2. These results, correlation between apparent growth and dilution factor, are shown in the Figure 3.8.2-1.

True growth rates of phytoplankton, grazing rates of microzooplankton and grazing pressures of microzooplankton in the Stns. K2-1 and KNOT are summarized in Table 3.8.2-2, and results between MR07-05 and MR08-05 are compared in Table 3.8.2-3.
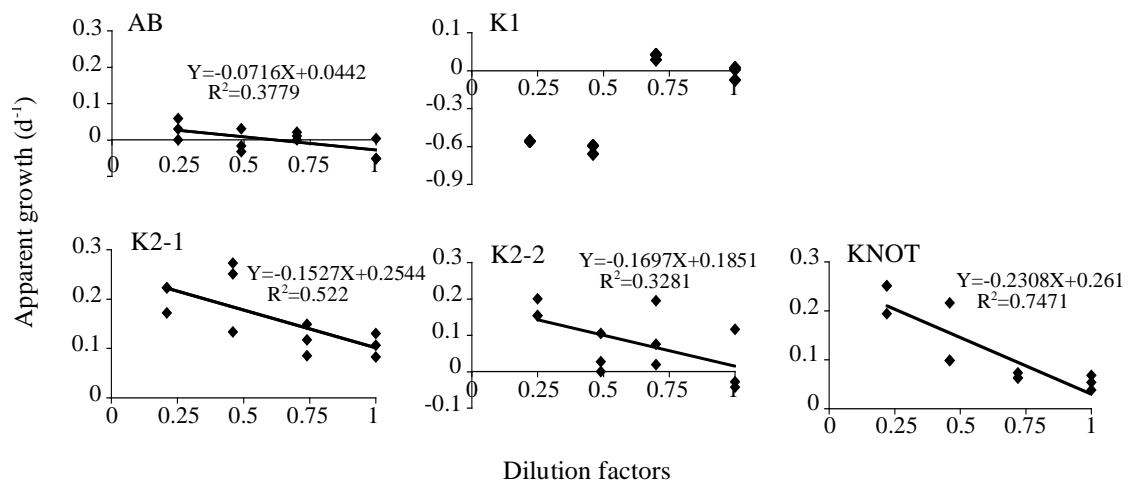
Fig.3.8.2-1. Correlation between apparent growth rates of phytoplankton and dilution factors in the five dilution incubation experiments during MR08-05, October and November 2007.

Table 3.8.2-2. Results of dilution incubation experiments for estimation of microzooplankton grazing.

Stn.	Date	μ	g	P_p
AB	14-15 Oct.	-	-	-
K1	20-21 Oct.	-	-	-
K2-1	27-28 Oct.	0.254	0.152	62.9
K2-2	29-30 Oct.	-	-	-
KNOT	31 Oct.-1 Nov.	0.261	0.230	89.4

μ : growth rate of phytoplankton (d^{-1})

g: grazing rate of microzooplankton (d^{-1})

P_p: grazing pressure on primary production (%)

Table 3.8.2-3. Comparison between results of MR07-05 and MR08-05.

Stn.	Date	μ	g	P_p
MR07-05				
K2-1	15-16 Sept.	0.55	0.30	62.0
K2-2	25-26 Sept.	0.32	0.18	60.2
MR08-05				
K2	27-28 Oct.	0.25	0.15	62.9

1

3.8.3 Micrometer particles size spectrum and microbial activities in a twilight zone

Hideki FUKUDA (Ocean Research Institute, The University of Tokyo)
Ayako OKAMOTO (Ocean Research Institute, The University of Tokyo)
Koji HAMASAKI (Ocean Research Institute, The University of Tokyo)

(1) Objectives
Microbial degradation of organic matter particles and its physicochemical transformation are the key processes of controlling vertical fluxes of organic matters in ocean's interior. Since the size of primary producers in the ocean (mainly phytoplankton) ranged from ca. 1 to 100 micrometers, it is important to reveal the dynamics of micrometer size particles as an initial form of organic particles and a major source of large and fast-sinking particles in order to understand the fluctuation of organic matter fluxes due to degradation, aggregation and/or condensation. The objectives of this study is to determine bacterial community structures and their activities in sub-euphotic twilight zones where hetrotrophic degradation overwhelms photosynthetic production and also determine size spectrum and sinking rates of micrometer size particles and transparent exopolymer particles concentration that provide key parameters to model their dynamics (aggregation, condensation and sinking).

(2) Methods
   Seawater samples were collected from all the depths of 'Ocean Research Institute (ORI) shallow cast' at all the four stations (i.e., Station AB, K1, K2 and KNOT) (see the meta-data sheet for detail). Concentrations of chlorophyll a, POC/PON, DOC are measured as environmental parameters. Abundance of particle-attached bacteria is counted by fluorescent microscopy after filtering fixed seawater with 3 µm pore-size polycarbonate filters. Bacterial community structures are analyzed by PCR-DGGE method after extracting DNA from 0.22 µm filtrates with Sterivex filters. Activities of free and particle-attached bacteria are analyzed by immunocytochemistry of bromodeoxyuridine-incorporating bacteria after BrdU labeling and filtering fixed seawater with 0.2 and 3 µm pore-size polycarbonate filters, respectively. Also, the phylotypes of actively growing bacteria are determined by combined BrdU-immunocapture with PCR-DGGE method.
   Size spectrum of micrometer particles (5.21-196 µm in diameter) was measured by the submersible laser-scattering particle sensor, LISST 100X (Sequoia Scientific Inc., USA).

(3) Preliminary results
Particle size distributions at each of the stations showed that suspended particles were accumulated within mixing layer. Figure 1A and B show typical particle size distributions at station AB. Depth profiles of concentration of chlorophyll *a* suggest that suspended particles actively produced by planktonic organisms within the mixed layer (Figure 2). Remarkable accumulation of larger particles (> 50 µm) appeared within pycnocline suggesting that difference in density between sinking particles and fluid decreases with increase of particle diameter.
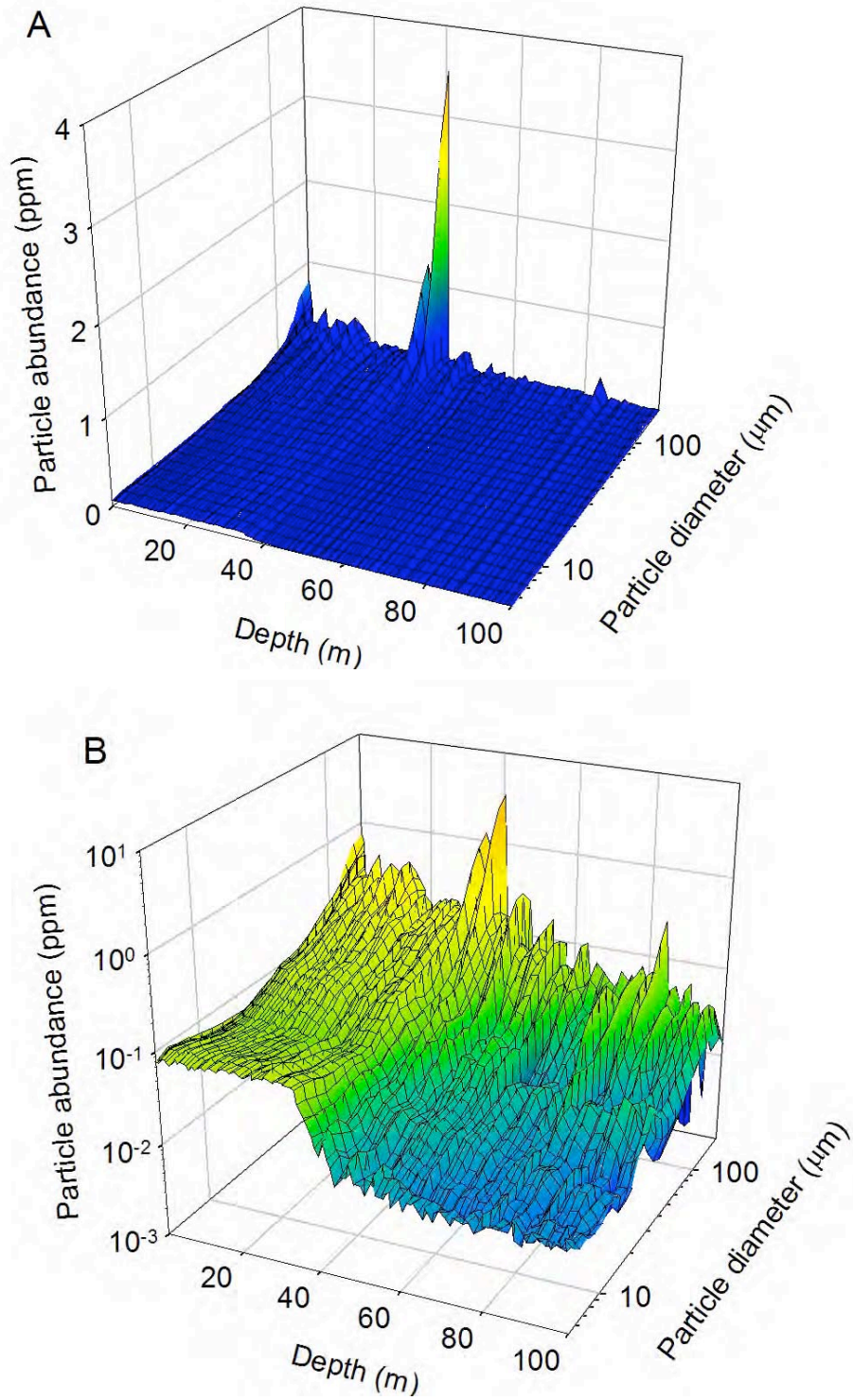
Fig. 1 Depth profiles of particle size distribution at station AB showed in linear scale (A), in logarithmic scale (B).
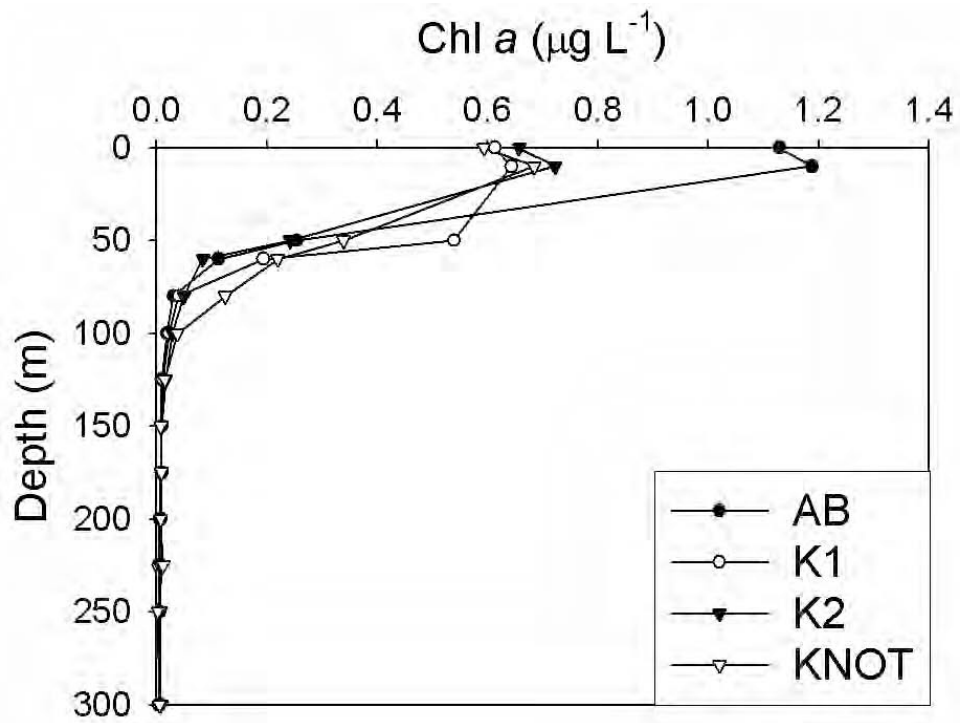
Fig. 2 Depth profiles of concentration of chlorophyll a at station AB, K1, K2 and KNOT.

3.8.4 Full-depth analysis of microbial community structures and their auto- and heterotrophic activities

Toshi NAGATA (Ocean Research Institute, The University of Tokyo)
Taichi YOKOKAWA (Royal Netherlands Institute for Sea Research)

(1) Objective
Prokaryotes (i.e., Bacteria and Archaea) account for a large fraction of pelagic biomass and play an important role in biogeochemical cycles in the ocean. While the importance of prokaryotes in the oceanic carbon cycle have been well established, particularly for surface waters, our knowledge about magnitude and variation of metabolic activities of prokaryotes in the meso- and bathy-pelagic ocean are rather undeveloped. The objective of our study conducted during the MR08-05 cruise was to investigate i) Full-depth profiles of prokaryotic activity and abundance, ii) Depth profiles of dissolved inorganic carbon incorporation rate, iii) Distribution and activity of Bacteria and Archaea in water columns.

(2) Method
i) Full-depth profiles of prokaryotic activity and abundance
   Prokaryotic abundance: Flow cytometry
   Prokaryotic production: ^{3}H-leucine incorporation

ii) Depth profiles of dissolved inorganic carbon (DIC) incorporation rate
   DIC incorporation rate: ^{14}C-bicarbonate incorporation

iii) Distribution and activity of Bacteria and Archaea in water columns.
   Distribution and activity of Bacteria and Archaea is determind by using a combining microautoradiography with catalyzed reporter deposition fluorescence in situ hybridization (Micro-CARD-FISH). To determine uptake of organic matter and inorganic carbon, ^{3}H-leucine and ^{14}C-bicarbonate were used as substrates.

Measurements: Samples of the both prokaryotic abundance and production were collected from all the depths of 'Ocean Research Institute (ORI) cast' at all the four stations (i.e., Station AB, K1, K2 and KNOT). Samples of the DIC incorporation rate and the Micro-CARD-FISH were collected from the selected depths of ORI casts at all the four stations (*details are described in the meta-data sheet*).

(3) Preliminary results
Leucine incorporation rate ranged from 0.1 – 1052.8 pmol L^{-1} d^{-1} in whole through the water columns (Fig. 1). Leucine incorporation rate in surface waters (up to 40 m) varied within one order of magnitude and showed higher values than that below 40 m. These rates were decreased rapidly along the depth below 40 m. The patterns of leucine incorporation rate between 50 m and 1000 m were a function of depth at all the stations, while the patterns of this rate below 1000 m showed a depth-related pattern in three out of the four stations (Table 1). The magnitude of decreases (regression slops) were variable between the two layer (50 – 1000 m and below 1000 m) and among
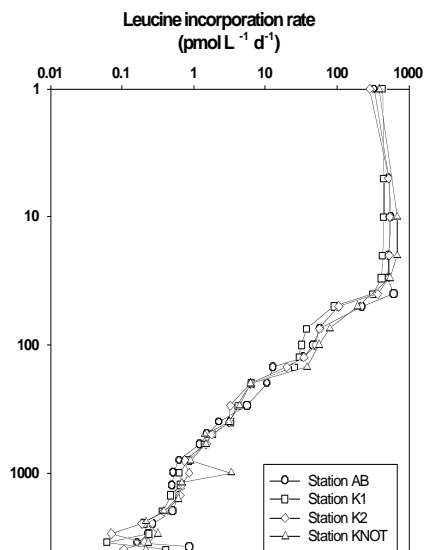
the four stations.

Figure 1. Depth profiles of leucine incorporation rate at the four stations.

Table 1. The log-log regression results for the decrease of leucine incorporation rate with depth.

Station	Layer	Slope b	SE	n	r^2	p
AB		-2.003	0.067	12	0.99	< 0.001
K1	40 -	-1.699	0.080	12	0.98	< 0.001
K2	1000	-1.781	0.095	12	0.97	< 0.001
KNOT		-1.744	0.206	11	0.89	< 0.001
AB		-0.424	0.433	8	0.14	0.37
K1	1000 -	-1.108	0.317	10	0.60	0.008
K2	Bottom	-1.173	0.491	10	0.41	0.044
KNOT		-1.408	0.266	10	0.78	< 0.01

3.9 Dissolved Organic Carbon

Masahide WAKITA (JAMSTEC MIO)

(1) Purpose of the study

Fluctuations in the concentration of dissolved organic carbon (DOC) in seawater have a potentially great impact on the carbon cycle in the marine system, because DOC is a major global carbon reservoir. A change by < 10% in the size of the oceanic DOC pool, estimated to be ~ 700 GtC, would be comparable to the annual primary productivity in the whole ocean. In fact, it was generally concluded that the bulk DOC in oceanic water, especially in the deep ocean, is quite inert based upon ^{14}C-age measurements. Nevertheless, it is widely observed that in the ocean DOC accumulates in surface waters at levels above the more constant concentration in deep water, suggesting the presence of DOC associated with biological production in the surface ocean. This study presents the distribution of DOC during autumn in the northwestern North Pacific Ocean.

(2) Sampling

Seawater samples were collected at all stations and brought the total to ~700. Seawater from each Niskin bottle was transferred into 60 ml High Density Polyethylene bottle (HDPE) or 50 ml ampoule rinsed with same water three times. Water taken from the surface to 250 m is filtered using precombusted (450°C) GF/F inline filters as they are being collected from the Niskin bottle. At depths > 250 m, the samples are collected without filtration. After collection, samples are frozen upright in 60 ml acid-cleaned HDPE bottles, and remain cold until analysis in our land laboratory. Each ampoule was sealed with a torch, quick-frozen, and preserved at ~ -20 °C until the analysis. Before use, all glassware was muffled at 550 °C for 5 hrs.

(3) Analysis

Prior to analysis, samples are returned to room temperature and acidified to pH < 2 with concentrated hydrochloric acid. DOC analysis was basically made with a high-temperature catalytic oxidation (HTCO) system improved a commercial unit, the Shimadzu TOC-V (Shimadzu Co.). In this system, the non-dispersive infrared was used for carbon dioxide produced from DOC during the HTCO process (temperature: 680 °C, catalyst: 0.5% Pt-Al$_2$O$_3$).

(4) Preliminary result

The distributions of DOC will be determined as soon as possible after this cruise.

(5) Data Archive

All data will be submitted to JAMSTEC Data Management Office (DMO) within 2 years.

3.10 Chlorofluorocarbons

Masahide WAKITA (JAMSTEC): Principal Investigator
Ken'ichi SASAKI (JAMSTEC)
Katsunori SAGISHIMA (MWJ)
Shoko TATAMISASHI (MWJ)

(1) Objectives

Chlorofluorocarbons (CFCs) are chemically and biologically stable gases that have been man-made synthesized at 1930's or later. The atmospheric CFCs can slightly dissolve in sea surface water by air-sea gas exchange and then are spread into the ocean interior. Three chemical species of CFCs, namely CFC-11 (CCl_3F), CFC-12 (CCl_2F_2), CFC-113 ($C_2Cl_3F_3$) can be used as transient tracers for the decadal time scale ocean circulation. We determined concentrations of these compounds in seawater on board.

(2) Apparatus

Dissolved CFCs are measured by an electron capture detector (ECD) – gas chromatograph attached with a purging & trapping system.

Table   1   Instruments

Gas Chromatograph:	GC-14B (Shimadzu Ltd.)
Detector:	ECD-14 (Shimadzu Ltd)
Analytical Column:	
Pre-column:	Silica Plot capillary column [i.d.: 0.53mm, length: 8 m, thick: 0.25µm]
Main column:	Connected two capillary columns (Pola Bond-Q [i.d.: 0.53mm, length: 9 m, thick: 6.0µm] followed by Silica Plot [i. d.: 0.53mm, length: 15 m, thick: 0.25µm])
Purging & trapping:	Developed in JAMSTEC.Trap column are 1/16" SUS tubing packed column (Porapak type N)

(3) Procedures

a) Sampling

Seawater sub-samples were collected from 12 litter Niskin bottles to 300 ml glass bottles(Developed in JAMSETC).The bottles were filled by nitrogen gas before sampling. Two times of the bottle volumes of seawater sample were overflowed. The seawater samples were kept in water bathes roughly controlled on sample temperature. The CFCs concentrations were determined as soon as possible after sampling.

In order to confirm CFC concentrations of standard gases and their stabilities and also to check CFC saturation levels in sea surface water with respect to overlying air, CFC mixing ratios in background air were periodically analyzed. Air samples were continuously led into laboratory by 10 mm OD Dekaron® tubing. The end of the tubing was put on a head of the compass deck and another end was connected onto a macro air pump in the laboratory. The tubing was relayed by a T-type union which had a small stop cock. Air sample was collected from the flowing air into a 200ml glass cylinder attached on the cock.

b) Analysis

The analytical system is modified from the original design of Bullister and Weiss

(1988). Constant volume of sample water (50ml) is taken into the purging & trapping system. Dissolved CFCs are de-gassed by N_2 gas purge and concentrated in a trap column cooled to -40 degree centigrade. The CFCs are desorbed by electrically heating the trap column to 140 degree centigrade within 1.5 minutes, and lead into the pre-column. CFCs and other compounds are roughly separated in the pre-column and CFCs are sent to main analytical column. And then the pre-column is switched to another line and flushed back by counter flow of pure nitrogen gas. CFCs sent into main analytical column are separated further and detected by an electron capture detector (ECD).

Table 2 Analytical conditions of dissolved CFCs in seawater.

Temperature

Analytical Column:	95 deg-C
Detector (ECD):	240 deg-C
Trap column:	-45 deg-C (at adsorbing) & 140 deg-C (at desorbing)

Mass flow rate of nitrogen gas (99.9999%)

Carrier gas:	11ml/min
Detector make-up gas:	26ml/min
Back flush gas:	20ml/min
Sample purge gas:	120 ml/min

All nitrogen gases through one or two gas purifier tube containing Molecular Sieve 13X (MS-13X).

Standard gas (Japan Fine Products co. ltd.)

Base gas:	Nitrogen
CFC-11:	300 ppt (v/v)
CFC-12:	160 ppt (v/v)
CFC-113:	30 ppt (v/v)

(4) Preliminary results

The analytical precisions are estimated from replicate sample analyses. The precisions of CFCs were calculated to be ± 0.006 pmol/kg (n =41), ± 0.008 pmol/kg (n = 41) and ± 0.006 pmol/kg (n = 41) for CFC-11, -12 and -113, respectively.

(5) Data archive

All data will be submitted to JAMSTEC Data Management office (DMO) and under its control.

(6) Reference

Bullister, J.L and Weiss R.F. 1988. Determination of CCl_3F and CCl_2F_2 in seawater and air. Deep Sea Research, 35, 839-853.

3.11 Argo float

Nobuyuki SHIKAMA   (IORGC): Principal Investigator (not on board)
Tomoyuki TAKAMORI (MWJ): Technical Staff
Hiroshi MATSUNAGA (MWJ): Technical Staff

(1) Objectives
        The objective of deployment is to clarify the structure and temporal/spatial variability of water masses in the northwest Pacific and the Bering Sea. Floats are deployed at the request of Dr. Howard Freeland of Institute of Ocean Sciences, Fisheries and Oceans Canada, under Argo Project.
        The profiling floats launched in this cruise measure vertical profiles of temperature and salinity automatically every ten days. The data from the floats will enable us to understand the phenomenon mentioned above with time/spatial scales much smaller than in previous studies.

(2) Parameters
        Water temperature, salinity, and pressure

(3) Methods
  Profiling float deployment
        We launched 6 APEX floats manufactured by Webb Research Ltd. These floats equip an SBE41 CTD sensor manufactured by Sea-Bird Electronics Inc.
        The floats usually drift at a depth of 2000 dbar (called the parking depth), rising up to the sea surface every ten days by increasing their volume and thus changing the buoyancy. During the ascent, they measure temperature, salinity, and pressure. They stay at the sea surface for approximately nine hours, transmitting the CTD data to the land via the ARGOS system, and then return to the parking depth by decreasing volume.   The status of floats and their launches are shown in Table 1.

(4) Data archive
        The real-time data are provided to meteorological organizations, research institutes, and universities via Global Data Assembly Center (GDAC:
http://www.usgodae.org/argo/argo.html, http://www.coriolis.eu.org/) and Global
Telecommunication System (GTS), and utilized for analysis and forecasts of sea conditions.

Table 1 Status of floats and their launches

Float

Float Type	APEX floats manufactured by Webb Research Ltd.
CTD sensor	SBE41 manufactured by Sea-Bird Electronics Inc.
Cycle	10 days (approximately 9 hours at the sea surface)
ARGOS transmit interval	45 sec
Target Parking Pressure	2000 dbar
Sampling layers	70 (1950, 1900, 1850, 1800, 1750, 1700, 1650, 1600, 1550, 1500, 1450, 1400, 1350, 1300, 1250, 1200, 1150, 1100, 1050, 1000, 950, 900, 850, 800, 750, 700, 650, 600, 550, 500, 450, 400, 380, 360, 350, 340, 330, 320, 310, 300, 290, 280, 270, 260, 250, 240, 230, 220, 210, 200, 190, 180, 170, 160, 150, 140, 130, 120, 110, 100, 90, 80, 70, 60, 50, 40, 30, 20, 10, 5 dbar)

Launches

Float S/N	ARGOS PTT ID	Date and Time of Launch (UTC)	Location of Launch	CTD St. No.
3875	82956	11:24, Oct. 12	55-47.99 N, 176-29.87 W	N/A
3876	82957	20:18, Oct. 12	56-35.91 N, 179-59.81 W	N/A
3877	82958	04:42, Oct. 16	57-00.34 N, 175-58.90 E	S1(AB)
3878	82959	15:37, Oct. 16	56-12.08 N, 175-00.23 E	N/A
3879	82960	01:49, Oct. 21	50-59.45 N, 165-13.41 E	S7(K1)
3888	83249	23:45, Oct. 29	45-58.89 N, 158-20.01 E	S12

3.12 Biofouling

Tetsuichi FUJIKI (JAMSTEC MIO)

(1) Objective

      When the buoy system is utilized for long-term observations in the ocean, the instruments are susceptible to biofouling in the form of microbial and algal films. Tributyltin self-copolymer paints have been the most successful in reducing biofouling. However it also has been reported that tributyltin affect adversely the marine organisms (e.g. defective growth, imposex and debilitation of the immunological defense). In the present study, tin-free antifouling paint was tested during this cruise.

(2) Methods

      As the tin-free antifouling paint, we tested a silicone-based paint (CMP Bioclean, Chugoku Marine Paints, clear and colorless) which provides a low critical surface tension, i.e., a "slippery" surface. First, anti-corrosion paint (Ecomax, Chugoku Marine Paints, black color) was applied on aluminum plates (5 cm ×5 cm). After drying, CMP Bioclean was overpainted on these plates. The Bioclean-painted and control (only anti-corrosion paint) plates were placed in an on-deck water tank for a period of three weeks (Fig. 1). Duplicates were made for each treatment. Three weeks later, the samples were fixed with neutralized formalin (final concentration: 3%, v/v). For assessing biofouling on the plates, attached organisms are examined by using a light microscope.

(a)   (b)
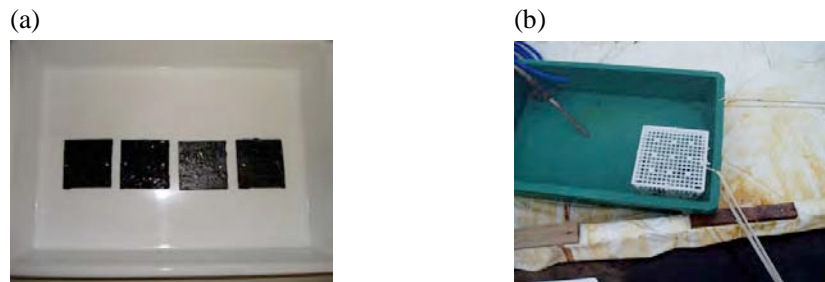
Fig. 1. Photographs of (a) Bioclean-painted [two plates on the left] and control [two plates on the right] samples and (b) the on-deck water tank experiment.

3.13 Stable carbon and nitrogen isotopes of suspended particles

Toshiro SAINO (JAMSTEC)
Yoshihisa MINO (HyARC, Nagoya Univ.)

(1) Objective

Stable carbon and nitrogen isotopes in marine organic matter can provide information on the environmental condition and its related algal physiology when the organic matter was formed. In order to understand algal physiology and its implications on biogeochemistry of high productive subarctic north Pacific, we examined spatial variations in carbon and nitrogen isotopic compositions in suspended particulate organic matter in surface waters of along a transect extending from the Bering Sea to the western subarctic north Pacific, crossing the Aleutian Islands.

(2) Methods

For the determination of ^{13}C and ^{15}N in suspended POM, about 20 liters of surface seawaters were collected with a plastic bucket at 14 stations along the track (S1-14). These samples were filtered through precombusted GF/F filters (Whatman, 47mm diameter). After filtration, the filters were rinsed with particle free salt water and stored frozen until isotopic analysis onshore.

4. Geophysical observation

Takeshi MATSUMOTO (University of the Ryukyus) : Principal Investigator*
Masao NAKANISHI (Chiba University) : Principal Investigator*
Wataru TOKUNAGA (GODI)
Kazuho YOSHIDA (GODI)
* not on board

4.1 Swath Bathymetry

(1)   Introduction

R/V MIRAI is equipped with a Multi narrow Beam Echo Sounding system (MBES), SEABEAM 2112.004 (SeaBeam Instruments Inc.), add system Sub-Bottom Profiler (SBP). The objective of MBES is collecting continuous bathymetric data along ship's track to make a contribution to geological and geophysical investigations and global datasets.

In addition, we surveyed and collected data at the Station of Aleutian basin, K1, K2 and Shimokita off with SBP (see; 3.7). And we need to estimate the depth at the location of deployment of BGC buoy in order to design these mooring systems.

(3)   Data Acquisition

The "SEABEAM 2100" on R/V MIRAI was used for bathymetry mapping during the MR08-05 cruise from 11 October 2008 to 7 November 2008, except for the territorial waters of U.S.A.

To get accurate sound velocity of water column for ray-path correction of acoustic multibeam, we used Surface Sound Velocimeter (SSV) data to get the sea surface (6.2m) sound velocity, and the deeper depth sound velocity profiles were calculated by temperature and salinity profiles from CTD data by the equation in Mackenzie (1981) during the cruise.

Table 4.1-1 shows system configuration and performance of SEABEAM 2112.004 system.

Table 4.1-1 System configuration and performance

SEABEAM 2112.004 (12 kHz system)

Frequency:	12 kHz
Transmit beam width:	2 degree
Transmit power:	20 kW
Transmit pulse length:	3 to 20 msec.
Depth range:	100 to 11,000 m
Beam spacing:	1 degree athwart ship
Swath width:	150 degree (max)
	120 degree to 4,500 m
	100 degree to 6,000 m
	90 degree to 11,000 m
Depth accuracy:	Within < 0.5% of depth or +/-1m,
	whichever is greater, over the entire swath.
	(Nadir beam has greater accuracy;

typically within < 0.2% of depth or +/-1m, whichever is greater)

Sub-Bottom Profiler (4kHz system)	
Frequency:	4 kHz
Transmit beam width:	5 degree
Sweep:	5 to 100 msec
Depth Penetration:	As much as 75 m (varies with bottom composition)
Resolution of sediments:	Under most condition within < tens-of-centimeters range (dependent upon depth and sediment type)

(4)　　Preliminary Results
　　　The results will be published after primary processing.

(5)　　Data Archives
　　Bathymetric data obtained during this cruise will be submitted to the Marine-Earth Data and Information Department (MEDID) in JAMSTEC, and will be archived there.

(6)　　Remark
　　　We did not collect data in the territorial waters of U.S.A at following term.
　　Departure from Dutch Harbor - 02:16 UTC, 11 Oct.

4.2 Sea surface gravity

(1)   Introduction

The local gravity is an important parameter in geophysics and geodesy. We collected gravity data at the sea surface.

(3)   Parameters

Relative Gravity [CU: Counter Unit]

[mGal] = (coef1: 0.9946) * [CU]

(4)   Data Acquisition

We measured relative gravity using LaCoste and Romberg air-sea gravity meter S-116 (Micro-g LaCoste, LLC) during the MR08-05 cruise from 10 October 2008 to 8 October 2008, except for the territorial waters of the U.S.A.

To convert the relative gravity to absolute one, we measured gravity, using portable gravity meter (Scintrex gravity meter CG-3M), at Sekinehama (MR08-04 was started) and Onahama as the reference points.

(5)   Preliminary Results

Absolute gravity shown in Tabel 4.2-1

Table 4.2-1

No.	Date	U.T.C.	Port	Absolute Gravity [mGal]	Sea Level [cm]	Draft [cm]	Gravity at Sensor [1] [mGal]	L&R [2] Gravity [mGal]
#1	10 Oct.	20:35	Dutch Harbor	---------	325	625	--------	--------
#2	07 Nov.	07:03	Onahama					

[1]: Gravity at Sensor = Absolute Gravity + Sea Level*0.3086/100 + (Draft-530)/100*0.0431

[2]: LaCoste and Romberg air-sea gravity meter S-116

(6)   Data Archives

Surface gravity data obtained during this cruise will be submitted to the Marine-Earth Data and Information Department (MEDID) in JAMSTEC, and will be archived there.

(7)   Remark

We did not collect data in the territorial waters of U.S.A at following term.
Departure from Dutch Harbor - 02:16 UTC, 11 Oct.

4.3 Sea Surface three-component magnetic field

(1) Introduction
   Measurements of magnetic force on the sea are required for the geophysical investigations of marine magnetic anomaly caused by magnetization in upper crustal structure. We measured geomagnetic field using a three-component magnetometer during the MR08-05 cruise from 10 October 2008 to 7 November 2008, except for the territorial waters of the U.S.A.

(3) Principle of ship-board geomagnetic vector measurement
   The relation between a magnetic-field vector observed on-board, $\mathbf{H}$ob, (in the ship's fixed coordinate system) and the geomagnetic field vector, $\mathbf{F}$, (in the Earth's fixed coordinate system) is expressed as:

$$\mathbf{H}ob = \mathbf{A} \, \mathbf{R} \, \mathbf{P} \, \mathbf{Y} \, \mathbf{F} + \mathbf{H}p \qquad\qquad (a)$$

   where $\mathbf{R}$, $\mathbf{R}$ and $\mathbf{Y}$ are the matrices of rotation due to roll, pitch and heading of a ship, respectively. $\tilde{\mathbf{A}}$ is a 3 x 3 matrix which represents magnetic susceptibility of the ship, and $\mathbf{H}p$ is a magnetic field vector produced by a permanent magnetic moment of the ship's body.   Rearrangement of Eq. (a) makes

$$\mathbf{B} \, \mathbf{H}ob + \mathbf{H}bp = \mathbf{R} \, \mathbf{P} \, \mathbf{Y} \, \mathbf{F} \qquad\qquad (b)$$

   where $\mathbf{B} = \mathbf{A}^{-1}$, and $\mathbf{H}bp = \mathbf{-B} \, \mathbf{H}p$.   The magnetic field, $\mathbf{F}$, can be obtained by measuring $\mathbf{R}$, $\mathbf{P}$, $\mathbf{Y}$ and $\mathbf{H}ob$, if $\mathbf{B}$ and $\mathbf{H}bp$ are known.   Twelve constants in $\mathbf{B}$ and $\mathbf{H}bp$ can be determined by measuring variation of $\mathbf{H}ob$ with $\mathbf{R}$, $\mathbf{P}$ and $\mathbf{Y}$ at a place where the geomagnetic field, $\mathbf{F}$, is known.

(4) Instruments on *R/V MIRAI*
   A shipboard three-component magnetometer system (Tierra Technica SFG1214) is equipped on-board *R/V MIRAI*.   Three-axes flux-gate sensors with ring-cored coils are fixed on the fore mast.   Outputs of the sensors are digitized by a 20-bit A/D converter (1 nT/LSB), and sampled at 8 times per second.   Ship's heading, pitch, and roll are measured utilizing a ring-laser gyro installed for controlling attitude of a Doppler radar.   Ship's position (GPS) and speed data are taken from LAN every second.

(5) Data Archives
   Magnetic force data obtained during this cruise will be submitted to the Marine-Earth Data and Information Department (MEDID) in JAMSTEC, and will be archived there.

(6) Remarks
   1.   We did not collect data in the territorial waters of U.S.A at following term.
      Departure from Dutch Harbor - 02:16 UTC 11 Oct.
   2.   For calibration of the ship's magnetic effect, we made a "Figure eight" turn (a pair of clockwise and anti-clockwise rotation). The periods were follows;

i) 09:02 - 09:26 UTC, 15 Oct. about at 57-00N, 175-59E

ii) 01:00 - 01:32 UTC, 05 Nov. about at 37-58N, 143-24E

3. Data logging was stopped because of file operation error as following term.
00:47:11 - 00:47:43 UTC, 26 Oct.

4.4 Tectonic history of the Pacific Plate

The Pacific Plate is the largest oceanic lithospheric plate on the Earth. The Pacific Plate was born around 190 Ma, Middle Jurassic (Nakanishi et al., 1992). The tectonic history of the Pacific Plate has been exposed by many studies based on magnetic anomaly lineations. However, the tectonic history in some periods is still obscure because of lack of geophysical data. To reveal the entire tectonic history of the Pacific Plate from Middle Jurassic to the present, increase in geophysical data is indispensable.

Identification of magnetic anomaly lineations has been the most common method for tectonic studies of oceanic plates. After improvement of the multi-narrow beam echo sounder, we become able to describe lineated abyssal hills for the tectonic studies in detail. Abyssal hills are related to the nature of the mid-ocean ridges at which they form (e.g. Goff et al., 1997). For example, abyssal hills heights and widths tend to correlate inversely with spreading rates. Abyssal hills also change morphology depending on crustal thickness and magma supply, factors which can vary within a single ridge segment and/or can vary from one ridge segment to another. Abyssal hills are therefore an off-axis indicator of mid-ocean ridge spreading history.

We collected bathymetric data using SeaBeam 2112 during MR08-04 and MR08-05. Figure 4.4.1 shows an example of abyssal hills. The abyssal hills has an N60°E strike. The seafloor was formed at the Pacific-Izanagi Ridge (Nakanishi et al., 1989) and is getting progressively younger to the north. Magnetic anomaly lineations with an N70°E trend, which age is around 130 Ma, are identified to the south of the survey area (Nakanishi et al., 1989). The result of the bathymetric survey may imply that the strike of the Pacific-Izanagi Ridge changed after 130 Ma.

References

Goff, J. A., Y. Ma, A. Shah, J.R. Cochran, and J.-C. Sempere, 1997, Stochastic analysis of seafloor morphology on the flank of the Southeast Indian Ridge: The influence of ridge morphology on the formation of abyssal hills, *J. Geophys. Res*., 102, 15,521-15,534.

Searle, R., 1984, GLORIA survey of the East Pacific Rise Near 3.5°S: Tectonic and volcanic characteristics of a fast spreading mid-ocean rise, *Tectonophysics*, 101, 319-344.

Nakanishi, M., K. Tamaki, and K. Kobayashi, 1989, Mesozoic magnetic anomaly lineations and seafloor spreading history of the northwestern Pacific, *J. Geophys. Res.*, 94, 15437-15462.

Nakanishi, M., K. Tamaki, and K. Kobayashi, 1992, A new Mesozoic isochron chart of the whole western Pacific Ocean: Paleomagnetic and tectonic implications, *Geophys. Res. Lett*., 19, 693-696.
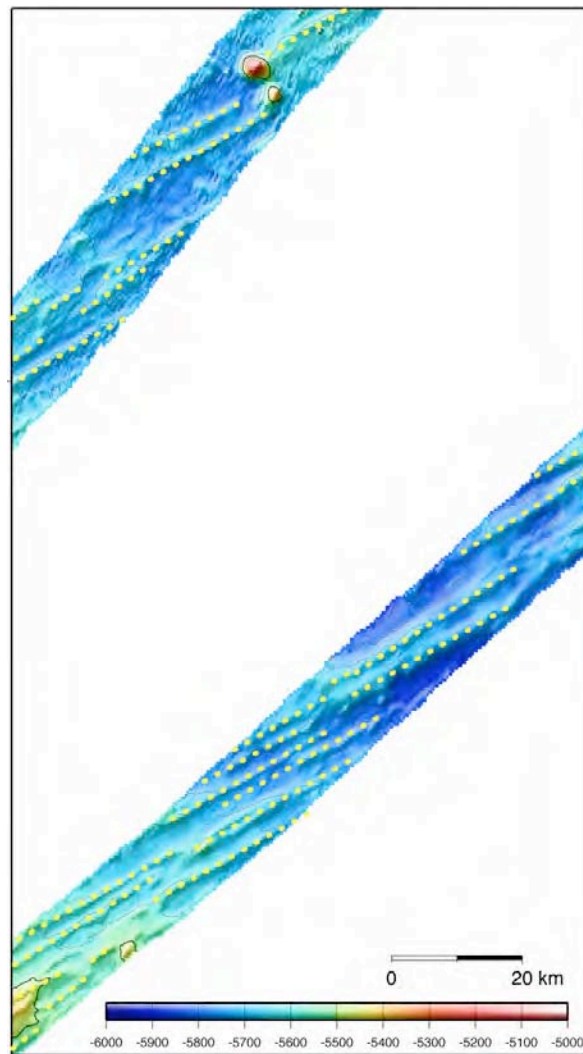
Figure 4.4.1 An example of lineated abyssal hills. Contour interval is 100 m. Bathymetry is illuminated from the northwest. Yellow dotted lines represent abyssal hills.

5. Satellite Image Acquisition (MCSST from NOAA/HRPT)

Makio HONDA   **(JAMSTEC) : Principal Investigator**
Kazuhiko MATSUMOTO   **(JAMSTEC)**
Wataru TOKUNAGA   **(GODI)**
Kazuho YOSHIDA   **(GODI)**

(1)   Objectives

It is our objectives to collect data of sea surface temperature in a high spatial resolution mode from the Advance Very High Resolution Radiometer (AVHRR) on the NOAA polar orbiting satellites and to build a time and depth resolved primary productivity model.

(2)   Method

We receive the down link High Resolution Picture Transmission (HRPT) signal from NOAA satellites. We processed the HRPT signal with the in-flight calibration and computed the sea surface temperature by the Multi-Channel Sea Surface Temperature (MCSST) method. A daily composite map of MCSST data is processed for each day on the R/V MIRAI for the area, where the R/V MIRAI located.

We received and processed NOAA data throughout MR08-05 cruise from 11 October 2008 to 7 November 2008.

The sea surface temperature data will be applied for the time and depth resolved primary productivity model to determine a temperature field for the model.

(3)   Preliminary results

Fig.5-1 showed MCSST composite image during this cruise from 11 October 2008 to 6 November 2008 at the Northern-west Pacific Ocean.

(4)   Data archives

The raw data obtained during this this cruise will be submitted to the Marine-Earth Data and Information Department (MEDID) in JAMSTEC, and will be archived there.
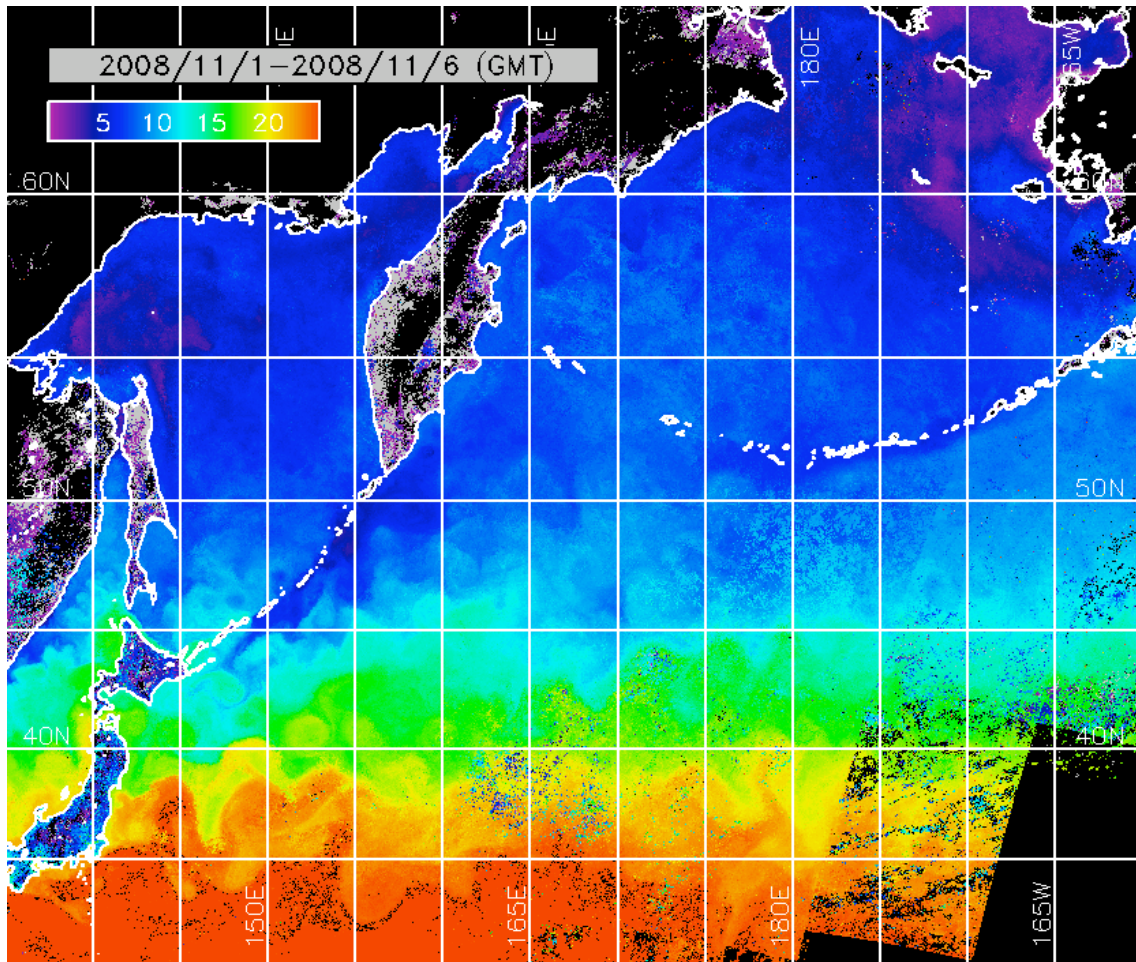
Fig.5-1   MCSST composite image at Northern-west Pacific Ocean.
11 Oct. - 06 Nov. 2008

6. Ship Operation

Masaharu AKAMINE (Master of R/V "MIRAI)
Ship's Crew

6.1 Ship's Handling for Deployment of BGC mooring

(1) Objectives
・**To deploy it accurately and efficiently to a spot where a mooring is required.**
・**To prevent damage of an observation equipment and a sensor.**
Results are analyzed from the standpoint of ship's maneuvering to achieve two purposes that mentioned above, and it aims to make the results useful for observation work in the future.

(2) Observation parameters

・Ship's position, course, speed
・Directions of the wind and the current, velocities of the wind and the current
・ Vectors of the wind and the current, the resultant force
・ Working hours
・ Catenary of the mooring line while towing
・ Position of the sinker

(3) Methods
   (3.1) Measurement of the actual ship-movement
       Measurement of the ship-movement at engine stopped is executed by a set-drift which is measured before deploying the BGC mooring in order to make in advance a comparison between reality and expectation. A direction and a velocity of the ship-movement in the external force influence is measured by a radio navigation device " Sains" assembled by Sena Co., Ltd. Japan and a Doppler sonar "DS-30" assembled by FURUNO Electric Co., Ltd. Japan.

   (3.2) Measurement of the wind and the current
       The wind direction and speed is measured by KOAC-7800 weather data processor and sensors assembled by Koshin Denki Co., Ltd.
       The current direction and speed are continuously measured by a Doppler sonar "DS-30" installed at the bottom of the ship.

   (3.3) Ship's speed
       According to the results measured in past, and the instruction from the marine technician of Woods Hole Oceanographic Institution, the ship's speed is set up so as to keep her speed on 1.0~ 2.0 knots at ship's through-the-water while the mooring lines are paid out, to keep her speed on about 1 knot at ship's through-the-water while the various instruments such as sensors, sediment traps, glass balls /releasers/sinker etc. are attached. In order to avoid their instrument accident and to

maintain a safety of the work, an average speed in all the works being around 1.5 knots at through-the-water is made an aim in deploying. At the stage of the start, the ship's way is most stopped while some instruments are attached in the top buoy.

(3.4) Ship's course

The standard of the ship's course is to make the ship proceed to upwind. The final decision is done in consideration of the external force influence such as the wind-drift, the wave, the current, and the swell, making reference to the data of the set-drift carried out before the deploying operation of the BGC mooring.

It is important to lessen the angle between the ship's course and the wind direction in order to prevent the ship drifting to the lee. The ship shall be managed to make the mooring lines paid out from the stern, straight behind. It is necessary to grasp the current influence in the long span to set a sinker to the target point accurately.

It is also necessary to consider the direction of the swell that influences the shift of the ship.

(3.5) Working hours for the deployment of the BGC mooring

The time that the ship needs in each work is investigated and recorded referring to past data. An example in principle is given as follows.

"Total of Distance" means the navigating distance from the work beginning to the sinker dropping. This is a standard without a big flow influence in accordance with data in past. Each ship's speed is the numerical value of the above standard in (4.3).

BGC mooring

Works	Time	Ship's speed	Distance
Stand by the top-buoy	0.5 hour	0 knot	0 mile
Attachment of the sediment traps	4.0	1.0	4.0
Paying out the mooring ropes	0.5	1.5	0.8
Towing	1.0	1.7	1.7
Setting the sinker	0.5	1.0	0.5
Total	6.5 hours	1.4 knots	7.0 miles

(3.6) Catenary of the BGC mooring line while towing

It is necessary to know catenary of the BGC mooring line in order to keep straight the tension of it before the sinker is dropped.

After all of the BGC mooring line are paid out from the stern, a distance between the stern and the top buoy of the BGC mooring line is measured by radar of the ship while they are being towed to the place where the sinker is dropped.

The ship's radar: "JMA9000 X band" and "JMA 9000 S band" assembled by JRC Ltd. "MM950 X & S band" assembled by Consilium Selesmar, Italy.

(3.7) Designated mooring location (Target point) Targets at K2 station are fixed based on the sounding result of execution in 2001.

BGC mooring **: Lat.47° 00'.35N, Long. 159° 58'.32E** Depth 5206.2 meter

(3.8) Decision of the anchored position

　　As soon as the sinker dropped into the ocean, the ship returns to the position of the top-buoy, watches the top-buoy disappearing from the surface by the ship's radars and etc. The movement of the sinker dropped in the sea is taken hold of in real time and the position of the sinker arrived at the seabed is fixed by an acoustic navigation device (System), a radio navigation device.

　　The acoustic navigation device: "SSBL processor (transmit 9 kHz or 13 kHz, receipt 13.5 kHz to 15.5 kHz)" assembled by Oki Electric Co. Ltd. Japan The acoustic transducer & releaser: Edgetech Inc. USA

　　　(receipt 9 kHz & 11 kHz, transmit 11 kHz & 12 kHz but 12 kHz was changed to 14kHz in this time)

　　The radio navigation device: "Sains" assembled by Sena Co., Ltd. Japan.

　　The ship's radar: "JMA9000 X band" and "JMA 9000 S band" assembled by JRC Ltd. "MM950 X & S band" assembled by Consilium Selesmar, Italy.

(4) Results

　(4.1) Ship's speed

　　The results are shown in Fig.6.1-1 and Table 6.1-1, 6.1-2.

　　An approximate speed at through-the-water in each work is shown in the following.

During setting the top buoy	0.4 (0.6) knots
During paying out mooring ropes with sediment traps	1.3(1.6)
During towing at the final stage	1.8 (2.1)
During setting the sinker	1.1 (1.3)
The average speed during the deployment	1.4 (1.7)

　　(　) An average speed at over-the -ground.

　　The ship's speed in deploying the mooring was according to the standard.

　　The speed at over-the-ground is more bigger than speed at through-the water because the ship ran with the following current.

　　The speed of the ship and revolutions of the winch are adjusted so as not to hang a big stress in the cable/ropes actually paid out from her stern, checking the past data and the cable/ropes tension measurement by skilled hands of marine technicians and chief officer at ship's stern.

　(4.2) Ship's course (Table 6.1-1)

　　The deployment course on which the ship advances toward the wind was decided based on the set drift and the past data.

　　The course-made-good and the heading of the ship are shown as follows.

Course	CMG	Towing Co.	Overshooting Co.	Unit: degrees
<161>	<161>	<162>	<163>	

"Course" is the course set when the development of the mooring started.

"CMG" stands for "course-made-good ". It means the furrow that the ship actually navigated from the deployment start to the sinker drop.

"Towing Co." means the furrow in navigation from the towing start to the sinker drop.

"Overshooting Co." means an actual result that the ship ran in a certain distance beyond the target point. It is shown in (5.6) Sinker position.

The course of the ship was set to 161 degrees to receive the wind in the bow and moderate head swell. The influence of the wind is a little because the wind was almost unchanged as shown in Fig.6.1-2, 6.1-3 & table 6.1-1.

The irregular current made the choice of her course difficult at the stage of start of the deployment. Consequentially, the direction of the current has changed from 143 degrees to 242 degrees as shown in Fig.6.1-4 , 6.1-5, 6.1-6 and Table 6.1-1.

The hull shift to the right was forced with the current in two-thirds of the deployment work, but it reverted by using the powerful side thruster. Although the ship's heading was changed variously, the ship navigated on the course nearly. It is clear because there is no difference between the setting course and the CMG.

After the ship passed through the target point, she was controlled with the helm and the side thrusters as the external force influence to the right due to the current increased by reducing speed.

(4.3) Working hours

The results are shown in Table 6.1-2 and the following tables.

The time spent in paying out mooring ropes was short very much because they had already been connected and they were being wound around the drum tidily.

From 1055SMT to 1115SMT the additional lashing of the sinker on the deck was carried out with reducing the ship's speed because it was found that it was unstable as soon as the towing had started. Accordingly the time in towing increased a little in comparison with the last time.

Working hours in deployment of the BGC mooring line on 29th October 2008

①The time spent in setting a top buoy and instruments .... 18 minutes
②The time spent in paying out mooring lines with sediment traps 2 hours 43 minutes
   (including the time spent in setting glass balls)
③The time spent on towing .... 1 hour17 minutes
④The time spent in setting releasers and sinker .... 5 minutes

                                              Total   4 hours 23 minutes

The following table shows past actual results as to each work mentioned in the above table. The work item of this table is referred to the numbers which are marked for each work item mentioned in the above table.
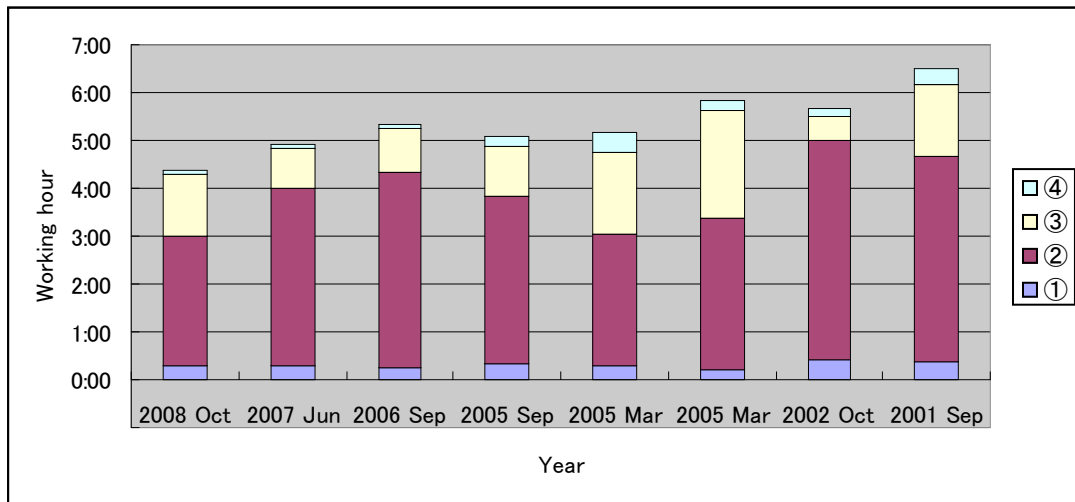
I t is found that the working hours has been shortened gradually by having an experience.

(4.4) Catenary of the BGC mooring line while towing

After all of the BGC mooring line was paid out from the stern a horizontal distance from the stern to the top buoy of the BGC mooring line was measured with radar of the ship each 20 minutes during towing to the place where the sinker was dropped.

SMT	Radar distance	BGC mooring length	Catenary
10:51(Towing starts)	4965 meters	5186 meters	221 meters
11:11	5039	5186	147
11:31	5039	5186	147
11:51	5039	5186	147
12:13 (Let go sinker)	5039	5186	147

Radar distance means the horizontal length between the stern and the top buoy of the BGC mooring measured by the ship's radar. The amount of Catenary is shown in the difference from the radar distance and the BGC mooring length.
When the towing started, Catenary of the mooring lines was 221 meters. After the towing was carried out for 20 minutes, Catenary was shortened to 147m and the length was unchanged until a sinker was dropped in the sea.

(4.5) Dropping sinker

The preparation to drop a sinker started about 200 meters on this side of the spot where the sinker is dropped.
The distance to the dropped point was informed with the communication device from the bridge to a team of technician and deck personnel in every 10 meters. And the bridge counted down from 10 meters before the point dropping the sinker.

After the sinker had been dropped, the ship made a U-turn and pursued it so as to make sure that the top buoy disappeared from surface. The ship went near the top buoy as soon as possible to catch it clearly by radar because it was unable to be found due to poor visibility.

After all, the top buoy was unable to be caught until it disappeared from the surface of the sea. The ship ran on the point where a top buoy disappeared from the radar screen, and confirmed that it had sunk certainly.

The movement of the sinker being dropped into the sea was grasped by the acoustic navigation device continuously. The information grasped here is diagrammed in the Fig 6.1-7.

UTC +11 h

Movement	Position	Time (SMT)	Direction and Distance
Top buoy into sea	47-06.98N	08:08	<degree>
	159-55.00E		
Top buoy's position	47-02.82N	12:13	
(Sinker was dropped)	159-57.06E		
Top buoy disappeared	47-01.33N	13:02	
	159-57.66E		<165>2852m
Target point	47-00.35N		
	159-58.32E		
Sinker reached seabed	47-00.36N	13:08	
(Sinker point)	159-58.16E		<161>1908m <276>204m
Sinker drop point	47-00.03N		
(Ship's position)	159-58.46E	<161>13594m <161>5465m <163>611m	

Remark: The bearing /distance from the sinker point to the sinker drop point are <148>/722 m.

The time from the drop of the sinker to the disappearance of the top buoy was 49 minutes and that of previous deployment was as follows.40 minutes (2007), 41 minutes (2006), 38 minutes (2005), 50 minutes (Long 2005) and 47 minutes (Test 2005). After the top buoy got free, it ran on the surface at average speed 1.9 knots in the direction of 165 degrees. In the above-mentioned table, the horizontal distance and the time from the point where the top buoy disappeared from the surface to the sinker point were 1908 meters and 6 minutes. There is no big difference between this answer and the actual result in 2005 (2093 meters and 5 minutes).

(4.6) Sinker's position (Fig 6.1-7)

Because the response signal of the releaser was changed to 14kHz in this time, it was possible to know the movement of the sinker thrown into the sea by the acoustic navigation device on board in real time. The time when the sinker arrived at the bottom of the sea, and its position were able to know by this device as well.

The difference between the position that **the sinker was dropped (Sinker drop point)** and the position that **the sinker reached the seabed** (**Sinker point**) is shown in the following numerical data.

Sinker drop point to Target point	Sinker drop point to **Sinker point**	**Difference**
direction/ distance	direction/ distance	**Sin/ Cos**
343 degrees/ 519 meters	326 degrees/ 630 meters	152/ -134 meters

Above-mentioned numerical value shows that the straight-line distance between the sinker drop point and the target point or the sinker point.

"Sinker drop point" means the distance from the position of the sinker dropped to the target point**.** The distance was obtained with the simulation program of Marine Works Japan Ltd.

"Sinker point" was obtained by the measurement of the acoustic navigation device which the ship is equipped with.

The **"Sin of Difference"** and the **"Cos of Difference"** are the amount of difference in the X/Y directions to the sinker point from the target point. The plus sign of Sin shows that the sinker point exists in the right side of the target point toward the sinker drop point. The plus sign of Cos shows that the sinker point exists in the far side of the target point toward the sinker drop point. The minus sign shows the reverse in each.

These values is including 84 meters of the horizontal distance between the GPS position of the bridge and the ship's stern where the mooring lines are paid out.

Though the mooring line being towed by the ship passed on the target point precisely, after the sinker was dropped into the sea the whole of the BGC mooring line including the sinker streamed in the WNW direction by the flow in SW direction and the SSE'ly wind.

(4.7) Required depth

The mooring was actually anchored within the same depth contour as shown in Fig 6.1-8 and the depth of 5220 meters was obtained by a SEA-BEAM 2000.

(4.8) Distance for deployment of the mooring (Table 6.1-2)

Results are shown in the following Table.

Actual	Tow	T/A
7.37 miles	2.65 miles	36.0 % (1.7 knots)

"Actual" is the distance from the starting point to the position of the dropped sinker.
"Tow" is the distance between the point where the tow begins and the point where the sinker is slung. The distance of "Actual" includes that of "Tow".
"T/A" is the ratio of the distance for towing to the actual distance. Figures in parentheses show the speed at over-the -ground. The following are the past data of the ratio.

28.3 % in 2007 (1.4knots), 24.4 % in 2006 (1.3knots), 30.1 % in 2005 (1.5knots), 40.5 % in 2005(Long-term) (1.3knots), 43.1 % in 2005(Test) (1.7knots), 9.1 % in 2002 (1.4knots) , 30.8 % in 2001 (1.3knots).

In 2002 (Long-term), the time in towing was shortened because time for setting sediment traps attached extra compared with others was consumed much.

There is relationship between this percent and the average OG speed of the

deployment buoy work. In other words, the percent is showing a tendency to grow big when the OG speed is fast.

(5) Data archive

All data will be archived on board.

(6) Remarks

By changing the response signal of the releaser being used for BGC mooring system from 12kHz to 14kHz, the movement of the sinker thrown into the sea could be grasped in real time, and moreover the position of the sinker that reached the bottom of the sea could be known easily in a short time.

According to measurement of Catenary of the BGC mooring line while towing at the through-the-water speed about 2 knots, it found that the BGC mooring line had to be towed for more than twenty minutes to make straight it tension before the sinker was dropped.

Fig 6.1-1 Ship's speed in deployment at K2 station (MR08-05)
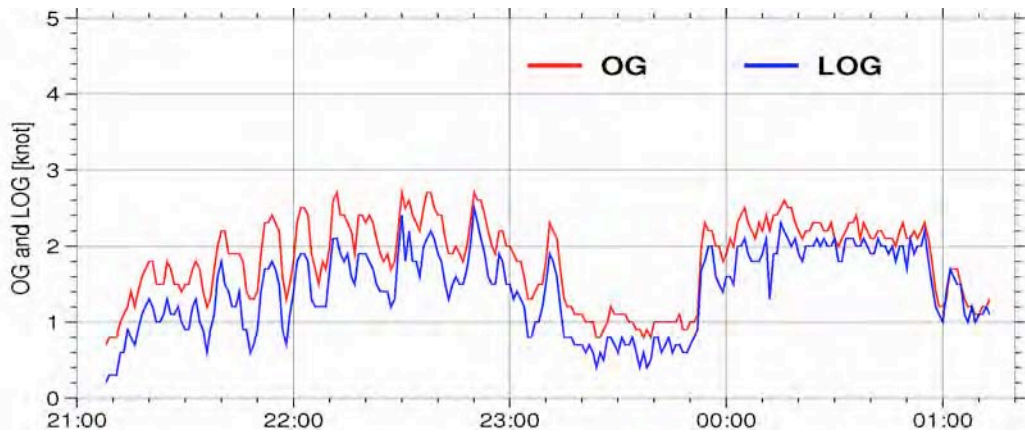

Fig 6.1-2 Relative wind in deployment at K2 station (MR08-05)
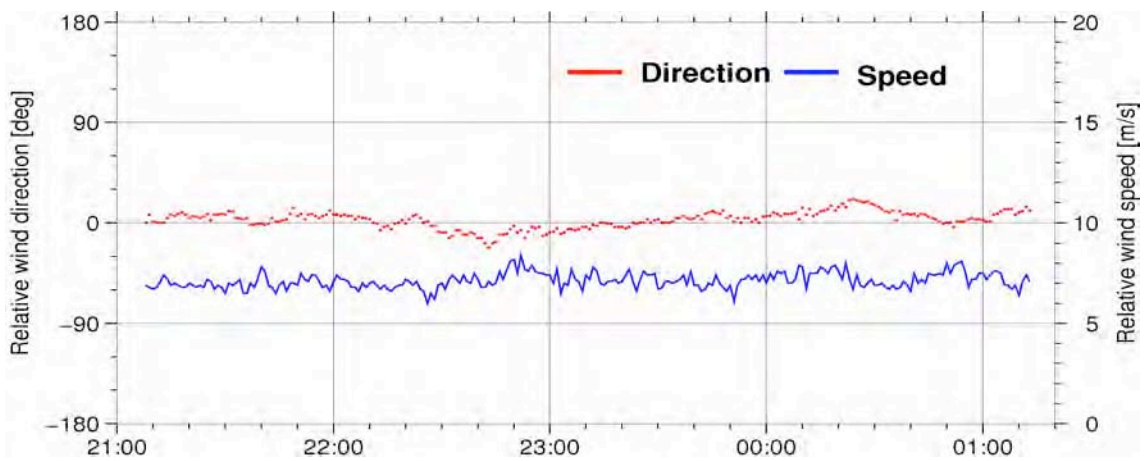

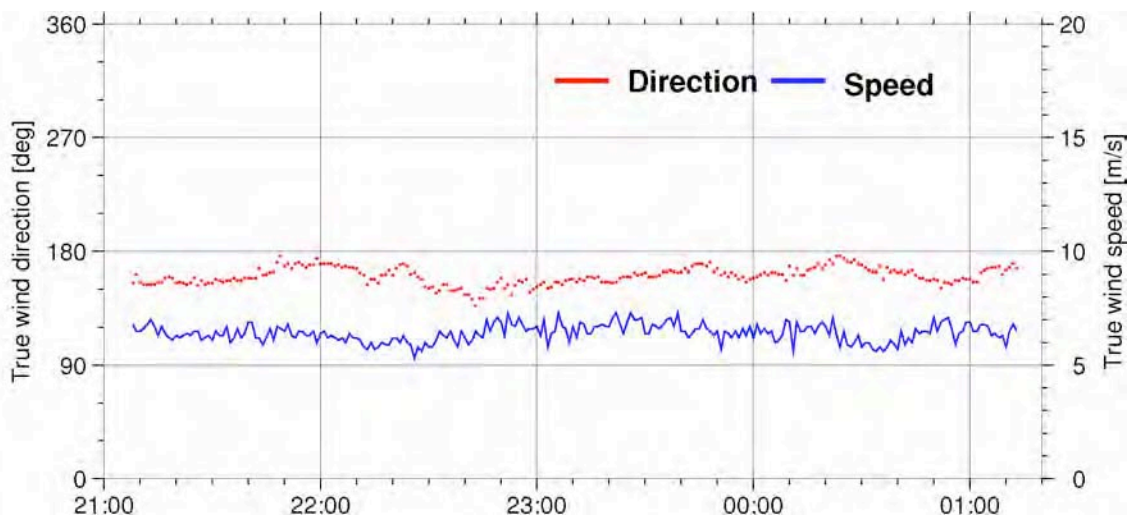Fig 6.1-3 True wind in deployment at K2 station (MR08-05)

Fig 6.1-4 True current to ship's track in deployment at K2 station (MR08-05)
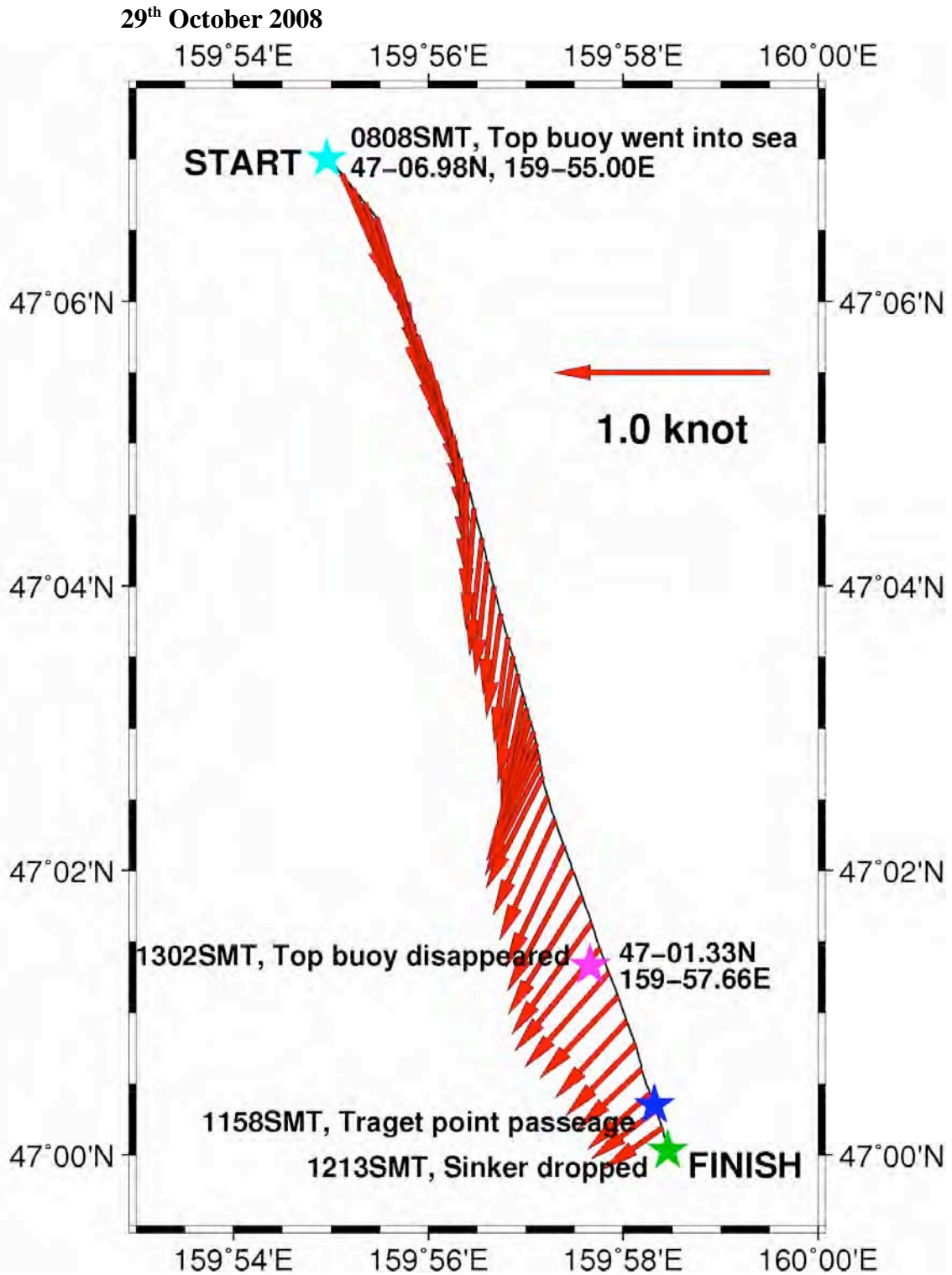

29th October 2008

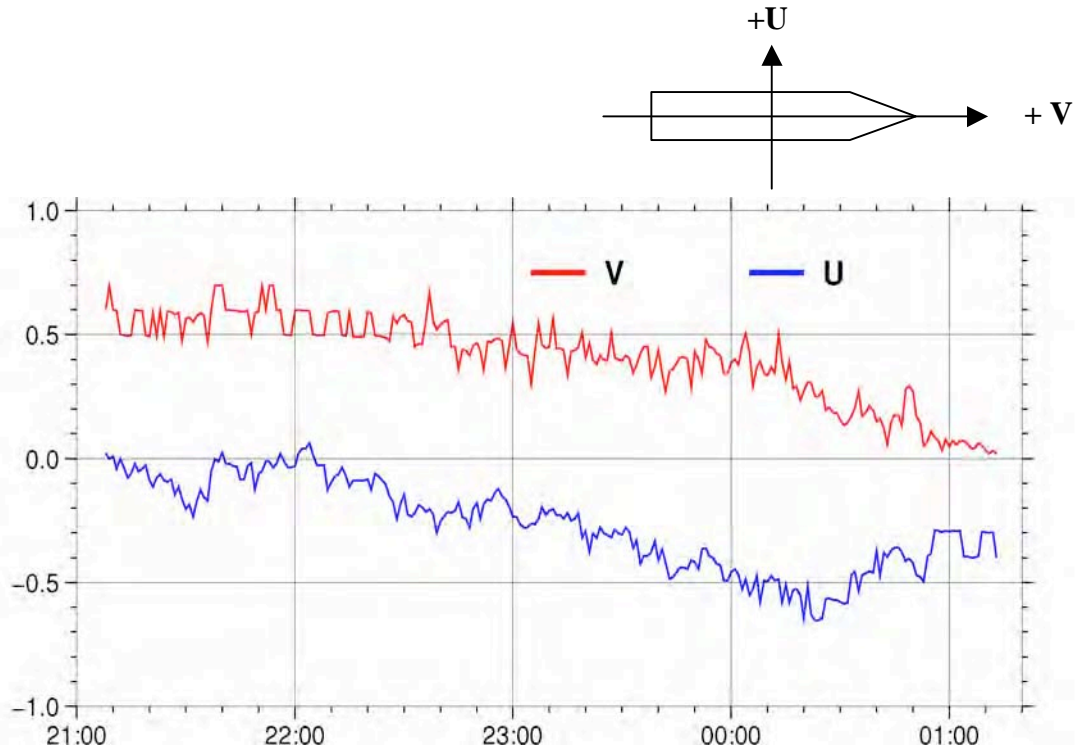Fig 6.1-5 Current influence in deployment at K2 station (MR08-05)

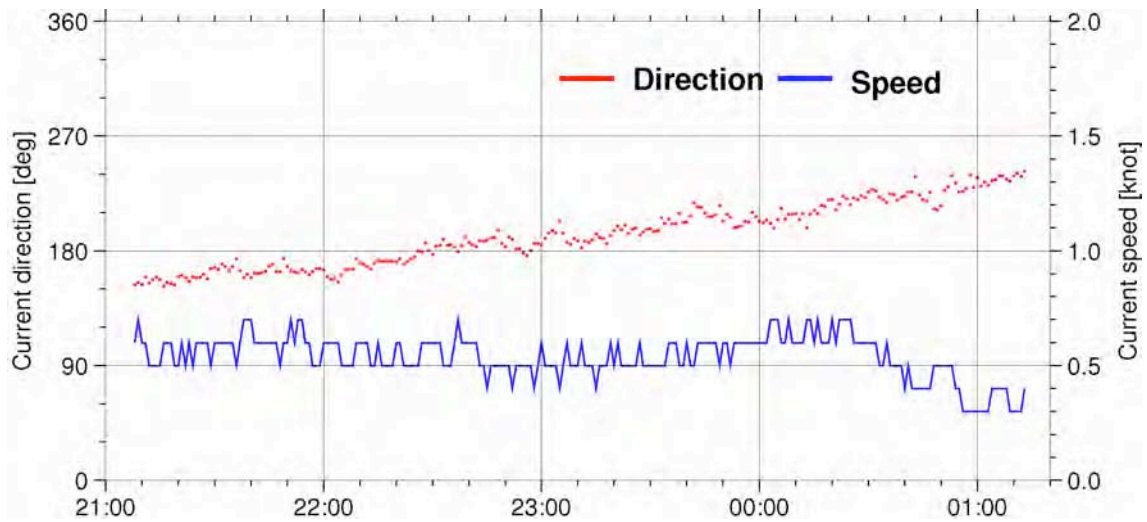Fig 6.1-6 Current in deployment at K2 station (MR08-05)

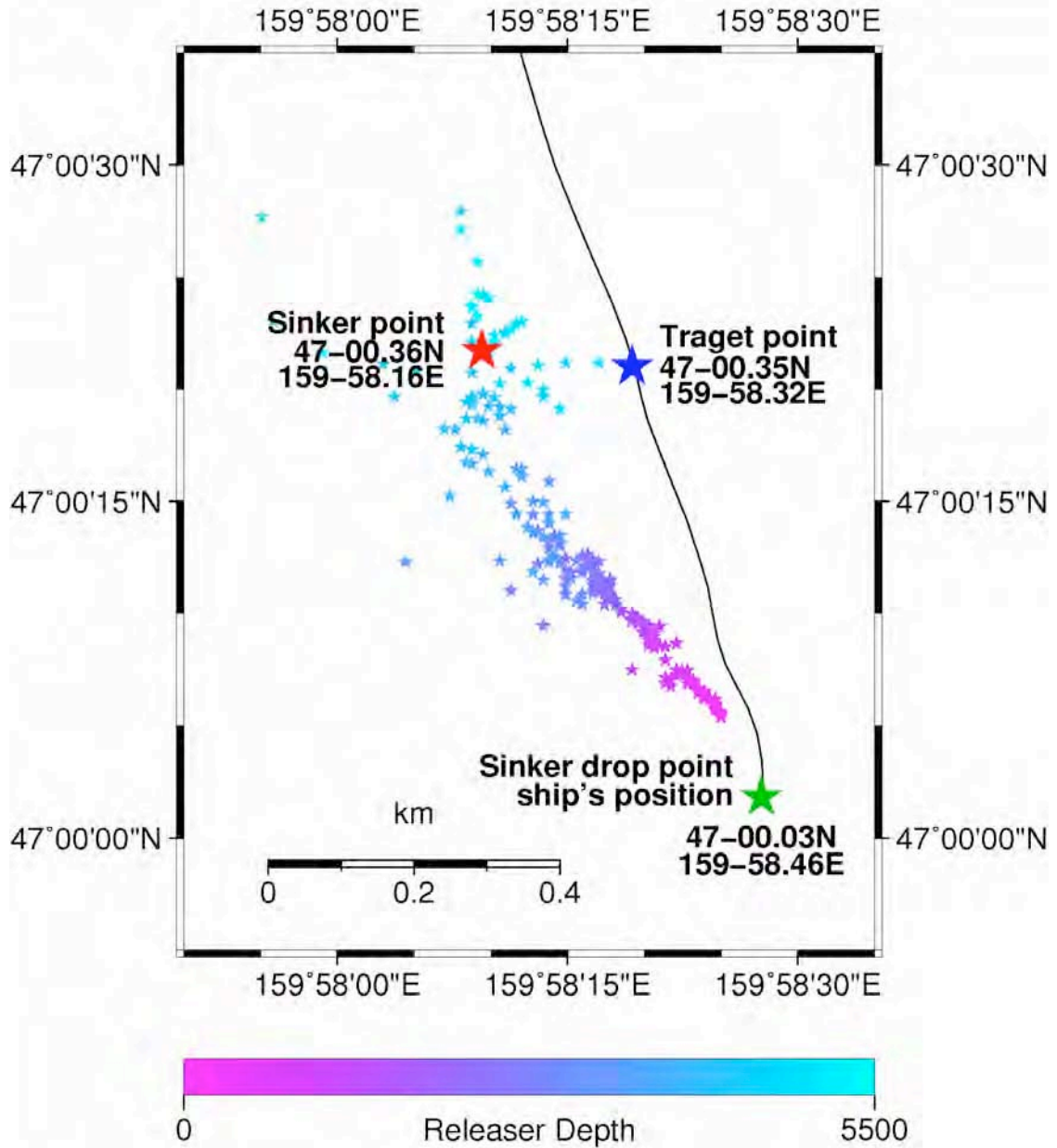Fig 6.1-7 Mooring point at K2 station (MR08-05)

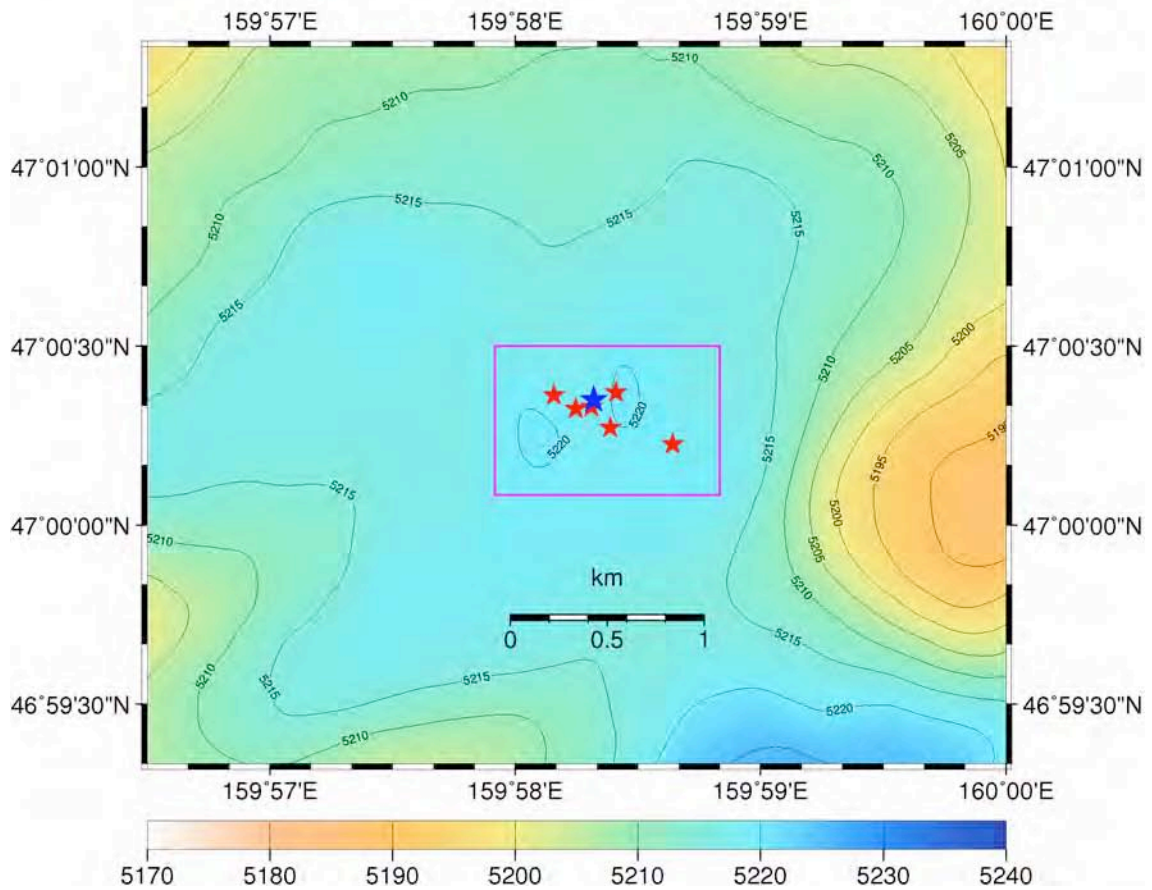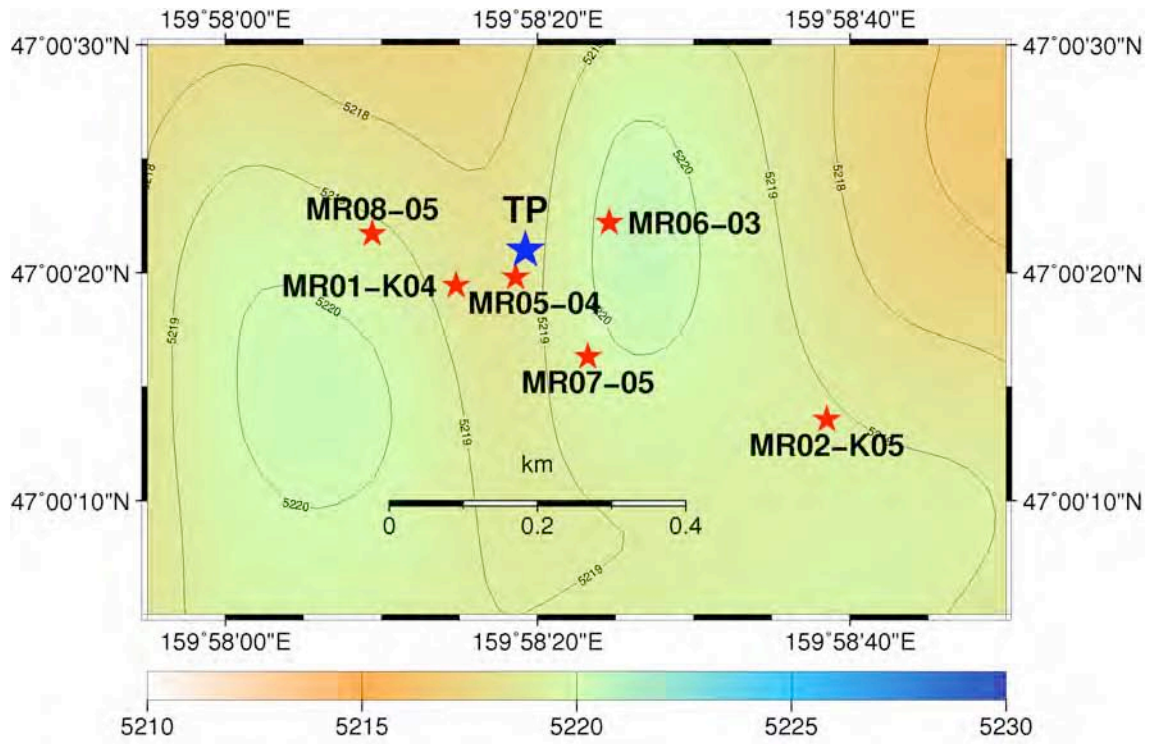Fig 6.1-8 Terrain of ocean floor at K2 station (MR08-05)

Table 6.1-1 Navigational data in deployment at K2 station (MR08-05)

UTC+11h

Time	Position		Head	Log	CO	OG	Relative Wind		True Wind		Current	
(SMT)	Lat.	Long.	(deg)	(knot)	(deg)	(knot)	(deg)	(m/S)	(deg)	(m/s)	(deg)	(knot)
21:05	47-06.99 N	159-54.95 E	154	0.3	111	0.5	1	7	156	6.8	143	0.5
21:15	47-06.89 N	159-55.11 E	150	0.8	141	1.4	7	6.9	156	6.3	157	0.5
21:25	47-06.68 N	159-55.35 E	150	1.3	143	1.8	8	7.2	159	6.5	159	0.6
21:35	47-06.46 N	159-55.53 E	153	0.9	171	1.4	3	6.5	157	6	168	0.6
21:45	47-06.17 N	159-55.69 E	160	1.4	154	1.9	1	6.9	162	6.2	168	0.6
21:55	47-05.88 N	159-55.81 E	162	1.7	159	2.3	6	7.4	169	6.5	164	0.6
22:05	47-05.57 N	159-56.00 E	163	1.3	158	1.9	6	6.8	169	6.1	161	0.5
22:15	47-05.24 N	159-56.16 E	162	1.9	160	2.3	-3	6.7	158	5.7	173	0.6
22:25	47-04.89 N	159-56.32 E	163	1.4	162	1.8	0	6.6	162	5.9	175	0.5
22:35	47-04.54 N	159-56.47 E	162	1.6	166	2.2	-7	7	154	6.2	185	0.5
22:45	47-04.16 N	159-56.60 E	162	1.6	167	2	-17	7	143	6.2	188	0.4
22:55	47-03.80 N	159-56.74 E	162	1.5	166	2	-4	7.9	157	7.1	178	0.5
23:05	47-03.49 N	159-56.86 E	162	0.8	163	1.3	-6	6.9	156	6.5	203	0.4
23:15	47-03.22 N	159-56.97 E	160	0.8	165	1.3	0	6.9	160	6.4	193	0.4
23:25	47-03.05 N	159-57.04 E	160	0.6	167	0.8	0	7.2	160	6.9	197	0.5
23:35	47-02.89 N	159-57.10 E	160	0.6	167	0.9	4	7.1	164	6.8	205	0.6
23:45	47-02.73 N	159-57.15 E	160	0.6	170	1	10	6.9	170	6.6	210	0.6
23:55	47-02.51 N	159-57.22 E	157	2	163	2.2	4	7.4	161	6.5	199	0.6
0:05	47-02.17 N	159-57.39 E	153	2.1	160	2.5	8	7.6	163	6.5	205	0.7
0:15	47-01.81 N	159-57.57 E	154	2.3	160	2.5	10	7.8	165	6.7	212	0.6
0:25	47-01.45 N	159-57.75 E	150	2.1	161	2.3	20	7.4	174	6.5	217	0.7
0:35	47-01.11 N	159-57.94 E	155	2.1	162	2.3	11	6.9	168	5.8	218	0.6
0:45	47-00.77 N	159-58.12 E	156	1.9	160	2.1	5	7.5	161	6.6	220	0.4
0:55	47-00.42 N	159-58.27 E	153	2.2	157	2.3	1	7.7	154	6.6	227	0.4
1:05	47-00.18 N	159-58.40 E	155	1.5	164	1.5	10	7.5	166	6.7	236	0.4
1:13	47-00.03 N	159-58.46 E	155	1.1	177	1.3	11	7.1	166	6.5	242	0.4

Table 6.1-2 SUMMARY OF WORKING TIME FOR DEPLOYMENT BGC MOORING ON MR0805 CRUISE

U+11

Mooring No.	K2	K2	K2	K2	K2(Long-term)	K2(Test)	K2	K2	
Fixed position	47-00.36N	47-00.27N	47-00.34N	47-00.33N	47-00.47N	47-00.48N	47-00.23N	47-00.32N	
	159-58.16E	159-58.39E	159-58.41E	159-58.31E	159-58.06E	159-57.97E	159-58.42E	159-58.25E	
Works Date	29.Oct.08	12.Sep.07	6.Jun.06	26.Sep.05	18.Mar.05	5.Mar.05	25.Oct.02	9.Sep.01	
SEABEAM Depth (m)	5220	5206	5217	5217	5214	5216	5215	5214	
Com'ced deployment	7:50	7:51	7:57	8:24	7:51	8:25	10:30	10:09	
Top buoy into sea	8:08	8:09	8:13	8:43	8:09	8:38	10:54	10:32	
Sediment(1) into sea	8:17	8:18	8:24	8:49	8:24	8:47	11:19	11:23	
Sediment(2) into sea	8:22	8:27	8:35	8:59	8:36	8:59	13:09	12:09	
Sediment(3) into sea	8:35	8:45	8:45	9:13	8:48	9:11	15:02	14:22	
Sediment(4) into sea	8:49	9:03	9:02	9:35	9:00	9:44			
Glass balls(1) into sea	9:08	9:43	9:23	10:07	9:19	10:00			
Glass balls(2) into sea	9:28	10:06	10:10	10:58	9:39	10:28			
Glass balls(3) into sea	9:47	10:34	11:10	11:45	10:02	10:53			
Sediment(5) into sea	10:08	11:03	11:32	11:54	10:29	11:15			
Set Glass balls/Releaser	10:51	11:51	12:17	12:13	10:54	11:47	15:31	14:48	
Stand by sinker	12:08	12:42	13:11	13:16	12:36	14:02	15:59	16:20	
Let go sinker	12:13	12:45	13:17	13:30	13:01	14:14	16:11	16:40	Average
H for top buoy/sensors	0:18	0:18	0:16	0:19	0:18	0:13	0:24	0:23	0:18
o for sediments	2:43	3:42	4:04	3:30	2:45	3:09	4:37	4:16	3:35
u for towing	1:17	0:51	0:54	1:03	1:42	2:15	0:28	1:32	1:15
r for S/B sinker	0:05	0:03	0:06	0:14	0:25	0:12	0:12	0:20	0:12
Total	4:23	4:54	5:20	5:06	5:10	5:49	5:41	6:31	5:21
D for top buoy (mile)	0.19	0.08	0.16	0.26	0.2	0.15	0.09	0	0.14
I for sediments (mile)	4.42	4.67	4.86	4.6	3.42	5.37	6.69	5.29	4.92
s for towing (mile)	2.65	1.9	1.66	2.3	2.75	4.38	0.71	2.56	2.36
t for sinker (mile)	0.11	0.07	0.11	0.32	0.42	0.26	0.28	0.45	0.25
Total (mile)	7.37	6.72	6.79	7.48	6.79	10.16	7.77	8.30	7.67
S for top buoy (knot)	0.6	0.3	0.6	0.8	0.7	0.7	0.2	0.0	0.5
p for sediments (knot)	1.6	1.3	1.2	1.3	1.2	1.7	1.4	1.2	1.4
ee for towing(knot)	2.1	2.2	1.8	2.2	1.6	1.9	1.5	1.7	1.9
d for sinker (knot)	1.3	1.4	1.1	1.4	1.0	1.3	1.4	1.3	1.2
Average OG speed (knot)	1.7	1.4	1.3	1.5	1.3	1.7	1.4	1.3	1.4
Average LOG speed (knot)	1.4	1.1	1.4	1.3	1.3	1.6	1.3	1.7	1.4

	0:18	0:18	0:16	0:19	0:18	0:13	0:24	0:23
	2:43	3:42	4:04	3:30	2:45	3:09	4:37	4:16
	1:17	0:51	0:54	1:03	1:42	2:15	0:28	1:32
	0:05	0:03	0:06	0:14	0:25	0:12	0:12	0:20
	2008 Oct	2007 Jun	2006 Sep	2005 Sep	2005 Mar	2005 Mar	2002 Oct	2001 Sep

6.2 Ship's Handling for the recovery of the BGC moorings

(1) Objectives

When a BGC mooring is recovered, after separating it from the seabed, it is important to know in what direction it will be adrift by the wind, the current, and the swell, etc. in order to catch it safely, and efficiently. Moreover, it is greatly helpful to grasp actual working hours when performing future work.

It aims at recording results of recovering the mooring systems such as the BGC from the standpoint of the ship's handling.

(2) Observation parameters
- ・ Movement of the BGC mooring released from the seabed
- ・ Ship's position, course, speed
- ・ Directions of the wind/the current/the swell, velocities of the wind/the current

(3) Methods

  (4.1) Measurement of the actual ship-movement

Measurement of the ship-movement at coming close to the top buoy and the glass ball floats is carried out in a radio navigation device assembled by Sena Co., Ltd. Japan.

  (4.2) Measurement of the wind and the current

The wind direction and speed are measured by KOAC-7800 weather data processor and sensors assembled by Koshin Denki Co., Ltd.

The current direction and speed are continuously measured by a Doppler sonar installed at the bottom of the ship. The Doppler sonar is assembled by FURUNO Electric Co., Ltd.

  (4.3) Measurement of the releaser-movement in the sea

The releaser is operated with an acoustic transducer which is made by Edgetech Inc. USA and an acoustic navigation device.

Releaser: Edgetech Inc. USA (transmit 11 kHz or 12 kHz, receipt 9 kHz or 11 kHz)

Acoustic navigation device: "SSBL processor (Transmit 11 kHz or 13 kHz, receipt 13.5 kHz to 15.5 kHz)" assembled by Oki Electric Co. Ltd. Japan.

(4) Maneuver

  (4.1) Surfacing of the moorings

    (a) The ship is located leeward or downstream on a distance of 200 - 400 meters from the sinker position of the mooring. The clutches of the CPP are disengaged and the operation of the stern thruster and the SEABEAM are suspended except the bow thruster for adjusting the ship's head if necessary.The "Enable" signal is sent from the stern of the ship by the transducer or from ship's bottom by the acoustic navigation device and the signal reception is confirmed. It is demanded to be nearly over the moored point when the signal reception is difficult. After the reception is confirmed, it is necessary to go away from the moored point by about 400 meters

because the point where the top buoy surfaces might shift by about 200 meters.

(b) The BGC mooring is released from the seabed by using the acoustic transducer on 11 and 12 kHz at the mooring deck of the ship's stern or by using the acoustic transmission device at the bottom of the ship.

(c) On the assumption that the mooring point is correct, a top buoy of the mooring is surfaced in the direction of the current. In case there is hardly a flow, the top buoy surfaces right above the mooring point. The top buoy receives the influence of the wind after it surfaces, and drifts.

(4.2) How to approach the top buoy/the glass ball floats

(a) When the ship approaches buoy etc, the angle between the ship's course and the wind direction is made as small as possible in order to lessen the external force influence of the wind. In addition the ship's course is decided to make her locate in the lee of buoys/glass ball floats.

(b) To prevent the ropes etc. from twining round the ship's propeller, the clutch of the propeller in the recovery-side is discharged until the handling rope is connected to buoy etc. from the time that the ship approaches buoys etc.

(c) In case of calm sea state, the work to catch the top buoy is carried out with the working boat after all of the system appear on the surface. When the working boat is lowered, and the working boat is drawn up, the ship makes the lee to have calm water, an ample berth for it.

(d) In case of rough sea state, the ship is handled to approach the top buoy most and the top buoy is caught from the upper deck of the ship by a grapnel or a hook and a long pole because the working boat is not able to use due to rough sea. Because delicate measuring instruments are installed under the top buoy, it is prohibited to push the buoy strongly, and to hit it the discharging current from CPP and propeller of the side-thruster.

Be careful when the hook/pole is used to catch the top buoy since the various instruments installed under the top buoy might be damaged. Therefore the hook installed the end of the long pole, a long rope connected with the hook is used as the second plan.

(e) While recovering mooring ropes/cables, the ship is steered by side thrusters in order to tow them straight behind. It is easy to carry out the work if the ship proceeds to upwind.

(f) Since the BGC mooring in which a lot of observation equipments and sediment traps are installed, it cannot be strongly towed. The ship's speed is kept about 1 knot or less. When these observation equipments are slung up the ship, Care is
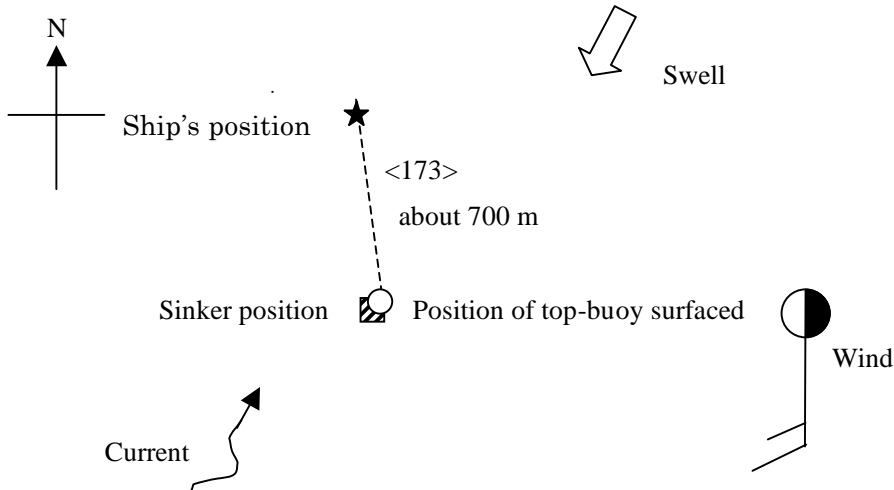
needed in handling them not to upset the observation equipment.

(5) Results
  (5.1) Surfacing of the BGC mooring (Fig 6.2-1)
    The results are shown in following figures and these are characterized as follows.

In case of the BGC mooring at K2 site

(a) The ship was stopped at the leeward and the downstream about 500 meters from the sinker position.

(b) The ship's starboard was turned to the sinker position for transmitting signals and the operation of machines (CPP, bow/stern thrusters and the SEABEAM) which influence the acoustic devices was suspended. Firstly the acoustic navigation device was tried out for communicating with the releasers but was unable to receive a confirmation signal from the releasers. Afterwards, the acoustic transducer was lowered over the starboard stern. As soon as the release signal from the transducer was sent, the mooring was separated from the seabed because the releaser had been already waked by the enable signal sent from the acoustic navigation device.

(c) The top buoy surfaced at the position of 173 degrees and about 700 meters from the ship **in 1 minute** after confirming the release. The point was near the sinker position.

(d) After the top buoy had surfaced, the glass floats being connected near the bottom of the mooring surfaced **47 minutes later**. The point was in the direction of about 200 degrees from the top buoy at the distance of about 150 meters by influence of the wind and the current. The middle glass floats surfaced **51 minutes later** after confirming the release. The middle glass floats bobbed up and down between the waves and ropes connected with them were sinking.

177

(6.2) Working hours for recovering the BGC mooring

The result is shown in Table 6.2-1 and the following matters are pointed out.

(a) The time consumed in recovery of the BGC mooring was 4 hours and 45 minutes.

The working hours in this time are long in comparison with the past results because the hours in recovery of sediment traps took so much time since ropes and glass floats were entangled to each other. Other working hours except for the recovery of the sediment traps were much the same as past results.

(b) The top buoy of the BGC mooring was caught by the workboat because it was ensured to recover various delicate equipments safely. The operation hours from the time when the workboat was lowered to the time when the workboat entered the shed were 28 minutes. This was almost the same as the last working hours.

(c) The ropes/wires in which glass floats were entangled were cut in the suitable place without disentangling the knots. In the end this extra work due to the tangle caused the delay of the working hours. Compared with previous works, tangles of glass floats were much.

⑹ Data archive

All data will be archived on board.

(7) Remarks

The recovery of the BGC buoy which many delicate sediments/sensors are installed with must be basically carried out by using a working boat. However the operation of the working boat is restricted because of the rough sea. In this time, the recovery of the BGC buoy was postponed until the following day as the sea was rough. It is to prevent tangles with glass floats and ropes to achieve shortening of the working hours any further. There is an idea that all BGC system including the top buoy is towed by the working boat or the ship as soon as the top buoy rises to the surface of the sea in order to prevent the tangle of glass floats.

Fig.6.2-1 RECOVERY OF BGC MOORING

Location: 47-00.27N, 159-58.39E

Date: 25th October 2008
Wind: <180> 7.1 m/s, Current: <015> 0.5 knot
Swell: NNE, Wave height: 2.3 m, 7.3 sec
Weather: c, Depth: 5220m
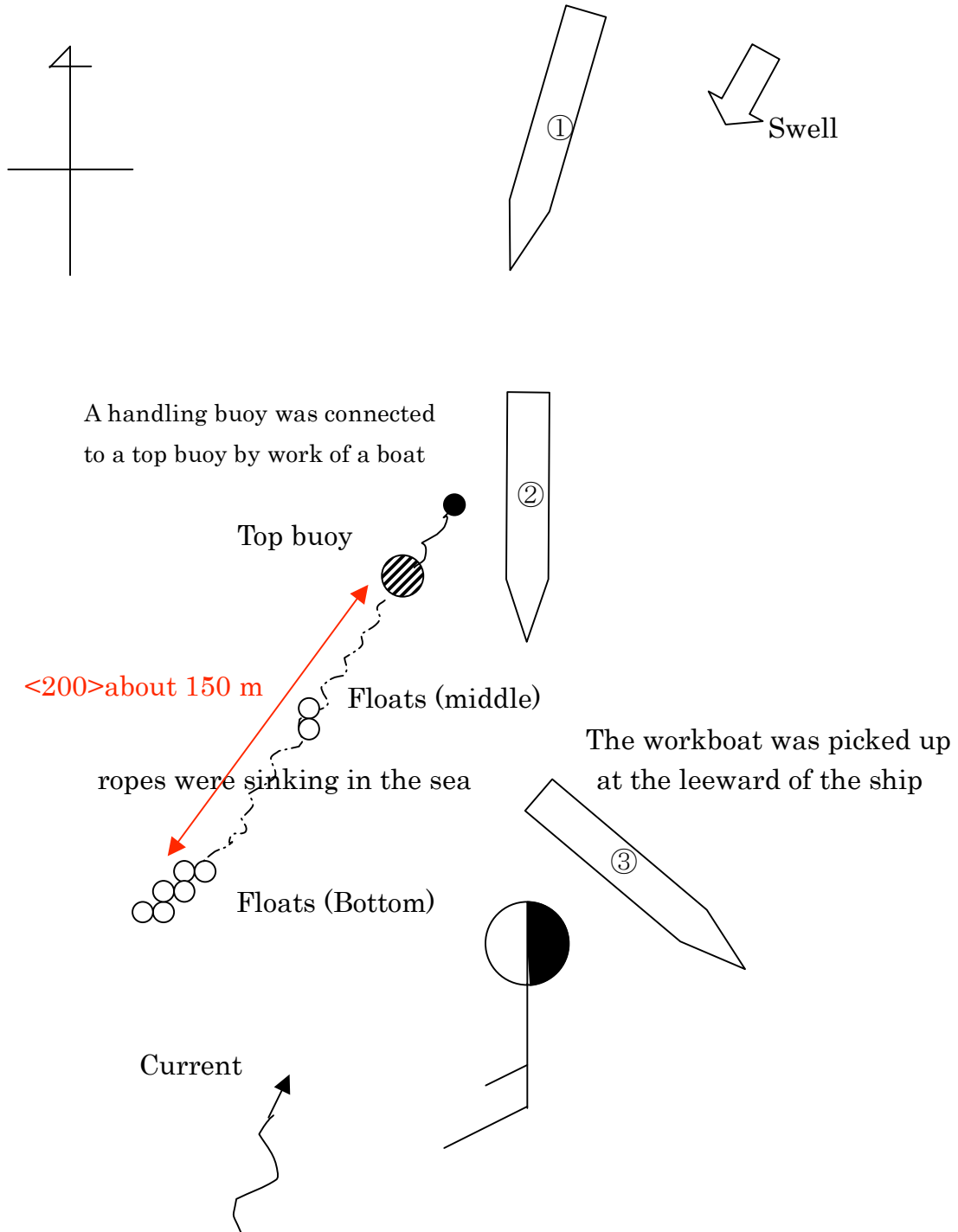
①

Swell

A handling buoy was connected
to a top buoy by work of a boat

②

Top buoy

<200>about 150 m

Floats (middle)

The workboat was picked up
ropes were sinking in the sea   at the leeward of the ship

③

Floats (Bottom)

l

Current

Table 6.2-1 RECOVERY OF BGC MOORING ON MR08-05 CRUISE

Mooring No.		K2-BGC	K2-BGC	K2-BGC	K2-BGC	K2-BGC
Location	lat	47-00.27N	47-00.34N	47-00.33N	47-00.47N	47-00.48N
	Long	159-58.39E	159-58.41E	159-58.31E	159-58.06E	159-57.97E
Date		25.Oct.08	17.Jul.06	31.May.06	23.Sep.05	17.Mar.05
Water depth (m)		5215	5200	5206.2	5206.2	5206.2
Com'ced work (Set transducer)		6:39	6:53	7:10	7:07	7:03
Released from sinker		6:42	6:55	7:13	7:14	7:05
Top buoy surfaced		6:43	6:56	7:14	7:15	7:06
Floats (Bottom) surfaced		7:30	7:46	8:00	8:03	7:53
Catched handling buoy by workboat		7:58	8:11	8:06	8:28	8:34
Slinged top buoy at stern		8:29	8:30	8:40	8:55	8:41
Winded up top buoy (on deck)		8:34	8:36	8:45	9:04	8:47
Recovery of equipments		8:36	8:42	8:53	9:15	8:57
Recovery of sediment (1)		8:50	8:53	9:10	9:25	9:08
Recovery of sediment (3)		9:20	9:10	9:31	9:47	9:41
Recovery of sediment (5)		11:11	10:39	10:57	11:19	11:52
Recovery of floats (Bottom)/releaser		11:22	10:48	11:05	11:31	12:16
Finished work (Releaser on deck)		11:24	10:51	11:06	11:32	12:18
Total working hours		4:45	3:58	3:56	4:25	5:15

Time consumed

in preparation for recovery		0:03	0:02	0:03	0:07	0:02
in rising of glass balls (Bottom)		0:48	0:51	0:47	0:49	0:48
in catching of top buoy		0:28	0:25	0:06	0:25	0:41
in recovery of top buoy		0:36	0:25	0:39	0:36	0:13
in recovery of sediments		2:37	2:03	2:12	2:15	3:05
in recovery of floats/releaser		0:13	0:12	0:09	0:13	0:26
Total working hours		4:45	3:58	3:56	4:25	5:15

Maneuvering data

MOORING NUMBER	K2(Oct.'08)	K2(Jul.'06)	K2(May,'06)	K2(Sep.'05)	K2(Mar.'05)
Course when approaching (deg)	185	280	145	290	260
Course when catching buoy (deg)	175	270	145	280	220
Wind direction (deg)	180	270	145	290	290
Wind velocity (m/s)	7.1	6.1	9.1	11.5	3.7
Current direction (deg)	15	60	70	170	Various
Current velocity (knot)	0.5	0.4	0.5	0.8	0.2
Swell direction	NNE	West	SE	WNW	WSW
Wave height (m)	2.3	1.7	1.5	2.8	2.4